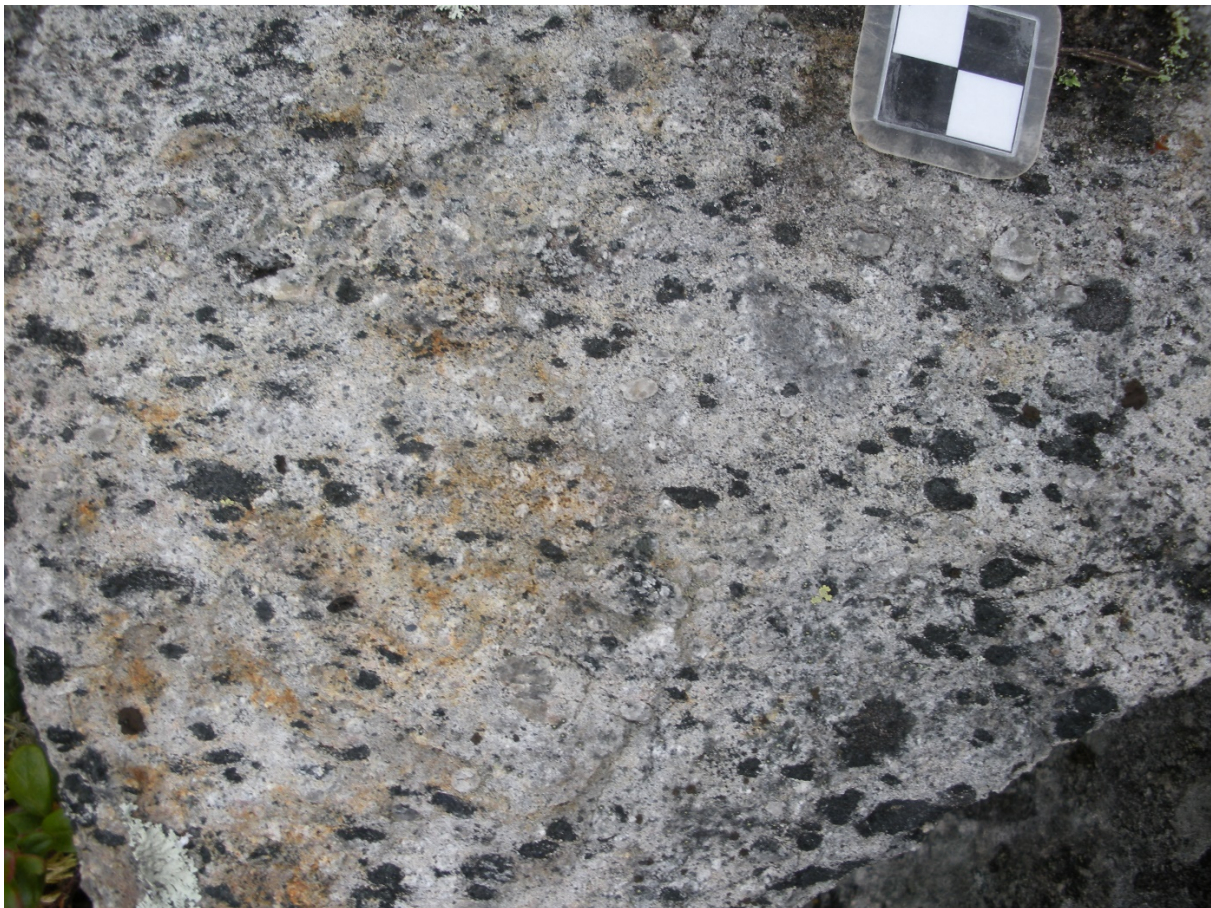


U-Pb zircon geochronology of rocks from the mid and southwestern part of Norrbotten County, Sweden

Dick Claeson & Ildikó Antal Lundin (Editors)

oktober 2018

SGU-rapport 2018:22



Cover: Newly discovered 1.77 Ga volcanic succession at Tjäckåure.
Photographer: Dick Claeson

Editors: Dick Claeson & Ildikó Antal Lundin
Reviewed by: Stefan Bergman, Benno Kathol, Lena Persson
Responsible head of division: Ildikó Antal Lundin
Projektnamn: Mellersta Norrbotten, Sydvästra Norrbotten

Geological Survey of Sweden
Sveriges geologiska undersökning
Box 670, 751 28 Uppsala
tel: 018-17 90 00
fax: 018-17 92 10
e-post: sgu@sgu.se

www.sgu.se

TABLE OF CONTENTS

Sammanfattning.....	8
Introduction	9
Map sheet 27K Nattavaara area.....	10
U-Pb zircon age of an intermediate volcanic rock at Sammakkovaara, map sheet 27K Nattavaara.....	12
Introduction.....	13
Sample description.....	13
Analytical results and interpretation of geochronological data.....	15
Discussion and conclusion	17
References	18
U-Pb zircon age of quartz and feldspar porphyric rhyolite from 2.5 km NW of Kiltekorronen, map sheet 27K Nattavaara, Norrbotten County	19
Introduction.....	20
Sample description.....	20
Analytical results and interpretation of geochronological data.....	23
Discussion and conclusion	26
References	27
U-Pb zircon age of subvolcanic granite to rhyolite porphyry at Linavare, map sheet 27K Nattavaara, Norrbotten County.....	28
Introduction.....	29
Sample description.....	29
Analytical results and interpretation of geochronological data.....	32
U-Pb zircon analyses.....	32
Results.....	33
Discussion and conclusion	35
References	35
U-Pb zircon age of metagranite with relict phenocryst texture at Linavare, map sheet 27K Nattavaara, Norrbotten County.....	36
Introduction.....	37
Sample description.....	37
Analytical results and interpretation of geochronological data.....	38
Discussion and conclusion	41
References	41

U-Pb zircon age of quartz monzonite to granite at Urtjuvare, map sheet 27K Nattavaara, Norrbotten County	42
Introduction	43
Sample description	43
Analytical results and interpretation of geochronological data.....	46
Analytical procedures	46
Analytical results and interpretation of geochronological data.....	46
Discussion and conclusion	49
References	49
U-Pb zircon age of strongly deformed, recrystallised granite at Kaltisberget, map sheet 27K Nattavaara, Norrbotten County	50
Introduction	51
Sample description	51
Analytical results and interpretation of geochronological data.....	52
Discussion and conclusion	55
References	56
U-Pb zircon age of quartz monzonite to monzonite at Tiurevaara, map sheet 27K Nattavaara, Norrbotten County	57
Introduction	58
Sample description	58
Analytical results and interpretation of geochronological data.....	61
U-Pb zircon analyses.....	61
Results.....	63
Discussion and conclusion	65
References	65
U-Pb zircon age of monzonite to syenite at Ahmavaara, close to the Aitik ore deposit, Norrbotten County	66
Introduction	67
Sample description	68
Analytical results and interpretation of geochronological data.....	69
U-Pb zircon analyses.....	69
Results.....	71
Discussion and conclusion	73
References	74
Map sheet 27J Porjus SV area	75

U-Pb zircon age of quartz trachyte to rhyolite at St. Samonåive, map sheet 27J Porjus SV, Norrbotten County	77
Introduction	78
Sample description	78
Analytical results and interpretation of geochronological data.....	81
Discussion and conclusion	85
References	86
U-Pb zircon age of rhyolite at Kaddåive, map sheet 27J Porjus SV, Norrbotten County	87
Introduction	88
Sample description	88
Analytical results and interpretation of geochronological data.....	91
Discussion and conclusion	94
References	95
U-Pb zircon age of the host granite of the REE and Mo (U, Th, Nb, Ta) mineralisation at Tåresåive, map sheet 27J Porjus SV, Norrbotten County	96
Introduction	97
Sample description	97
Analytical results and interpretation of geochronological data.....	100
Discussion and conclusion	104
References	105
U-Pb zircon age of monzonite at Njuorramjauratj, map sheet 27J Porjus SV, Norrbotten County	106
Introduction	107
Sample description	107
Analytical results and interpretation of geochronological data.....	110
Discussion and conclusion	114
References	115
Map sheet 26J Jokkmokk NV, NO area	116
U-Pb zircon age of rhyolite to trachyte west of Lagmans-graven, map sheet 26J Jokkmokk NV, Norrbotten County	117
Introduction	118
Sample description	119
Analytical results and interpretation of geochronological data.....	123
Discussion and conclusion	126
Acknowledgments.....	126
References	127

U-Pb zircon age of granite to quartz monzonite north of Tårrajaur, map sheet 26J Jokkmokk NV, Norrbotten County	128
Introduction	129
Sample description	132
Analytical results and interpretation of geochronological data.....	135
Discussion and conclusion	139
Acknowledgements	139
References	140
U-Pb zircon age of gabbro pegmatite at the Ruotevare intrusion, map sheet 26J Jokkmokk NO, Norrbotten County	141
Introduction	142
Sample description	143
Analytical results and interpretation of geochronological data.....	144
Discussion and conclusion	148
Acknowledgements	149
References	149
U-Pb zircon age of porphyric quartz monzonite to monzonite south of Tvärträsket, map sheet 26J Jokkmokk NO, Norrbotten County	151
Introduction	152
Sample description	153
Analytical results and interpretation of geochronological data.....	157
Discussion and conclusion	160
Acknowledgements	160
References	161
Map sheet 27I Tjåmotis SV, SO area	162
U-Pb zircon age of granite to quartz monzonite at Ritavare, map sheet 27I Tjåmotis SO, Norrbotten County	163
Introduction	164
Sample description	165
Analytical results and interpretation of geochronological data.....	168
Discussion and conclusion	171
References	172
U-Pb zircon age determination of the Hárrevárddo intrusion using quartz monzonite at Jervas, map sheet 27I Tjåmotis SV, Norrbotten County	173
Introduction	174
Sample description	176

Analytical results and interpretation of geochronological data.....	179
Discussion and conclusion	183
References	184
U-Pb zircon age of host quartz trachyte at the Kallak iron ore deposit east of Björkholmen, map sheet 27I Tjåmotis SO, Norrbotten County.....	186
Introduction	187
Sample description	187
Analytical results and interpretation of geochronological data.....	191
Discussion and conclusion	194
Acknowledgements	194
References	195
New volcanic succession at 1.77 Ga determined by U-Pb zircon age of andesitoid at Tjåkkaure, map sheet 27I Tjåmotis SO, Norrbotten County	196
Introduction	197
Sample description	197
Analytical results and interpretation of geochronological data.....	202
Discussion and conclusion	206
Acknowledgments.....	206
References	207
Concluding remarks and future issues.....	208

SAMMANFATTNING

Syftet med SGU:s dateringar är att skapa goda underlag för intressenter inom prospekteringsindustrin, gruvnäringen, länsstyrelser, kommuner och andra. Dessutom bidrar de till att utöka de akademiska kunskaperna om regionens berggrundsgeologi.

Denna rapport presenterar nya radiometriska dateringar av bergarter med uran-bly-metoden på zirkon från berggrundskarteringsprojekt vid SGU som löpt under 2006 till 2015 i södra Norrbotten.

Åtta U-Pb zirkonåldrar av vulkaniska bergarter, elva U-Pb zirkonåldrar av sura till intermediära plutoniska bergarter och en U-Pb zirkonålder av en gabbropegmatit redovisas här. Några resultat är viktiga nya fynd relaterade till tidpunkten för händelser som är relevanta för malmbildningar som Aitik, Kallak och andra i regionen. Andra åldersbestämningar har använts för att bättre förstå berggrundens utveckling. En tidigare helt okänd vulkanisk succession bildad vid 1,77 Ga beskrivs nedan.

INTRODUCTION

This report presents radiometric age determination results from bedrock mapping programmes carried out at the Geological Survey of Sweden in parts of southern Norrbotten between 2006 and 2015. The different chapters of map sheet areas; 27K Nattavaara, 27J Porjus SV, 26J Jokkmokk NV, NO, 27I Tjåmotis SV, SO, all start with geophysical maps of the magnetic total field and of the gravity and sample locations shown. The separate age determinations for the specific area then follows.

Eight U-Pb zircon ages of volcanic rocks, eleven U-Pb zircon ages of acid to intermediate plutonic rocks, and one U-Pb zircon age of a gabbro pegmatite rock are reported here. Some results are important new findings related to the timing of events of relevance for ore deposits at Aitik, Kallak, and others of the region. Other age determinations are used to understand the crustal evolution of the bedrock. An earlier unknown volcanic succession at 1.77 Ga is described.

The U-Pb zircon ages were determined using either the high-spatial resolution secondary ion mass spectrometer (SIMS) Cameca IMS 1270/1280 at the Nordsim facility at the Swedish Museum of Natural History in Stockholm, the thermal ionization mass spectrometer (TIMS) at the Laboratory of Isotope Geology at the Swedish Museum of Natural History in Stockholm or laser ablation sector field inductively coupled plasma mass spectrometry (LA-SF-ICP-MS) at the the ICPMS laboratory, Ministry of Climate and Energy, GEUS, Copenhagen, Denmark. The Laboratory for Isotope Geology/Nordsim of the Swedish Museum of Natural History in Stockholm and the ICPMS laboratory, Ministry of Climate and Energy, GEUS, Copenhagen, Denmark are greatly acknowledged for their first-class analytical support.

MAP SHEET 27K NATTAVAARA AREA

All but one of the age determined rocks of this area occur within the map sheet 27K Nattavaara, except for the rock at Ahmavaara that is located within the map sheet 28K Gällivare SV. Eight rocks were sampled for age determination, two volcanic and six intrusive, in order to better constrain the mapping effort and contribute to new data and knowledge of the magmatic events in the area.

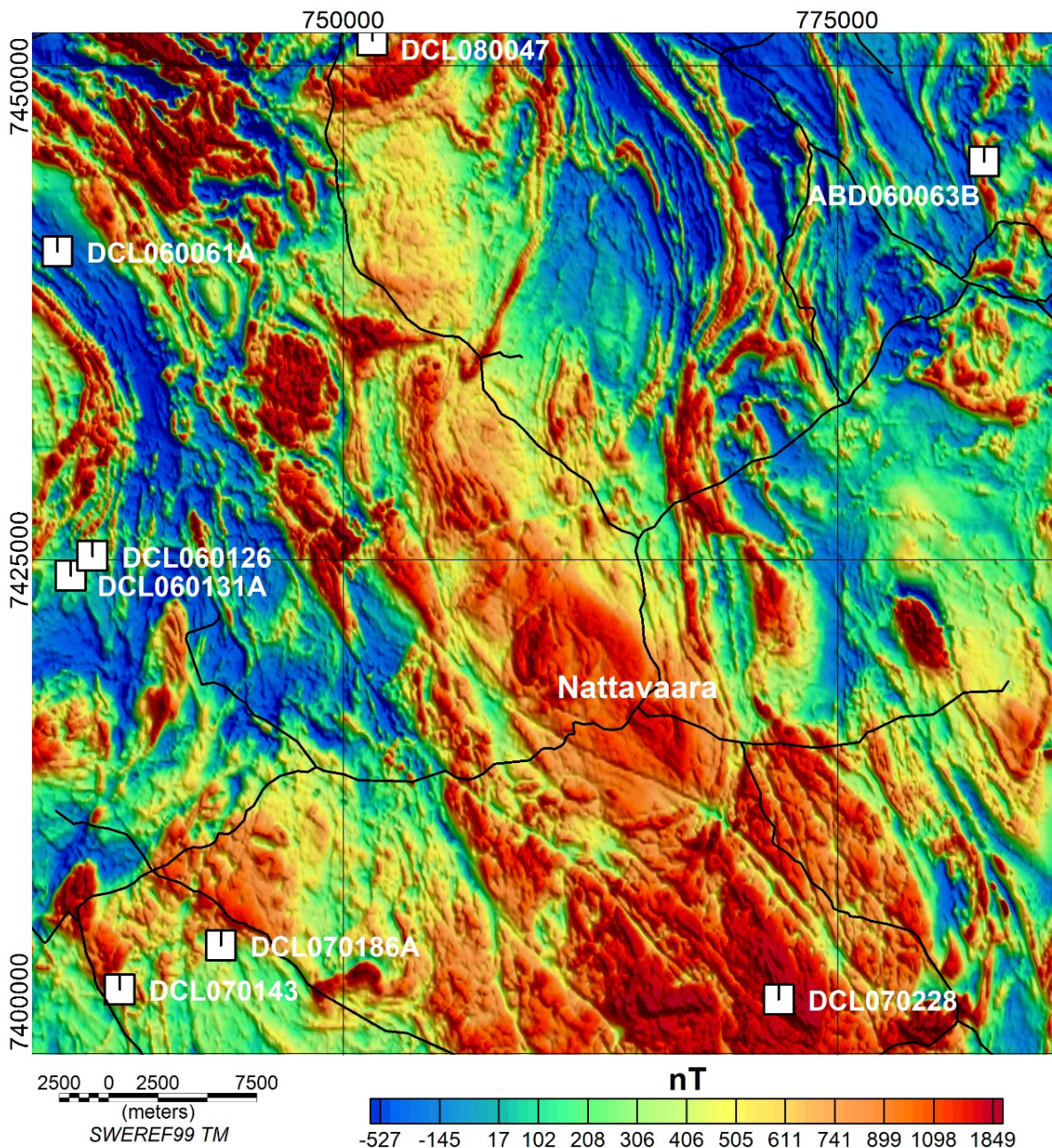


Figure 1. Magnetic total field after subtraction of the geomagnetic reference field (DGRF 1965.0) covering map area 27K Nattavaara. The sample locations are shown with white rectangles.

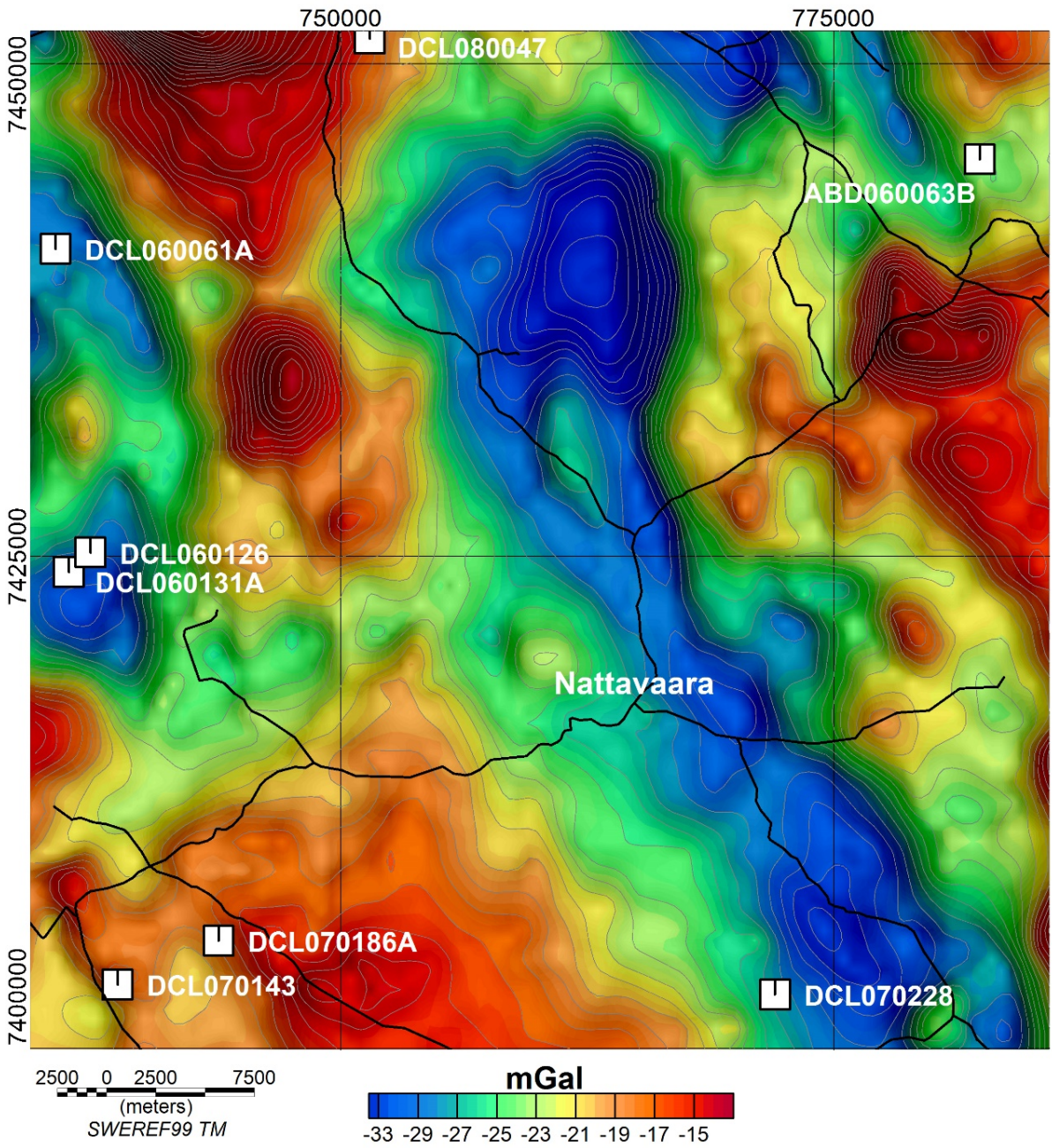


Figure 2. Bouguer gravity map covering map area 27K Nattavaara. The sample locations are shown with white rectangles.

U-Pb ZIRCON AGE OF AN INTERMEDIATE VOLCANIC ROCK AT SAMMAKKOVAARA, MAP SHEET 27K NATTAVAARA

Authors: Dick Claeson, Ildikó Antal Lundin, Andrius Rimsa & Fredrik Hellström

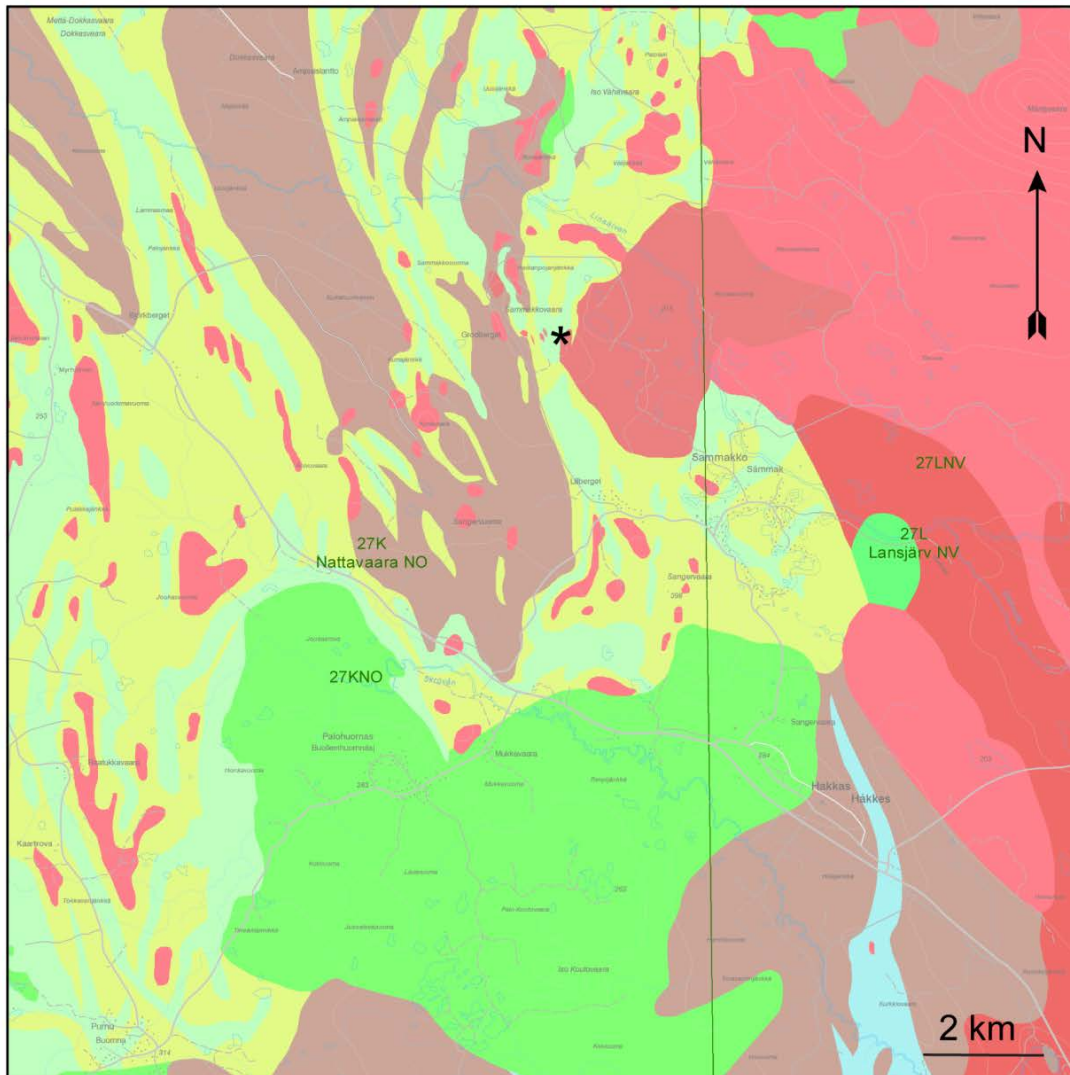


Figure 3. Bedrock map of the area, sampling location marked with black star.

Introduction

The aim of this study is to determine the age of an intermediate volcanic rock that occurs at Sammakkovaara, 24 km east of the world-class Aitik ore deposit in the north-eastern part of the map area 27K Nattavaara in Norrbotten County (Fig. 1–3). The result would increase the knowledge of the volcanic stratigraphy in the area and furthermore, age determinations of volcanic rocks in the region are scarce. The sampled rock is part of the same units that are subject to prospecting efforts in 2017 for Cu, Au, Ag, and Mo at e.g. Dokkas, Sadjem, Liikavaara, Leipovaara, and Aitik.

Sample description

The investigated rock is a relatively well-preserved intermediate volcanic rock (andesitic composition, $\text{SiO}_2 = 60.3\%$) with very fine to fine-grained, dark grey matrix. Metamorphic facies of the rock are estimated to be epidote amphibolite. The rock at the outcrop is partly an agglomerate with clasts of more basaltic compositions as well (Fig. 4) and shows a high magnetic susceptibility between $3\,000$ and $5\,000 \times 10^{-5}$ SI and low gamma ray values; $K = 1.9\%$, $U = 1.5$ ppm, and $\text{Th} = 5.9$ ppm. Petrophysical measurements of two different samples from the outcrop show density at $2\,755$ and $2\,876$ kg/m^3 , magnetic susceptibility $5\,406$ and 300×10^{-5} SI and remanent magnetization intensity of $1\,690$ and 78 mA/m, respectively.

The andesitoid at Sammakkovaara shows a LREE-enriched and flat HREE pattern, with a minor negative Eu anomaly (Fig. 5). The LREE enrichment is due to fractional crystallisation, the flat, unfractionated HREE pattern shows that no garnet was left in the residue at the location of magma genesis, and the minor Eu anomaly is indicative of insignificant plagioclase fractionation. The lack of a Sr anomaly in the multi-element diagram also suggests insignificant plagioclase fractionation (Fig. 5). The small negative anomalies shown in the multi-element diagram of P indicate some apatite fractionation, and the Ti anomaly of modest Fe-Ti oxide fractionation (Fig. 5). The strong negative Nb anomaly and positive Pb anomaly suggest a subduction related petrogenesis (Fig. 5). In contact with the sampled rock is an undeformed, massive, potassium feldspar porphyritic quartz monzonite, monzonite to granite, interpreted to belong to the same 1.80 Ga old generation of similar rocks as seen at Ahmavaara (this paper).

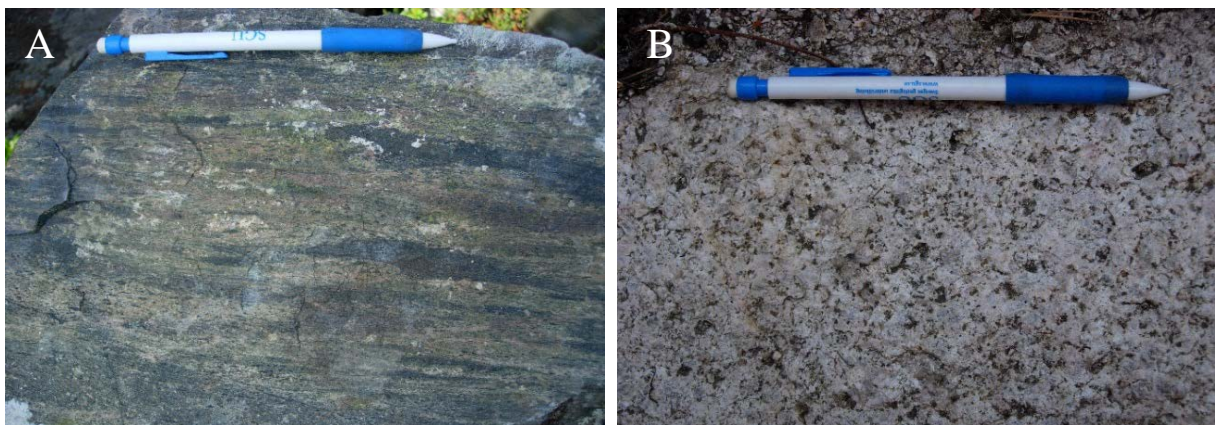


Figure 4. **A.** The intermediate volcanic rock at Sammakkovaara is partly an agglomerate and shows clasts of basalt. **B.** The pristine quartz monzonite to monzonite that is seen in contact with the andesitoid. Photos: Dick Claeson.

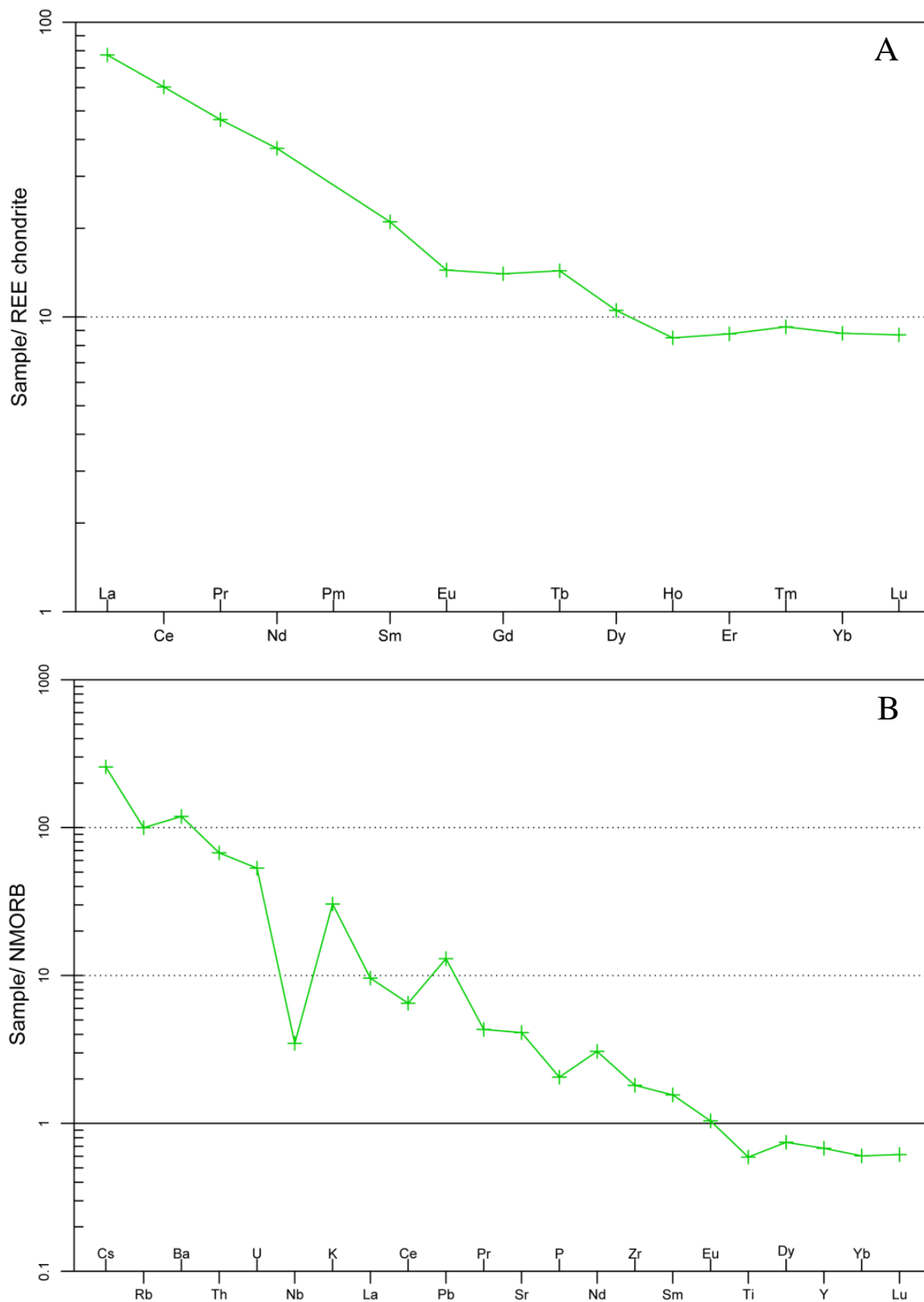


Figure 5. A. REE-diagram of andesite at Sammakovaara. Normalizing values for chondrite from Boynton (1984). **B.** Multi-element diagram, same rock as in A. Normalizing values for N-MORB from Sun & McDonough (1989).

Analytical results and interpretation of geochronological data

In situ U-Pb-Th SIMS analysis of zircon was performed at the Nordsim facility at the Museum of Natural History in November 2007. Detailed descriptions of the analytical procedures are given in Whitehouse et al. (1997, 1999). Pb/U ratios, elemental concentrations and Th/U ratios were calibrated relative to the Geostandards zircon 91 500 reference, which has an age of c. 1 065 Ma (Wiedenbeck et al. 1995, 2004). Common Pb corrected isotope values were calculated using modern common Pb composition (Stacey & Kramers 1975) and measured ^{204}Pb . Decay constants follow the recommendations of Steiger & Jäger (1977). Diagrams and age calculations of isotopic data were made using software Isoplot 4.15 (Ludwig 2012). The analytical results are shown in Table 1. Zircon in the sample is generally euhedral to subhedral, prismatic crystals or fragments of crystals. In cathodoluminescence (CL) images most grains show an internal oscillatory zonation, but CL-dark unzoned rims are occasionally present (Fig. 6).

The U content varies between 113 and 436 ppm. Th/U ratios are 0.50–0.74 ($n = 7$; Table 1). The analyses yield a concordia age of $1\,886 \pm 5$ Ma (2σ , MSWD = 8.0, Fig. 7). One of the analyses (7) is weakly discordant at the 2σ limit (0.1 %). Excluding this weakly discordant analysis (14c) the concordia age is calculated at $1\,887 \pm 6$ Ma (2σ , MSWD = 4.4) and the MSWD of concordance is lower. The data set is limited and the difference in concordia ages between the seven or six-point data set is negligible. The weighted average $^{207}\text{Pb}/^{206}\text{Pb}$ age is 1882 ± 6 Ma (2σ , $n=7$, MSWD = 0.80), independent if six or seven analyses are used and within error same as the concordia ages. The low MSWD indicates a low spread in $^{207}\text{Pb}/^{206}\text{Pb}$ ages and the $^{207}\text{Pb}/^{206}\text{Pb}$ weighted average age of $1\,882 \pm 6$ Ma is therefore chosen as the best estimate of the igneous crystallisation of the intermediate volcanic rock.

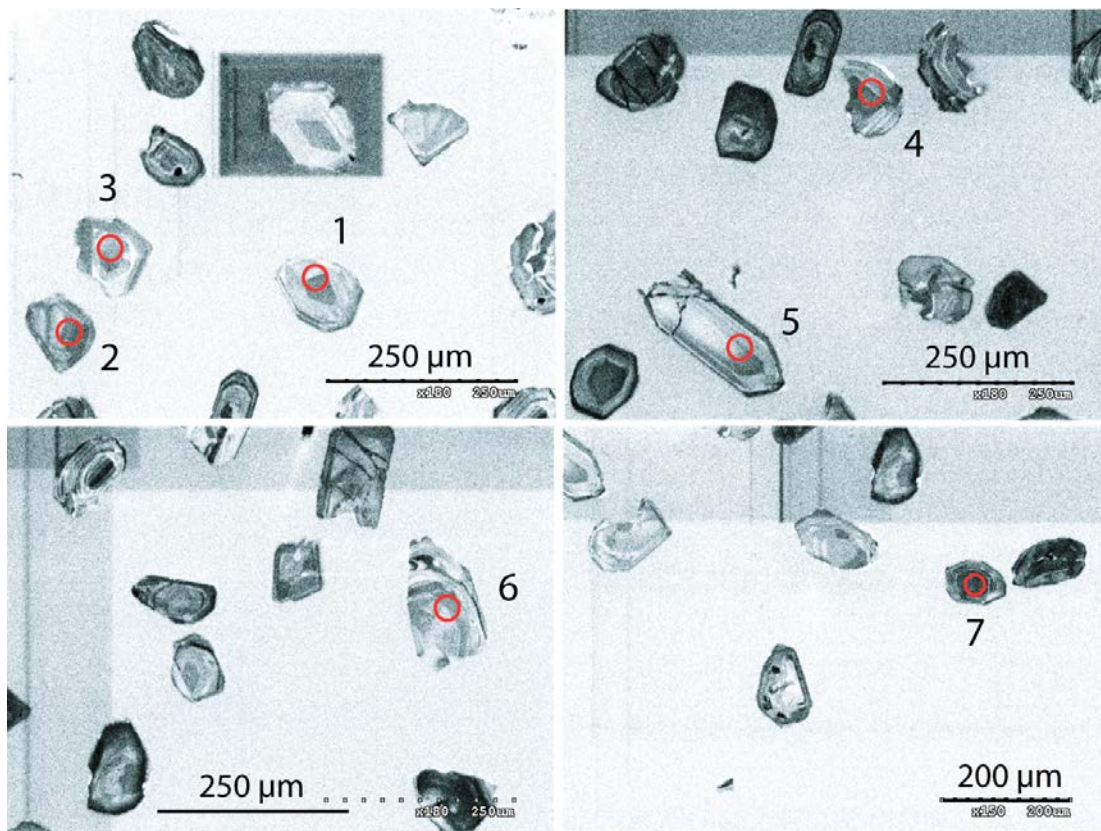


Figure 6. CL-images of zircon from the investigated intermediate volcanic rock. Red circles mark the approximate location of analyses spots. Numbers refer to analytical spots in Table 1.

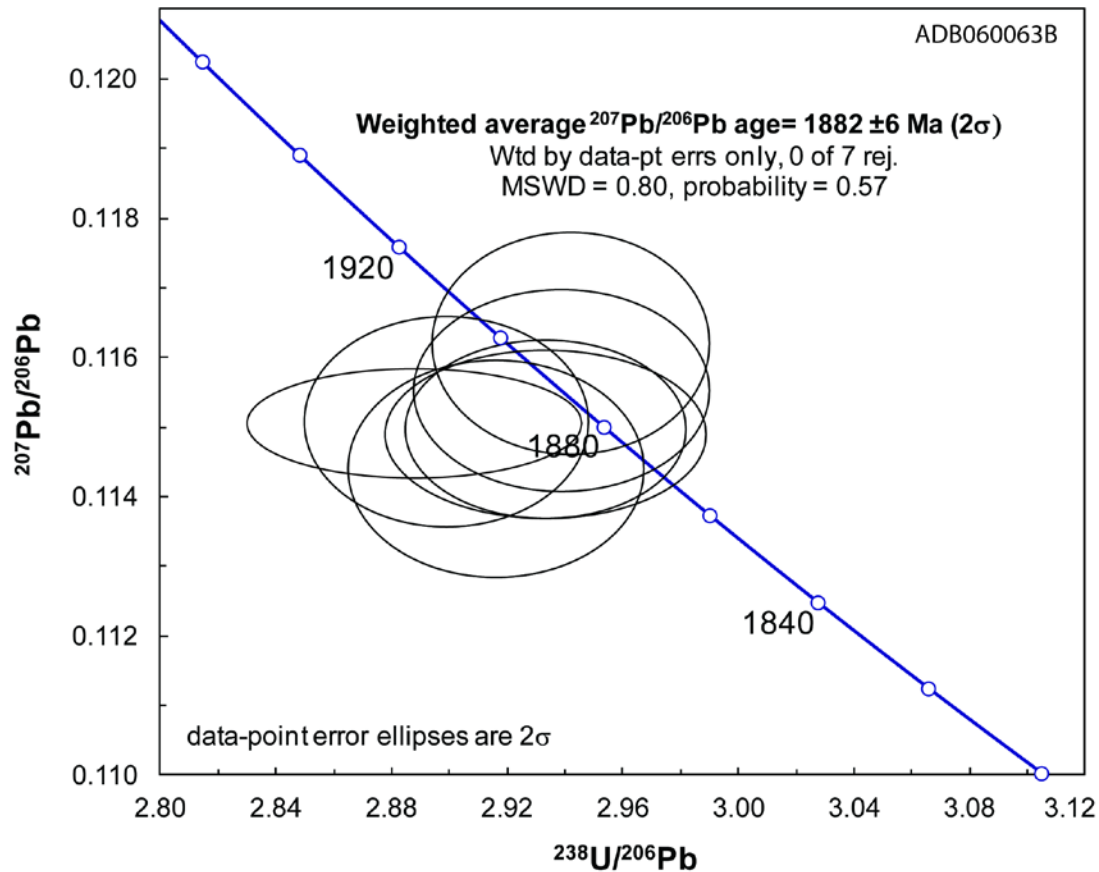


Figure 7. Tera-Wasserburg diagram showing U-Pb zircon data from an intermediate volcanic rock at Sammakkoavaara.

Table 1. SIMS U-Pb-Th zircon data.

Sample/ spot #	U ppm	Th ppm	Pb ppm	Th/U calc ^{*1}	^{207}Pb ^{235}U	$\pm\sigma$	^{208}Pb ^{232}Th	$\pm\sigma$	^{238}U ^{206}Pb	$\pm\sigma$	^{207}Pb ^{206}Pb	$\pm\sigma$	ρ *2	Disc. % conv. *3	^{207}Pb ^{206}Pb	$\pm\sigma$	^{206}Pb ^{238}U	$\pm\sigma$	$^{206}\text{Pb}/^{204}\text{Pb}$ measured	$f_{206}\%$ *4
n2857-1	243	176	110	0.74	5.401	0.88	0.0993	2.6	2.933	0.77	0.1149	0.43	0.87	0.8	1885	8	1891	13	253271	{0.01}
n2857-2	206	130	91	0.64	5.404	0.82	0.0980	3.1	2.933	0.68	0.1150	0.45	0.83	0.7	1886	7	1891	11	57032	0.03
n2857-3	148	73	63	0.50	5.420	0.88	0.0997	2.7	2.939	0.71	0.1155	0.52	0.81	0.0	1888	8	1888	12	45495	0.04
n2857-4	113	67	50	0.61	5.409	0.91	0.1007	2.6	2.916	0.72	0.1144	0.56	0.79	1.9	1886	8	1901	12	79866	{0.02}
n2857-5	116	82	52	0.72	5.446	0.87	0.0999	3.0	2.942	0.67	0.1162	0.56	0.77	-0.7	1892	8	1886	11	22452	0.08
n2857-6	128	62	56	0.51	5.473	0.87	0.1020	2.7	2.899	0.69	0.1151	0.54	0.79	1.8	1896	8	1910	11	53578	0.03
n2857-7	436	212	190	0.51	5.494	0.87	0.1031	2.8	2.888	0.82	0.1151	0.28	0.95	2.2	1900	7	1917	14	134346	0.01

Isotope values are common Pb corrected using modern common Pb composition (Stacey & Kramers 1975) and measured ^{204}Pb .

*1 Th/U ratios calculated from $^{206}\text{Pb}/^{206}\text{Pb}$ and $^{207}\text{Pb}/^{206}\text{Pb}$ ratios, assuming a single stage of closed U-Th-Pb evolution

*2 Error correlation in conventional concordia space. Do not use for Tera-Wasserburg plots.

*3 Age discordance in conventional concordia space. Positive numbers are reverse discordant.

*4 Figures in parentheses are given when no correction has been applied, and indicate a value calculated assuming present-day Stacey-Kramers common Pb.

Discussion and conclusion

The intermediate volcanic rock is situated east of the Aitik mine and according to earlier maps (e.g. Geological map of the Fennoscandian Shield, Koistonen et al. 2001), it is part of the Kiruna-Arvidsjaur complex (upper part/Liikavaaragroup). The igneous crystallisation age of $1\ 882 \pm 6$ Ma rather puts the rock in the older stages of volcanism associated with the magmatism between 1.86–1.89 Ga in the area and is now possibly better referred to as belonging to the lower part of the Kiruna-Arvidsjaur complex. It is also more or less coeval with the quartz monzodiorite just east of the Aitik mine dated at $1\ 887 \pm 8$ Ma (Wanhainen et al. 2006). The results were integrated in the mapping of the Nattavaara area (Claeson & Antal Lundin 2012). Summary of sample data is given in Table 2.

Table 2. Summary of sample data.

Rock type	Intermediate volcanic rock
Lithotectonic unit	Norrbottn lithotectonic unit of the Svecokarelian orogen
Lithological unit	
Sample number	ADB060063B
Lab_id	n2857
Coordinates	7445143/782397 (Sweref99TM)
Map sheet	27K Nattavaara NE (RT90)
Locality	Sammakkovaara
Project	Mellersta Norrbotten (1108701/80010)

References

- Boynton, W.V., 1984: Cosmochemistry of the Rare Earth Elements: Meteorite studies. In P. Henderson (ed.): *Rare earth element geochemistry*. Elsevier Science B.V. 63–114.
- Claeson, D. & Antal Lundin, I., 2012: Beskrivning till berggrundskartorna 27K Nattavaara NV, NO, SV & SO. *Sveriges geologiska undersökning K 383–386*, 22 pp.
- Koistonen, T., Stephens, M.B., Bogatchev, V., Nordgulen, Ø., Wennerström, M. & Korhonen, J., 2001: *Geological map of the Fennoscandian Shield, scale 1:2 000 000*. Geological Survey of Finland, Norway and Sweden and the North-West Department of Natural Resources of Russia.
- Ludwig, K.R., 2012: User's manual for Isoplot 3.75. A Geochronological Toolkit for Microsoft Excel. *Berkeley Geochronology Center Special Publication No. 5*, 75 pp.
- Stacey, J.S. & Kramers, J.D., 1975: Approximation of terrestrial lead isotope evolution by a two-stage model. *Earth and Planetary Science Letters* 26, 207–221.
- Steiger, R.H. & Jäger, E., 1977: Convention on the use of decay constants in geo- and cosmochronology. *Earth and Planetary Science Letters* 36, 359–362.
- Sun, S.S. & McDonough, W.F., 1989: Chemical and isotopic systematic of oceanic basalts: implications for mantle composition and processes. In A.D. Saunders & M.J. Norry (eds.): *Magmatism in ocean basins*. Geological Society of London, Special Publication 42, 313–345.
- Wanhainen, C. Billström, K. & Martinsson, O., 2006: Age, petrology and geochemistry of the porphyritic Aitik intrusion, and its relation to the disseminated Aitik Cu-Au-Ag deposit, northern Sweden. *GFF* 128, 273–286.
- Whitehouse, M.J., Claesson, S., Sunde, T. & Vestin, J., 1997: Ion-microprobe U–Pb zircon geochronology and correlation of Archaean gneisses from the Lewisian Complex of Gruinard Bay, north-west Scotland. *Geochimica et Cosmochimica Acta* 61, 4 429–4 438.
- Whitehouse, M.J., Kamber, B.S. & Moorbath, S., 1999: Age significance of U–Th–Pb zircon data from Early Archaean rocks of west Greenland: a reassessment based on combined ion-microprobe and imaging studies. *Chemical Geology (Isotope Geoscience Section)* 160, 201–224.
- Wiedenbeck, M., Allé, P., Corfu, F., Griffin, W.L., Meier, M., Oberli, F., Quadt, A.V., Roddick, J.C. & Spiegel, W., 1995: Three natural zircon standards for U-Th-Pb, Lu-Hf, trace element and REE analyses. *Geostandards Newsletter* 19, 1–23.
- Wiedenbeck, M., Hanchar, J.M., Peck, W.H., Sylvester, P., Valley, J., Whitehouse, M., Kronz, A., Morishita, Y., Nasdala, L., Fiebig, J., Franchi, I., Girard, J.P., Greenwood, R.C., Hinton, R., Kita, N., Mason, P.R.D., Norman, M., Ogasawara, M., Piccoli, P.M., Rhede, D., Satoh, H., Schulz-Dobrick, B., Skår, O., Spicuzza, M.J., Terada, K., Tindle, A., Togashi, S., Vennemann, T., Xie, Q. & Zheng, Y.F., 2004: Further Characterisation of the 91500 Zircon Crystal. *Geostandards and Geoanalytical Research* 28, 9–39.

U-Pb ZIRCON AGE OF QUARTZ AND FELDSPAR PORPHYRIC RHYOLITE FROM 2.5 KM NW OF KILTEKORRONEN, MAP SHEET 27K NATTAVAARA, NORRBOTTEN COUNTY

Authors: Dick Claeson, Ildikó Antal Lundin, Fredrik Hellström & Andrius Rimša

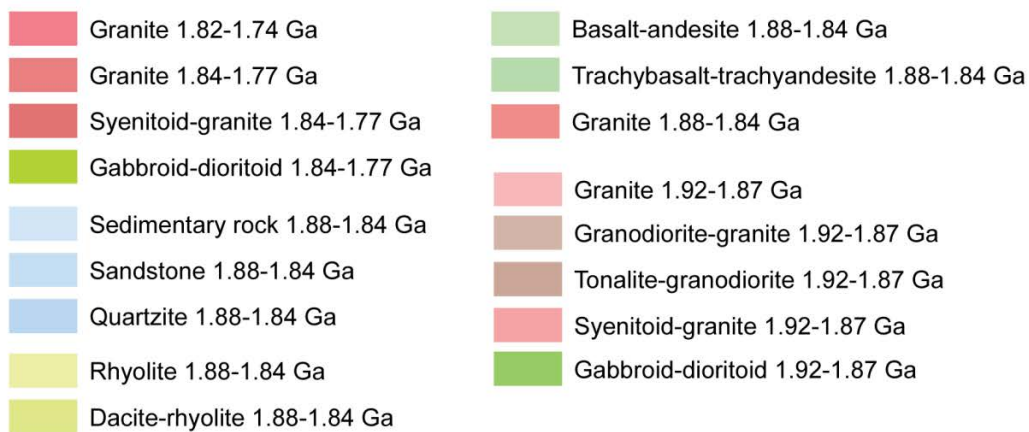
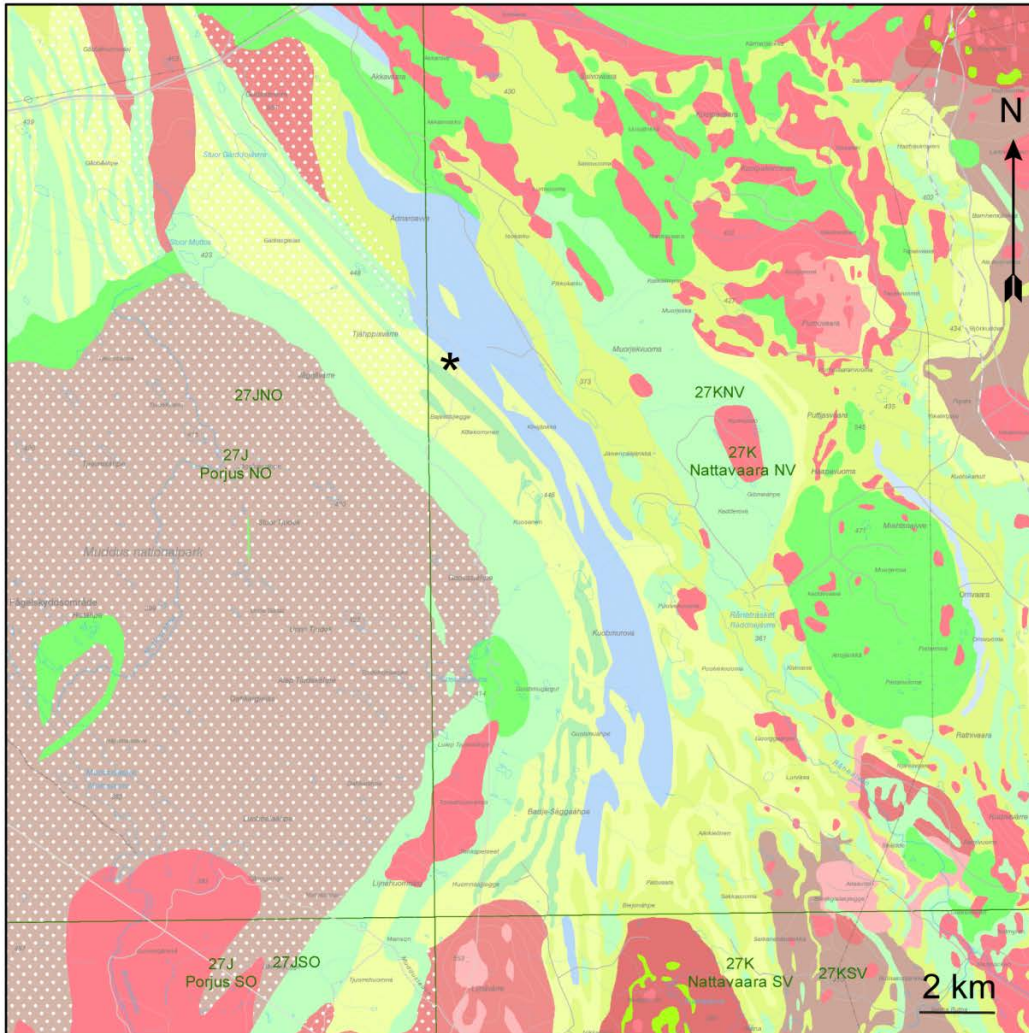


Figure 8. Bedrock map of the area, sampling location marked with black star.

Introduction

Norrbottnen, Sweden is a key area of Europe for future exploration and mining. To establish age relations for magmatic activity and metamorphic overprinting in this area, the sampled rock was selected (Fig. 1, 2, 8). The volcanogenic rocks in the western part of map area 27K Nattavaara NV are seen to continue north from interpretation of the geophysical data, possibly to Kiruna. Accordingly, it is a regional structure that should be age determined. The rhyolite at hand is extremely well-preserved and as such may also be used to infer that regional metamorphism and deformation should be of an older age than the rhyolite or that this section entirely escaped such an event.

The purpose of this study was to determine the age of a quartz and feldspar porphyric rhyolite that is overlaying quartzite to arkose rocks, which also display minor parts of more clay-rich metasedimentary rocks east of the rhyolite. Thereby also determine a maximum age of the sedimentary clastic rocks that occur stratigraphically below the rhyolite. Furthermore, age determinations of volcanic rocks in the region are scarce even though they host world-class ore deposits.

Sample description

The age determined sample is a well-preserved rhyolite ($\text{SiO}_2 = 76.4\%$), with quartz and euhedral potassium feldspar phenocrysts in a very fine to fine-grained, grey to reddish grey matrix (Fig. 9). The quartz and potassium feldspar phenocrysts are 1–3 mm, 5–10 % of each in total 10–20 %. A few plagioclase phenocrysts are present as well. The Zr content of the rock is 496 ppm. The well-preserved nature is clearly seen in the panoramic microscopy image of a thin-section of the rock (Fig. 10). At several outcrops the rhyolite is an ignimbrite showing eutaxitic texture, which is a layered or banded texture that often originates by the compaction and flattening of glass shards and pumice fragments around undeformed crystals and phenocrysts (Fig. 10).

The rhyolite unit shows low magnetic susceptibility measured on outcrops, usually less than 30×10^{-5} SI and appears as low magnetic anomalies on the magnetic anomaly map (Fig. 1). At an outcrop 1.2 km southeast of Kiltokorronen the rhyolite shows gamma ray radiation as $K = 4.3\text{--}5.3\%$, $U = 3.5\text{--}4.6$ ppm, and $Th = 15.7\text{--}16.3$ ppm. Petrophysical measurements of two rhyolite samples from that outcrop show densities of 2 615 and 2 634 kg/m^3 respectively, magnetic susceptibility $16\text{--}19 \times 10^{-5}$ SI, and remanent magnetization intensity of 20–50 mA/m. The low-density values obtained from the petrophysical measurements correlate well with the gravity low in the western part of the map area (Fig. 2).

The porphyric rhyolite 2.5 km NW of Kiltokorronen shows a LREE-enriched and flat HREE pattern, with a pronounced negative Eu anomaly (Fig. 11). The LREE enrichment is due to fractional crystallisation, the flat, unfractionated HREE pattern shows that no garnet was left in the residue at the location of magma genesis, and the Eu anomaly is indicative of extensive plagioclase fractionation. The negative anomalies shown in the multi-element diagram of Sr is due to plagioclase fractionation, the P anomaly of apatite fractionation, and the Ti anomaly of Fe-Ti oxide fractionation (Fig. 11). The strong negative Nb anomaly suggests a subduction related petrogenesis but the minor negative Pb anomaly shows that it is not unambiguous and may infer e.g. lesser input of sediment in the source region of the subduction zone (Fig. 11).

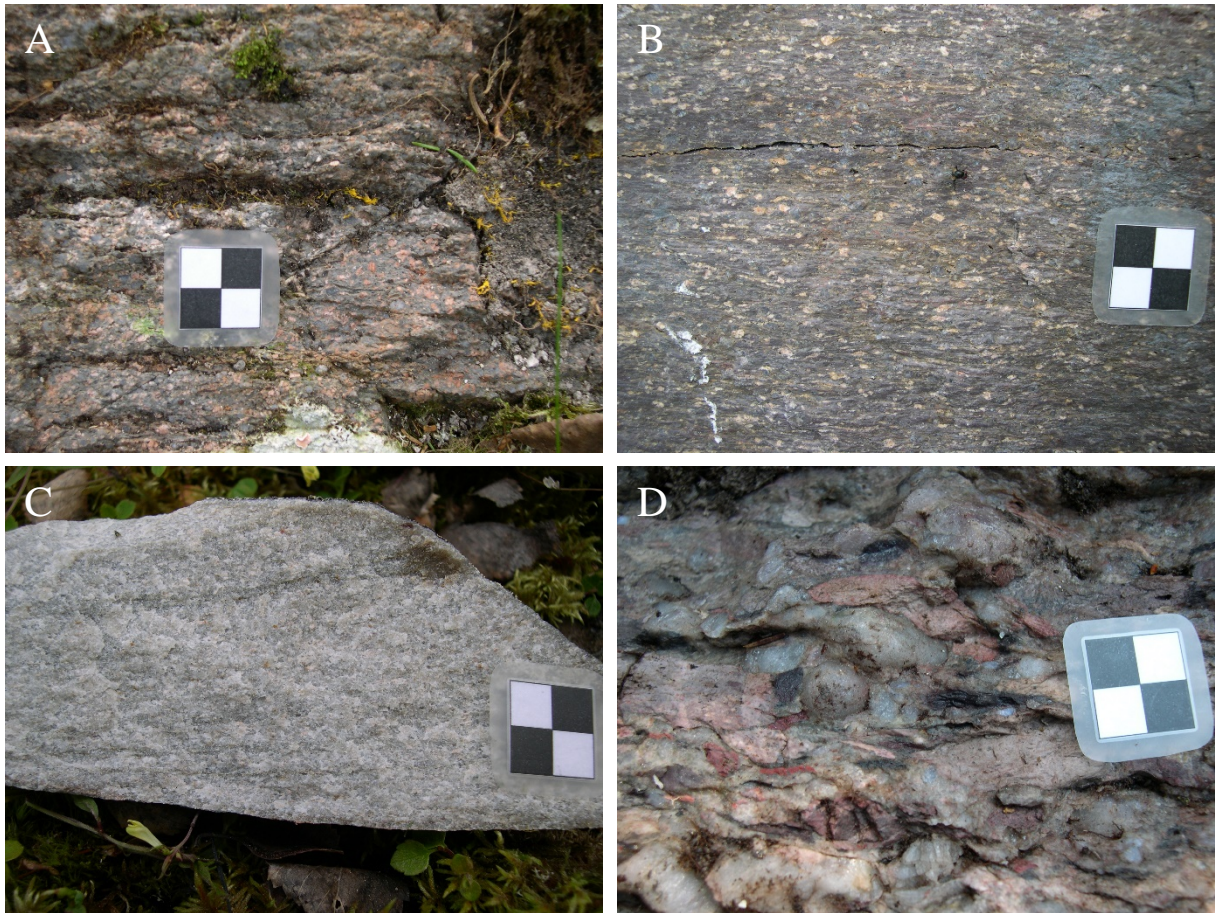


Figure 9. **A.** Rhyolite with quartz and euhedral feldspar phenocrysts at sample location for age determination (7440594/735518). **B.** Same rhyolite unit but further to SE (7437790/737924). **C.** Close-up of quartzitic rock (7437837/737983). **D.** Conglomerate at the very top of the sedimentary unit, with spherical clasts of quartzite and assortment of clasts of volcanic rocks with different origins and compositions (7438515/737424, cm-scale). Photos: Dick Claeson.

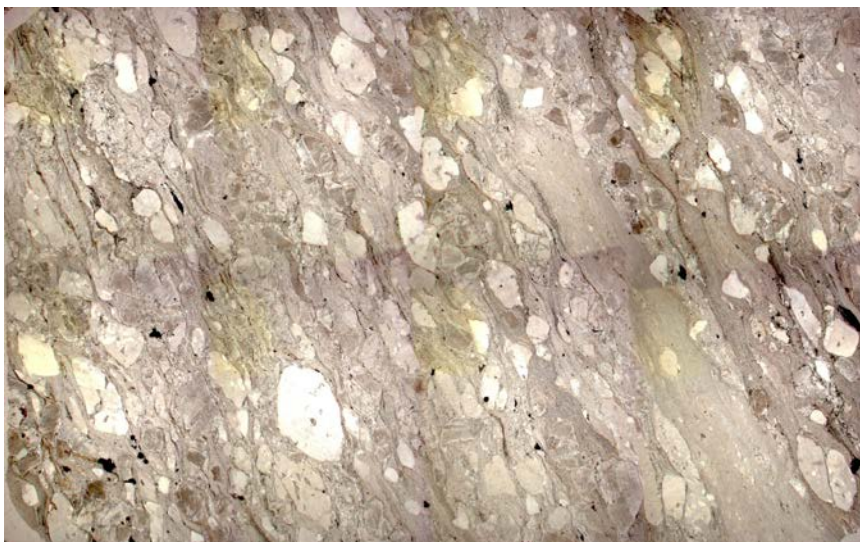


Figure 10. Full thin-section panorama made from eight images of rhyolite with quartz and euhedral feldspar phenocrysts. Note the eutaxitic texture. Width of image c. 40 mm. Some shading is due to orientation in the microscope. Micrograph: Dick Claeson.

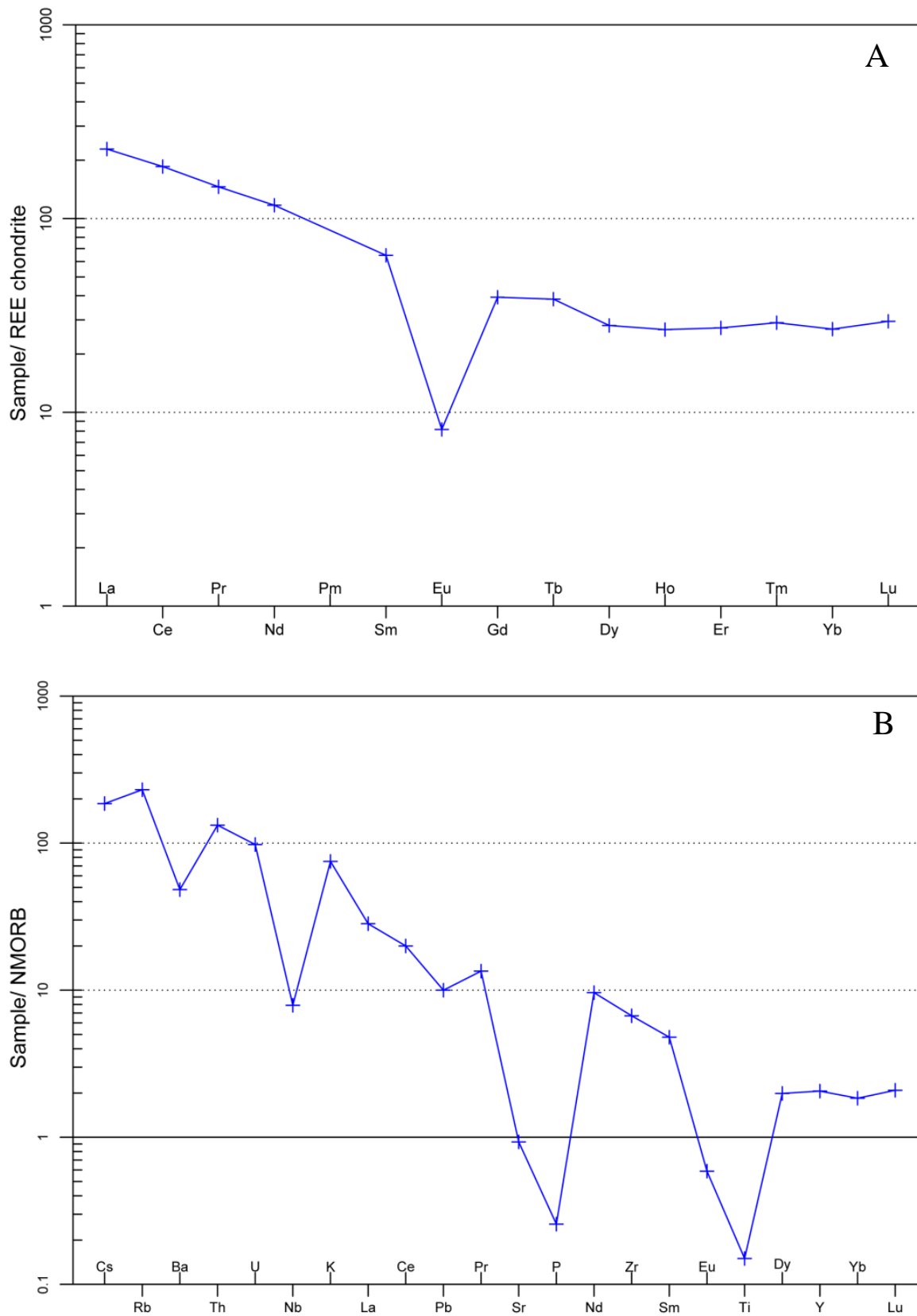


Figure 11. A. REE-diagram of rhyolite. Normalizing values for chondrite from Boynton (1984). **B.** Multi-element diagram, rock as in A. Normalizing values for N-MORB from Sun & McDonough (1989).

Analytical results and interpretation of geochronological data

In situ U-Pb-Th SIMS analysis of zircon was performed at the Nordsim facility at the Museum of Natural History in November 2007. Detailed descriptions of the analytical procedures are given in Whitehouse et al. (1997, 1999). Pb/U ratios, elemental concentrations and Th/U ratios were calibrated relative to the Geostandards zircon 91 500 reference, which has an age of c. 1 065 Ma (Wiedenbeck et al. 1995, 2004). Common Pb corrected isotope values were calculated using modern common Pb composition (Stacey & Kramers 1975) and measured ^{204}Pb . Decay constants follow the recommendations of Steiger & Jäger (1977). Diagrams and age calculations of isotopic data were made using software Isoplot 4.15 (Ludwig 2012). The analytical results are shown in Table 3. The sample contains fragments or whole crystals of euhedral zircon. In CL-images some grains show partially a weak internal oscillatory zonation, while other grains lack an obvious zonation altogether (Fig. 12).

The U content of the analysed zircon varies between 159 and 258 ppm and Th/U ratios are between 0.22 and 0.43 ($n = 7$; Table 3). Together, seven concordant analyses yield a concordant age of $1\,868 \pm 6$ Ma (2σ , MSWD = 0.22; Fig. 13), near identical to the weighted average $^{207}\text{Pb}/^{206}\text{Pb}$ age of $1\,869 \pm 8$ Ma (2σ , MSWD = 0.36). The concordia age of $1\,868 \pm 6$ Ma is interpreted to date igneous crystallisation of the rhyolite.

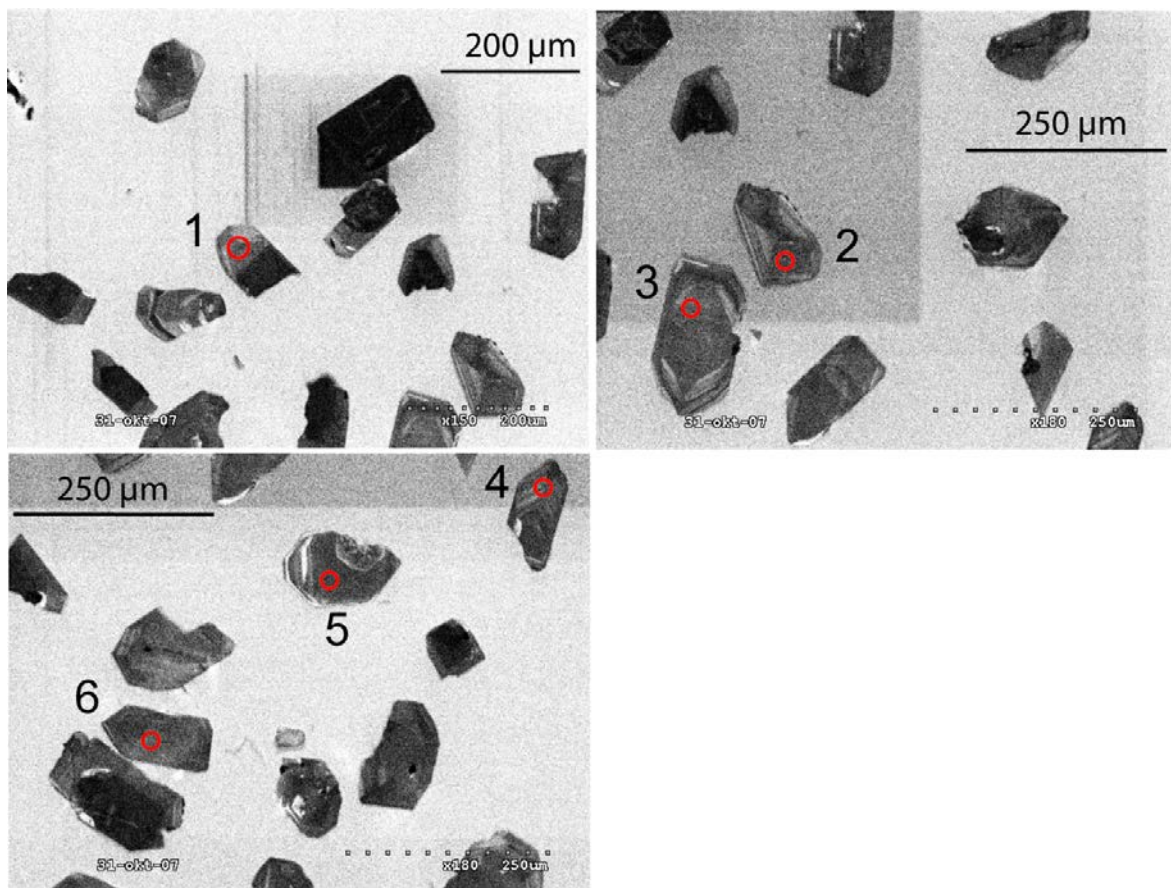


Figure 12. CL-images of zircon from the rhyolite. Red circles mark the approximate location of analyses spots. Numbers refer to analytical spot number in Table 3.

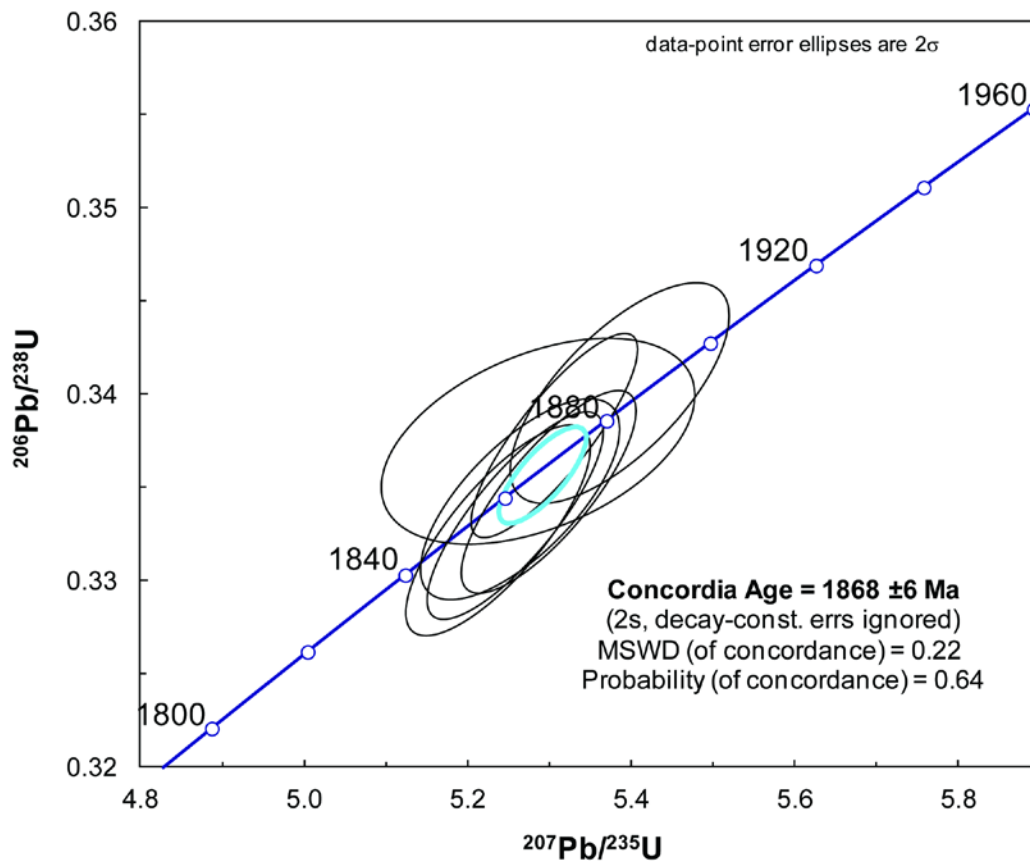


Figure 13. Tera-Wasserburg diagram showing U-Pb zircon data of rhyolite from 2.5 km NW of Kiltekorronen.

Table 3. SIMS U-Pb-Th zircon data of rhyolite from 2.5 km NW of Kiltokorronen.

Sample/ spot #	U ppm	Th ppm	Pb ppm	Th/U calc* ¹	²⁰⁷ Pb ²³⁵ U	±σ	²⁰⁸ Pb ²³² Th	±σ	²³⁸ U ²⁰⁶ Pb	±s	²⁰⁷ Pb ²⁰⁶ Pb	±s	ρ	Disc. % conv. * ³	²⁰⁷ Pb ²⁰⁶ Pb	±s	²⁰⁶ Pb ²³⁸ U	±s	²⁰⁶ Pb/ ²⁰⁴ Pb measured	f ₂₀₆ % * ⁴
n2849-1	159	44	63	0.27	5.237	0.89	0.0936	7.6	3.006	0.69	0.1142	0.55	0.78	-1.0	1867	10	1851	11	35847	0.05
n2849-2	258	110	107	0.41	5.286	1.49	0.0930	8.2	2.963	0.66	0.1136	1.33	0.45	1.0	1858	24	1875	11	5308	0.35
n2849-3	194	52	77	0.26	5.258	0.84	0.0944	7.6	2.999	0.68	0.1143	0.49	0.81	-0.9	1870	9	1855	11	345933	{0.01}
n2849-4	191	42	75	0.22	5.264	0.95	0.0956	7.6	2.991	0.66	0.1142	0.68	0.70	-0.4	1867	12	1860	11	83045	0.02
n2849-5	251	111	105	0.43	5.306	0.78	0.0945	7.5	2.960	0.66	0.1139	0.42	0.84	0.8	1863	8	1876	11	108660	0.02
n2849-6	228	56	91	0.25	5.299	0.83	0.0973	7.6	2.987	0.66	0.1148	0.50	0.80	-0.9	1877	9	1862	11	50066	0.04
n2849-7	195	42	78	0.21	5.387	1.01	0.0973	7.6	2.940	0.71	0.1149	0.72	0.70	0.6	1878	13	1887	12	39590	0.05

Isotope values are common Pb corrected using modern common Pb composition (Stacey & Kramers 1975) and measured ²⁰⁴Pb.

*1 Th/U ratios calculated from ²⁰⁸Pb/²⁰⁶Pb and ²⁰⁷Pb/²⁰⁶Pb ratios, assuming a single stage of closed U-Th-Pb evolution

*2 Error correlation in conventional concordia space. Do not use for Tera-Wasserburg plots.

*3 Age discordance in conventional concordia space. Positive numbers are reverse discordant.

*4 Figures in parentheses are given when no correction has been applied, and indicate a value calculated assuming present-day Stacey-Kramers common Pb.

Discussion and conclusion

The concordia age of $1\,868 \pm 6$ Ma is interpreted to date igneous crystallisation and deposition of the rhyolite upon the quartzite and arkose rocks to the east. This shows that the rhyolite is part of the later stages of volcanism associated with the magmatism between 1.86–1.89 Ga in the study area. Earlier maps (e.g. Geological map of the Fennoscandian Shield, Koistonen et al. 2001) show the rhyolite as belonging to the Kiruna-Arvidsjaur complex and within its lower, older part. The rhyolite is now better referred to as belonging to the upper part of the Kiruna-Arvidsjaur complex.

Further east of the mostly quartzitic unit within the mapping area 27K Nattavaara (but not in contact with), an intermediate volcanic rock indicates an igneous crystallisation age of $1\,882 \pm 6$ Ma (this issue). This suggests the age bracket for deposition of the sedimentary clastic unit to the east of the rhyolite at 1.87–1.88 Ga. The extremely well-preserved rhyolite demonstrate that regional metamorphism and deformation are older than $1\,868 \pm 6$ Ma or less likely that this volcanic sequence entirely escaped such an event. The results were integrated in the mapping of the Nattavaara area (Claeson & Antal Lundin 2012). Summary of sample data is given in Table 4.

Table 4. Summary of sample data.

Rock type	Rhyolite
Lithotectonic unit	Norrbotten lithotectonic unit of the Svecokarelian orogen
Lithological unit	
Sample number	DCL060061A B
Lab_id	n2849
Coordinates	7440594/735518 (Sweref99TM)
Map sheet	27K Nattavaara NV (RT90)
Locality	2.5 km NW of Kiltokorronen
Project	Mellersta Norrbotten (80010)

References

- Boynton, W.V., 1984: Cosmochemistry of the Rare Earth Elements: Meteorite studies. *In* P. Henderson (ed.): *Rare earth element geochemistry*. Elsevier Science B.V. 63–114.
- Claeson, D. & Antal Lundin, I., 2012: Beskrivning till berggrundskartorna 27K Nattavaara NV, NO, SV & SO. *Sveriges geologiska undersökning K 383–386*, 22 pp.
- Koistonen, T., Stephens, M.B., Bogatchev, V., Nordgulen, Ø., Wennerström, M. & Korhonen, J., 2001: *Geological map of the Fennoscandian Shield, scale 1:2 000 000*. Geological Survey of Finland, Norway and Sweden and the North-West Department of Natural Resources of Russia.
- Ludwig, K.R., 2012: User's manual for Isoplot 3.75. A Geochronological Toolkit for Microsoft Excel. *Berkeley Geochronology Center Special Publication No. 5*, 75 pp.
- Stacey, J.S. & Kramers, J.D., 1975: Approximation of terrestrial lead isotope evolution by a two-stage model. *Earth and Planetary Science Letters* 26, 207–221.
- Steiger, R.H. & Jäger, E., 1977: Convention on the use of decay constants in geo- and cosmochronology. *Earth and Planetary Science Letters* 36, 359–362.
- Sun, S.S. & McDonough, W.F., 1989: Chemical and isotopic systematic of oceanic basalts: implications for mantle composition and processes. *In* A.D. Saunders & M.J. Norry (eds.): *Magmatism in ocean basins*. Geological Society of London, Special Publication 42, 313–345.
- Whitehouse, M.J., Claesson, S., Sunde, T. & Vestin, J., 1997: Ion-microprobe U–Pb zircon geochronology and correlation of Archaean gneisses from the Lewisian Complex of Gruinard Bay, north-west Scotland. *Geochimica et Cosmochimica Acta* 61, 4 429–4 438.
- Whitehouse, M.J., Kamber, B.S. & Moorbath, S., 1999: Age significance of U–Th–Pb zircon data from Early Archaean rocks of west Greenland: a reassessment based on combined ion-microprobe and imaging studies. *Chemical Geology (Isotope Geoscience Section)* 160, 201–224.
- Wiedenbeck, M., Allé, P., Corfu, F., Griffin, W.L., Meier, M., Oberli, F., Quadt, A.V., Roddick, J.C. & Spiegel, W., 1995: Three natural zircon standards for U–Th–Pb, Lu–Hf, trace element and REE analyses. *Geostandards Newsletter* 19, 1–23.
- Wiedenbeck, M., Hanchar, J.M., Peck, W.H., Sylvester, P., Valley, J., Whitehouse, M., Kronz, A., Morishita, Y., Nasdala, L., Fiebig, J., Franchi, I., Girard, J.P., Greenwood, R.C., Hinton, R., Kita, N., Mason, P.R.D., Norman, M., Ogasawara, M., Piccoli, P.M., Rhede, D., Satoh, H., Schulz-Dobrick, B., Skår, O., Spicuzza, M.J., Terada, K., Tindle, A., Togashi, S., Vennemann, T., Xie, Q. & Zheng, Y.F., 2004: Further Characterisation of the 91500 Zircon Crystal. *Geostandards and Geoanalytical Research* 28, 9–39.

U-Pb ZIRCON AGE OF SUBVOLCANIC GRANITE TO RHYOLITE PORPHYRY AT LINAVARE, MAP SHEET 27K NATTAVAARA, NORRBOTTEN COUNTY

Authors: Dick Claeson, Ildikó Antal Lundin, Jenny Andersson & Anders Scherstén¹

¹Department of geology, Lund University, Sölvegatan 12, SE-223 62 Lund, Sweden

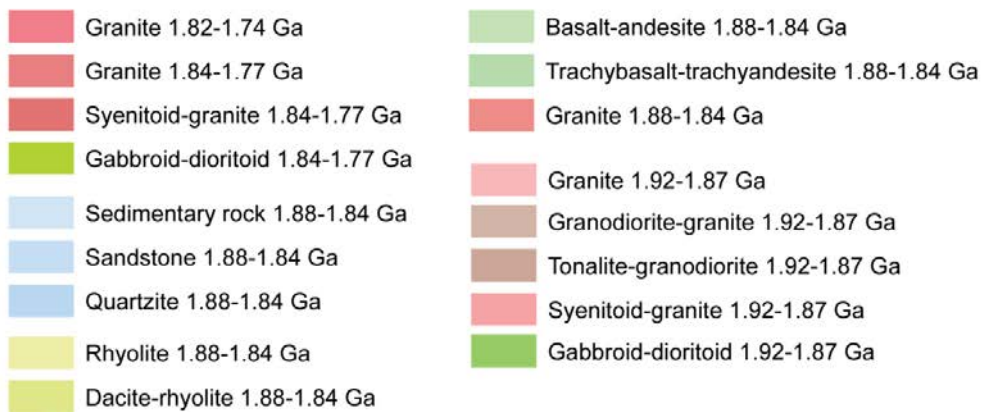
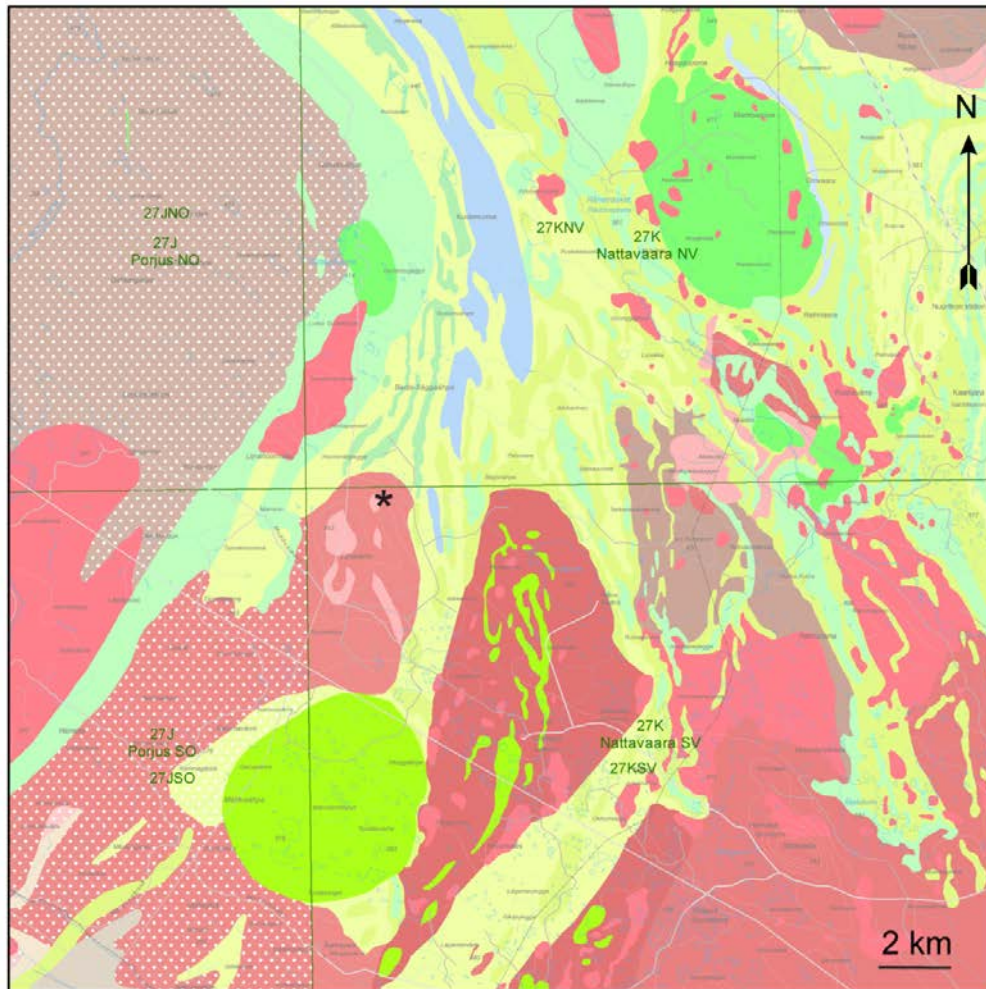


Figure 14. Bedrock map of the area, sampling location marked with black star.

Introduction

Norrbotnen, Sweden is a key area of Europe for future exploration and mining. To establish age relations for magmatic activity and metamorphic overprinting in this area, the sampled rock was selected (Fig. 1, 2, 14). The magmatic age of the subvolcanic granite to rhyolite porphyry is the main aim of the study. Within this rock there are mega-xenoliths of strongly deformed, recrystallised and low-radiation granite that was age determined to $1\,876 \pm 8$ Ma at Linavare (this issue). The regional metamorphic event, which the latter rock register but shows no sign of secondary zircon overgrowths, may be deduced from the age of the host subvolcanic granite to rhyolite porphyry giving a lower age of the metamorphism.

Sample description

Subvolcanic granite to rhyolite porphyry, massive, very fine-grained to fine-grained groundmass was sampled for age determination (Fig. 15). Phenocrysts of feldspar, mostly K-feldspar, and quartz, 2–15 mm (10–50 %), a few feldspar phenocrysts are 20 mm and some quartz are 5 mm large. The rock consists of potassium feldspar, plagioclase, undulose quartz, biotite that is altered to chlorite (degree of alteration 30–50 %), opaque minerals, and titanite (Fig. 15). The Zr content of the rock is 459 ppm. Outcrop measurement of magnetic susceptibility yielded $897\text{--}1\,690 \times 10^{-5}$ SI. Ground measurements of gamma ray radiation show K = 3.9–4 %, U = 3.2–4.5 ppm, and Th = 26.9–27.5 ppm. Petrophysical measurements of a sample show density at $2\,609 \text{ kg/m}^3$, magnetic susceptibility $2\,301 \times 10^{-5}$ SI, and remanent magnetization intensity of 420 mA/m.

The granite to rhyolite porphyry, subvolcanic intrusion at Linavare shows a LREE-enriched and flat HREE pattern, with a pronounced negative Eu anomaly (Fig. 16). The LREE enrichment is due to fractional crystallisation, the flat, unfractionated HREE pattern shows that no garnet was left in the residue at the location of magma genesis, and the Eu anomaly is indicative of extensive plagioclase fractionation. The negative anomalies shown in the multi-element diagram of Sr is due to plagioclase fractionation, the P anomaly of apatite fractionation, and the Ti anomaly of Fe-Ti oxide fractionation (Fig. 16). The strong negative Nb anomaly and minor positive Pb anomaly suggest a subduction related petrogenesis (Fig. 16).



Figure 15. **A.** Outcrop of the sampled subvolcanic granite to rhyolite porphyry. **B.** Close-up of the outcrop in A. **C.** The subvolcanic granite to rhyolite porphyry sample used for age determination (cm-scale). **D.** Micrograph of subvolcanic granite to rhyolite porphyry. Photos: Dick Claeson.

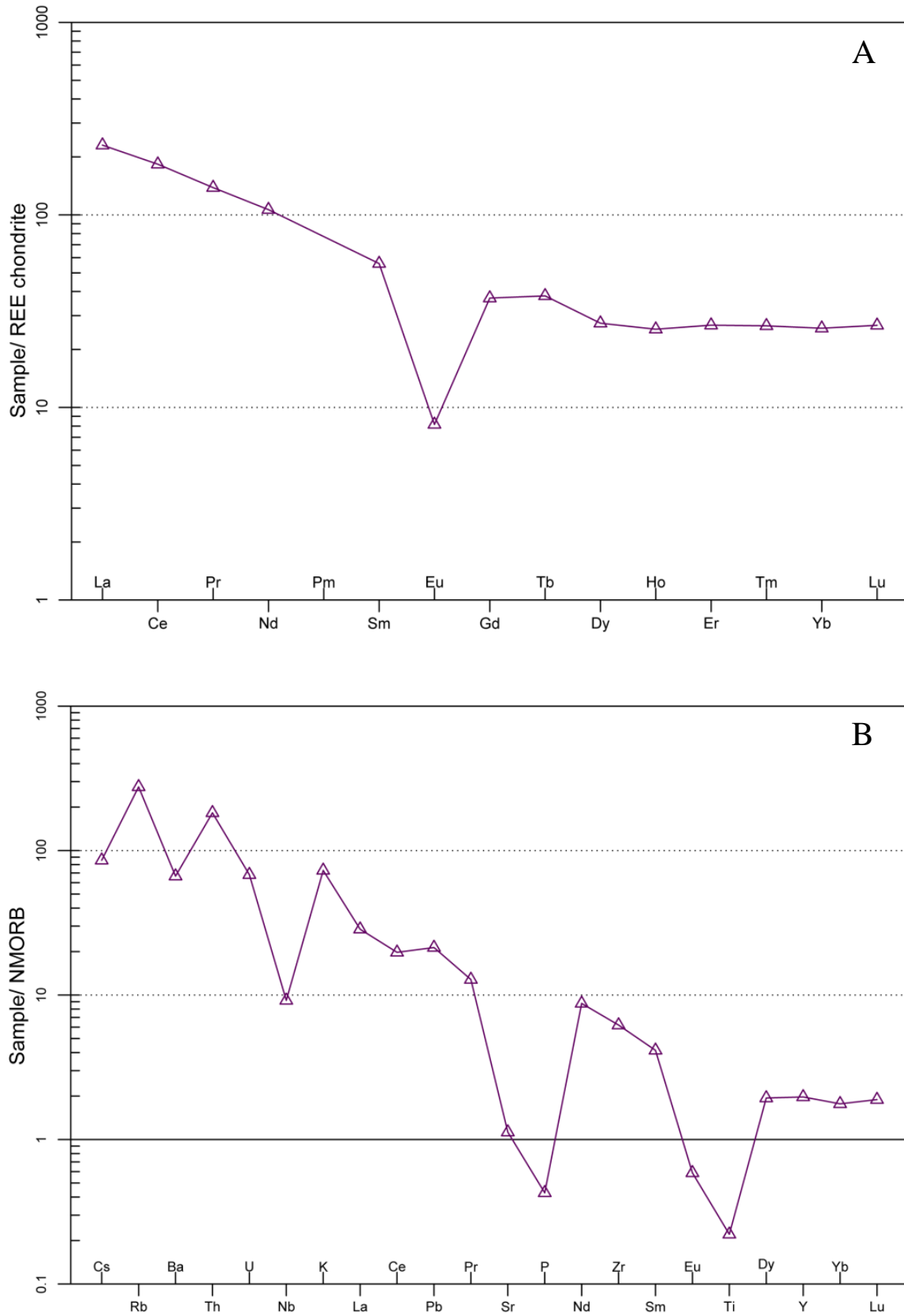


Figure 16. A. REE-diagram of subvolcanic granite to rhyolite porphyry. Normalizing values for chondrite from Boynton (1984). **B.** Multi-element diagram, rock as in A. Normalizing values for N-MORB from Sun & McDonough (1989).

Analytical results and interpretation of geochronological data

U-Pb zircon analyses

Zircon was extracted from a c. 0.5 kg large rock sample and U-Pb-Th analyses were made using a Laser-Ablation Sector Field Inductively Coupled Plasma Mass Spectrometer (LA-SF-ICPMS) at the Geological Survey of Denmark and Greenland (GEUS) in Copenhagen. All analytical procedures are described in the appendix of Andersson (2012).

The sample was rich in zircon (Fig. 17). The zircon are typically euhedral and short prismatic crystals with sharp terminations that show no signs of secondary alteration. The grains are typically between 50–200 μm in size. They are overall colourless, translucent and clear crystals of high analytical quality with few cracks and inclusions. Complex core-rim growth relations have not been observed.

In Cathodoluminescence (CL) images, the zircon typically shows CL-dark to CL-grey oscillatory zonation. The zonation varies from thinly laminated to wide broad banded. Minor fields of CL-bright unzoned sectors are in places seen to disrupt the oscillatory zonation (Fig. 18). The oscillatory zonation typically continues all the way to the crystal margin.

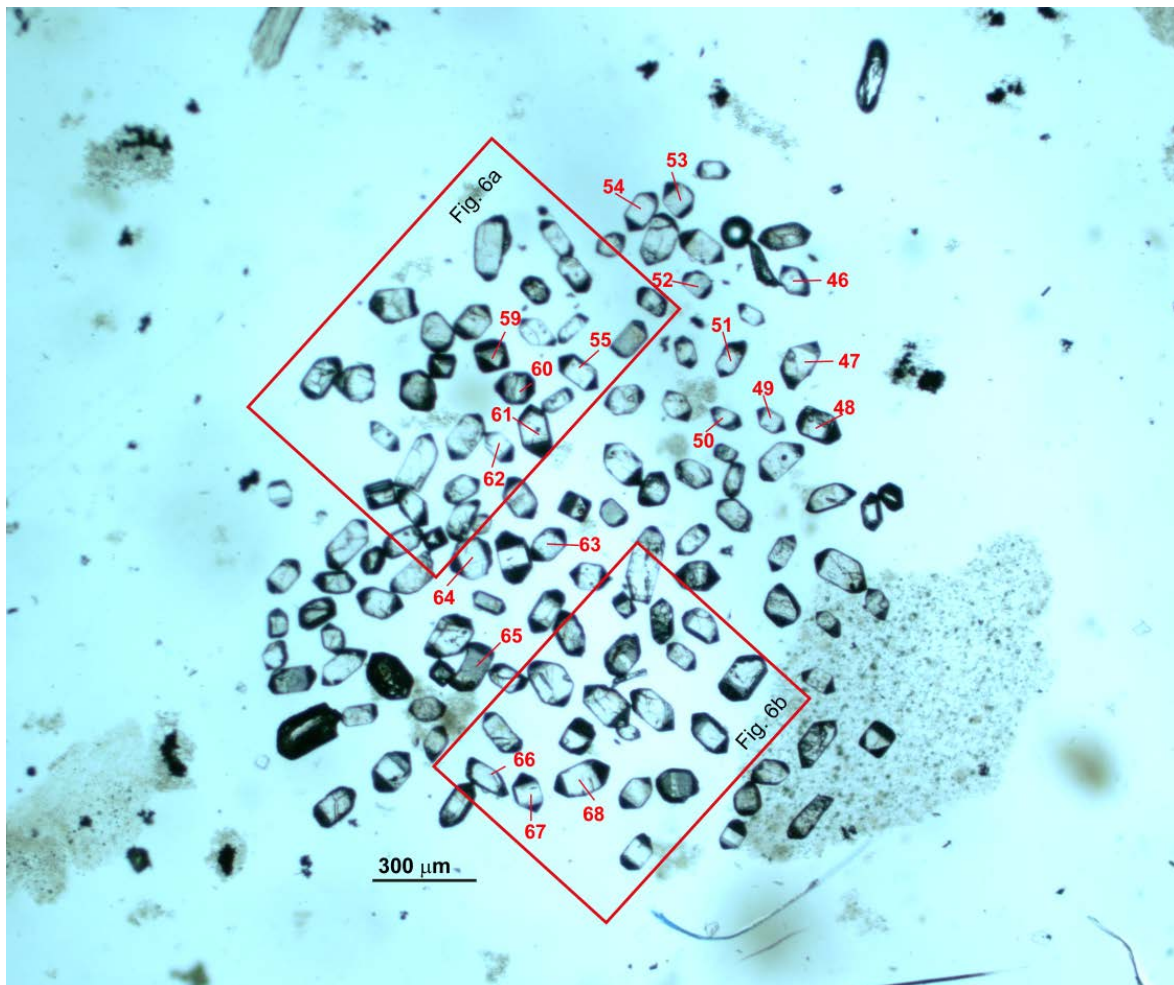


Figure 17. Optical microscope photo (plane polarized light) of representative zircon from sample DCL060126 in a polished section of the epoxy mount used for LA-SF-ICP MS analyses. Numbers refer to analytical ID in Table 5. Location of the CL-images in Figure 18 is indicated with red squares.

Results

Twenty analytical spots were placed in 20 different zircon crystals. The analysed crystals are shown in Figure 17. CL-images of representative grains analysed are shown in Figure 18. The analytical data is given in Table 5. The analysed zircon have U-contents between 304–112 ppm, and Th/U ratios between 0.45–0.73; values common for igneous zircon. The 20 analyses cluster on, or close to the Concordia, but do not conform to define a common concordia age. The spread of the data point error ellipses follows a more or less horizontal trend in the Tera-Wasserburg plot (Fig. 19) and do not indicate any significant ancient disturbance of the U-Pb system. The horizontal spread reflects either recent Pb-loss or is caused by over correction (calibration) of analytical data. Together the 20 analyses define a weighted average $^{206}\text{Pb}/^{207}\text{Pb}$ age of $1\,870 \pm 6$ Ma (MSWD = 0.36, 95 % conf., Fig. 19, 20). This age dates igneous crystallization of the granitic porphyry.

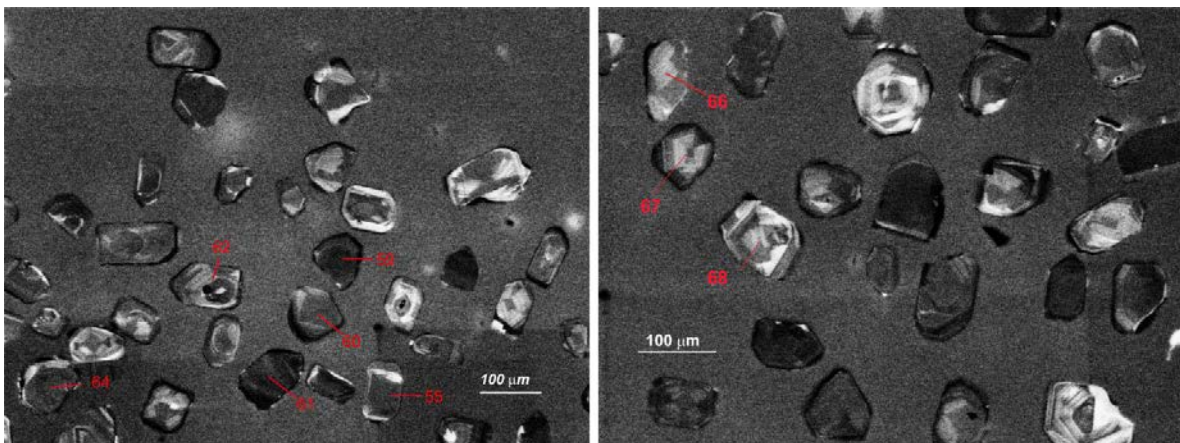


Figure 18. CL-images of detail of analysed zircon mount from sample DCL060126. Numbers refer to ID of spot analysed with LA-SF-ICP MS, cf. Table 5. The location of the CL-image area outlined in Figure 17.

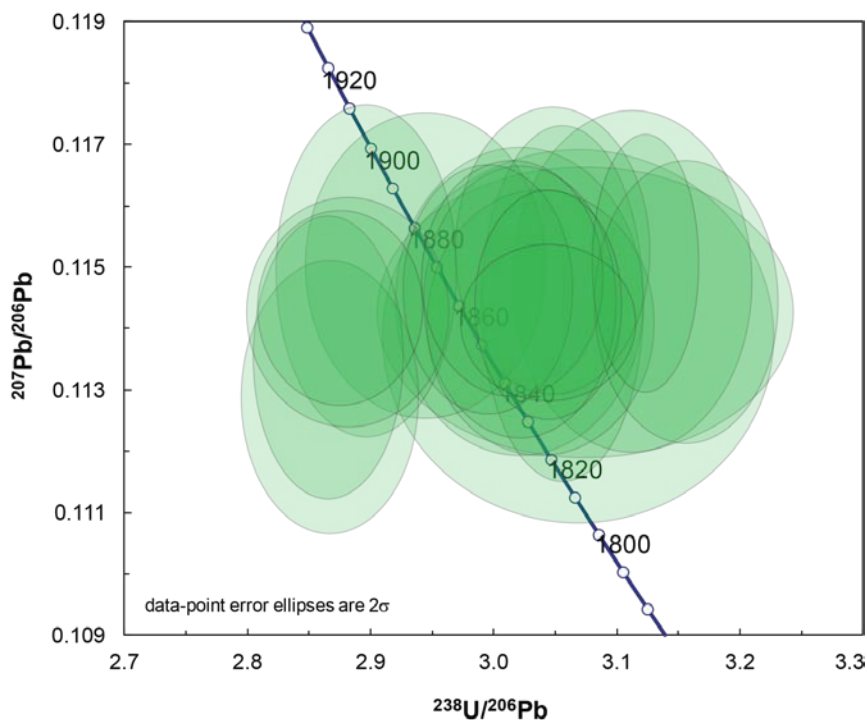


Figure 19. Tera-Wasserburg diagram showing U-Pb zircon data from subvolcanic granite to rhyolite porphyry at Linavare.

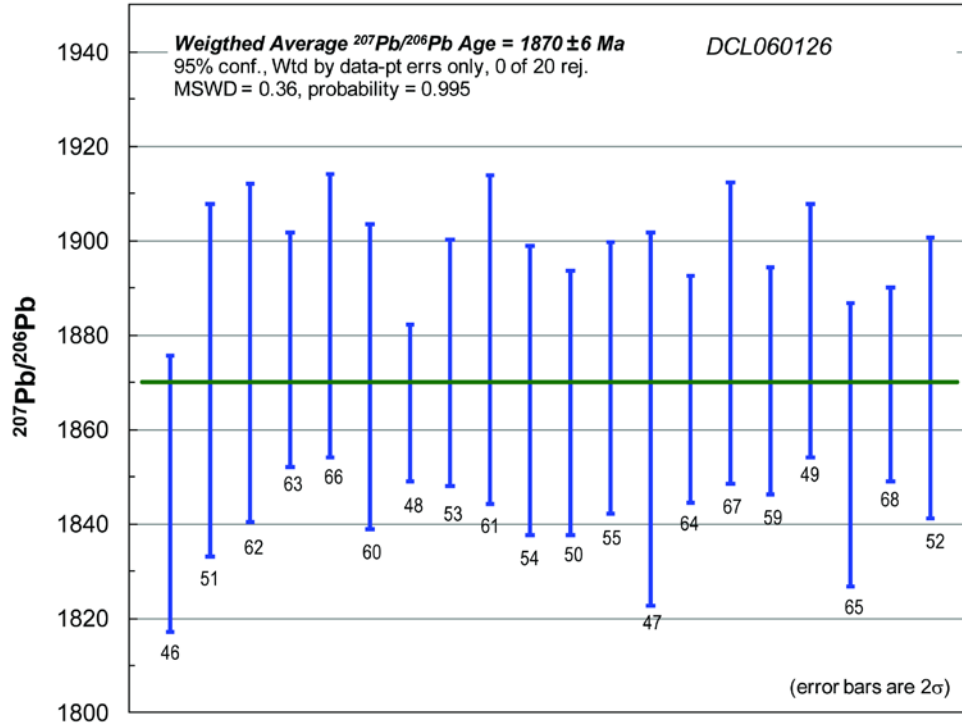


Figure 20. Plot of $^{207}\text{Pb}/^{206}\text{Pb}$ ages in Ma for the twenty analyses obtained from zircon in sample DCL060126. Weighted average $^{207}\text{Pb}/^{206}\text{Pb}$ age is shown as green horizontal line. Numbers refer to ID of spot analysed with LA-SF-ICP MS, cf. Table 5.

Table 5. LA-SF-ICPMS U-Th-Pb zircon data from sample DCL060126

Spot #	CL image class ^a	[U] ppm	Th/U calc.	^{206}Pb		^{207}Pb		Conc. %	^{206}Pb		^{207}Pb		
				^{204}Pb meas.	^{238}U	$\pm 2\sigma$ %	^{206}Pb		$\pm 2\sigma$ %	Age (Ma)	$\pm 2\sigma$	Age (Ma)	$\pm 2\sigma$
46	CLG osc zon	143	0.50	775	0.349	2.06	0.113	1.61	102	1929	34	1846	29
47	CLG unzoned	192	0.55	14600	0.327	1.77	0.114	2.07	99	1825	28	1871	37
48	CLG osc zon	112	0.51	9171	0.321	2.57	0.115	1.99	98	1797	40	1876	36
49	CLG bb zon	147	0.53	26495	0.332	1.99	0.115	1.38	99	1847	32	1877	25
50	CLG osc zon	167	0.55	12313	0.328	2.11	0.115	1.67	99	1830	34	1884	30
51	CLG bb zon	139	0.53	2466	0.331	2.72	0.114	1.79	99	1844	44	1871	32
52	CLD osc zon conv	304	0.57	99999	0.329	1.91	0.114	0.92	99	1831	31	1866	17
53	CLG osc zon sect	222	0.73	10271	0.334	1.89	0.115	1.45	100	1857	30	1874	26
54	CLG bb zon	135	0.54	11843	0.345	2.07	0.115	1.93	101	1913	34	1879	35
55	CLG bb zon	188	0.55	12678	0.325	4.50	0.114	1.70	99	1816	71	1868	31
59	CLD bb zon	265	0.51	21699	0.329	2.48	0.114	1.55	99	1835	40	1866	28
60	CLG bb zon	182	0.56	5874	0.331	2.11	0.114	1.59	99	1844	34	1871	29
61	CLD bb zon	261	0.46	11596	0.326	4.24	0.114	2.19	99	1819	67	1862	39
62	CLG osc zon	159	0.62	2798	0.347	2.33	0.114	1.34	101	1921	39	1869	24
63	CLG osc zon	129	0.57	4657	0.340	2.72	0.115	1.77	100	1885	44	1881	32
64	CLG osc zon	287	0.72	18060	0.329	1.60	0.114	1.34	99	1831	26	1870	24
65	CLG osc zon conv	172	0.55	41627	0.320	1.13	0.115	1.49	98	1791	18	1881	27
66	CLG osc zon sect	138	0.53	5197	0.349	1.75	0.114	1.66	102	1930	29	1857	30
67	CLG osc zon	127	0.45	19307	0.348	1.91	0.114	1.14	101	1924	32	1870	21
68	CLG osc zon sect	163	0.58	48270	0.317	1.94	0.114	1.65	98	1775	30	1871	30

^a) Abbreviations: CLG=CL-grey; CLD=CL-dark; CLB=CL-bright; osc=oscillatory; zon=zonation
bb=broad banded; conv=convoluted; sect= with sectors

Discussion and conclusion

The magmatic age of the host subvolcanic granite to rhyolite porphyry at $1\,870 \pm 6$ Ma and the magmatic age of the older $1\,876 \pm 8$ Ma mega-xenoliths of relict K-feldspar porphyric granite at Linavare, bracket the age of the high-grade metamorphic event the latter rock has experienced. The results were integrated in the mapping of the 27K Nattavaara area (Claeson & Antal Lundin 2012). Summary of sample data is given in Table 6.

Table 6. Summary of sample data.

Rock type	Granite to rhyolite porphyry, subvolcanic
Lithotectonic unit	Norrbottnen lithotectonic unit of the Svecofennian orogen
Lithological unit	
Sample number	DCL060126
Lab_id	DCL060126
Coordinates	7425183/737293 (Sweref99TM)
Map sheet	27K Nattavaara SV (RT90)
Locality	Linavare
Project	Mellersta Norrbotten (80010)

References

- Andersson, J. (ed.) 2012: U-Pb zircon geochronology of granitic and syenitoid rocks across the southern part of the Sveconorwegian orogen. *Sveriges geologiska undersökning SGU-rapport 2012:14*, appendix p. 26.
- Boynnton, W.V., 1984: Cosmochemistry of the Rare Earth Elements: Meteorite studies. In P. Henderson (ed.): *Rare earth element geochemistry*. Elsevier Science B.V. 63–114.
- Claeson, D. & Antal Lundin, I., 2012: Beskrivning till berggrundskartorna 27K Nattavaara NV, NO, SV & SO. *Sveriges geologiska undersökning K 383–386*, 22 pp.
- Sun, S.S. & McDonough, W.F., 1989: Chemical and isotopic systematic of oceanic basalts: implications for mantle composition and processes. In A.D. Saunders & M.J. Norry (eds.): *Magmatism in ocean basins*. Geological Society of London, Special Publication 42, 313–345.

Introduction

Norrbottnen, Sweden is a key area of Europe for future exploration and mining. To establish age relations for magmatic activity and metamorphic overprinting in this area, the sampled rock was selected (Fig. 1, 2, 21). This rock occurs at Linavare as mega-xenoliths of strongly deformed, foliated, recrystallised and low-radiation metagranite in massive subvolcanic granite to rhyolite porphyry that was age determined to $1\,870 \pm 6$ Ma, giving a lower age of the high-grade metamorphic event (this issue). The age of the regional metamorphic event may be deduced from the age of these two rocks, occurring between their igneous crystallisation ages. Determine the magmatic age of the metagranite is the main aim and if the zircon display metamorphic rims or overgrowths, these should be studied to.

Sample description

The metagranite is red to greyish red, with amphibole and biotite content estimated at 15 %, in a relict medium-grained, now fine-grained groundmass (Fig. 22). The rock is deformed, recrystallised, and displaying relict potassium feldspar phenocryst texture (Fig. 22). The foliation is oriented 5/54. Petrophysical measurements of a sample show density at $2\,629$ kg/m³, magnetic susceptibility $2\,100 \times 10^{-5}$ SI, and remanent magnetization intensity of 110 mA/m.



Figure 22. The sampled metagranite with relict potassium feldspar phenocrysts.

Analytical results and interpretation of geochronological data

U-Pb TIMS analysis of zircon was performed at the Laboratory of Isotope Geology at the Museum of Natural History in Stockholm. The analytical results are shown in Table 7. The zircon are of poor quality, metamict, and with plenty of cracks. A few, colourless crystals are of better quality and these were selected for abrasion. Euhedral, as well as rounded and anhedral grains occur. Most of the selected grains are euhedral with sharp edges and pyramid tips. Middle sized and large crystals were abraded separately. Magmatic zonation is common, but no signs of cores or overgrowths are seen. The analysed fractions consist of 1 to 3 crystals. Fractions 1 to 4 are from abrasion 1 (middle sized) and fraction 5 from abrasion 2 (large; Fig. 23).

The five data points define a discordia with concordia intercepts at $1\,876 \pm 8$ Ma and 315 ± 140 Ma (2σ ; MSWD of 2.1). The upper intercept age at $1\,876 \pm 8$ Ma is interpreted as the igneous crystallisation age of the granite (Fig. 24).

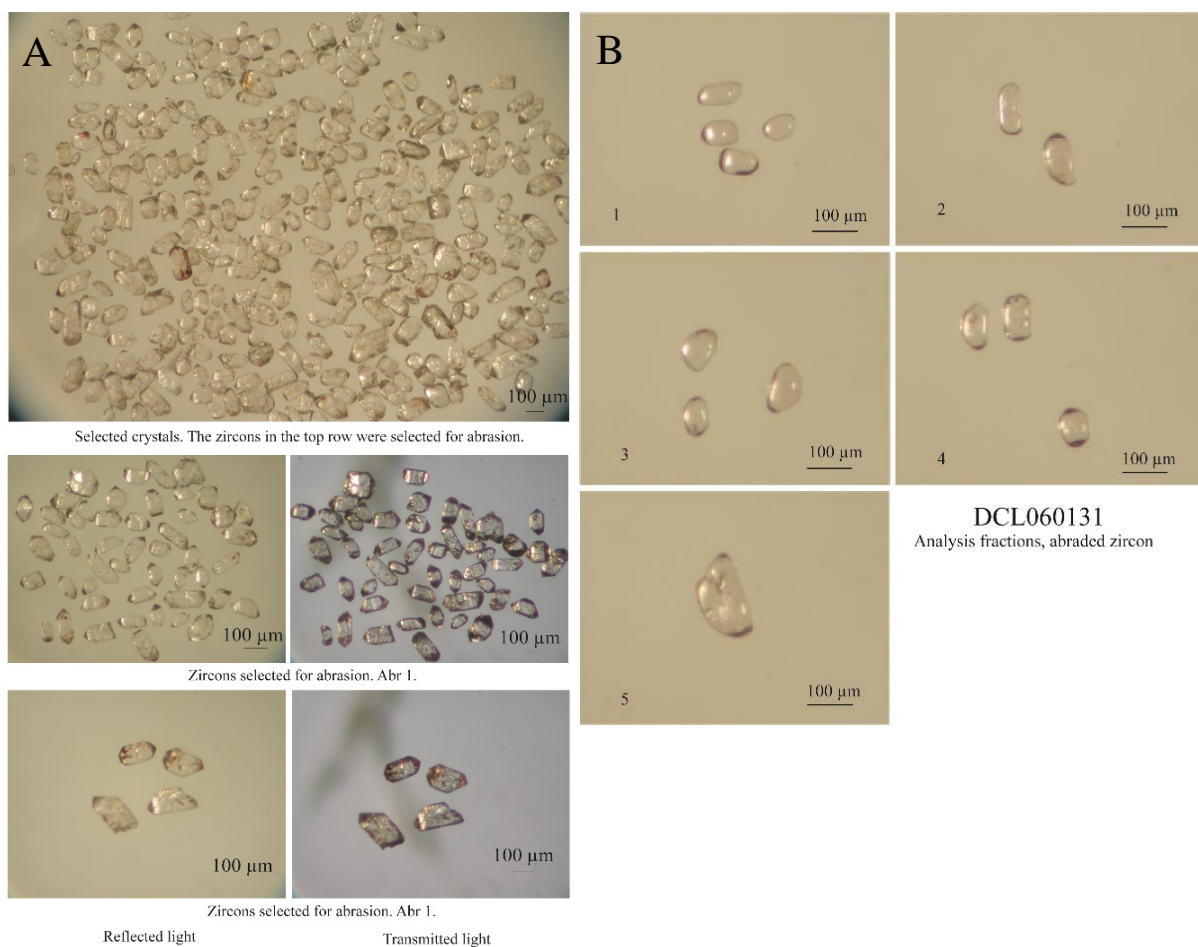


Figure 23. **A.** The left part of the image shows the selected zircon crystals prior to abrasion. **B.** The right part shows the analysed fractions. Fraction 1 consists of two clear crystals with no visible inner structures. (Two of the crystals on the photo were lost during the washing procedure.) Fraction 2 contains two clear, more elongated crystals. Fraction 3 holds three clear crystals with observed magmatic zonation. Fraction 4 consists of three clear crystals with inclusions seen in some of them. Fraction 5 contains one large, broken crystal with sparse cracks.

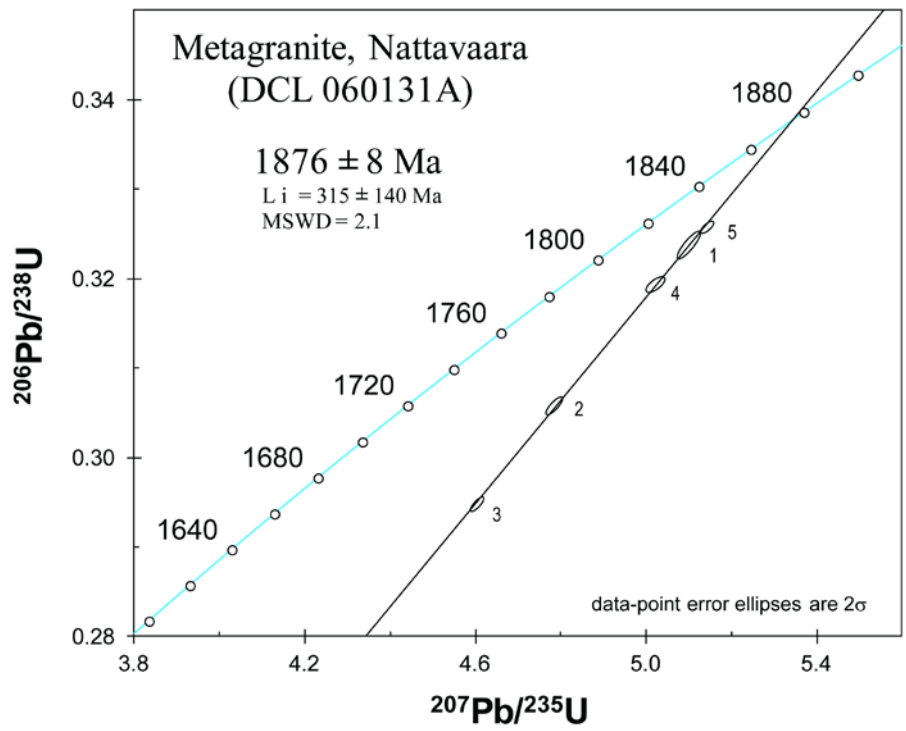


Figure 24. Concordia diagram showing U-Pb zircon data.

Table 7. SIMS U-Pb-Th zircon data.

Analysis	Weight (μg)	No. of crystals	U (ppm)	Th (ppm) ¹	Pb tot (ppm)	Pb com (ppm)	²⁰⁶ Pb/ ²⁰⁴ Pb 2	²⁰⁶ Pb - ²⁰⁷ Pb - ²⁰⁸ Pb (At %) ³	²⁰⁶ Pb/ ²³⁸ U 4	2s (%)	²⁰⁷ Pb/ ²³⁵ U 4	2s (%)	²⁰⁷ Pb/ ²⁰⁶ Pb 4	2s (%)	²⁰⁶ Pb/ ²³⁸ U Ma	²⁰⁷ Pb/ ²³⁵ U Ma	²⁰⁷ Pb/ ²⁰⁶ Pb Ma	corr. coeff. 5
1	1.5	2	330	148	118	3.2	1418	80.2 - 9.2 - 10.6	0.32376	0.39	5.09925	0.45	0.11423	0.23	1808.0	1836.0	1867.8 \pm 4.1	0.863
2	1.5	2	296	131	101	4.3	963	80.4 - 9.1 - 10.5	0.30580	0.26	4.78532	0.32	0.11350	0.19	1720.0	1782.3	1856.1 \pm 3.4	0.818
3	3	3	452	196	143	1.0	4828	80.5 - 9.1 - 10.4	0.29478	0.22	4.60471	0.28	0.11329	0.17	1665.4	1750.1	1852.9 \pm 3.0	0.802
4	3	3	294	121	101	1.6	2528	80.9 - 9.2 - 9.9	0.31933	0.22	5.02062	0.36	0.11403	0.26	1786.4	1822.8	1864.6 \pm 4.8	0.688
5	3.5	1	413	171	144	1.1	4812	80.8 - 9.3 - 9.9	0.32576	0.17	5.14402	0.25	0.11453	0.17	1817.8	1843.4	1872.5 \pm 3.0	0.745

1. Calculated from ²⁰⁸Pb content. Corrected for Pb loss.

2. Corrected for mass fractionation and spike.

3. Radiogenic Pb, i.e. corrected for common Pb and blank.

4. Corrected for mass fractionation, spike, common Pb and blank.

5. Correlation coefficient for errors in ²⁰⁶Pb/²³⁸U and ²⁰⁷Pb/²³⁵U.

The mass fractionation for Pb is 0.10 % per a.m.u.

The mass fractionation for U is calculated during measurement by monitoring the ²³³U/²³⁶U ratio.

Pb blank is 1-5 pg. Standard value is 2 pg.

U blank is 1 pg.

The samples were not weighed and, consequently, the concentrations given in the table are only approximate.

This does not affect the isotope ratios or errors or the positions of the data points in the concordia diagram.

Discussion and conclusion

The igneous age of the $1\,876 \pm 8$ Ma mega-xenoliths of relict K-feldspar porphyric granite at Linavare and the host subvolcanic granite to rhyolite porphyry age at $1\,870 \pm 6$ Ma, bracket the age of the high-grade metamorphic event the former rock has experienced. The results were integrated in the mapping of the 27K Nattavaara area (Claeson & Antal Lundin 2012). Summary of sample data is given in Table 8.

Table 8. Summary of sample data.

Rock type	Metagranite with relict phenocryst texture
Lithotectonic unit	Norrbottn lithotectonic unit of the Svecokarelian orogen
Lithological unit	
Sample number	DCL060131A
Lab_id	NRM TIMS
Coordinates	7424193/736193 (Sweref99TM)
Map sheet	27K Nattavaara SV (RT90)
Locality	Linavare
Project	Mellersta Norrbotten (80010)

References

- Claeson, D. & Antal Lundin, I., 2012: Beskrivning till berggrundskartorna 27K Nattavaara NV, NO, SV & SO. *Sveriges geologiska undersökning K 383–386*, 22 pp.
- Stacey, J.S. & Kramers, J.D., 1975: Approximation of terrestrial lead isotope evolution by a two-stage model. *Earth and Planetary Science Letters* 26, 207–221.
- Steiger, R.H. & Jäger, E., 1977: Convention on the use of decay constants in geo- and cosmochronology. *Earth and Planetary Science Letters* 36, 359–362.

Introduction

Norrbotnen, Sweden is a key area of Europe for future exploration and mining. In order to establish age relations for magmatic activity and metamorphic overprinting in this area, the sampled rock was selected (Fig. 1, 2, 25). The igneous age of the quartz monzonite to granite at Urtjuvare is unknown. The rock is in contact with strongly deformed, recrystallised granite that locally display relict K-feldspar phenocrysts. The latter rock was age determined at $1\,876 \pm 5$ Ma, which was designated its igneous crystallisation age (this issue). According to earlier maps (e.g. Geological map of the Fennoscandian Shield, Koistonen et al. 2001) both of these rocks belong to the so called Lina suite and thus formed around 1.80 Ga ago.

This is clearly not the case and the rock at Urtjuvare is more analogous to the so called Edefors suite. From the previous dating effort of the deformed granite an analysis of a rim area of a zircon shows a low Th/U ratio and a dark hue in cathodoluminescence (this issue). These are interpreted as signs of secondary growth or recrystallisation of zircon and thus indicative of when the deformation and metamorphism occurred. The analysis of the secondary zircon shows an age of c. 1.80 Ga, which might be the age of the undeformed quartz monzonite to granite or the latter is slightly younger than that, if the former is due to a regional metamorphic event.

Sample description

The quartz monzonite to granite at Urtjuvare is massive to weakly foliated, the latter interpreted to be related to flow at magmatic conditions (Fig. 26). The rock is medium-grained to coarse-grained, greyish red to reddish grey, uneven-grained to porphyric with feldspar phenocrysts, mostly potassium feldspar and some plagioclase, 5–20 mm large (0–15 %). Accessory minerals are biotite, opaque minerals, muscovite, apatite, titanite, and zircon. Saussurite-sericite alteration of plagioclase is minor at 0–10 %, very minor biotite alteration to chlorite is seen, and weakly undulose quartz. The Zr content of the rock is 371 ppm. Outcrop measurement of magnetic susceptibility yielded $2\,540\text{--}3\,720 \times 10^{-5}$ SI. Measurements of gamma ray radiation show K = 3.9–4 %, U = 3.2 ppm, and Th = 20.7–21.1 ppm. Petrophysical measurements of a sample show density at $2\,640\text{ kg/m}^3$, magnetic susceptibility $2\,985 \times 10^{-5}$ SI, and remanent magnetization intensity of 200 mA/m.

The quartz monzonite to granite at Urtjuvare shows a LREE-enriched and flat HREE pattern, with a negative Eu anomaly (Fig. 27). The LREE enrichment is due to fractional crystallisation, the flat, unfractionated HREE pattern shows that no garnet was left in the residue at the location of magma genesis, and the Eu anomaly is indicative of plagioclase fractionation. The negative anomalies shown in the multi-element diagram of Sr is due to plagioclase fractionation, the P anomaly of apatite fractionation, and the Ti anomaly of Fe-Ti oxide fractionation (Fig. 27). The strong negative Nb anomaly and positive Pb anomaly suggest a subduction related petrogenesis (Fig. 27).

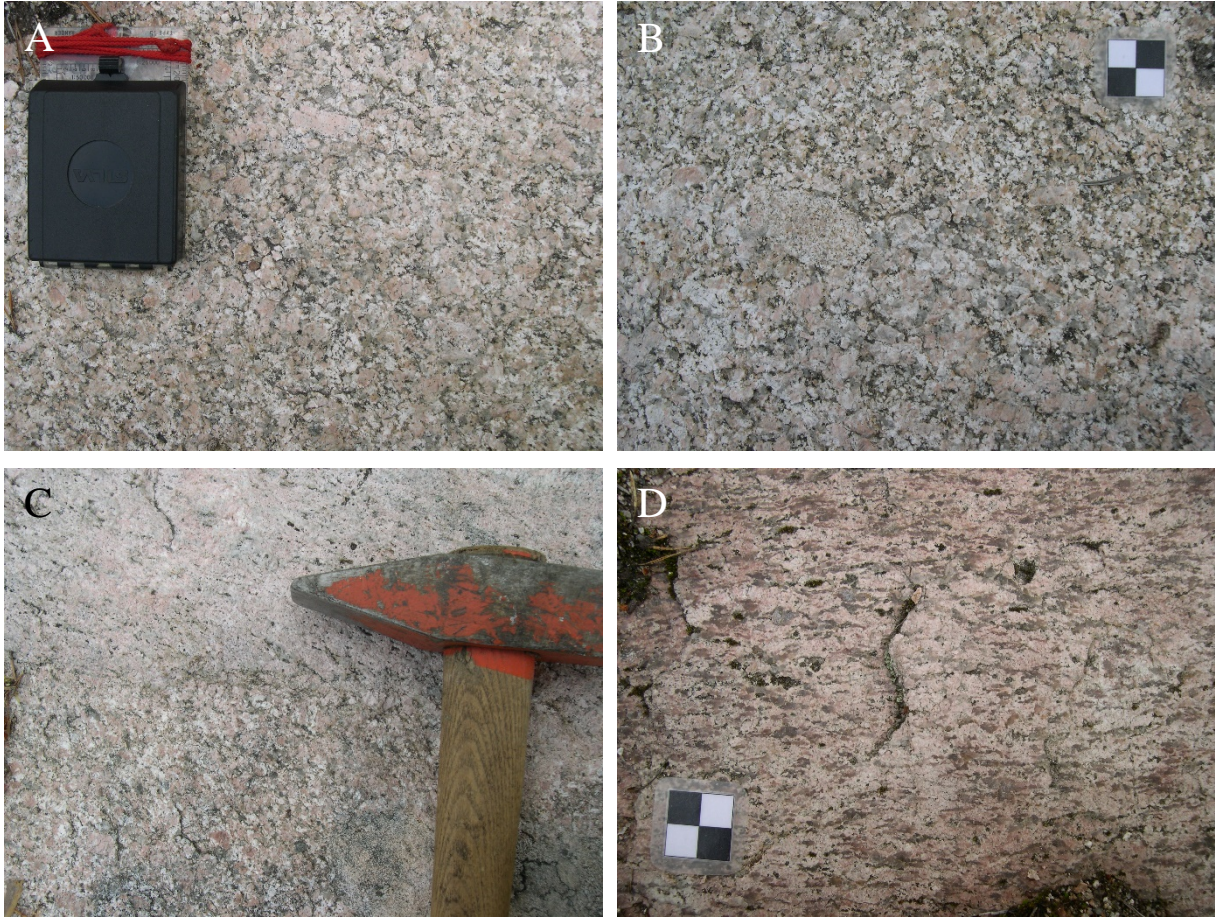


Figure 26. A. The age determined quartz monzonite to granite at Urtjuvare. B. A fine-grained enclave in quartz monzonite to granite, note the variation in phenocryst content (cm-scale). C. Contact between older, deformed, and recrystallised granite at the top of the image and the quartz monzonite to granite at Urtjuvare. D. Older, deformed, and recrystallised granite at Urtjuvare. Photos: Dick Claeson.

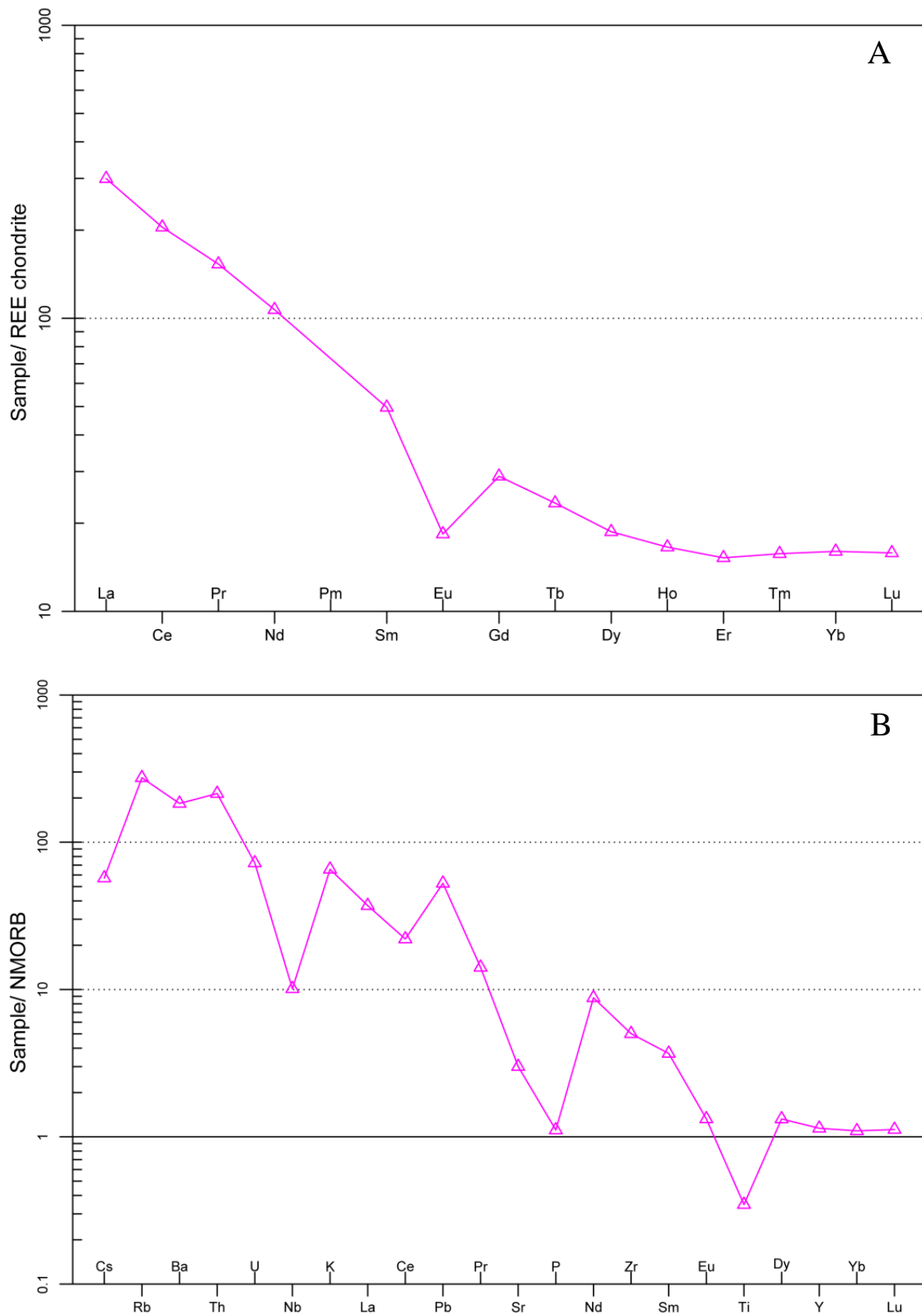


Figure 27. A. REE-diagram of quartz monzonite to granite. Normalizing values for chondrite from Boynton (1984). **B.** Multi-element diagram, rock as in A. Normalizing values for N-MORB from Sun & McDonough (1989).

Analytical results and interpretation of geochronological data

Analytical procedures

Zircon mineral separates were obtained from density separation of about 0.5 kg of rock sample grinded to a fine powder using a swing mill and then loaded on a Wilfley water table. The magnetic minerals were removed from the heavy residue by hand magnet. Zircon were hand-picked under a stereomicroscope and about 100–200 crystals from each sample were mounted on double-faced tape. The 1 065 Ma Geostandards zircon 91 500 (Wiedenbeck et al. 1995) was added to the mount used for ion microprobe SIMS analysis. The mounts were casted in transparent epoxy resin and after hardening polished to expose the central parts of the crystals. Cathodoluminescence imaging was performed on polished, gold-coated mounts using a Gatan CL3 detector on a Hitachi S-4300 electron microscope at the Swedish Museum of Natural History. The mounts were cleaned in an ultrasonic bath and with ethanol prior to loading it into the analytical chambers.

High-spatial resolution secondary ion mass spectrometer (SIMS) analysis was made using a Cameca IMS 1280 at the NordSIM facility at the Swedish Museum of Natural History in Stockholm. Detailed descriptions of the analytical procedures are given in Whitehouse et al. (1999) and Whitehouse & Kamber (2005). The instrument was operating with a spot size less than 25 μm . Age calculations of isotopic data were made using software Isoplot 4.15 (Ludwig 2012). The amount of common ^{206}Pb in measured ^{206}Pb is estimated from ^{204}Pb assuming a present day terrestrial Pb following the model of Stacey & Kramers (1975). Statistical precisions of age estimates are given at the 95% confidence level. Mean square weighted deviation (MSWD) for the concordia age is reported including both equivalence and discordance. Ages are reported without decay constant errors. Visual examination of the analysed spots was done by back scattered electron (BSE) imaging using the electron microprobe at the Department of Geology, Uppsala University, Sweden.

Analytical results and interpretation of geochronological data

The size, technical quality (inclusions and cracks) and aspect ratio of the individual grains varies widely through the population (Fig. 28). Large, generally turbid and subhedral grains, are up to 150 μm across and have aspect ratios of about 1:2–3. The smaller grains are ca 50 micron across, preferentially stubby crystals with aspect ratios of 1:1–1.5. They are also typically more colourless and translucent, generally devoid of visible inclusions. The smaller crystals generally have better preserved euhedral morphology with pointed tips and sharp terminations (Fig. 28).

Eight out of totally 13 analyses are concordant and within or less than 1% discordant. They define a common concordia age of $1\,782 \pm 7$ Ma (MSWD = 2.3, probability of fit = 0.003) and an identical weighted average $^{207}\text{Pb}/^{206}\text{Pb}$ age of $1\,780 \pm 4$ Ma (Fig. 29; MSWD = 0.73, probability = 0.65). Five analyses were discarded from age calculation. Two of these were significantly discordant (n3287-04 and 09). The other three analyses had high proportions of common Pb, resulting in high correction and high uncertainty of the resulting isotopic ratios (analyses n3287-01, 06, and 07).

There are no indications of post-crystallisation disturbance of the U-Pb isotopic system of the analysed zircon domains. The concordia age of $1\,782 \pm 7$ Ma is thus set to date igneous crystallisation of the granite to quartz monzonite intrusion.

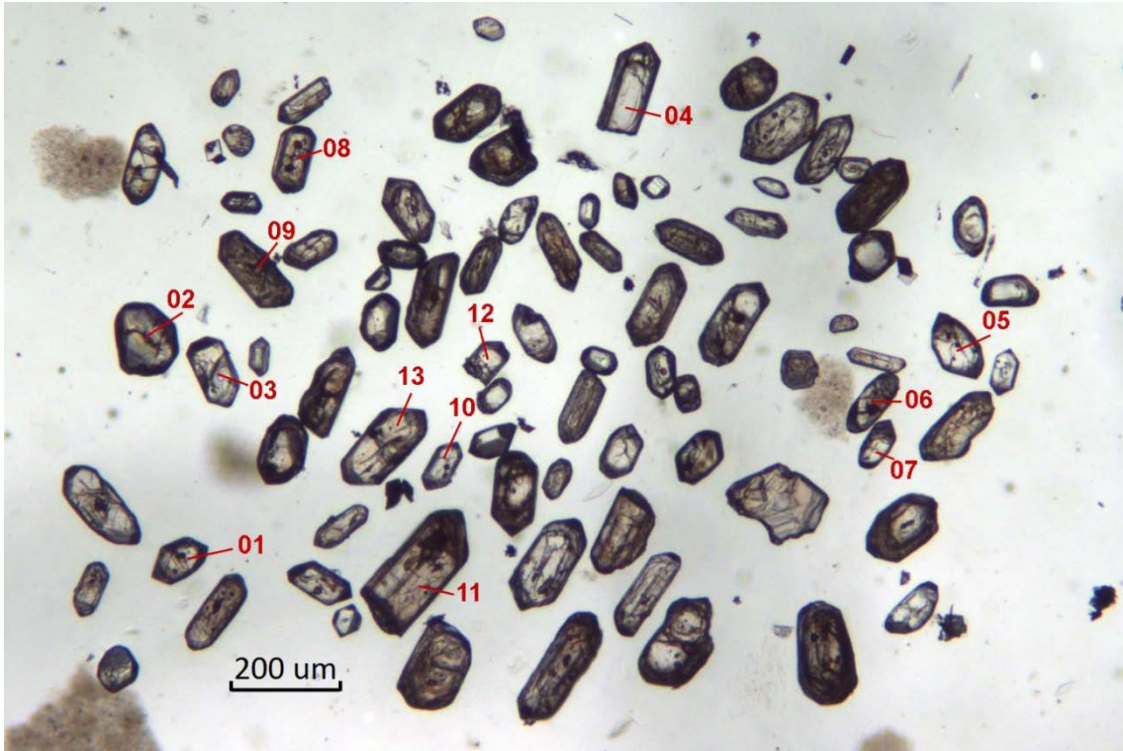


Figure 28. Optical microscope photo (plane polarized light) of representative zircon from sample DCL070143 in a polished section of the epoxy mount used for the SIMS analyses. Numbers refer to analytical ID in Table 9.

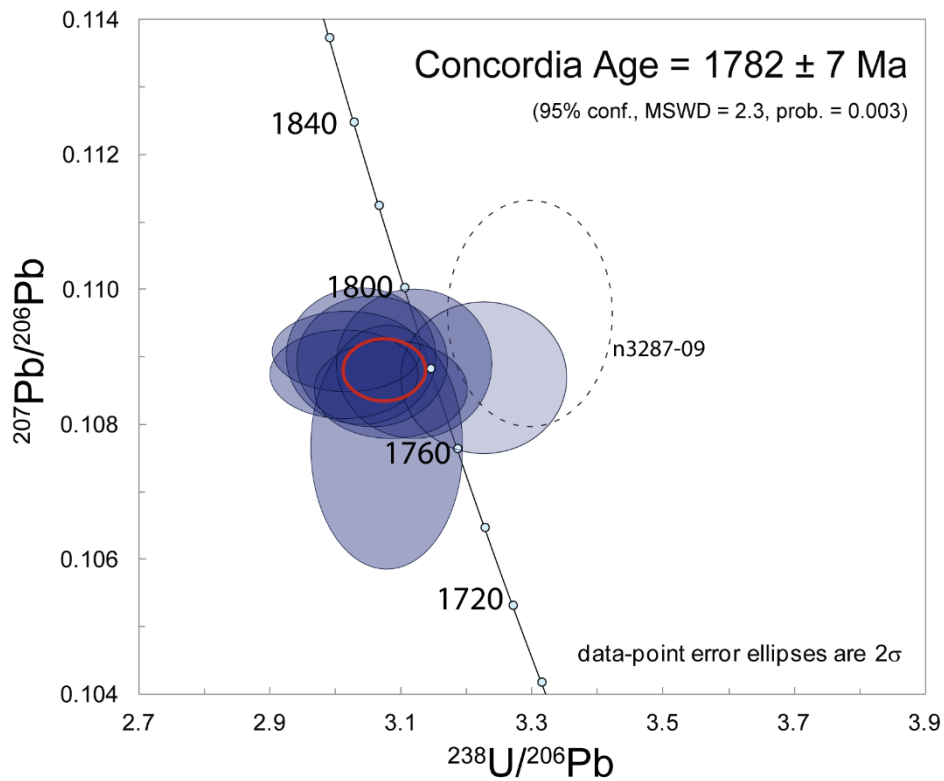


Figure 29. Tera-Wasserburg diagram showing U-Pb SIMS data for zircon from sample DCL070143. Concordia age error ellipse shown in red. Dashed line error ellipse marked with analytical ID shows data omitted from age calculation (cf. Table 9).

Table 9. SIMS U-Pb-Th zircon data.

Sample/ spot #	U ppm	Th ppm	Pb ppm	Th/U calc ^{*1}	²⁰⁷ Pb ²³⁵ U	±σ %	²⁰⁸ Pb ²³² Th	±σ %	²³⁸ U ²⁰⁶ Pb	±s %	²⁰⁷ Pb ²⁰⁶ Pb	±s %	ρ % ^{*2}	Disc. % conv. ^{*3}	²⁰⁷ Pb ²⁰⁶ Pb	±s Ma	²⁰⁶ Pb ²³⁸ U	±s Ma	²⁰⁶ Pb/ ²⁰⁴ Pb measured	f ₂₀₆ % ^{*4}
n3287-01	156	199	54	0.90	3.534	2.40	0.0630	3.5	4.138	1.54	0.1061	1.84	0.64	-21.6	1733	33	1395	19	220	{8.49}
n3287-02	697	700	322	1.03	4.977	1.56	0.0943	2.9	3.012	1.54	0.1087	0.25	0.99	4.5	1778	4	1848	25	59373	{0.03}
n3287-03	376	379	157	0.81	4.645	1.67	0.0733	4.3	3.226	1.61	0.1087	0.42	0.97	-2.4	1778	8	1741	25	3390	{0.55}
n3287-04	100	97	40	0.80	4.402	3.25	0.0768	4.4	3.447	3.08	0.1101	1.03	0.95	-9.9	1800	19	1642	45	16050	{0.12}
n3287-05	142	152	65	1.09	4.823	1.68	0.0928	3.0	3.078	1.54	0.1077	0.68	0.91	3.5	1760	12	1814	24	15922	{0.12}
n3287-06	375	290	125	0.57	3.686	3.66	0.0638	5.7	3.876	1.54	0.1036	3.32	0.42	-13.9	1690	60	1480	20	251	{7.45}
n3287-07	215	154	75	0.43	3.993	1.80	0.0506	3.4	3.508	1.54	0.1016	0.93	0.86	-2.5	1654	17	1617	22	1155	{1.62}
n3287-08	332	285	147	0.87	4.916	1.58	0.0939	3.3	3.055	1.54	0.1089	0.36	0.97	2.8	1782	7	1825	25	8167	{0.23}
n3287-09	416	522	184	1.13	4.586	1.67	0.0838	3.4	3.296	1.55	0.1096	0.63	0.93	-5.4	1793	11	1708	23	2411	{0.78}
n3287-10	282	239	122	0.85	4.813	1.62	0.0926	3.0	3.120	1.56	0.1089	0.41	0.97	0.7	1781	8	1792	24	19893	{0.09}
n3287-11	506	208	201	0.40	4.851	1.57	0.0902	3.2	3.084	1.54	0.1085	0.28	0.98	2.3	1775	5	1810	24	81952	{0.02}
n3287-12	329	267	146	0.85	4.947	1.58	0.0967	2.9	3.038	1.54	0.1090	0.38	0.97	3.3	1783	7	1834	25	63025	{0.03}
n3287-13	811	105	308	0.14	4.985	1.55	0.0964	3.0	3.017	1.54	0.1091	0.22	0.99	4	1784	4	1845	25	57980	{0.03}

Isotope values are common Pb corrected using modern common Pb composition (Stacey & Kramers 1975) and measured ²⁰⁴Pb.

*1 Th/U ratios calculated from ²⁰⁸Pb/²⁰⁶Pb and ²⁰⁷Pb/²⁰⁶Pb ratios, assuming a single stage of closed U-Th-Pb evolution

*2 Error correlation in conventional concordia space. Do not use for Tera-Wasserburg plots.

*3 Age discordance in conventional concordia space. Positive numbers are reverse discordant.

*4 Figures in parentheses are given when no correction has been applied, and indicate a value calculated assuming present-day Stacey-Kramers common Pb.

Discussion and conclusion

The igneous crystallisation age $1\,782 \pm 7$ Ma of the pristine monzonite to granite at Urtjuvare strongly suggests that either a major regional metamorphism occurred between the formation of this intrusion and the zircon rim formation at c. 1.80 Ga of the metagranite at Kaltisberget (this issue) or that the bimodal magmatism in itself lead to the formation of secondary zircon at Kaltisberget. Other contributions in this issue do suggest that if a regional metamorphic event is invoked it should be older than their igneous age, e.g. pristine rocks at Ahmavaara $1\,806 \pm 7$ Ma, well-preserved rocks only displaying greenschist facies metamorphism at Tiurevaara $1\,788 \pm 13$ Ma.

The age $1\,782 \pm 7$ Ma of the monzonite to granite at Urtjuvare shows that the most pristine rocks in the southern parts of the map area 27K Nattavaara are also recording the youngest ages, about 10–15 million years (this issue).

The monzonite to granite at Urtjuvare is yet another occurrence at 1.78–1.80 Ga of bimodal magmatism with associated basic rocks that are coeval in the investigated map areas (Fig. 25, this issue). The results were integrated in the mapping of the 27K Nattavaara area (Claeson & Antal Lundin 2012) and used in the subsequent mapping project “Sydvästra Norrbotten” (this issue). Summary of sample data is given in Table 10.

Table 10. Summary of sample data.

Rock type	Quartz monzonite to granite
Lithotectonic unit	Norrbotten lithotectonic unit of the Svecokarelian orogen
Lithological unit	
Sample number	DCL070143
Lab_id	n3287
Coordinates	7403252/738664 (Sweref99TM)
Map sheet	27K Nattavaara SV (RT90)
Locality	Urtjuvare
Project	Mellersta Norrbotten (80010)

References

- Boynton, W.V., 1984: Cosmochemistry of the Rare Earth Elements: Meteorite studies. *In* P. Henderson (ed.): *Rare earth element geochemistry*. Elsevier Science B.V. 63–114.
- Claeson, D. & Antal Lundin, I., 2012: Beskrivning till berggrundskartorna 27K Nattavaara NV, NO, SV & SO. *Sveriges geologiska undersökning K 383–386*, 22 pp.
- Stacey, J.S. & Kramers, J.D., 1975: Approximation of terrestrial lead isotope evolution by a two-stage model. *Earth and Planetary Science Letters* 26, 207–221.
- Sun, S.S. & McDonough, W.F., 1989: Chemical and isotopic systematic of oceanic basalts: implications for mantle composition and processes. *In* A.D. Saunders & M.J. Norry (eds.): *Magmatism in ocean basins*. Geological Society of London, Special Publication 42, 313–345.

U-Pb ZIRCON AGE OF STRONGLY DEFORMED, RECRYSTALLISED GRANITE AT KALTISBERGET, MAP SHEET 27K NATTAVAARA, NORRBOTTEN COUNTY

Authors: Dick Claeson, Ildikó Antal Lundin, Fredrik Hellström & Andrius Rimsa

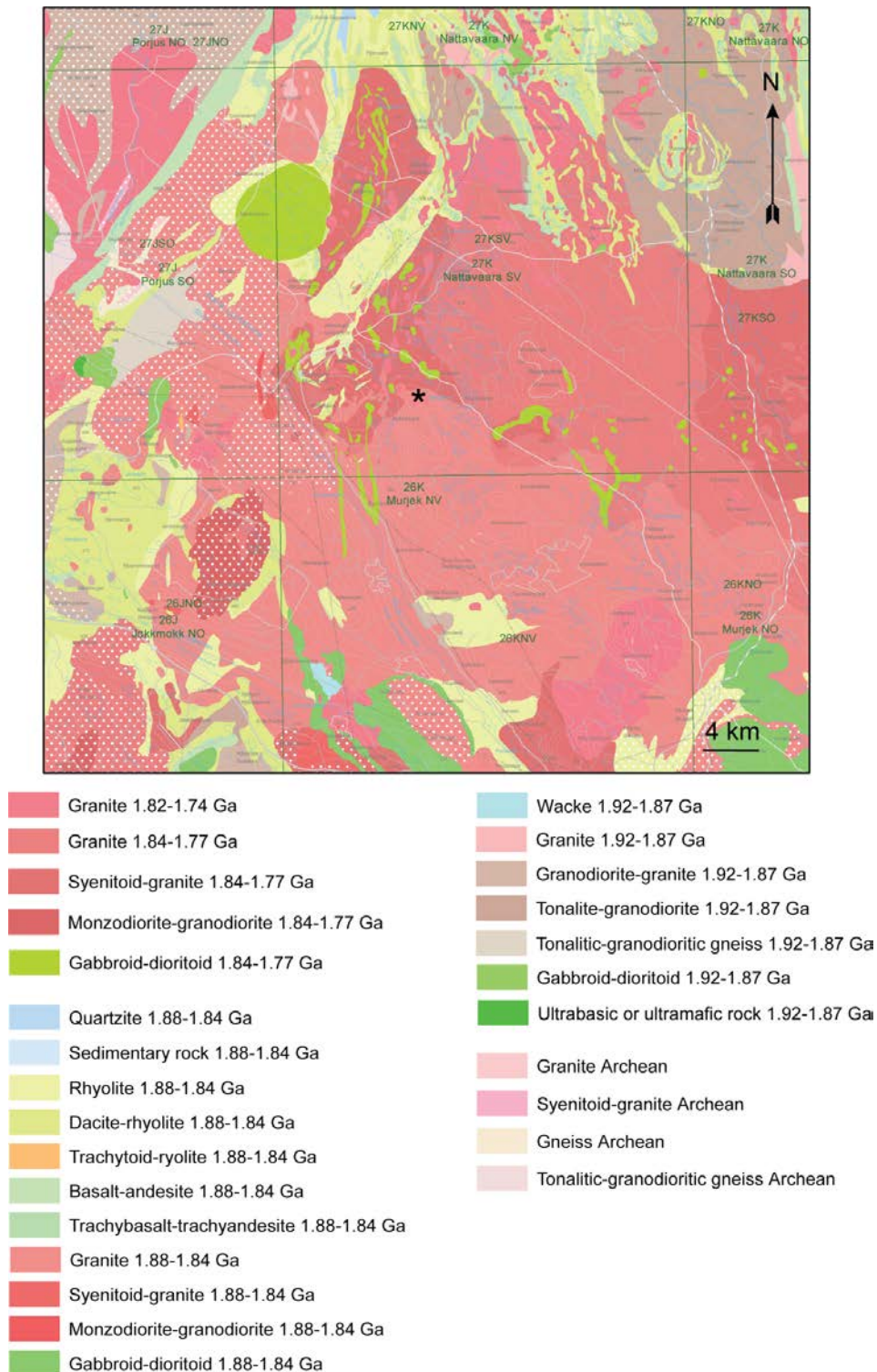


Figure 30. Bedrock map of the area, sampling location marked with black star.

Introduction

Strongly deformed, recrystallised granite occurs at Kaltisberget in the southwestern part of the map area 27K Nattavaara SV in Norrbotten County (Fig. 30). It is evident from the geophysical data that this type of rock is present in large areas west and south of map area 27K Nattavaara SV (Fig. 1, 2). The purpose of this study was to determine the protolith age of the metagranite and if possible also the age of metamorphic recrystallisation using secondary growth of zircon, if present.

Sample description

Strongly deformed, recrystallised granite that locally shows relict potassium feldspar phenocryst texture was sampled for age determination (Fig. 31). The rock is medium-grained to fine-grained, red to greyish red, and generally shows low contents of mafic minerals (1–5 % biotite and opaque minerals). Accessory minerals are biotite, opaque, allanite, fluorite, apatite, and zircon. Saussurite-sericite alteration of plagioclase is minor at 0–5 %, biotite alteration to chlorite is 50–75 %, and the sample shows undulose quartz. Quartz and biotite or chlorite usually defines the foliation and the rock is in places openly folded, giving a wavy appearance (Fig. 31). The metagranite is always showing low gamma ray radiation values and a ground measurement at the sample location shows K = 4.9 %, U = 1.4 ppm, and Th = 12.1 ppm. Petrophysical measurements of a sample show density at $2\,594\text{ kg/m}^3$, magnetic susceptibility $1\,928 \times 10^{-5}\text{ SI}$, and remanent magnetization intensity of 30 mA/m.



Figure 31. A. Deformed, recrystallised granite (dated sample). Photo: Fredrik Hellström. B. Deformed, recrystallised and openly folded granite (7402630/739436). Photo: Dick Claeson. C. Micrograph of sampled deformed, recrystallised granite. Photo: Dick Claeson.

Analytical results and interpretation of geochronological data

In situ U-Pb-Th SIMS analysis of zircon was performed at the NORDSIM facility at the Museum of Natural History in November 2007. Detailed descriptions of the analytical procedures are given in Whitehouse et al. (1997, 1999). Pb/U ratios, elemental concentrations and Th/U ratios were calibrated relative to the Geostandards zircon 91 500 reference, which has an age of c. 1 065 Ma (Wiedenbeck et al. 1995, 2004). Common Pb corrected isotope values were calculated using modern common Pb composition (Stacey & Kramers 1975) and measured ^{204}Pb . Decay constants follow the recommendations of Steiger & Jäger (1977). Diagrams and age calculations of isotopic data were made using software Isoplot 4.15 (Ludwig 2012). The analytical results are shown in Table 11. Zircon in the sample is of poor analytical quality, partly metamict. The zircon grains have generally euhedral to subhedral prismatic shapes but there are also anhedral crystals. In CL-images most grains show a weak internal oscillatory zonation, but CL-dark unzoned rims are occasionally also present (Fig. 32). The structurally old, typically oscillatory zoned core domains are interpreted to represent igneous zircon, while the CL-dark rims are interpreted to represent secondary growth of zircon (e.g. crystal 1a in Fig. 32).

One analysis (1a) displays higher U content (790 ppm) and a lower Th/U ratio (0.09) than the other analyses, which have 127–418 ppm U and Th/U ratios between 0.45 and 0.88 ($n = 7$; Table 11). The analysis of the low Th/U rim (1a, 2.8 % reversely discordant) record a younger age compared to the rest of the analyses (Fig. 33, Table 11). The other data points define a discordia line with intercept ages of $1\,875 \pm 6$ Ma and -138 ± 300 Ma (95 % confidence, $n = 7$, MSWD = 1.11), indicating no significant post-igneous isotopic disturbance in addition to recent Pb-loss. Five analyses are concordant and yield a concordia age at $1\,876 \pm 5$ Ma (2σ , MSWD = 1.9), identical to the weighted average $^{207}\text{Pb}/^{206}\text{Pb}$ age of $1\,876 \pm 6$ Ma (2σ , MSWD = 0.34) including the two discordant analyses (3, 5).

The concordia age of $1\,876 \pm 5$ Ma was obtained from analyses of apparently undisturbed oscillatory-zoned zircon domains and is interpreted to date crystallisation of igneous zircon in the granite. The single analysis with low Th/U ratio (1a) that yield an apparent $^{207}\text{Pb}/^{206}\text{Pb}$ age of 1.80 Ga is interpreted to reflect isotopic resetting of zircon in the metagranite at about 1.80 Ga, during metamorphism of the granitoid protolith. Additional analyses are needed to better constrain the age of this metamorphic event.

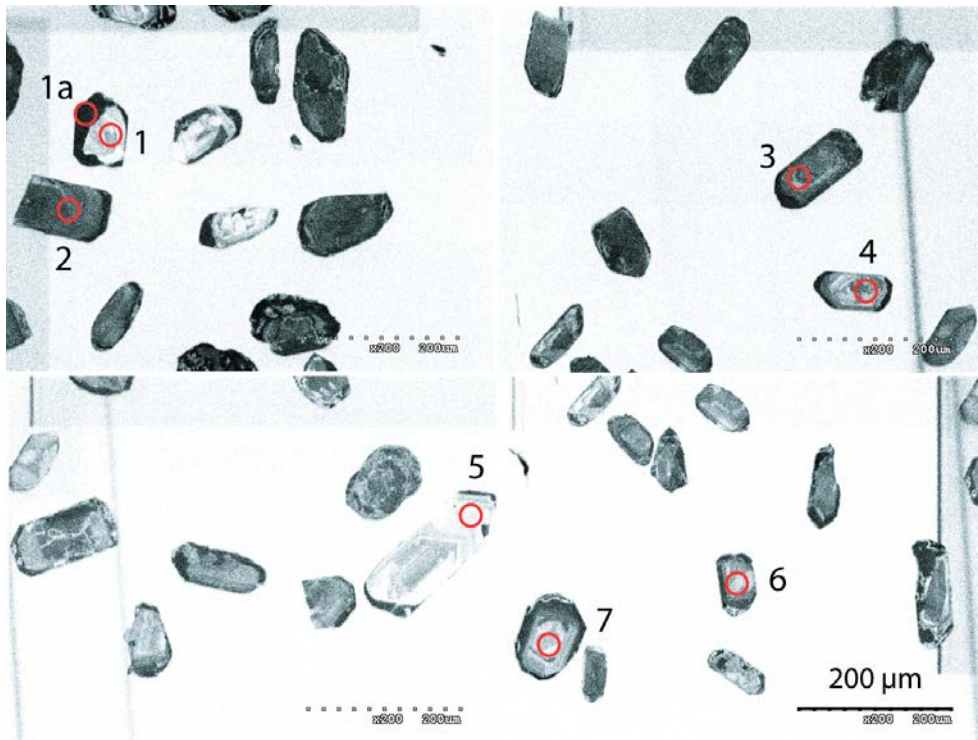


Figure 32. CL-images of zircon from the investigated metagranite at Kaltisberget. Red circles mark the approximate location of analysed spots. Numbers refer to analytical spot number in Table 11.

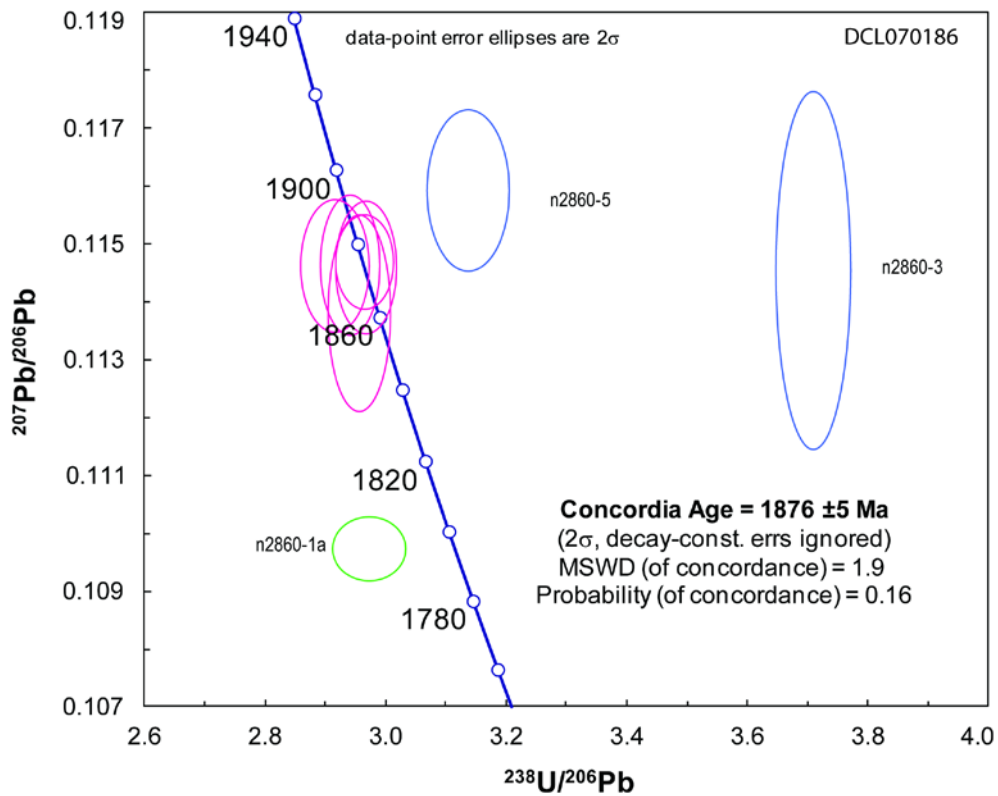


Figure 33. Tera-Wasserburg diagram showing U-Pb zircon data from the granite at Kaltisberget. Analyses used in age calculation are shown in red, discordant data points in blue and the CL-dark, reversely discordant rim analysis (1a) is shown in green.

Table 11. SIMS U-Pb-Th zircon data.

Sample/ spot #	U ppm	Th ppm	Pb ppm	Th/U calc ^{*1}	²⁰⁷ Pb		²⁰⁸ Pb		²³⁸ U		²⁰⁷ Pb		ρ *2	Disc. % conv. *3	²⁰⁷ Pb		²⁰⁶ Pb		²⁰⁶ Pb/ ²⁰⁴ Pb measured	f ₂₀₆ % *4
					$\pm\sigma$ % ²³⁵ U	$\pm\sigma$ % ²³² Th	$\pm\sigma$ %	$\pm\sigma$ %	$\pm\sigma$ %	$\pm\sigma$ %	$\pm\sigma$ Ma	$\pm\sigma$ Ma								
n2860-1	127	108	58	0.88	5.309	0.94	0.0996	2.7	2.956	0.72	0.1138	0.61	0.76	1.1	1861	11	1879	12	64154	0.03
n2860-1a	790	70	301	0.08	5.090	0.87	0.0892	7.4	2.972	0.84	0.1097	0.21	0.97	4.8	1795	4	1869	14	118124	0.02
n2860-2	418	310	177	0.48	5.334	0.73	0.0632	2.6	2.964	0.67	0.1147	0.29	0.92	-0.1	1875	5	1874	11	9982	0.19
n2860-3	276	144	95	0.45	4.258	1.30	0.0843	3.0	3.709	0.69	0.1145	1.10	0.53	-20.0	1873	20	1539	9	862	2.17
n2860-4	195	113	86	0.61	5.420	0.89	0.1019	2.7	2.915	0.79	0.1146	0.41	0.89	1.7	1874	7	1901	13	69230	0.03
n2860-5	136	61	55	0.46	5.095	1.02	0.0994	2.7	3.137	0.89	0.1159	0.49	0.88	-6.7	1894	9	1784	14	48308	0.04
n2860-6	198	103	85	0.53	5.326	0.81	0.0992	2.6	2.967	0.69	0.1146	0.41	0.86	-0.1	1874	7	1873	11	69741	0.03
n2860-7	188	115	83	0.62	5.373	0.81	0.0988	2.6	2.942	0.69	0.1146	0.43	0.85	0.7	1874	8	1886	11	77434	0.02

Isotope values are common Pb corrected using modern common Pb composition (Stacey & Kramers 1975) and measured ²⁰⁴Pb.

*1 Th/U ratios calculated from ²⁰⁸Pb/²⁰⁶Pb and ²⁰⁷Pb/²⁰⁶Pb ratios, assuming a single stage of closed U-Th-Pb evolution

*2 Error correlation in conventional concordia space. Do not use for Tera-Wasserburg plots.

*3 Age discordance in conventional concordia space. Positive numbers are reverse discordant.

*4 Figures in parentheses are given when no correction has been applied, and indicate a value calculated assuming present-day Stacey-Kramers common Pb.

Discussion and conclusion

The concordia age of $1\,876 \pm 5$ Ma is interpreted to date igneous crystallisation of the granite. Earlier maps (e.g. Geological map of the Fennoscandian Shield, Koistonen et al. 2001) show the Kaltisberget granite as belonging to the 1.80 Ga so called Lina suite, which is clearly not the case.

The single analysis with low Th/U ratio paired with a dark appearance in the CL-image shows the age of recrystallisation and metamorphism that this rock underwent c. 1.80 Ga ago. The major magmatic activity in the Kaltisberget rocks vicinity at c. 1.80 Ga probably was a major factor in the metamorphism (Claeson & Antal Lundin 2012, this issue). The results were integrated in the mapping of the 27K Nattavaara area (Claeson & Antal Lundin 2012). Summary of sample data is given in Table 12.

Table 12. Summary of sample data.

Rock type	Deformed, recrystallised granite
Lithotectonic unit	Norrbottn lithotectonic unit of the Svecokarelian orogen
Lithological unit	
Sample number	DCL070186
Lab_id	n2860
Coordinates	7405485/743795 (Sweref99TM)
Map sheet	27K Nattavaara SV (RT90)
Locality	Kaltisberget
Project	Mellersta Norrbotten (80010)

References

- Claeson, D. & Antal Lundin, I., 2012: Beskrivning till berggrundskartorna 27K Nattavaara NV, NO, SV & SO. *Sveriges geologiska undersökning K 383–386*, 22 pp.
- Koistonen, T., Stephens, M.B., Bogatchev, V., Nordgulen, Ø., Wennerström, M. & Korhonen, J., 2001: *Geological map of the Fennoscandian Shield, scale 1:2 000 000*. Geological Survey of Finland, Norway and Sweden and the North-West Department of Natural Resources of Russia.
- Ludwig, K.R., 2012: User's manual for Isoplot 3.75. A Geochronological Toolkit for Microsoft Excel. *Berkeley Geochronology Center Special Publication No. 5*, 75 pp.
- Stacey, J.S. & Kramers, J.D., 1975: Approximation of terrestrial lead isotope evolution by a two-stage model. *Earth and Planetary Science Letters* 26, 207–221.
- Steiger, R.H. & Jäger, E., 1977: Convention on the use of decay constants in geo- and cosmochronology. *Earth and Planetary Science Letters* 36, 359–362.
- Whitehouse, M.J., Claesson, S., Sunde, T. & Vestin, J., 1997: Ion-microprobe U–Pb zircon geochronology and correlation of Archaean gneisses from the Lewisian Complex of Gruinard Bay, north-west Scotland. *Geochimica et Cosmochimica Acta* 61, 4 429–4 438.
- Whitehouse, M.J., Kamber, B.S. & Moorbath, S., 1999: Age significance of U–Th–Pb zircon data from Early Archaean rocks of west Greenland: a reassessment based on combined ion-microprobe and imaging studies. *Chemical Geology (Isotope Geoscience Section)* 160, 201–224.
- Wiedenbeck, M., Allé, P., Corfu, F., Griffin, W.L., Meier, M., Oberli, F., Quadt, A.V., Roddick, J.C. & Spiegel, W., 1995: Three natural zircon standards for U-Th-Pb, Lu-Hf, trace element and REE analyses. *Geostandards Newsletter* 19, 1–23.
- Wiedenbeck, M., Hanchar, J.M., Peck, W.H., Sylvester, P., Valley, J., Whitehouse, M., Kronz, A., Morishita, Y., Nasdala, L., Fiebig, J., Franchi, I., Girard, J.P., Greenwood, R.C., Hinton, R., Kita, N., Mason, P.R.D., Norman, M., Ogasawara, M., Piccoli, P.M., Rhede, D., Satoh, H., Schulz-Dobrick, B., Skår, O., Spicuzza, M.J., Terada, K., Tindle, A., Togashi, S., Vennemann, T., Xie, Q. & Zheng, Y.F., 2004: Further Characterisation of the 91500 Zircon Crystal. *Geostandards and Geoanalytical Research* 28, 9–39.

U-Pb ZIRCON AGE OF QUARTZ MONZONITE TO MONZONITE AT TIUREVAARA, MAP SHEET 27K NATTAVAARA, NORRBOTTEN COUNTY

Authors: Dick Claesson, Ildikó Antal Lundin, Jenny Andersson & Anders Scherstén¹

¹Department of geology, Lund University, Sölvegatan 12, SE-223 62 Lund, Sweden

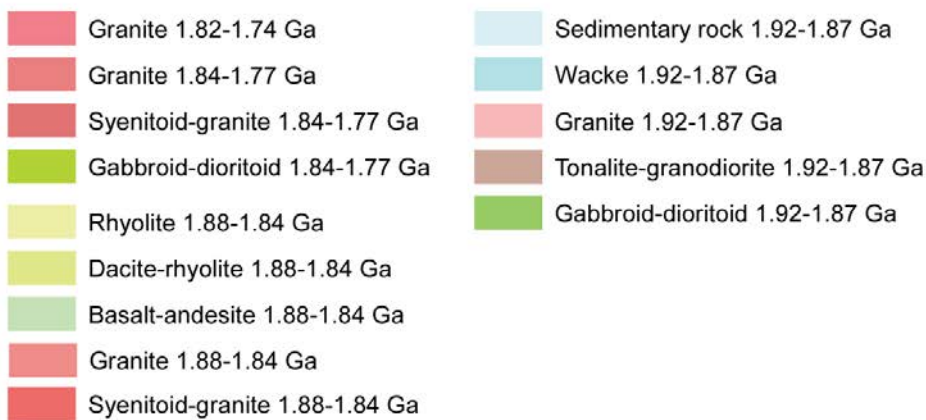
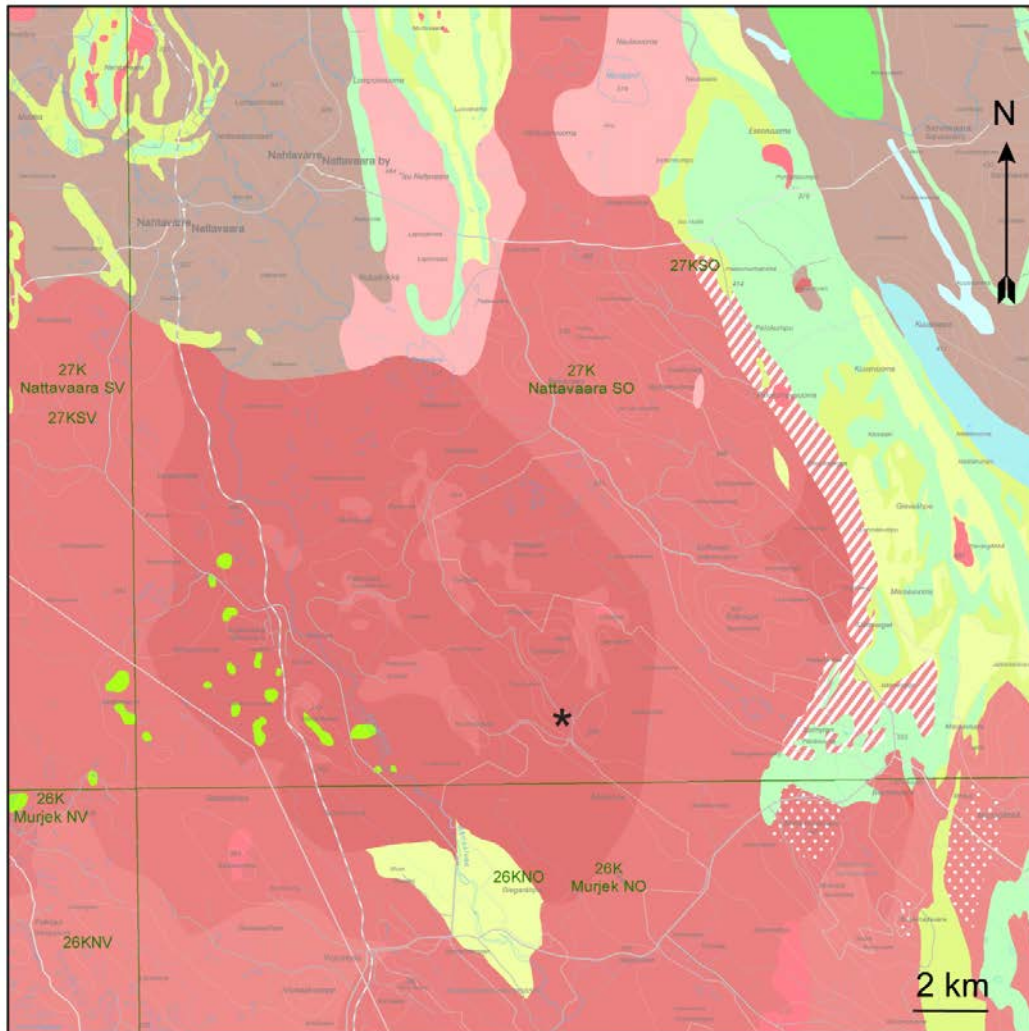


Figure 34. Bedrock map of the area, sampling location marked with black star.

Introduction

Norrbotten, Sweden is a key area of Europe for future exploration and mining. In order to establish age relations for magmatic activity and metamorphic overprinting in this area, the sampled rock was selected (Fig. 1, 2, 34). The often massive and at places foliated, potassium feldspar porphyric to uneven-grained quartz monzonite, monzonite to granite that make up a large proportion of the bedrock on the southern map areas of 27K Nattavaara, at some places show low-grade metamorphic overprinting to greenschist facies conditions (Claeson & Antal Lundin 2012, this issue). Are these coeval with the rocks interpreted as the youngest at c. 1.80 Ga age that do not display metamorphic overprinting or are they older intrusions, and if so how much older and when did the metamorphic overprinting take place?

The aim of this study is to determine the magmatic age of the quartz monzonite to monzonite at Tiurevaara map area 27K Nattavaara SO, and if there are any metamorphic overgrowths, determine these as well, since the latter might show ages for the redistribution of elements in the crust.

Sample description

The sampled quartz monzonite to monzonite is potassium feldspar porphyric to uneven-grained, medium-grained to coarse-grained, greyish red to reddish grey, massive, and often displays rapakivi texture (Fig. 35). The feldspar phenocrysts are 5 to 15 mm large (0–5 %). Biotite, opaque minerals, titanite, and apatite are accessory minerals. The rock shows low-grade metamorphic overprinting with epidote, saussurite-sericite alteration of plagioclase (15–40 %), minor alteration of biotite to chlorite, and undulose quartz (Fig. 35). The Zr content of the rock is 371 ppm. Outcrop measurement of magnetic susceptibility yielded $1\,330\text{--}3\,620 \times 10^{-5}$ SI. The quartz monzonite to monzonite displays gamma ray radiation of K = 3.8–4.4 %, U = 1.1–1.8 ppm, and Th = 5.7–13 ppm, values from ground measurements some 80 metres from the sample location. Petrophysical measurements of a sample show density at $2\,646 \text{ kg/m}^3$, magnetic susceptibility $4\,792 \times 10^{-5}$ SI, and remanent magnetization intensity of 260 mA/m.

The quartz monzonite to monzonite at Tiurevaara shows a LREE-enriched and flat HREE pattern, with a slight negative Eu anomaly (Fig. 36). The LREE enrichment is due to fractional crystallisation, the flat, unfractionated HREE pattern shows that no garnet was left in the residue at the location of magma genesis, and the Eu anomaly is indicative of plagioclase fractionation. The negative anomalies shown in the multi-element diagram of Sr is due to plagioclase fractionation, the P anomaly of apatite fractionation, and the Ti anomaly of Fe-Ti oxide fractionation (Fig. 36). The strong negative Nb anomaly and positive Pb anomaly suggest a subduction related petrogenesis (Fig. 36).

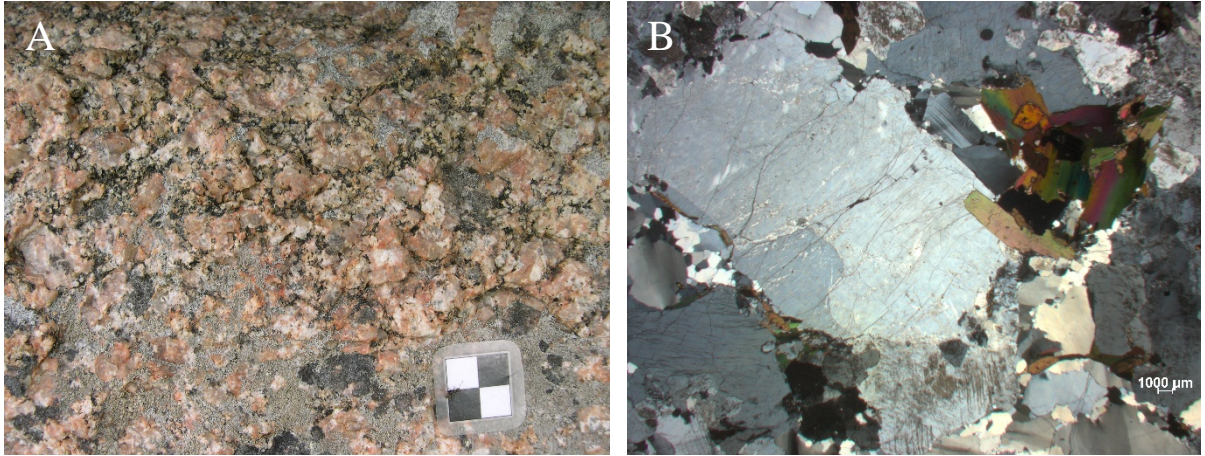


Figure 35. A. The age determined quartz monzonite to monzonite at Tiurevaara (cm-scale). **B.** Micrograph showing minor alteration and quartz recrystallisation in a potassium feldspar porphyric quartz monzonite to monzonite. Photos: Dick Claeson.

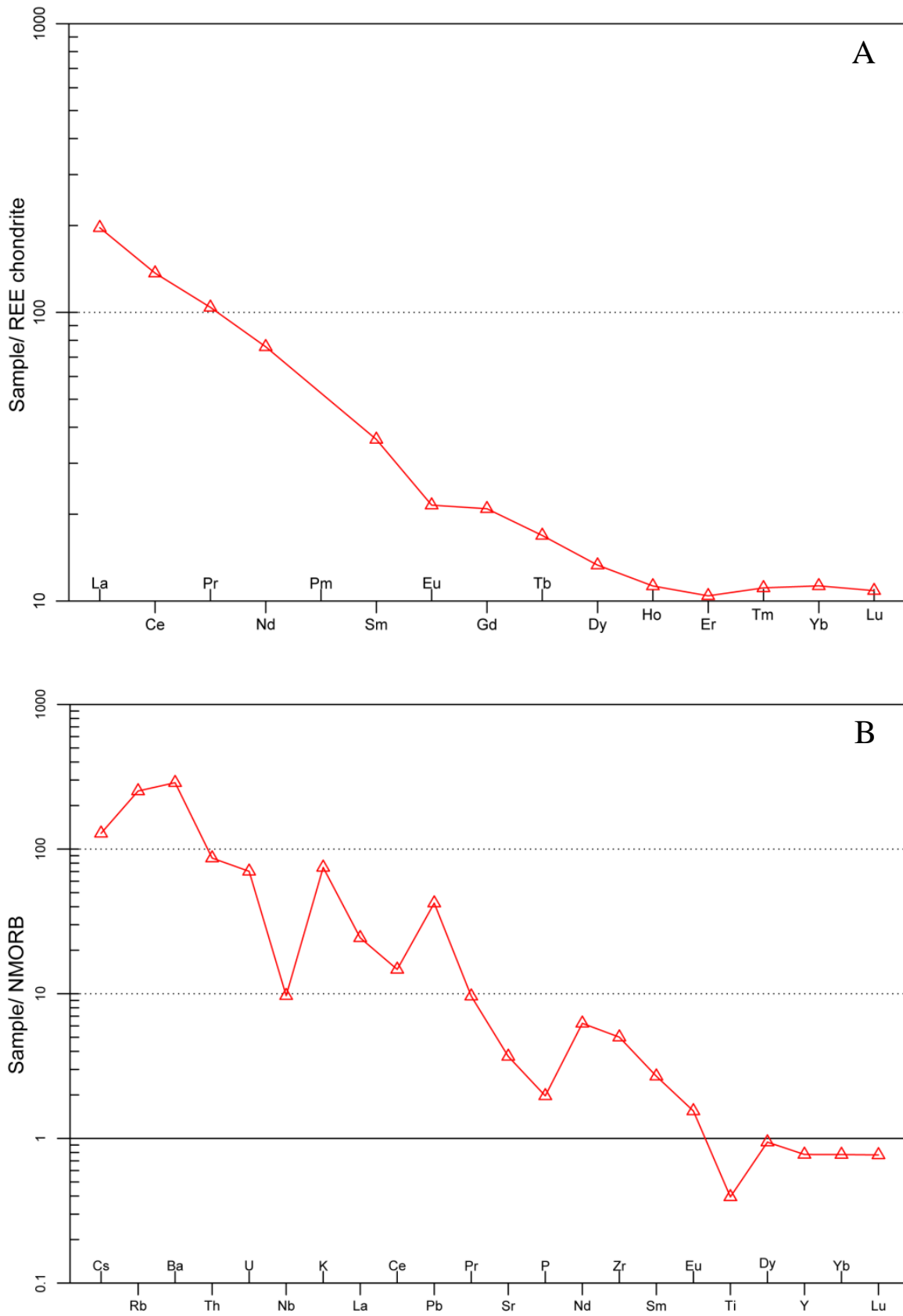


Figure 36. A. REE-diagram of quartz monzonite to monzonite. Normalizing values for chondrite from Boynton (1984). **B.** Multi-element diagram, rock as in A. Normalizing values for N-MORB from Sun & McDonough (1989).

Analytical results and interpretation of geochronological data

U-Pb zircon analyses

Zircon was extracted from a c. 0.5 kg large rock sample and U-Pb-Th analyses were made using a Laser-Ablation Sector Field Inductively Coupled Plasma Mass Spectrometer (LA-SF-ICPMS) at the Geological Survey of Denmark and Greenland (GEUS) in Copenhagen. All analytical procedures are described in the appendix of Andersson (2012).

The sample was rich in zircon (Fig. 37). The zircon are euhedral with sharp crystal terminations to sometimes slightly subhedral. They vary from short-prismatic stubby grains to long-prismatic large crystals and some are needle-shaped grains. The zircon are between 50 to more than 350–400 μm along the c-axis and have aspect ratios between 1 to more than 6. They are colourless, translucent and clear, and overall of high analytical quality; cracks and inclusions are subordinate. Complex core-rim growth relations are not observed.

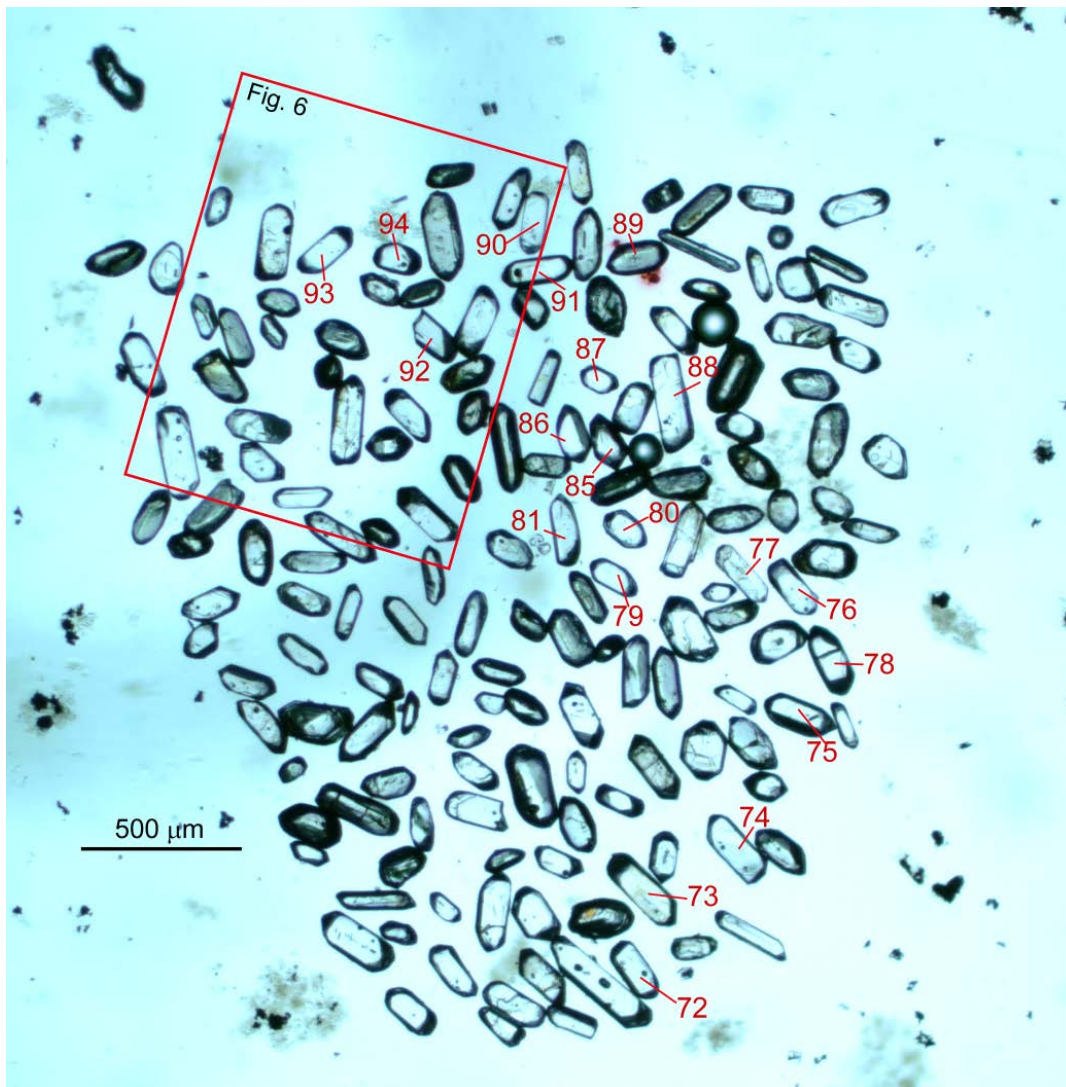


Figure 37. Optical microscope photo (plane polarized light) of representative zircon from sample DCL070228 in a polished section of the epoxy mount used for LA-SF-ICP MS analyses. Numbers refer to analytical ID in Table 13. Location of the CL image in Figure 38 is indicated with a red square.

In cathodoluminescence (CL) images, the zircon are typically oscillatory zoned (Fig. 38). The zonations vary from thinly laminated to broad banded. The outer margins are often CL-darker than the central domains, but the oscillatory zonation typically continues concordantly all the way to the crystal margin.

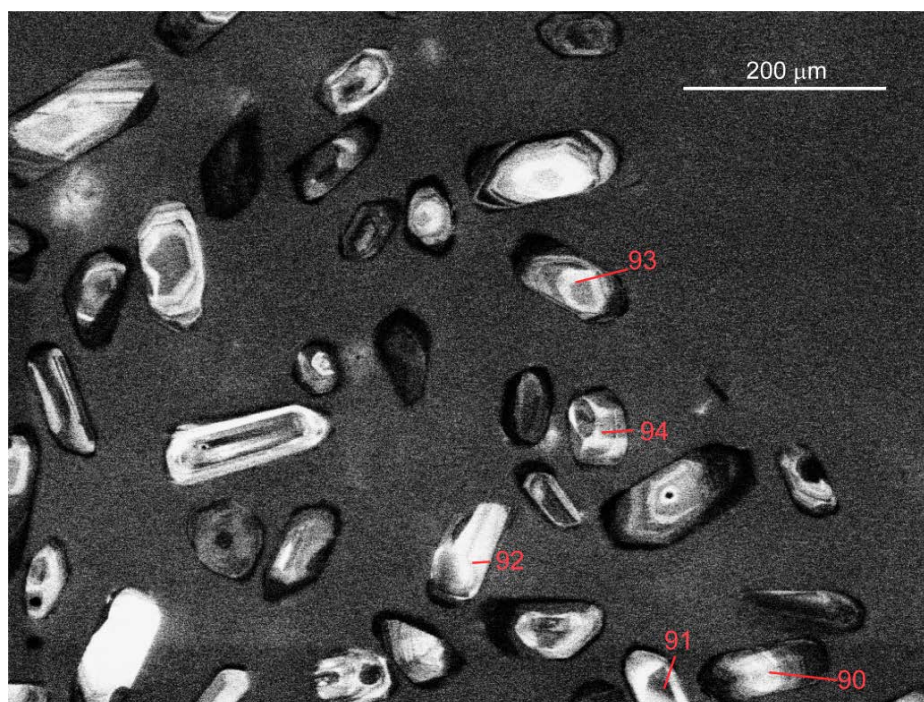


Figure 38. CL-image of detail of analysed zircon mount from sample DCL070228. Numbers refer to ID of spot analysed with LA-SF-ICP MS, cf. Table 13. The location of the CL-image area outlined in Figure 37.

Table 13. LA-SF-ICPMS U-Th-Pb zircon data from sample DCL070228.

Spot #	CL image class ^a	U ppm	Th/U calc.	²⁰⁶ Pb/ ²⁰⁴ Pb meas.	²⁰⁶ Pb/ ²³⁸ U ±2σ %	²⁰⁷ Pb/ ²⁰⁶ Pb ±2σ %	Conc. %	²⁰⁶ Pb/ ²³⁸ U ±2σ (Ma)	²⁰⁷ Pb/ ²⁰⁶ Pb ±2σ (Ma)				
72	CLG bb zon	57	0.76	5938	0.318	3.26	0.110	2.78	100	1782	51	1794	51
73	CLD-CLG bb zon	52	0.94	1131	0.389	2.52	0.111	3.77	108	2119	45	1812	69
74	CLG CLD osc zon	104	0.77	1396	0.299	2.42	0.111	2.60	97	1688	36	1808	47
75	CLG CLD osc zon	118	0.67	3930	0.315	2.35	0.110	1.73	99	1763	36	1794	32
76	CLB CLG osc zon	70	0.96	1756	0.336	3.55	0.109	2.10	102	1870	58	1780	38
77	CLG CLD bb zon	235	0.56	17283	0.304	2.56	0.111	2.51	97	1713	38	1818	46
78	CLB CLD bb zon	74	0.48	68024	0.329	6.73	0.110	3.81	101	1834	107	1795	69
79	CLB CLD bb zon	67	0.89	1564	0.318	2.60	0.111	2.81	99	1780	40	1815	51
80	CLB CLD osc zon	81	0.88	4895	0.313	3.41	0.109	3.35	99	1758	53	1790	61
81	CLG bb zon	119	0.71	22717	0.315	4.33	0.109	2.17	100	1767	67	1784	40
85	CLB osc zon	66	0.69	27912	0.309	4.12	0.108	2.49	99	1735	63	1771	46
86	CLB CLG bb zon	71	0.78	1692	0.302	5.47	0.109	3.34	98	1703	82	1781	61
87	CLB CLG bb zon	75	0.79	10112	0.300	4.13	0.109	3.65	98	1691	61	1775	67
88	CLG bb zon	123	0.6	4136	0.316	3.97	0.110	3.61	99	1769	61	1806	66
89	CLB CLG bb zon	94	0.82	5220	0.320	2.28	0.109	2.39	100	1789	36	1784	44
90	CLB CLD bb zon	104	0.76	7605	0.325	2.58	0.112	3.30	99	1812	41	1840	60
91	CLB CLG bb zon	102	0.98	8292	0.311	3.41	0.110	2.59	99	1746	52	1798	47
92	CLB CLG bb zon	59	0.84	2189	0.296	2.89	0.109	2.83	97	1673	43	1779	52
93	CLG CLD osc zon	88	0.58	9531	0.336	2.56	0.110	1.78	102	1867	42	1792	32
94	CLB CLG osc zon	55	0.72	7151	0.329	4.06	0.109	3.14	101	1835	65	1787	57

a) Abbreviations: CLG=CL-grey; CLD=CL-dark; CLB=CL-bright; osc=oscillatory; zon=zonation
bb=broad banded; data discarded from age calculation shown in italic (burned through sample)

Results

Twenty analytical spots were placed in 20 different zircon crystals. The analysed crystals are shown in Figure 37. CL-images of representative grains analysed are shown in Figure 38. The analytical data are given in Table 13. The analysed zircon have U-contents between 57 and 235 ppm, and Th/U ratios vary from 0.48 to 0.98, values common for igneous zircon (Hanchar & Hoskin 2003). Five analyses were omitted from age calculation. Three analyses (77, 90, 92) were discarded since the laser burned through the sample during data acquisition and two analyses (73, 74) were discarded due to high common Pb content. The latter analyses have $^{206}\text{Pb}/^{204}\text{Pb}$ ratios below 1 500 and both are significantly discordant (analysis 73 is strongly reversely discordant). Together the remaining 15 analyses define a concordia age of $1\,788 \pm 13$ Ma, with an MSWD of concordance and equivalence of 1.8 (Fig. 39). The weighted average $^{207}\text{Pb}/^{206}\text{Pb}$ age for the same 15 analyses is $1\,789 \pm 12$ Ma (MSWD=0.21; Fig. 40). The crystal morphology, internal growth textures and the U-Th-Pb isotopic analyses of zircon in sample DCL070228 demonstrate that the sample is composed of igneous zircon that show no or negligible post-crystallisation disturbance. Igneous crystallisation of sample DCL070228 is here best constrained by the concordia age at $1\,788 \pm 13$ Ma.

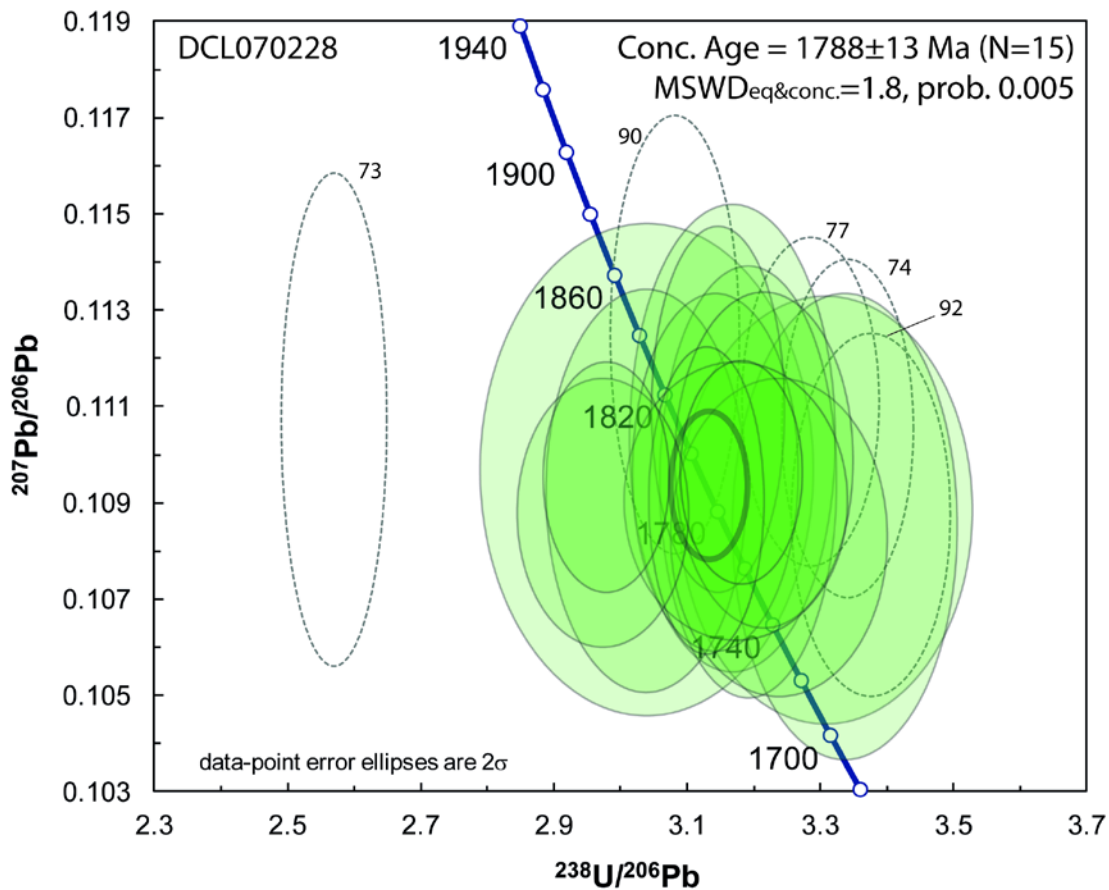


Figure 39. Tera-Wasserburg concordia plot of the 20 zircon U-Pb LA-SF-ICP MS analyses obtained from sample DCL070228. Error ellipses shown with dashed lines denote data omitted from age calculation and their spot ID numbers are indicated in the Figure.

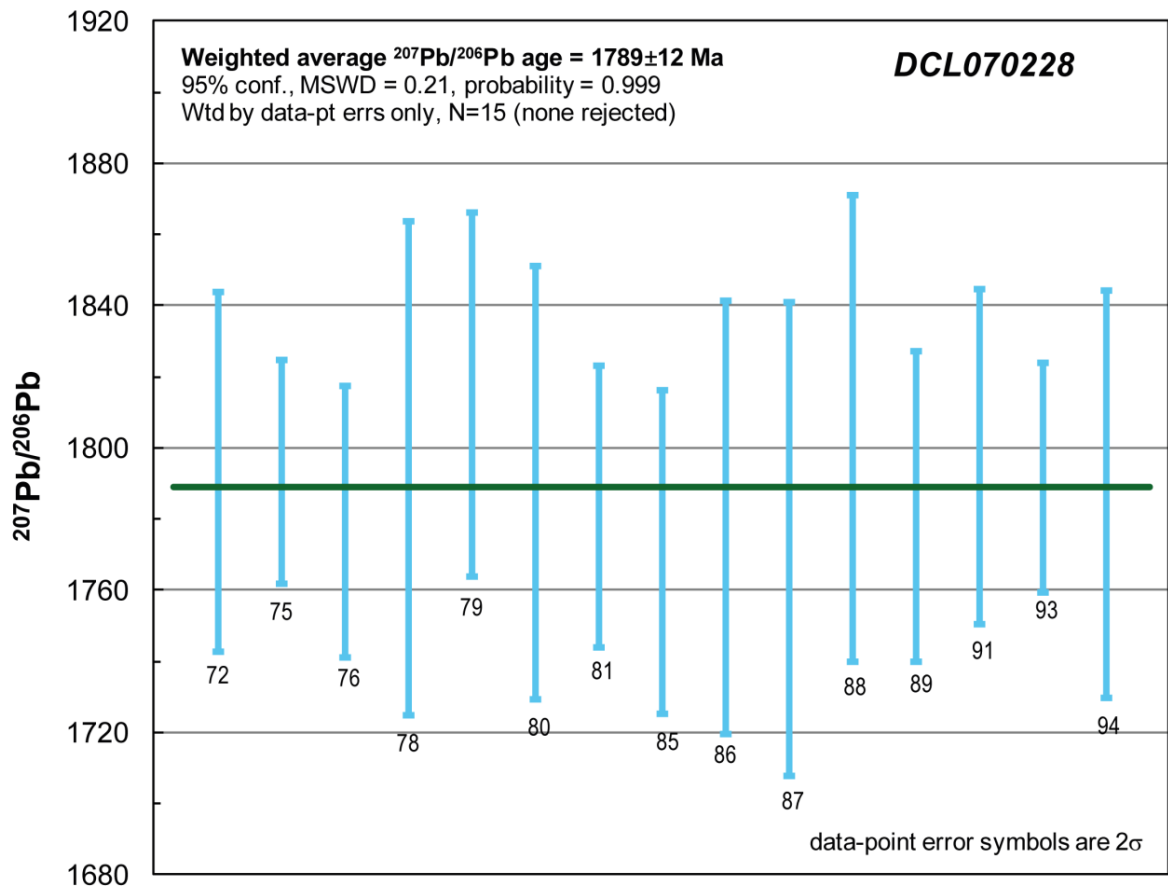


Figure 40. Plot of $^{207}\text{Pb}/^{206}\text{Pb}$ ages in Ma for the twenty analyses obtained from zircon in sample DCL070228. Weighted average $^{207}\text{Pb}/^{206}\text{Pb}$ age is shown as green horizontal line. Numbers refer to ID of spot analysed with LA-SF-ICP MS, cf. Table 13.

Discussion and conclusion

During the mapping of the 27K Nattavaara map area, foliated porphyric rocks located outside the largest, fully preserved and youngest intrusions, were age determined to about 10–15 million years older than these (this issue). In analogy with the observations and age data, the youngest and contemporary magmatic as well as tectonic activity gave rise to the deformation and greenschist facies metamorphism observed in the somewhat older separate intrusions or older parts of the younger, i.e., multiple intrusions that form over millions of years. To some extent, however, the observed deformations may be due to internal movements in the magma along cool contact zones that later were overprinted by new injections of magma. The results were integrated in the mapping of the 27K Nattavaara area (Claeson & Antal Lundin 2012). Summary of sample data is given in Table 14.

Table 14. Summary of sample data.

Rock type	Quartz monzonite to monzonite
Lithotectonic unit	Norrbottnen lithotectonic unit of the Svecokarelian orogen
Lithological unit	
Sample number	DCL070228
Lab_id	DCL070228
Coordinates	7402757/772018 (Sweref99TM)
Map sheet	27K Nattavaara SO (RT90)
Locality	Tiurevaara
Project	Mellersta Norrbotten (80010)

References

- Andersson, J. (ed.) 2012: U-Pb zircon geochronology of granitic and syenitoid rocks across the southern part of the Sveconorwegian orogen. *Sveriges geologiska undersökning SGU-rapport 2012:14*, appendix p. 26.
- Boynton, W.V., 1984: Cosmochemistry of the Rare Earth Elements: Meteorite studies. In P. Henderson (ed.): *Rare earth element geochemistry*. Elsevier Science B.V. 63–114.
- Claeson, D. & Antal Lundin, I., 2012: Beskrivning till berggrundskartorna 27K Nattavaara NV, NO, SV & SO. *Sveriges geologiska undersökning K 383–386*, 22 pp.
- Hanchar J.M. & Hoskin P.W.O. (eds.), 2003: Zircon. *Reviews in Mineralogy and Geochemistry*, vol. 53, *Mineralogical Society of America/Geochemical Society*. 500 pp.
- Sun, S.S. & McDonough, W.F., 1989: Chemical and isotopic systematic of oceanic basalts: implications for mantle composition and processes. In A.D. Saunders & M.J. Norry (eds.): *Magmatism in ocean basins*. Geological Society of London, Special Publication 42, 313–345.

U-Pb ZIRCON AGE OF MONZONITE TO SYENITE AT AHMAVAARA, CLOSE TO THE AITIK ORE DEPOSIT, NORRBOTTEN COUNTY

Authors: Dick Claeson, Ildikó Antal Lundin, Jenny Andersson & Anders Scherstén¹

¹Department of geology, Lund University, Sölvegatan 12, SE-223 62 Lund, Sweden

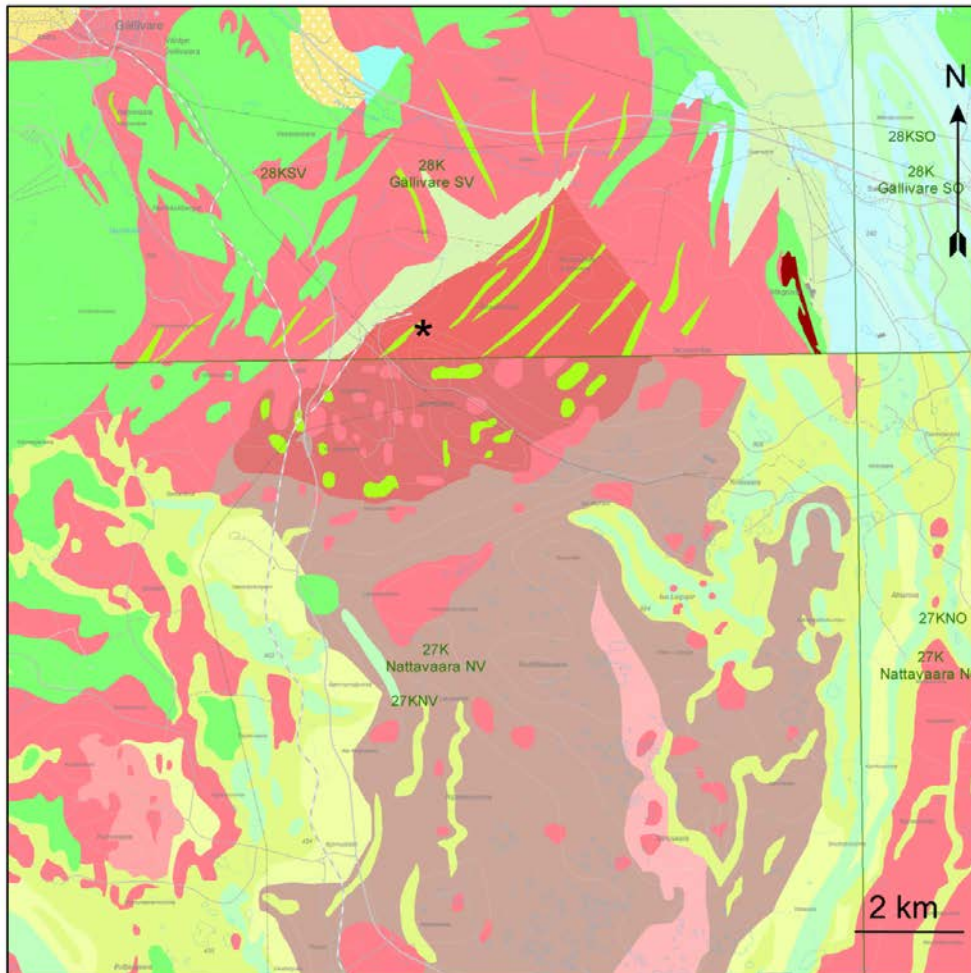


Figure 41. Bedrock map of the area, sampling location marked with black star.

Introduction

Knowledge of the magmatic activity close to a world-class deposit as the large volume, low grade porphyry-style copper-gold-silver ore at Aitik (Boliden Annual Report 2015), is vital in order to understand all aspects of its genesis. An earlier map of 28K Gällivare SV from SGU shows the magmatic age of the sampled rock as related to the Perthite-monzonite suite and intruded by dolerite dikes (Witschard 1996, Fig. 41, 42). The well-preserved field appearance of the rocks within this unit compared to the subvolcanic quartz monzodiorite at Aitik, 5km to the east and dated at $1\,887 \pm 8$ Ma (Wanhainen et al. 2006), suggested a relatively younger age than the Perthite-monzonite suite (1.88–1.87 Ga) to us.

The above was the main reason to request an age determination of these rocks, while carrying out mapping of the 27K Nattavaara NV, where no major outcrops were present. From the geophysical data it is obvious that the anomaly and thus the rock unit occurs on both map areas (Fig. 42). The aim of this study is to determine the magmatic age of the monzonite to syenite at Ahmavaara map area 28K Gällivare SV, and in the event that there are any metamorphic overgrowths, determine these as well, since the latter might show ages for the redistribution of elements in the crust.

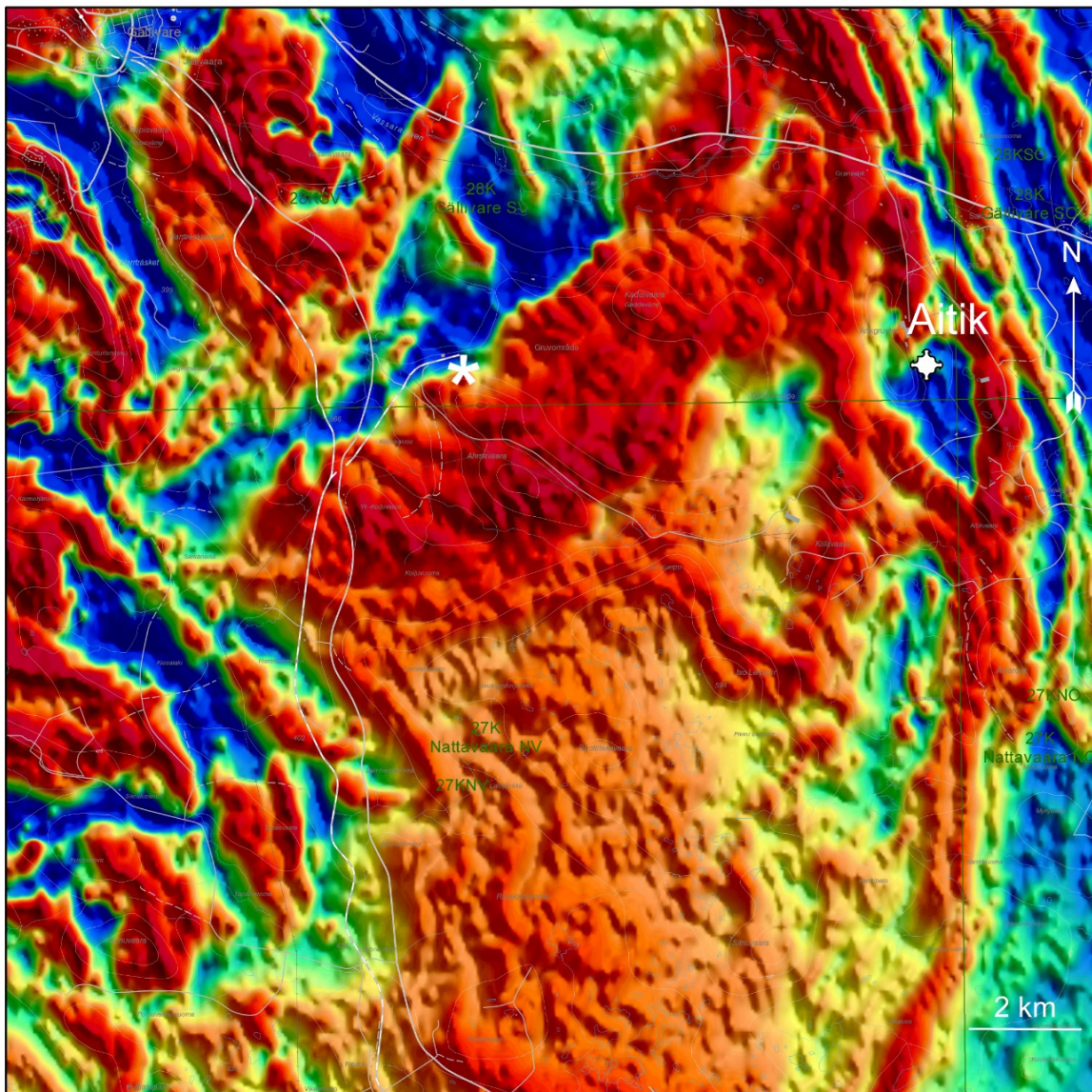


Figure 42. Magnetic anomaly map. Sampling site shown as white star and the Aitik ore deposit as white symbol.

Sample description

The sampled monzonite to syenite is from an outcrop at Ahmavaara close to the Aitik mine waste dam. It is medium-grained to coarse-grained, uneven grained to weakly porphyric with feldspar 5 to 15 mm (0–5 %), and purple tinted in colour (Fig. 43A). The monzonite to syenite occurs as relatively small parts within monzonite, monzodiorite, quartz monzonite to granite, which are medium-grained to coarse-grained, porphyric to uneven-grained, greyish red to reddish grey, massive and often display rapakivi texture as plagioclase-mantled K-feldspar phenocrysts (Fig. 43B, C). Larger areas of two-pyroxene monzogabbro are intermingled with the porphyric acid rocks (Fig. 43D). The monzogabbro displays darkly pigmented, inclusion-rich plagioclase. All rocks show contact relations that are interpreted as the rocks are coeval, lacking chilled margins, displaying mingling structures, and are thus of a bimodal magmatic nature (Fig. 43B).

The monzonite to syenite displays $K = 4.5 \%$, $U = 1.2 \text{ ppm}$, and $Th = 4.9 \text{ ppm}$, whereas the K-feldspar porphyric quartz monzonite to granite with rapakivi texture shows $K = 4.3\text{--}4.5 \%$, $U = 10 \text{ ppm}$, $Th = 13 \text{ ppm}$ and the monzogabbro around $K = 2.5 \%$. Outcrop measurement of magnetic susceptibility yielded for monzonite to syenite $3\ 200\text{--}3\ 790 \times 10^{-5} \text{ SI}$, K-feldspar porphyric quartz monzonite to granite $2\ 540\text{--}4\ 280 \times 10^{-5} \text{ SI}$, and monzogabbro $3\ 580\text{--}11\ 600 \times 10^{-5} \text{ SI}$. The high susceptibility values correlate well with the high magnetic anomalies on the magnetic anomaly map (Fig. 42)

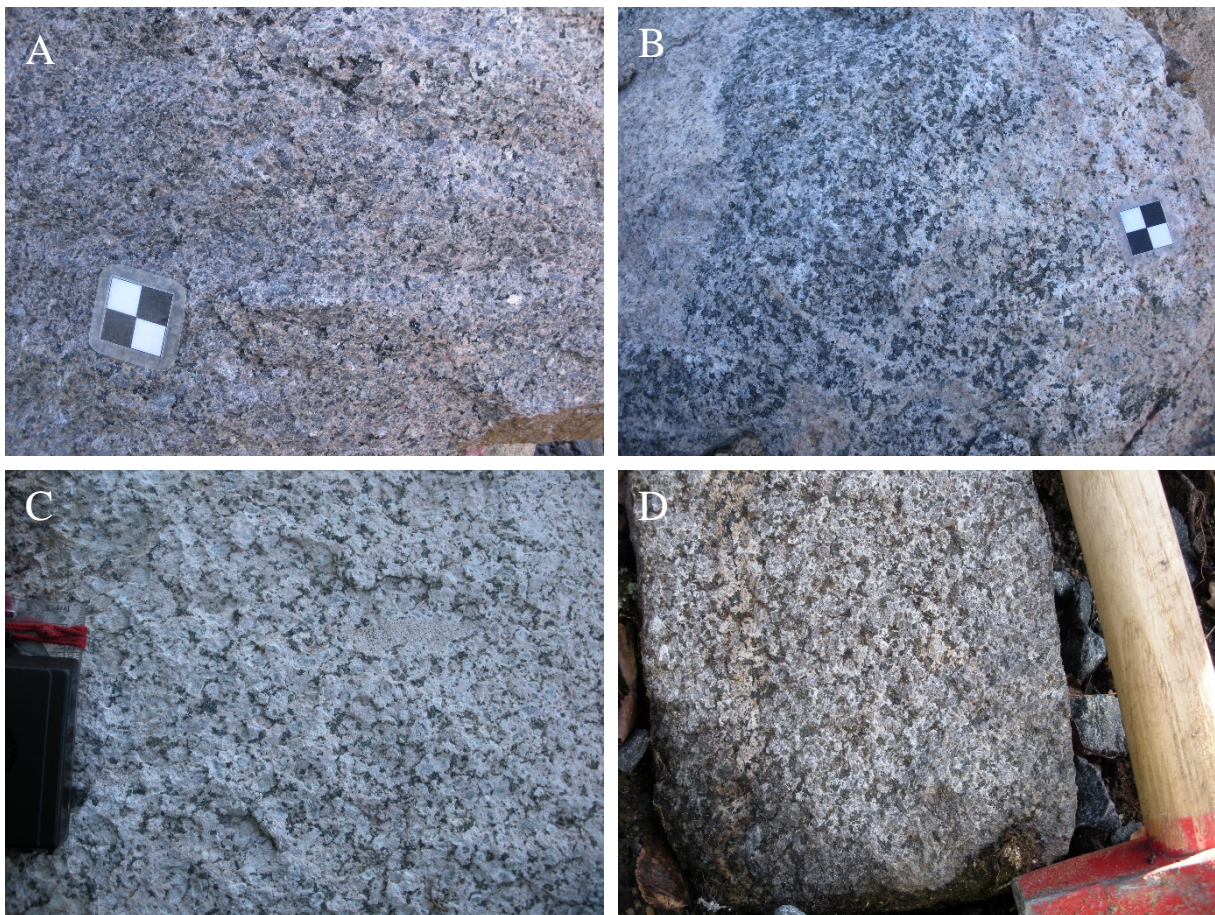


Figure 43. A. The age determined monzonite to syenite at Ahmavaara (7451266/751456, cm-scale). B. Mingling relation between monzonite to syenite and monzodiorite (7451266/751456). C. K-feldspar porphyric quartz monzonite to granite with rapakivi texture (7451147/751475). D. Massive two-pyroxene monzogabbro at Ahmavaara (7451164/750734). Photos: Dick Claeson.

Analytical results and interpretation of geochronological data

U-Pb zircon analyses

Zircon was extracted from a c. 0.5 kg large rock sample and U-Pb-Th analyses were made using a Laser-Ablation Sector Field Inductively Coupled Plasma Mass Spectrometer (LA-SF-ICPMS) at the Geological Survey of Denmark and Greenland (GEUS) in Copenhagen. All analytical procedures are described in the appendix of Andersson (2012).

The sample was rich in zircon crystals (Fig. 44). The zircon are dominated by large clear, colourless fragments where some grains are up to 500 μm in size. Well-developed prisms are rare, but the crystals do not have rounded terminations. The grains are of high analytical quality; cracks and inclusions are subordinate. Complex core-rim growth relations are not observed. The character of the zircon in the sample resembles zircon typically found in mafic and intermediate intrusive rocks (Hanchar & Hoskin 2003).

In cathodoluminescence (CL) images, the zircon are typically CL-grey to CL-dark with weak broad-banded zonation, some grains display well-developed, narrower oscillatory zonation (Fig. 45). The grains are overall homogeneously zoned throughout the exposed crystal.

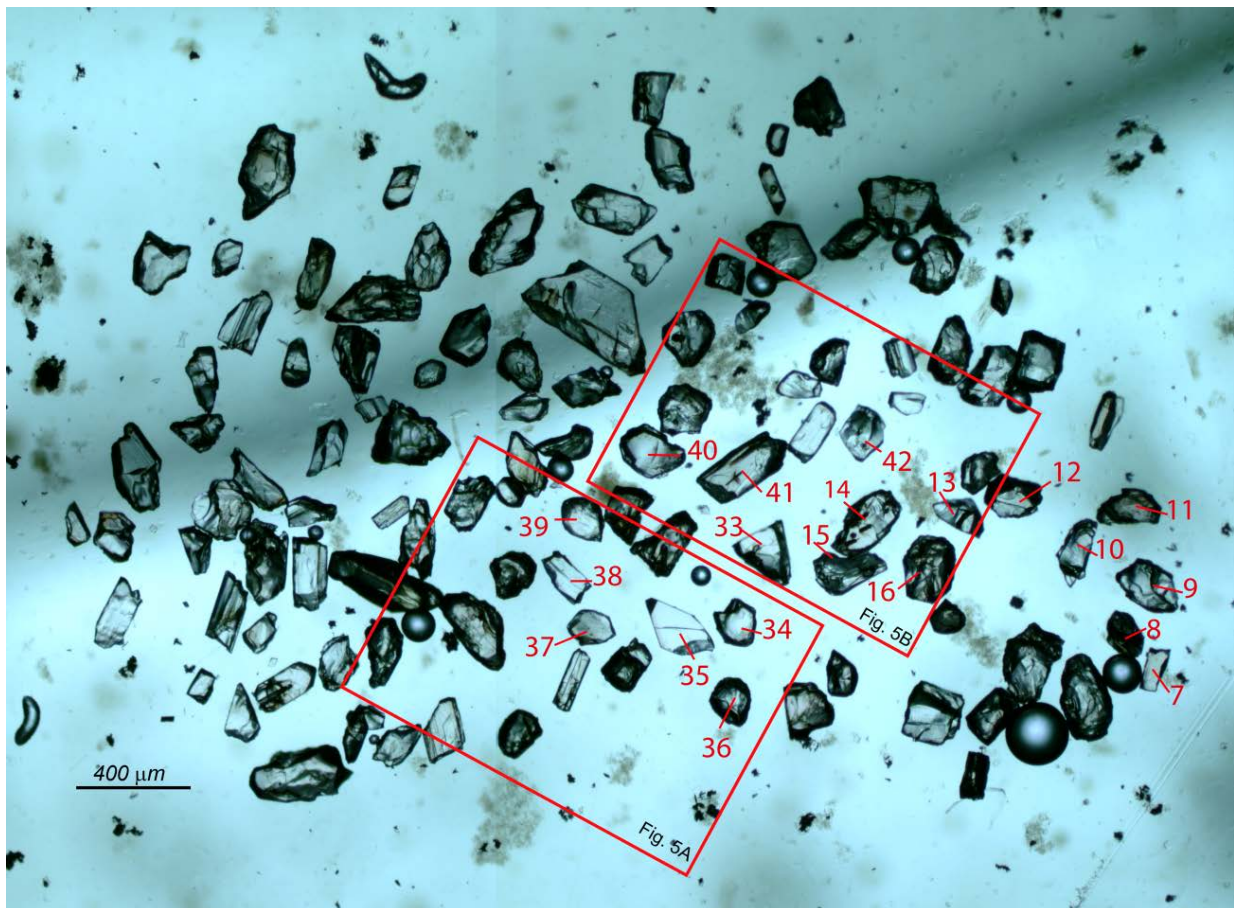


Figure 44. Optical microscope photo (plane polarized light) of representative zircon from sample DCL080047 in a polished section of the epoxy mount used for LA-SF-ICP MS analyses. Numbers refer to analytical ID in Table 15. Locations of the CL-images in Figure 45 are indicated with red squares.

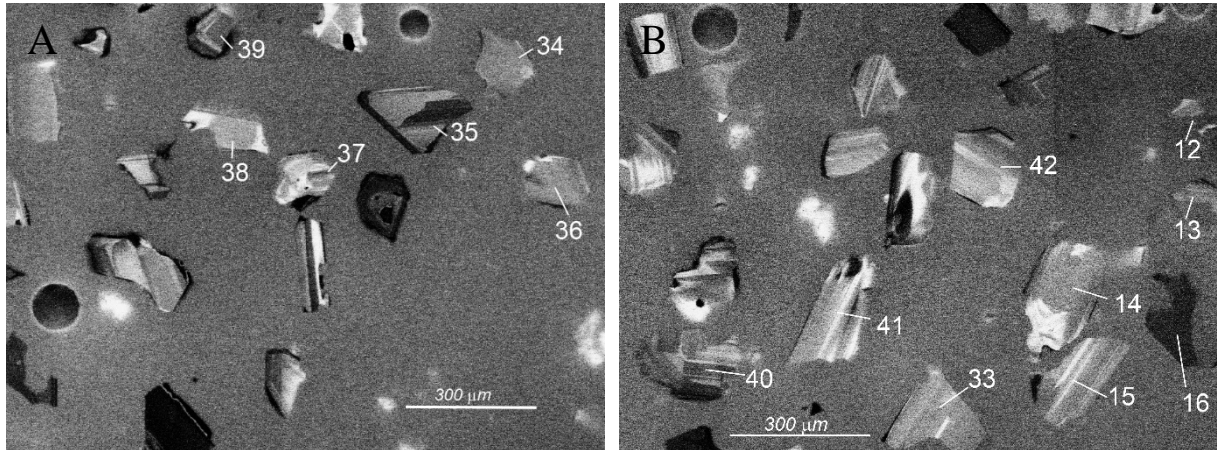


Figure 45. A and B. CL-image of detail of analysed zircon mount from sample DCL080047. Numbers refer to ID of spot analysed with LA-SF-ICP MS, cf. Table 15. The location of the CL-images area outlined in Figure 44.

Table 15. LA-SF-ICPMS U-Th-Pb zircon data from sample DCL080047.

Spot #	CL image class ^a	U ppm	Th/U calc.	²⁰⁶ Pb/ ²⁰⁴ Pb meas.	²⁰⁶ Pb/ ²³⁸ U ±2σ %	²⁰⁷ Pb/ ²⁰⁶ Pb ±2σ %	Conc. %	²⁰⁶ Pb/ ²³⁸ U (Ma) ±2σ	²⁰⁷ Pb/ ²⁰⁶ Pb (Ma) ±2σ				
7	CLD-G wk zon	90	0.36	4162	0.291	2.75	0.112	2.68	95	1648	40	1836	44
8	CLD uz	220	0.87	19398	0.301	3.32	0.110	1.82	97	1697	51	1798	30
9	CLG osc zon	115	0.82	40639	0.304	1.64	0.110	1.82	97	1710	24	1807	40
10	CLG uz	122	0.66	4303	0.320	2.19	0.110	1.82	100	1790	33	1792	39
11	<i>CLG bb zon</i>	<i>159</i>	<i>0.78</i>	<i>2750</i>	<i>0.311</i>	<i>2.89</i>	<i>0.120</i>	<i>4.17</i>	<i>95</i>	<i>1745</i>	<i>42</i>	<i>1956</i>	<i>75</i>
12	CLD uz	270	0.98	33541	0.306	2.61	0.110	0.91	98	1723	39	1802	23
13	CLG wk zon	184	0.75	15235	0.312	1.60	0.110	0.91	99	1748	26	1805	21
14	CLG wk zon	124	1.08	6539	0.312	2.56	0.111	0.90	98	1751	40	1822	22
15	CLG osc zon	114	0.81	3145	0.308	1.95	0.110	2.73	98	1731	30	1804	43
16	CLD-G bb zon	296	0.99	18068	0.306	1.96	0.111	1.80	97	1720	31	1819	27
33	CLG bb zon	196	1.09	10266	0.318	2.20	0.111	1.80	99	1778	34	1811	35
34	CLG uz	122	1.04	14926	0.317	1.58	0.111	1.80	99	1774	26	1808	34
35	CLG bb zon	159	1.00	12981	0.297	4.04	0.109	1.83	97	1674	60	1784	25
36	CLG wk zon	121	0.95	8327	0.310	1.94	0.110	1.82	98	1742	29	1805	34
37	CLG osc zon	106	0.82	13635	0.299	3.01	0.110	2.73	97	1685	47	1794	42
38	CLG bb zon	113	0.82	4065	0.313	1.60	0.110	1.82	99	1756	24	1803	31
39	CLG osc zon	136	0.92	5203	0.306	2.29	0.110	2.73	98	1722	35	1802	46
40	CLG osc zon	116	0.65	5723	0.319	1.88	0.113	2.65	99	1784	31	1843	42
41	CLG osc zon	104	0.90	4126	0.306	2.61	0.110	1.82	98	1723	40	1806	29
42	CLG osc zon	105	0.79	9843	0.314	2.55	0.110	1.82	99	1758	40	1796	30

a) Abbreviations: CLG=CL-grey; CLD=CL-dark; osc=oscillatory; zon=zonation; bb=broad banded; uz=unzoned; wk=weak; data discarded from age calculation shown in italic

Results

Twenty analytical spots were placed in 20 different zircon crystals. An optical microscope image of the analysed crystals is shown in Figure 44. CL-images of representative grains analysed are shown in Figure 45. The analytical data is given in Table 15. The analysed zircon have U-contents from 90 to 296 ppm, and Th/U ratios between 0.36 and 1.09, values commonly reported for igneous zircon (Hanchar & Hoskin 2003). One analysis plots significantly discordant off the concordia (analysis 11). It has the lowest $^{206}\text{Pb}/^{204}\text{Pb}$ ratio among the analysed spots, below 3 000, and was omitted from age calculation (Fig. 46). The remaining 19 analyses plot at or closely to the right of the concordia in a more or less coherent horizontal array. The spread of the data points does not allow calculation of a common concordia age but the horizontal spread of the data points in the Tera-Wasserburg diagram suggests no or negligible ancient disturbance of the U-Pb system. The observed spread in the data set reflects recent Pb-loss or problems with data correction.

Together the remaining 19 analyses define a weighted average $^{207}\text{Pb}/^{206}\text{Pb}$ age of $1\,806 \pm 7$ Ma (MSWD = 0.71, probability = 0.8, 95 % conf., Fig. 47). The crystal morphology, internal growth textures, and the U-Th-Pb isotopic analyses of zircon in sample DCL080047 show that the sample is composed of igneous zircon with no or negligible post-igneous crystallisation disturbance. Therefore, igneous crystallisation of sample DCL080047 is here constrained at $1\,806 \pm 7$ Ma.

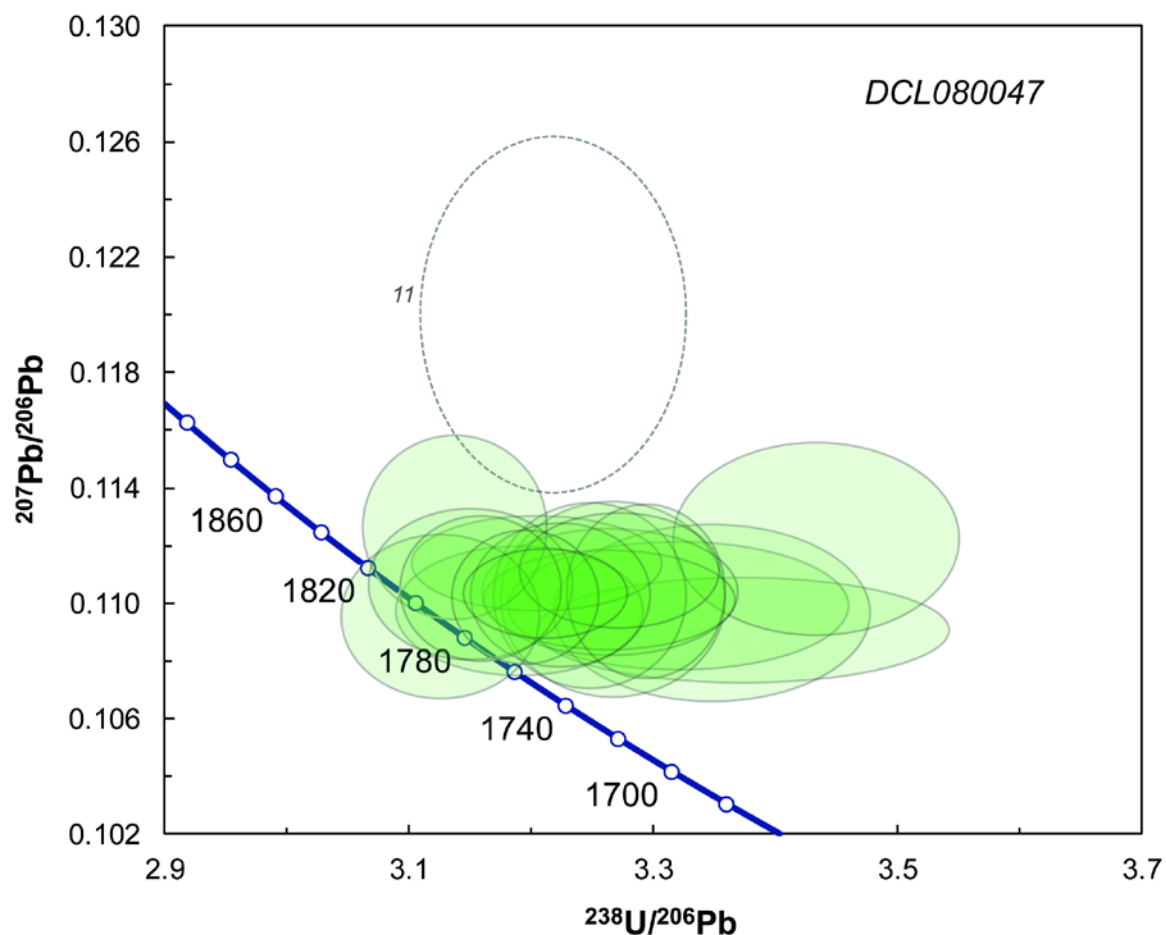


Figure 46. Tera-Wasserburg concordia plot of the 20 zircon U-Pb LA-SF-ICP MS analyses obtained from sample DCL080047. Error ellipse shown with a dashed line denote omitted data point 11.

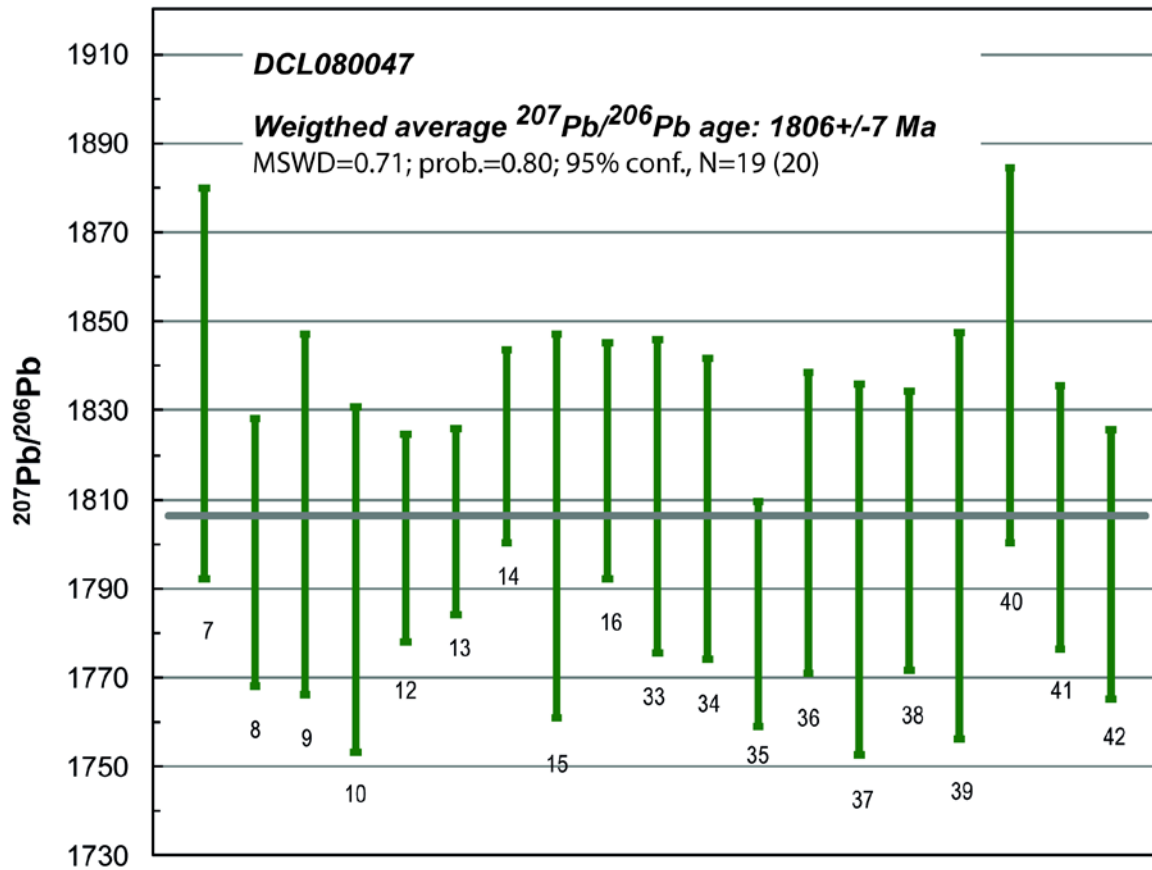


Figure 47. Plot of $^{207}\text{Pb}/^{206}\text{Pb}$ ages in Ma for 19 analyses obtained from zircon in sample DCL080047. Weighted average $^{207}\text{Pb}/^{206}\text{Pb}$ age is shown as grey horizontal line. Numbers refer to ID of spot analysed with LA-SF-ICP MS, cf. Table 15.

Discussion and conclusion

A protracted period of magmatic, hydrothermal, and metamorphic activity in the Aitik area is evident through Re–Os dating of molybdenite and U–Pb dating of titanite (Wanhainen et al. 2005). At Ahmavaara c. 7 km west of Aitik, there is a larger area with well-preserved feldspar porphyritic monzonite to monzodiorite. Small amounts of syenitic rocks are present and show gradual transitions to monzonite (Claeson & Lundin 2012). Together with these rocks, there is a monzogabbro showing mingling and mixing structures with the latter and thus interpreted as coeval and thus a bimodal magmatism is evident. Well-exposed outcrops of these rock associations are at the Aitik mine tailings pond.

The U–Pb zircon age determination of a monzonite to syenite from the site at the Aitik mine tailings pond indicates a formation age of about $1\,806 \pm 7$ Ma. This shows that these massive rocks are not related to the Perthite-monzonite suite as suggested by e.g. Witschard (1996, Fig. 41) but a 1.80 Ga old bimodal magmatic event. From the aeromagnetic geophysical data it is inferred that these intrusions might not be further away than a couple of km from the Aitik mine at the surface (Fig. 42).

The bimodal nature, having a basic component, is adding thermal influence on the surroundings at the magmatic stage as well. These facts should be used in future work to explain the protracted period of activity in the ore zone of Aitik. Other occurrences of this bimodal magmatism at c. 1.80 Ga may possibly be used for future exploration in the whole area, where one is looking for multiple remobilizations of ore elements or minerals through heat and hydrothermal input from magmatism.

The results were integrated in the mapping of the 27K Nattavaara area (Claeson & Antal Lundin 2012). However, the bedrock database at SGU is not harmonized in the area yet as is evident in Figure 41, where the new age relations are seen in the geology of the map sheet Nattavaara but not in the map sheet Gällivare to the north. Summary of sample data is given in Table 16.

Table 16. Summary of sample data.

Rock type	Monzonite to syenite
Lithotectonic unit	Norrbotten lithotectonic unit of the Svecokarelian orogen
Lithological unit	
Sample number	DCL080047
Lab_id	DCL080047
Coordinates	7451266/751456 (Sweref99TM)
Map sheet	28K Gällivare SV (RT90)
Locality	Ahmavaara
Project	Mellersta Norrbotten (80010)

References

- Andersson, J. (ed.) 2012: U-Pb zircon geochronology of granitic and syenitoid rocks across the southern part of the Sveconorwegian orogen. *Sveriges geologiska undersökning SGU-rapport 2012:14*, appendix p. 26.
- Boliden Annual Report 2015, 124 pp.
- Claeson, D. & Antal Lundin, I., 2012: Beskrivning till berggrundskartorna 27K Nattavaara NV, NO, SV & SO. *Sveriges geologiska undersökning K 383–386*, 22 pp.
- Hanchar J.M. & Hoskin P.W.O. (eds.), 2003: Zircon. *Reviews in Mineralogy and Geochemistry*, vol. 53, Mineralogical Society of America/Geochemical Society. 500 pp.
- Wanhainen, C., Billström, K., Martinsson, O., Stein, H. and Nordin, R., 2005. 160 Ma of magmatic/hydrothermal and metamorphic activity in the Gällivare area: Re–Os dating of molybdenite and U–Pb dating of titanite from the Aitik Cu–Au–Ag deposit, northern Sweden. *Mineralium Deposita* 40, 435–447.
- Wanhainen, C. Billström, K. & Martinsson, O., 2006: Age, petrology and geochemistry of the porphyritic Aitik intrusion, and its relation to the disseminated Aitik Cu-Au-Ag deposit, northern Sweden. *GFF* 128, 273–286.
- Witschard, F., 1996: Berggrundskartan 28K Gällivare SV 1:50 000. *Sveriges geologiska undersökning Ai 100*.

MAP SHEET 27J PORJUS SV AREA

Four rocks were sampled for age determination, two volcanic and two intrusive, in order to better constrain the mapping effort and contribute to new data and knowledge of the magmatic events in the area.

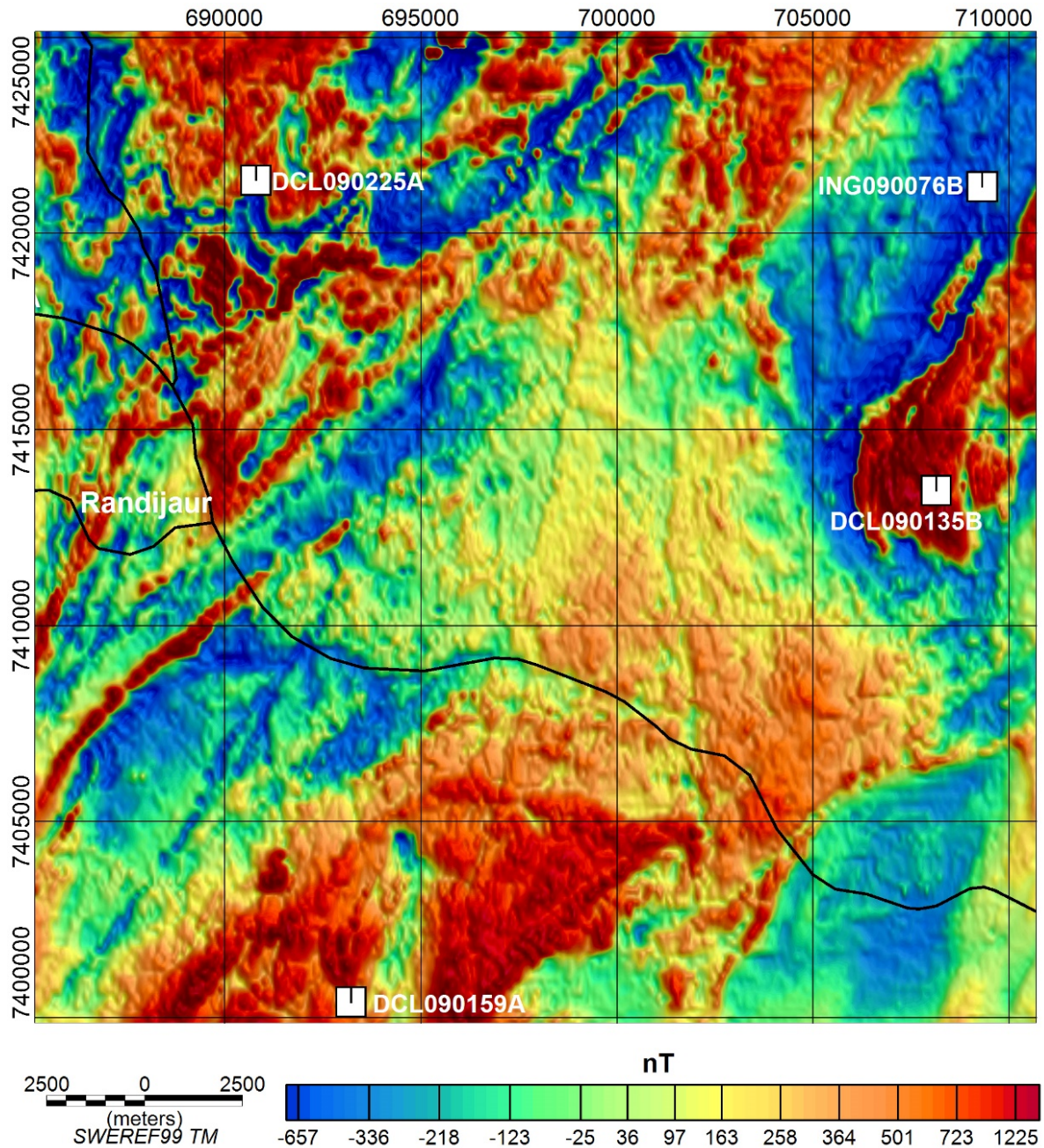


Figure 48. Magnetic total field after subtraction of the geomagnetic reference field (DGRF 1965.0) over the map area 27J Porjus SV. The sample locations are shown with white rectangles.

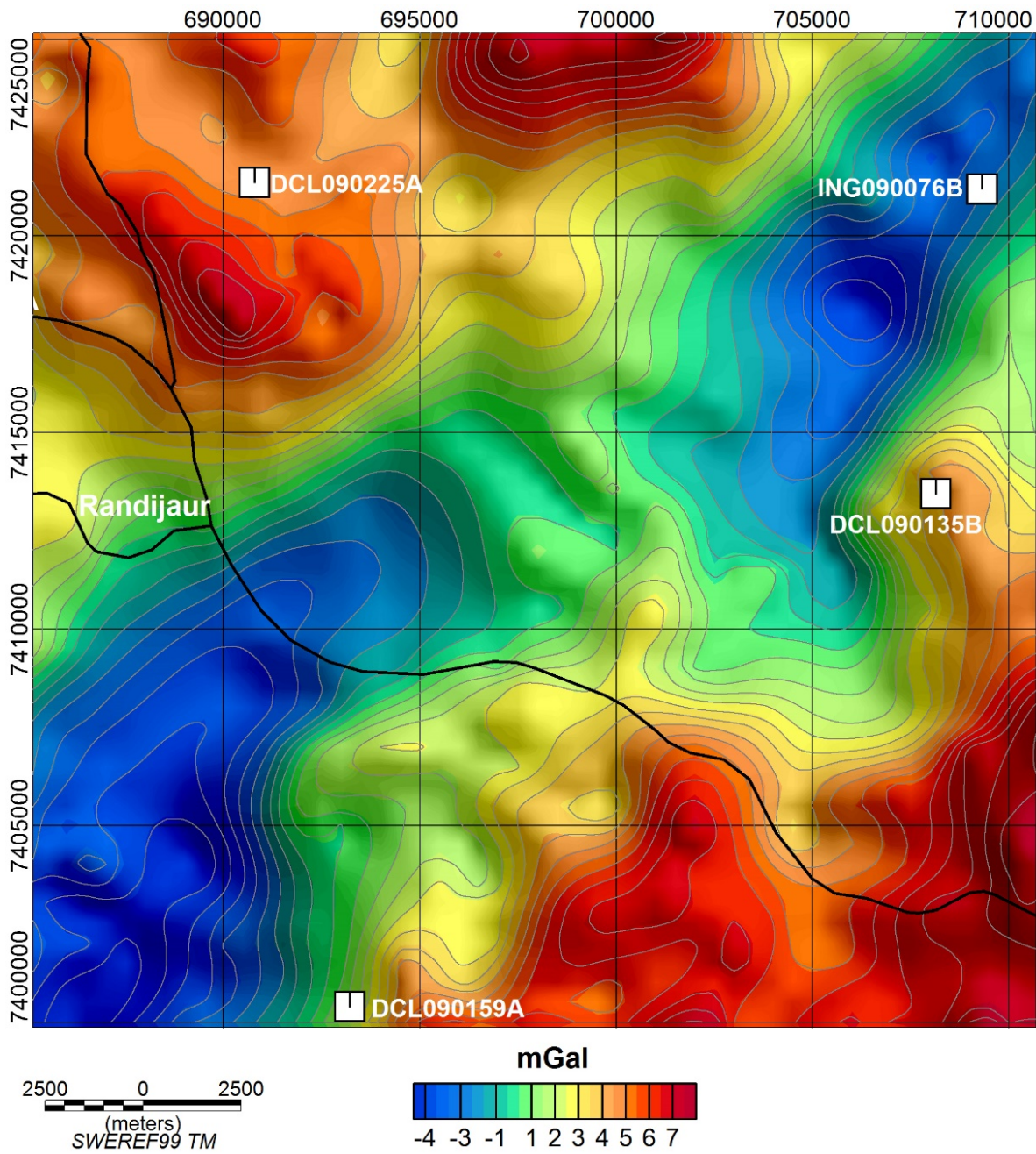


Figure 49. Residual gravity anomaly map over the map sheet 27J Porjus SV. Sample locations are shown with white rectangles.

U-Pb ZIRCON AGE OF QUARTZ TRACHYTE TO RHYOLITE AT ST. SAMONÅIVE, MAP SHEET 27J PORJUS SV, NORRBOTTEN COUNTY

Authors: Dick Claeson, Ildikó Antal Lundin & Fredrik Hellström

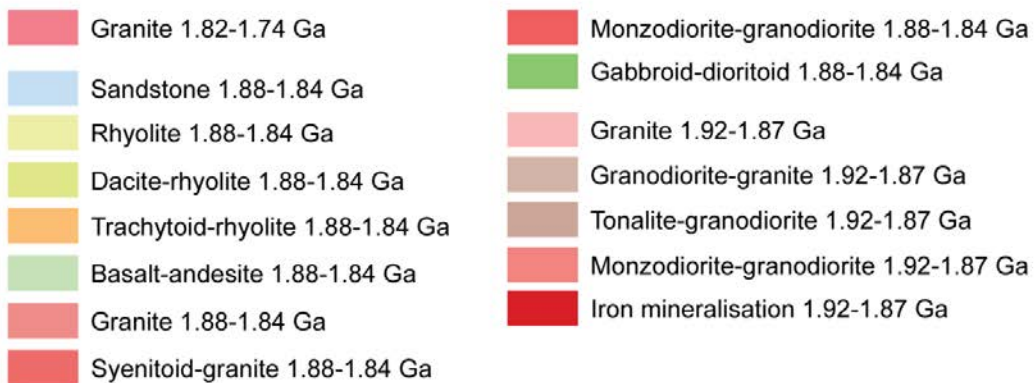
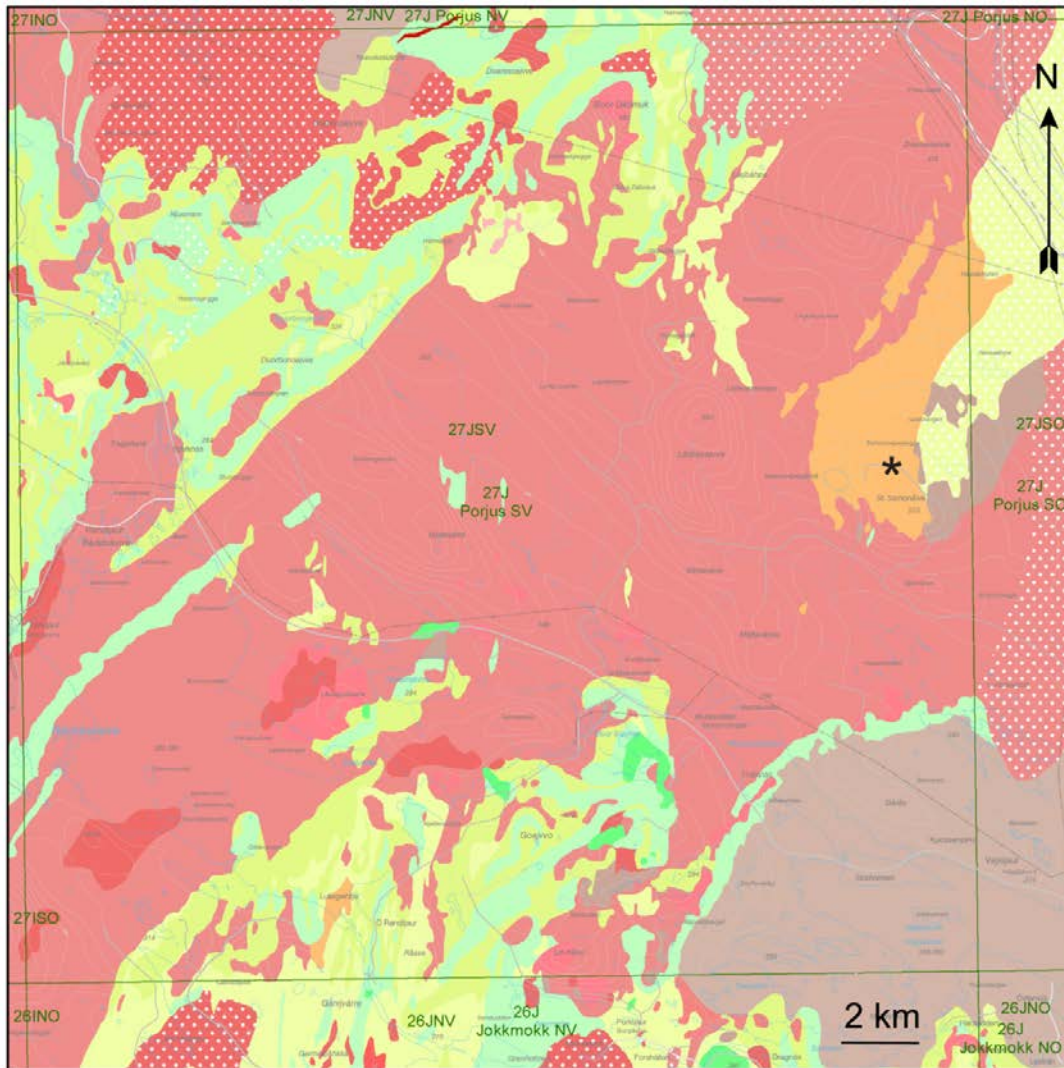


Figure 50. Bedrock map of the area, sampling location marked with black star.

Introduction

Norrbotnen, Sweden is a key area of Europe for future exploration and mining. The sampled rock is part of a large structure that is well-documented by the aeromagnetic data produced by the SGU (Fig. 48–50). Both on the magnetic and Bouguer anomaly maps the structure is clearly seen as a high magnetic pattern and in the southern part as a gravity high (Fig. 48, 49, Claeson & Antal Lundin *in press a*). The quartz trachyte to rhyolite is part of a volcanic succession that also demonstrates dacitoid and basaltoid rocks (Claeson & Antal Lundin *in press a*). The structure is interpreted as a body of extrusive rocks, which covers some of the eastern part of the map area 27J Porjus SV. The size of the sampled anomaly on the aeromagnetic map indicates that the extrusive rocks are part of a structure that stretches from St. Samonåive to Kiruna (Claeson & Antal Lundin *in press a*) and beyond, knowledge about the age is consequently important. Since some of these extrusive rocks are Au anomalous, from an exploration point of view, knowing their age is of great interest.

The aim of this study is to determine the magmatic age of the quartz trachyte to rhyolite at St. Samonåive map area 27J Porjus SV, and if there are any metamorphic overgrowths, determine these as well, since the latter might show ages for the redistribution of elements in the crust. Furthermore, age determinations of volcanic rocks in the region are scarce.

Sample description

The rock is a very fine-grained, porphyric quartz trachyte to rhyolite with a relatively well-preserved texture (Fig. 51, 52). It is sulphide-rich, grey to reddish grey and 1–4 mm large mostly alkali feldspar phenocrysts are present (2–4 %). The alkali feldspar phenocrysts show simple Carlsbad twinning (Fig. 52). Accessory amounts of biotite occur in the groundmass. The rock displays glomeroporphyritic texture with glomerocrysts of e.g. allanite, sulphide mineral, K-feldspar, plagioclase, and quartz (Fig. 52). Outcrop measurement of magnetic susceptibility yielded $2\,800\text{--}9\,870 \times 10^{-5}$ SI, with a geometric mean of $5\,200 \times 10^{-5}$ SI. Petrophysical measurements of two samples show density at 2 635 and 2 728 kg/m³, magnetic susceptibility 5 916 and $19\,701 \times 10^{-5}$ SI, and remanent magnetization intensity of 200 and 1 570 mA/m, respectively.

The quartz trachyte to rhyolite at St. Samonåive shows a LREE-enriched and flat HREE pattern, with a pronounced negative Eu anomaly (Fig. 53). The LREE enrichment is due to fractional crystallisation, the flat, unfractionated HREE pattern shows that no garnet was left in the residue at the location of magma genesis, and the Eu anomaly is indicative of extensive plagioclase fractionation. The negative anomalies shown in the multi-element diagram of Sr and Eu are due to plagioclase fractionation, the P anomaly of apatite fractionation, and the Ti anomaly of Fe-Ti oxide fractionation (Fig. 53).

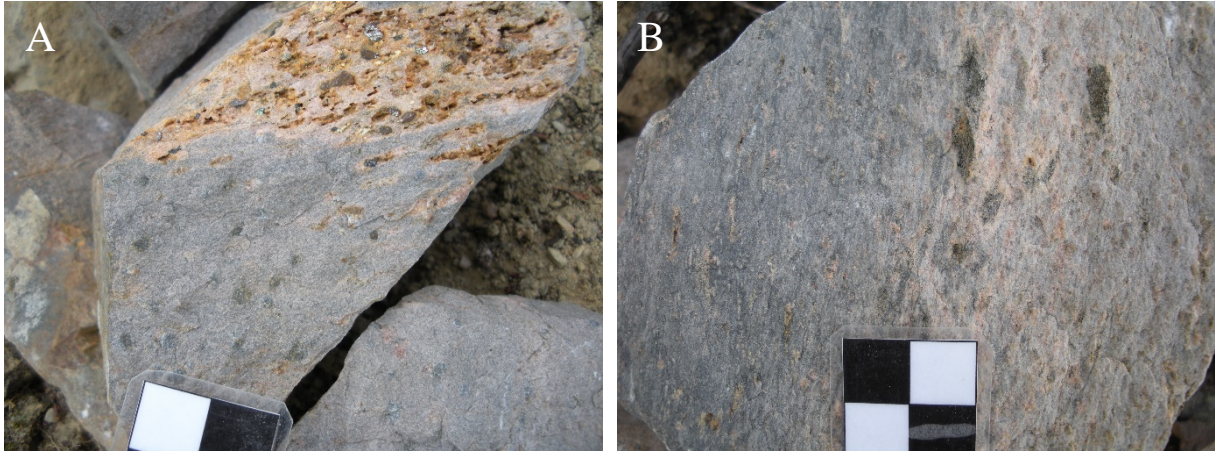


Figure 51. A. Alkali feldspar porphyric and sulphide-rich quartz trachyte to rhyolite at the sampling locality. B. Fragments of mafic volcanic rocks in quartz trachyte to rhyolite at sampling site (cm-scale). Photos: Dick Claeson.

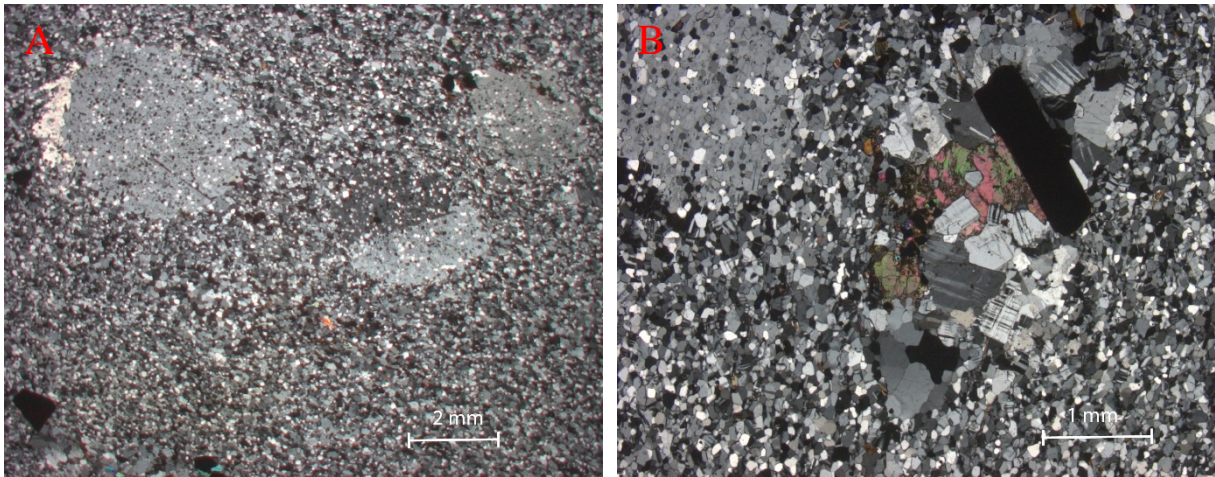


Figure 52. A. Alkali feldspar phenocrysts in very fine-grained matrix. B. Glomeroporphyritic texture with glomerocryst of allanite, sulphide mineral, K-feldspar, plagioclase, and quartz. Micrographs: Dick Claeson.

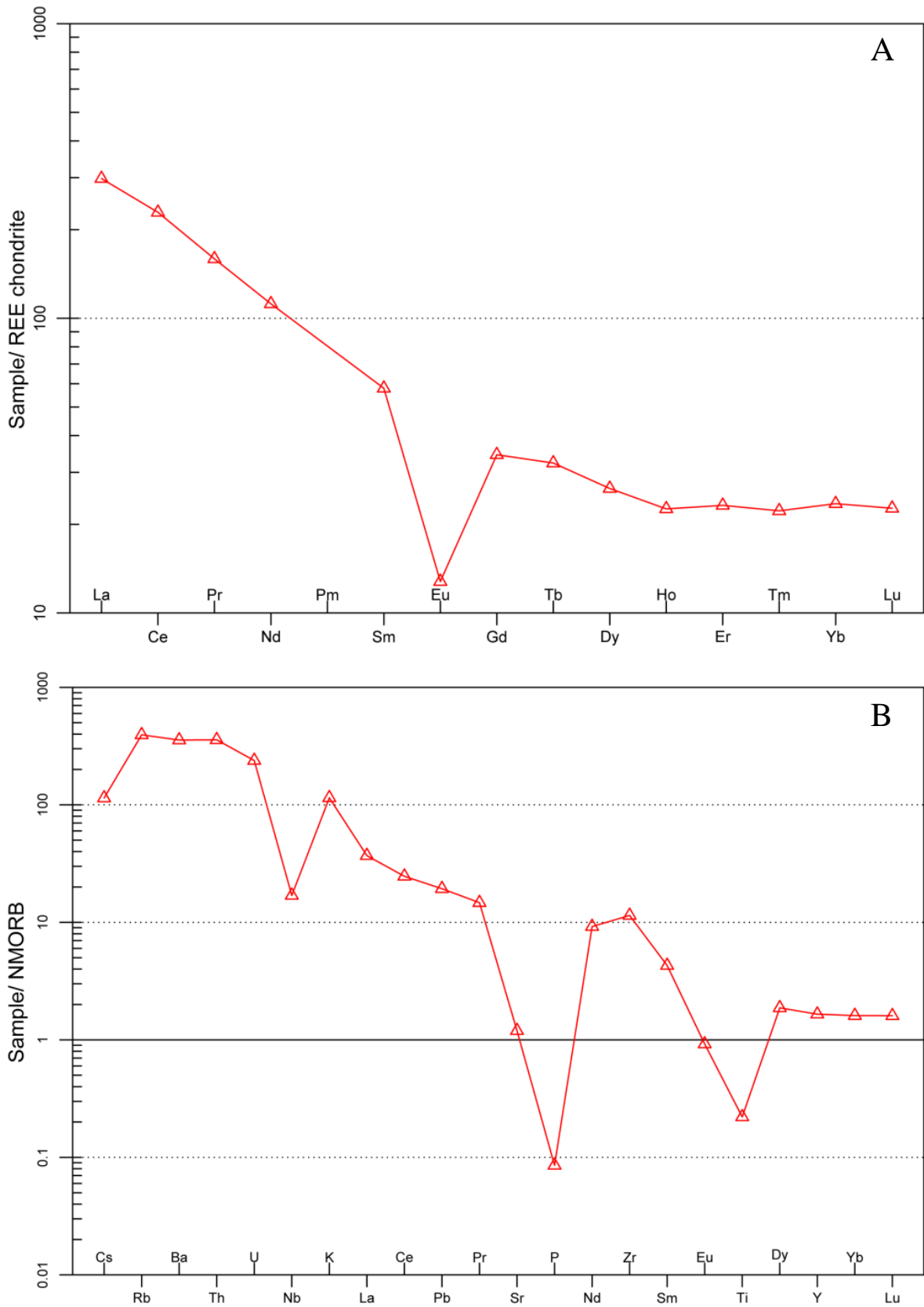


Figure 53. A. REE-diagram of quartz trachyte to rhyolite. Normalizing values for chondrite from Boynton (1984). **B.** Multi-element diagram, rock as in A. Normalizing values for N-MORB from Sun & McDonough (1989).

Analytical results and interpretation of geochronological data

In situ U-Pb-Th SIMS analysis of zircon was performed at the NordSIM facility at the Museum of Natural History in Mars 2010. Detailed descriptions of the analytical procedures are given in Whitehouse et al. (1997, 1999). Pb/U ratios, elemental concentrations and Th/U ratios were calibrated relative to the Geostandards zircon 91 500 reference, which has an age of c. 1 065 Ma (Wiedenbeck et al. 1995, 2004). Common Pb corrected isotope values were calculated using modern common Pb composition (Stacey & Kramers 1975) and measured ^{204}Pb . Decay constants follow the recommendations of Steiger & Jäger (1977). Diagrams and age calculations of isotopic data were made using software Isoplot 4.15 (Ludwig 2012). The analytical results are shown in Table 17.

The zircon grains in the sample are transparent to weakly turbid and have subhedral prismatic or anhedral shapes. There are also angular zircon fragments. BSE-images show an internal oscillatory or sector zonation in the selected zircon (Fig. 54). The U content of the analysed zircon varies between 121 and 374 ppm and Th/U ratios are 0.27–0.42 ($n = 8$, Table 17). The data points are concordant and yield a concordia age at $1\,876 \pm 6$ Ma (95 % confidence, MSWD = 3.3, Fig. 55), same as the weighted average $^{207}\text{Pb}/^{206}\text{Pb}$ age of $1\,874 \pm 5$ Ma (2σ , MSWD = 0.83). The concordia age at $1\,876 \pm 6$ Ma is interpreted to be the igneous crystallisation age of the studied quartz trachyte to rhyolite.

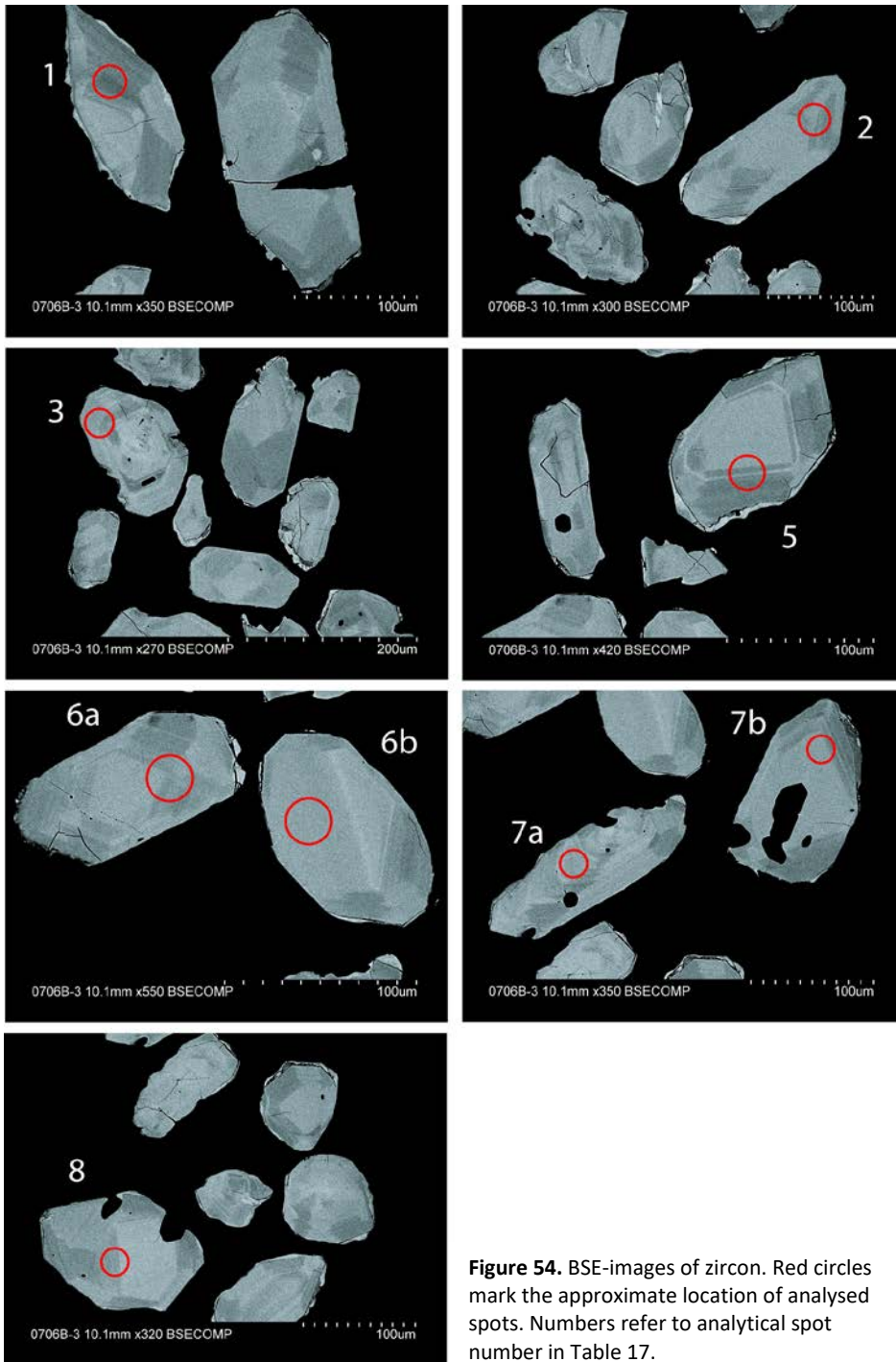


Figure 54. BSE-images of zircon. Red circles mark the approximate location of analysed spots. Numbers refer to analytical spot number in Table 17.

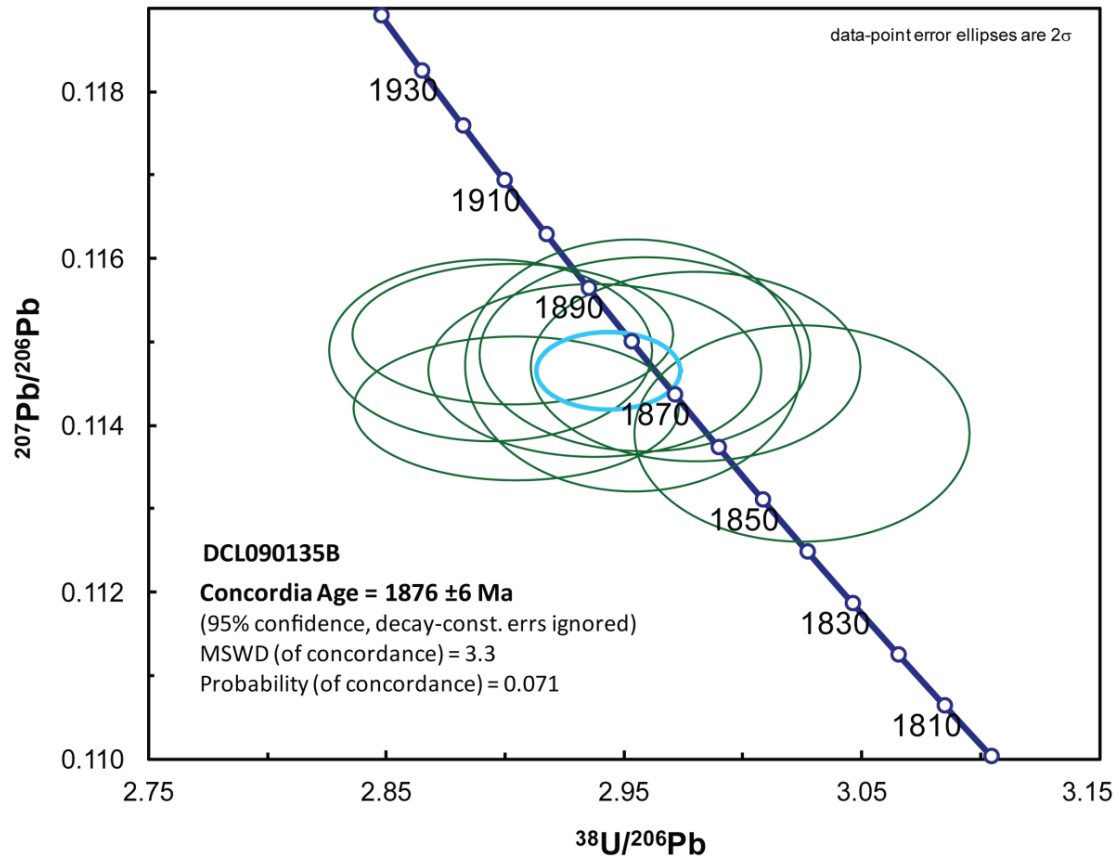


Figure 55. Tera-Wasserburg diagram showing U-Pb SIMS zircon data of the quartz trachyte to rhyolite.

Table 17. SIMS U-Pb-Th zircon data.

Sample/ spot #	U ppm	Th ppm	Pb ppm	Th/U calc ^{*1}	²⁰⁷ Pb ²³⁵ U	±σ %	²⁰⁸ Pb ²³² Th	±s %	²³⁸ U ²⁰⁶ Pb	±s %	²⁰⁷ Pb ²⁰⁶ Pb	±σ %	ρ *2	Disc. % conv. *3	²⁰⁷ Pb ²⁰⁶ Pb	±s Ma	²⁰⁶ Pb ²³⁸ U	±s Ma	²⁰⁶ Pb/ ²⁰⁴ Pb measured	f ₂₀₆ % *4
n3577-01	121	32	49	0.27	5.355	1.11	0.1002	3.9	2.954	0.98	0.1147	0.54	0.88	0.3	1875	10	1880	16	44961	{0.04}
n3577-02	281	100	115	0.35	5.307	1.03	0.0967	3.9	2.980	0.95	0.1147	0.40	0.92	-0.6	1875	7	1865	15	126447	{0.01}
n3577-03	232	67	96	0.31	5.474	1.03	0.1044	3.9	2.894	0.96	0.1149	0.39	0.93	2.2	1878	7	1913	16	89054	{0.02}
n3577-05	156	45	62	0.29	5.192	1.06	0.0965	3.9	3.025	0.95	0.1139	0.47	0.90	-1.3	1863	8	1841	15	232725	{0.01}
n3577-6a	260	76	106	0.30	5.381	1.04	0.0980	3.9	2.938	0.97	0.1147	0.37	0.94	0.9	1874	7	1889	16	66921	0.03
n3577-6b	374	149	159	0.42	5.466	1.00	0.1025	3.8	2.903	0.95	0.1151	0.30	0.95	1.6	1881	5	1908	16	166060	{0.01}
n3577-7b	287	112	119	0.40	5.352	1.05	0.0993	3.8	2.959	0.96	0.1148	0.41	0.92	-0,0	1878	7	1877	16	178012	{0.01}
n3577-8	358	145	152	0.42	5.421	1.01	0.1001	3.8	2.905	0.96	0.1142	0.31	0.95	2.5	1867	6	1907	16	126794	{0.01}

Isotope values are common Pb corrected using modern common Pb composition (Stacey & Kramers 1975) and measured ²⁰⁴Pb.

*1 Th/U ratios calculated from ²⁰⁸Pb/²⁰⁶Pb and ²⁰⁷Pb/²⁰⁶Pb ratios, assuming a single stage of closed U-Th-Pb evolution

*2 Error correlation in conventional concordia space. Do not use for Tera-Wasserburg plots.

*3 Age discordance in conventional concordia space. Positive numbers are reverse discordant.

*4 Figures in parentheses are given when no correction has been applied, and indicate a value calculated assuming present-day Stacey-Kramers common Pb.

Discussion and conclusion

Successful determination of the quartz trachyte to rhyolite crystallisation age at $1\,876 \pm 6$ Ma is in line with the field appearance as a relatively well-preserved volcanic sequence and suggests that it is part of the upper part of the Arvidsjaur Group. The results were integrated in the mapping of the Porjus SV area (Claeson & Antal Lundin *in press a*). Summary of sample data is given in Table 18.

Table 18. Summary of sample data.

Rock type	Quartz trachyte to rhyolite
Lithotectonic unit	Norrbottn lithotectonic unit of the Svecokarelian orogen
Lithological unit	
Sample number	DCL090135B
Lab_id	n3577
Coordinates	7413440/708143 (Sweref99TM)
Map sheet	27J Porjus SV (RT90)
Locality	St. Samonåive
Project	Sydvästra Norrbotten (80025)

References

- Boynnton, W.V., 1984: Cosmochemistry of the Rare Earth Elements: Meteorite studies. *In* P. Henderson (ed.): *Rare earth element geochemistry*. Elsevier Science B.V. 63–114.
- Claeson, D. & Antal Lundin, I., *in press a*: Beskrivning till berggrundskartan 27J Porjus SV. *Sveriges geologiska undersökning*.
- Ludwig, K.R., 2012: User's manual for Isoplot 3.75. A Geochronological Toolkit for Microsoft Excel. *Berkeley Geochronology Center Special Publication No. 5*, 75 pp.
- Stacey, J.S. & Kramers, J.D., 1975: Approximation of terrestrial lead isotope evolution by a two-stage model. *Earth and Planetary Science Letters* 26, 207–221.
- Steiger, R.H. & Jäger, E., 1977: Convention on the use of decay constants in geo- and cosmochronology. *Earth and Planetary Science Letters* 36, 359–362.
- Sun, S.S. & McDonough, W.F., 1989: Chemical and isotopic systematic of oceanic basalts: implications for mantle composition and processes. *In* A.D. Saunders & M.J. Norry (eds.): *Magmatism in ocean basins*. Geological Society of London, Special Publication 42, 313–345.
- Whitehouse, M.J., Claesson, S., Sunde, T. & Vestin, J., 1997: Ion-microprobe U–Pb zircon geochronology and correlation of Archaean gneisses from the Lewisian Complex of Gruinard Bay, north-west Scotland. *Geochimica et Cosmochimica Acta* 61, 4 429–4 438.
- Whitehouse, M.J., Kamber, B.S. & Moorbath, S., 1999: Age significance of U–Th–Pb zircon data from Early Archaean rocks of west Greenland: a reassessment based on combined ion-microprobe and imaging studies. *Chemical Geology (Isotope Geoscience Section)* 160, 201–224.
- Wiedenbeck, M., Allé, P., Corfu, F., Griffin, W.L., Meier, M., Oberli, F., Quadt, A.V., Roddick, J.C. & Spiegel, W., 1995: Three natural zircon standards for U-Th-Pb, Lu-Hf, trace element and REE analyses. *Geostandards Newsletter* 19, 1–23.
- Wiedenbeck, M., Hanchar, J.M., Peck, W.H., Sylvester, P., Valley, J., Whitehouse, M., Kronz, A., Morishita, Y., Nasdala, L., Fiebig, J., Franchi, I., Girard, J.P., Greenwood, R.C., Hinton, R., Kita, N., Mason, P.R.D., Norman, M., Ogasawara, M., Piccoli, P.M., Rhede, D., Satoh, H., Schulz-Dobrick, B., Skår, O., Spicuzza, M.J., Terada, K., Tindle, A., Togashi, S., Vennemann, T., Xie, Q. & Zheng, Y.F., 2004: Further Characterisation of the 91500 Zircon Crystal. *Geostandards and Geoanalytical Research* 28, 9–39.

U-Pb ZIRCON AGE OF RHYOLITE AT KADDÁIVE, MAP SHEET 27J PORJUS SV, NORRBOTTEN COUNTY

Authors: Dick Claeson, Ildikó Antal Lundin & Fredrik Hellström

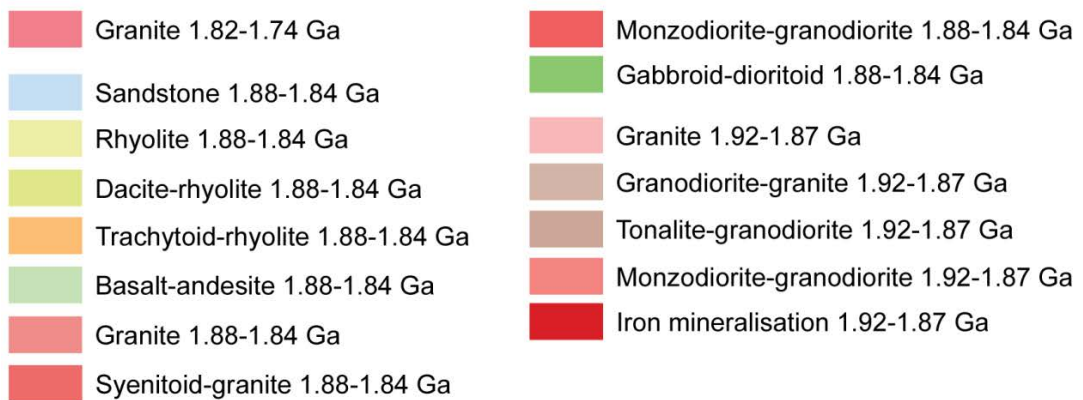
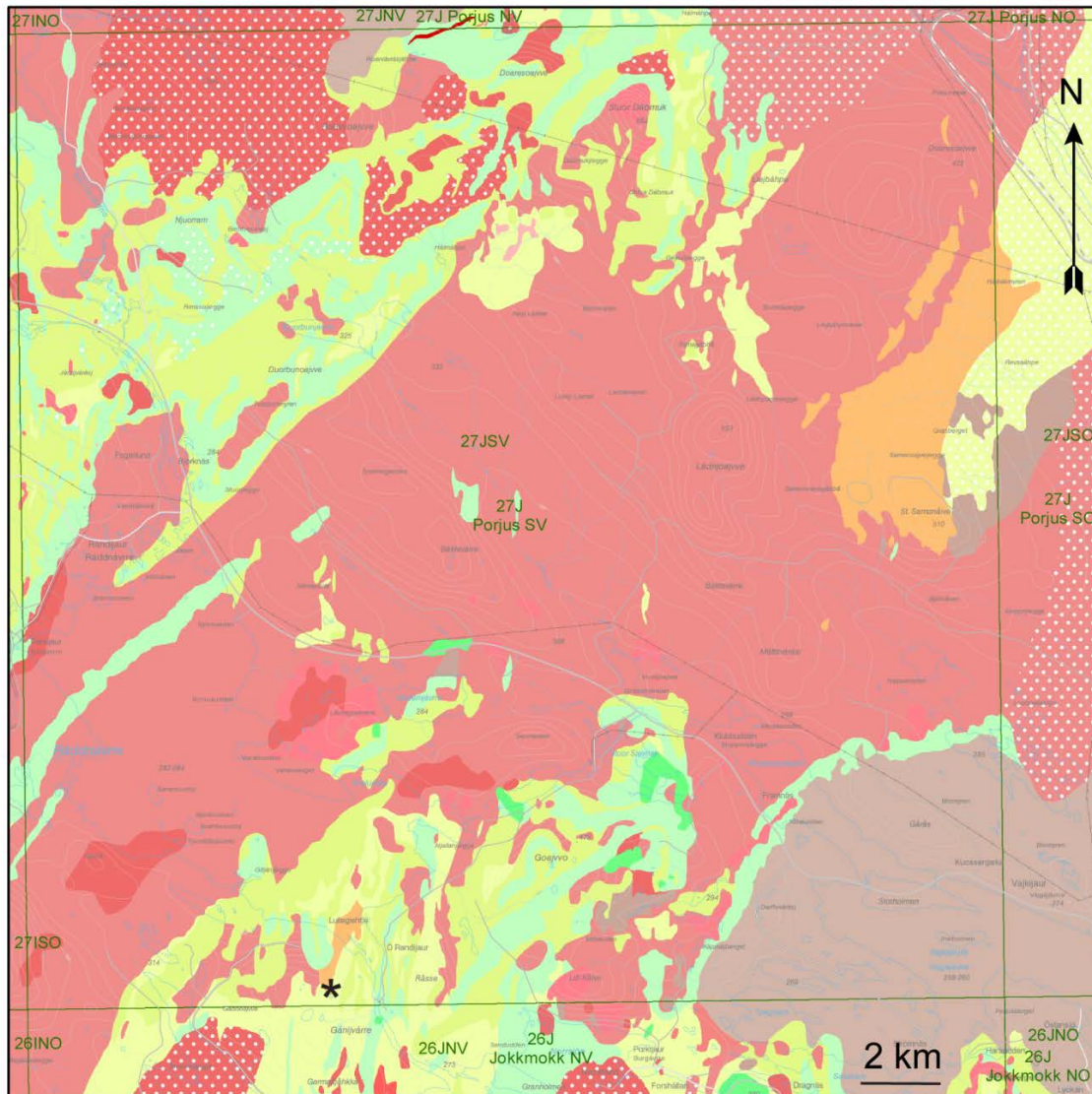


Figure 56. Bedrock map of the area, sampling location marked with black star.

Introduction

Norrbottnen, Sweden is a key area of Europe for future exploration and mining. The sampled rock is part of a large structure that is well-documented by the aeromagnetic data produced by the SGU (Fig. 48, 56). Both on the magnetic and Bouguer anomaly maps the structure is clearly seen as a high magnetic, banded pattern and as a gravity high (Fig. 48, 49). The structure is interpreted as a body of extrusive rocks, which covers parts of the map area 27J Porjus SV. The size of the sampled anomaly on the aeromagnetic map indicates that the extrusive rocks are stretching from Kaddåive to Kiruna (Claeson & Antal Lundin *in press a*) and beyond, knowledge about the age is consequently important. Since some of these extrusive rocks are Au anomalous, from an exploration point of view, knowing their age is of great interest.

The aim of this study is to determine the magmatic age of rhyolite at Kaddåive map area 27J Porjus SV, and if there are any metamorphic overgrowths, determine these as well, since the latter might show ages for the redistribution of elements in the crust. Furthermore, age determinations of volcanic rocks in the region are scarce.

Sample description

The rock is a banded, foliated, and very fine-grained to fine-grained volcanic rock of rhyolite composition (Fig. 57). It is light grey, grey to reddish grey. Accessory biotite occurs in the groundmass. The rock displays glomeroporphyritic texture with glomerocrysts of e.g. plagioclase, K-feldspar, Fe-Ti oxide, and quartz (Fig. 58). Outcrop measurement of magnetic susceptibility yielded $1\ 630\text{--}3\ 220 \times 10^{-5}$ SI. Petrophysical measurements of a sample show density at $2\ 649\ \text{kg/m}^3$, magnetic susceptibility $3\ 022 \times 10^{-5}$ SI, and remanent magnetization intensity of 80 mA/m.

The rhyolite at Kaddåive shows a LREE-enriched and flat HREE pattern, with a pronounced negative Eu anomaly (Fig. 59). The LREE enrichment is due to fractional crystallisation, the flat, unfractionated HREE pattern shows that no garnet was left in the residue at the location of magma genesis, and the Eu anomaly is indicative of extensive plagioclase fractionation. The negative anomalies shown in the multi-element diagram of Sr and Eu are due to plagioclase fractionation, the P anomaly of apatite fractionation, and the Ti anomaly of Fe-Ti oxide fractionation (Fig. 59). The small positive Pb anomaly as well as the negative Nb anomaly suggests a subduction related petrogenesis (Fig. 59).

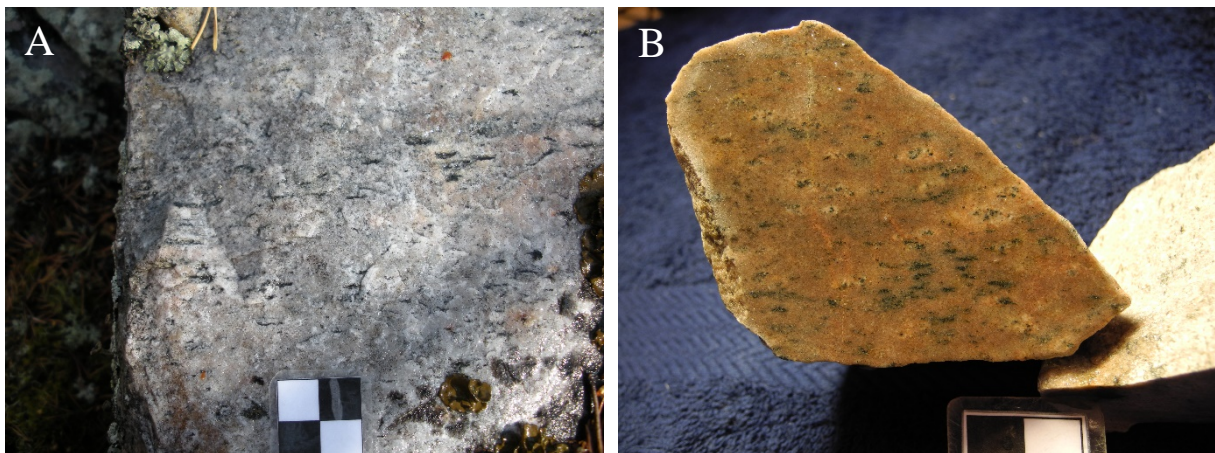


Figure 57. A. Outcrop of rhyolite (cm scale). B. Cut and wetted sample of rhyolite. Photos: Dick Claeson.

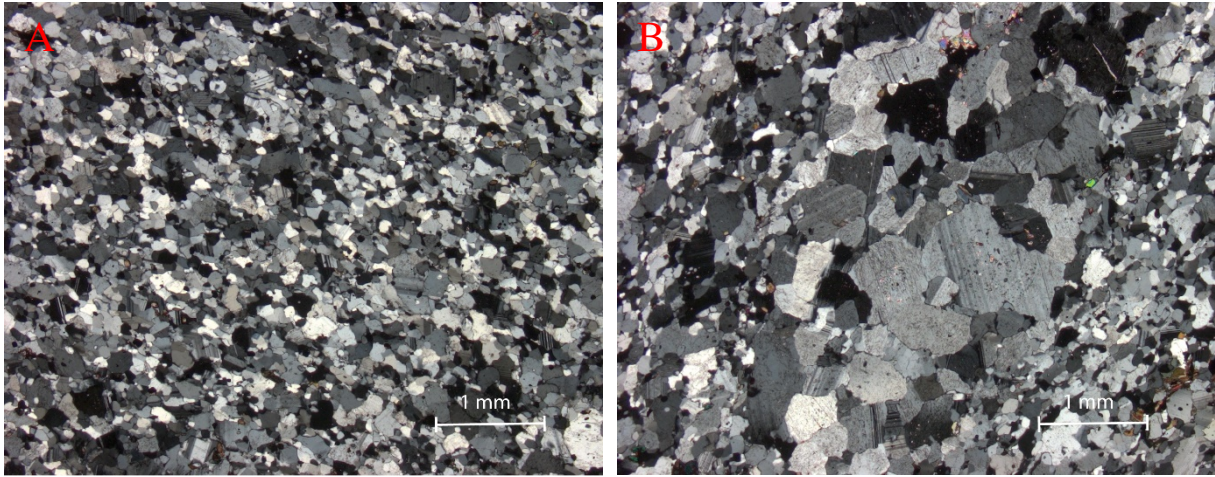


Figure 58. A. Very fine-grained matrix. **B.** Glomeroporphyritic texture with glomerocryst of plagioclase, K-feldspar, Fe-Ti oxide, and quartz. Micrographs: Dick Claeson.

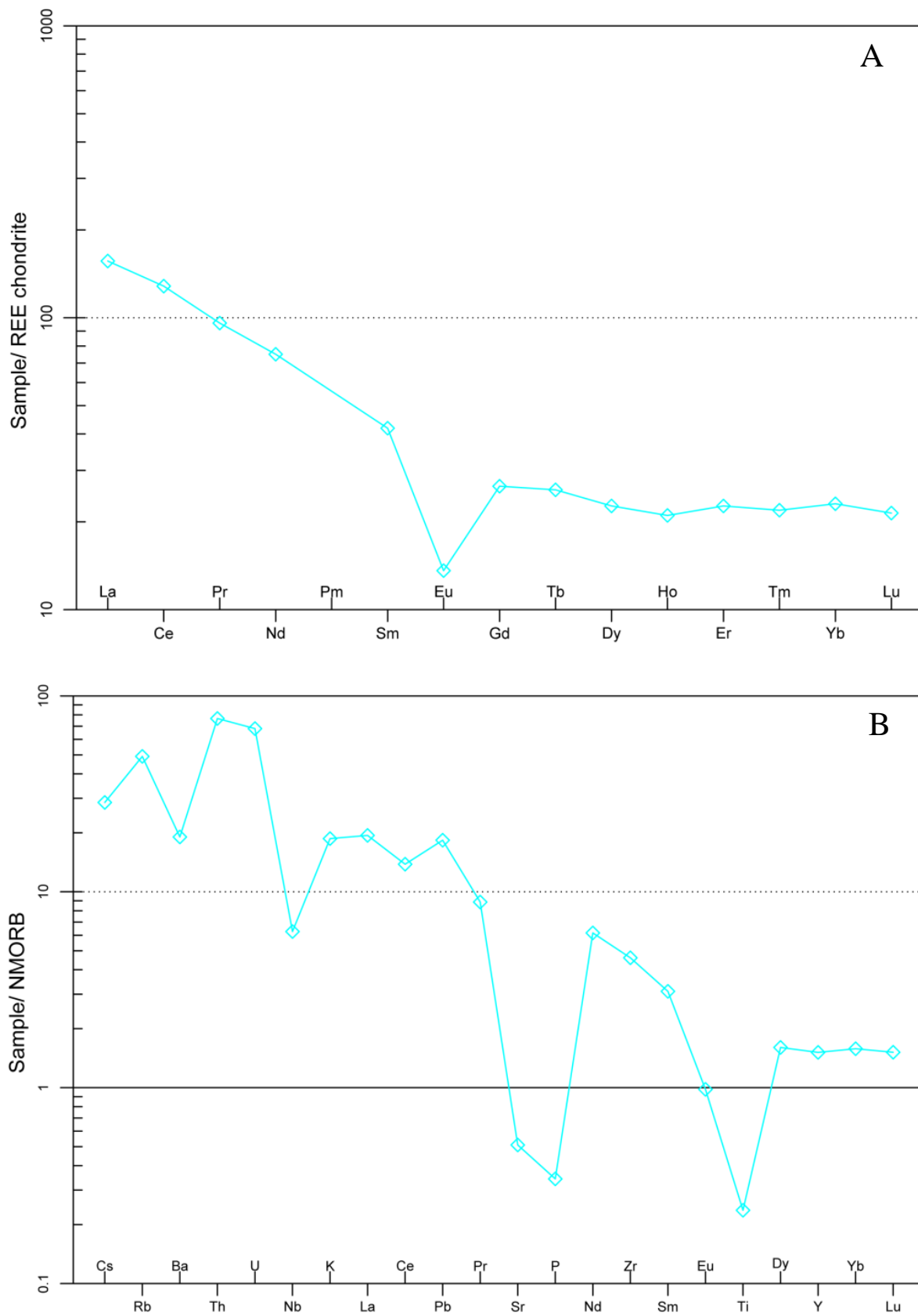


Figure 59. A. REE-diagram of rhyolite. Normalizing values for chondrite from Boynton (1984). **B.** Multi-element diagram, rock as in A. Normalizing values for N-MORB from Sun & McDonough (1989).

Analytical results and interpretation of geochronological data

In situ U-Pb-Th SIMS analysis of zircon was performed at the Nordsim facility at the Museum of Natural History in Mars 2010. Detailed descriptions of the analytical procedures are given in Whitehouse et al. (1997, 1999). Pb/U ratios, elemental concentrations and Th/U ratios were calibrated relative to the Geostandards zircon 91 500 reference, which has an age of c. 1 065 Ma (Wiedenbeck et al. 1995, 2004). Common Pb corrected isotope values were calculated using modern common Pb composition (Stacey & Kramers 1975) and measured ^{204}Pb . Decay constants follow the recommendations of Steiger & Jäger (1977). Diagrams and age calculations of isotopic data were made using software Isoplot 4.15 (Ludwig 2012). The analytical results are shown in Table 19. Zircon grains in the heavy mineral concentrate are transparent and have mainly sub to euhedral prismatic shapes. BSE-images show a weak internal oscillatory zonation in the selected zircon (Fig. 60). Many grains have inclusions and cracks. Metamict zircon domains are also common and some grains seem to have structurally older cores.

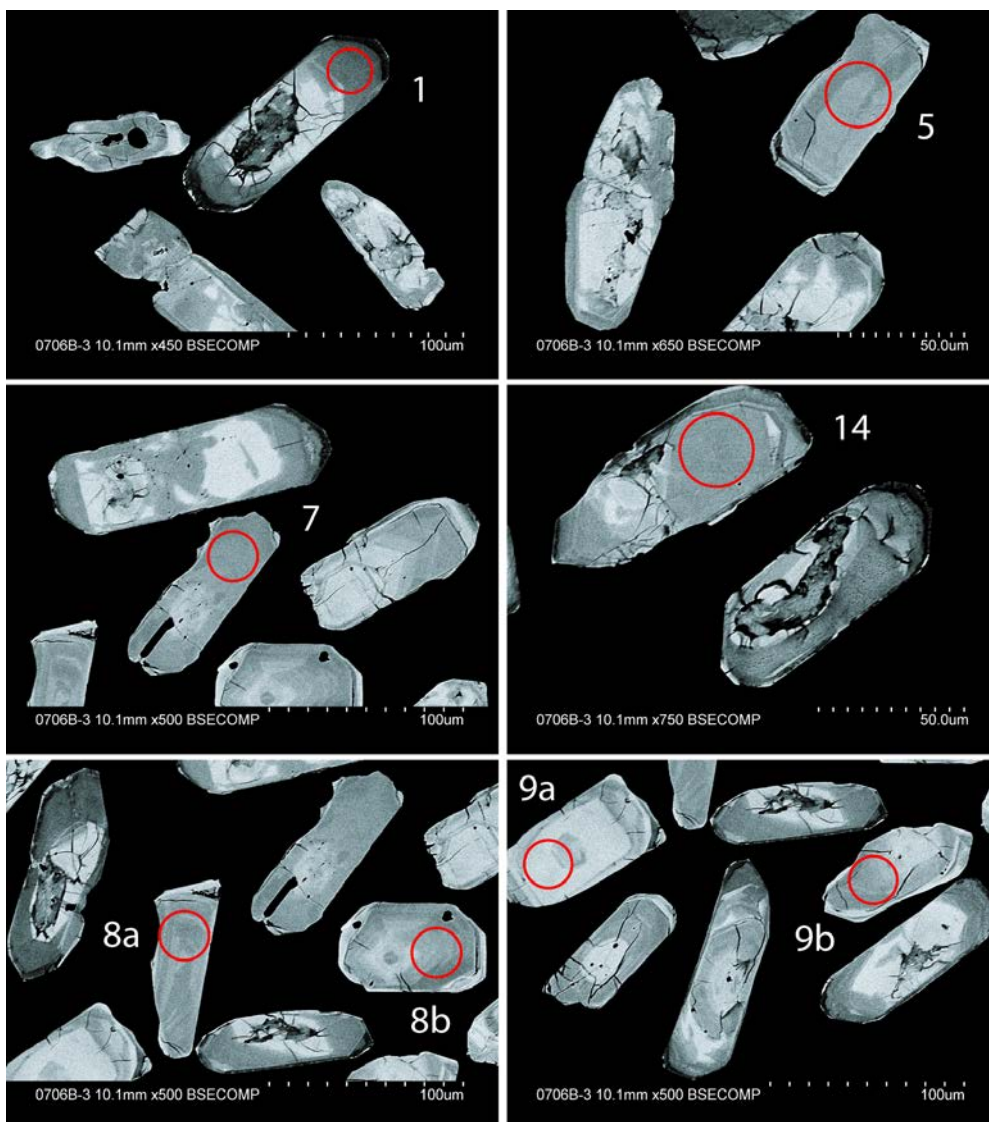


Figure 60. BSE-images of zircon from the rhyolite. Red circles mark the approximate location of analysed spots. Numbers refer to analytical spot number in Table 19.

The U content of the analysed zircon are 135–371 ppm and Th/U ratios are 0.30–0.44 (n = 6, Table 19), except for two analyses (No. 1, 14) that have U contents of 1 580 and 2 014 ppm and Th/U ratios of 0.10 and 0.14, respectively. These two uranium-rich zircon analyses show high values of common lead and are also strongly discordant (Table 19). Four data points are concordant and yield a concordia age at $1\,878 \pm 17$ Ma (95 % confidence, MSWD = 3.9). A weighted average $^{207}\text{Pb}/^{206}\text{Pb}$ age of $1\,873 \pm 7$ Ma (2σ , MSWD = 0.59; n = 6) is calculated using also two weakly discordant analyses (No. 5, 9a, Fig. 61). The weighted average $^{207}\text{Pb}/^{206}\text{Pb}$ age of $1\,873 \pm 7$ Ma is interpreted as when igneous crystallisation of the rhyolite occurred.

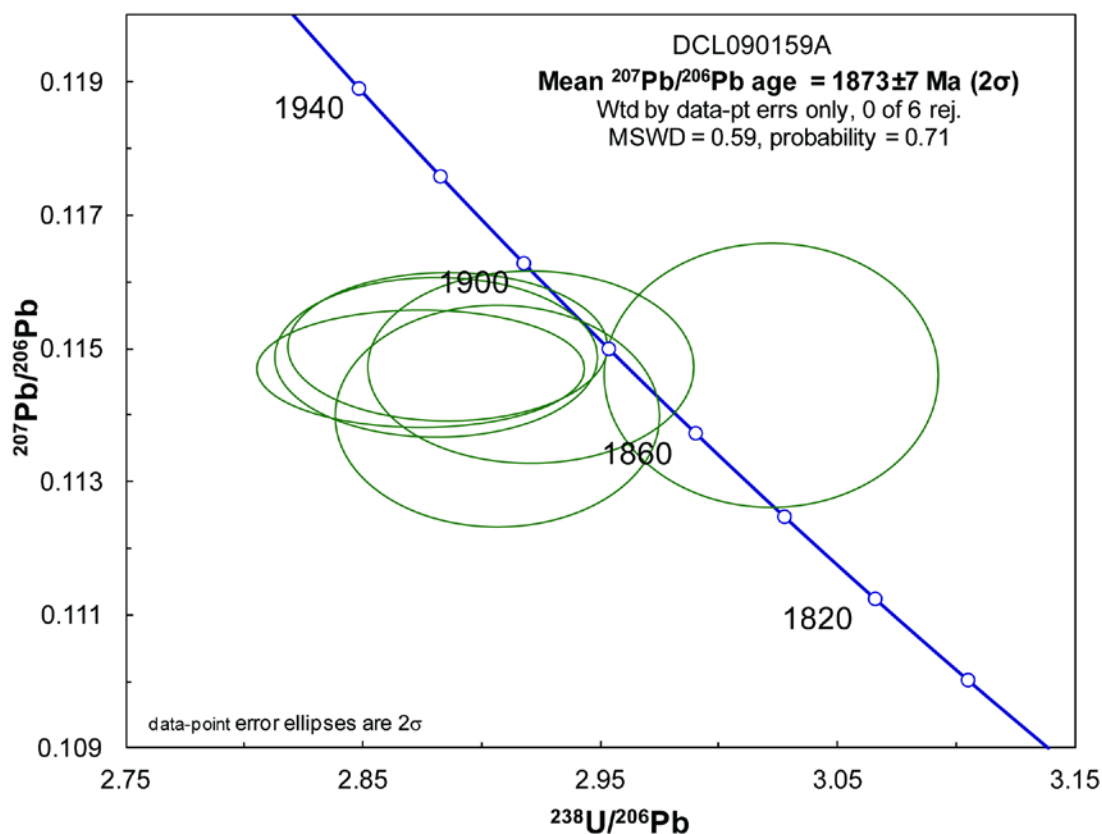


Figure 61. Tera-Wasserburg diagram showing U-Pb SIMS zircon data. Two strongly discordant analyses (1, 14) are not shown in the diagram and are not used in the age calculation (see Table 19).

Table 19. SIMS U-Pb-Th zircon data.

Sample/ spot #	U ppm	Th ppm	Pb ppm	Th/U calc* ¹	²⁰⁷ Pb ²³⁵ U	±σ %	²⁰⁸ Pb ²³² Th	±σ %	²³⁸ U ²⁰⁶ Pb	±s %	²⁰⁷ Pb ²⁰⁶ Pb	±s %	ρ * ²	Disc. % conv. * ³	²⁰⁷ Pb ²⁰⁶ Pb	±s Ma	²⁰⁶ Pb ²³⁸ U	±s Ma	²⁰⁶ Pb/ ²⁰⁴ Pb measured	f ₂₀₆ % * ⁴
n3579-1	2014	373	237	0.10	1.102	1.17	0.0311	4.3	9.605	0.97	0.0767	0.66	0.83	-44.8	1114	13	638	6	793	2.36
n3579-5	199	85	85	0.44	5.480	1.06	0.1002	3.9	2.882	0.96	0.1146	0.43	0.91	2.9	1873	8	1920	16	42525	0.04
n3579-7	171	54	71	0.34	5.407	1.13	0.1038	3.9	2.906	0.96	0.114	0.59	0.85	2.6	1864	11	1906	16	76245	{0.02}
n3579-8a	135	41	56	0.31	5.415	1.09	0.0996	3.9	2.921	0.96	0.1147	0.51	0.88	1.4	1875	9	1898	16	55816	{0.03}
n3579-8b	273	102	116	0.39	5.496	1.03	0.1008	4.0	2.886	0.95	0.115	0.39	0.92	2.3	1880	7	1918	16	92624	{0.02}
n3579-9a	371	140	158	0.39	5.494	1.03	0.1006	3.8	2.875	0.98	0.1146	0.32	0.95	3.2	1873	6	1924	16	95040	0.02
n3579-9b	153	46	61	0.30	5.181	1.20	0.096	4.0	3.026	0.95	0.1137	0.73	0.79	-1.1	1859	13	1841	15	14915	0.13
n3579-14	1580	389	301	0.15	2.141	1.16	0.0464	4.4	6.122	0.98	0.095	0.61	0.85	-39.0	1529	12	975	9	418	4.47

Isotope values are common Pb corrected using modern common Pb composition (Stacey & Kramers 1975) and measured ²⁰⁴Pb.

*¹ Th/U ratios calculated from ²⁰⁸Pb/²⁰⁶Pb and ²⁰⁷Pb/²⁰⁶Pb ratios, assuming a single stage of closed U-Th-Pb evolution

*² Error correlation in conventional concordia space. Do not use for Tera-Wasserburg plots.

*³ Age discordance in conventional concordia space. Positive numbers are reverse discordant.

*⁴ Figures in parentheses are given when no correction has been applied, and indicate a value calculated assuming present-day Stacey-Kramers common Pb.

Discussion and conclusion

Successful age determination of the rhyolite at $1\,873 \pm 7$ Ma shows that this volcanic sequence is part of the upper part of the Arvidsjaur Group and not an older part, which could be suggested by the metamorphic foliation seen in the rock. The results were integrated in the mapping of the 27J Porjus SV area (Claeson & Antal Lundin *in press a*). Summary of sample data is given in Table 20.

Table 20. Summary of sample data.

Rock type	Rhyolite
Lithotectonic unit	Norrbottnen lithotectonic unit of the Svecokarelian orogen
Lithological unit	
Sample number	DCL090159A
Lab_id	n3579
Coordinates	7400390/693216 (Sweref99TM)
Map sheet	27J Porjus SV (RT90)
Locality	Kaddåive
Project	Sydvästra Norrbotten (80025)

References

- Boynnton, W.V., 1984: Cosmochemistry of the Rare Earth Elements: Meteorite studies. In P. Henderson (ed.): *Rare earth element geochemistry*. Elsevier Science B.V. 63–114.
- Claeson, D. & Antal Lundin, I., *in press a*: Beskrivning till berggrundskartan 27J Porjus SV. *Sveriges geologiska undersökning*.
- Ludwig, K.R., 2012: User's manual for Isoplot 3.75. A Geochronological Toolkit for Microsoft Excel. *Berkeley Geochronology Center Special Publication No. 5*, 75 pp.
- Stacey, J.S. & Kramers, J.D., 1975: Approximation of terrestrial lead isotope evolution by a two-stage model. *Earth and Planetary Science Letters* 26, 207–221.
- Steiger, R.H. & Jäger, E., 1977: Convention on the use of decay constants in geo- and cosmochronology. *Earth and Planetary Science Letters* 36, 359–362.
- Sun, S.S. & McDonough, W.F., 1989: Chemical and isotopic systematic of oceanic basalts: implications for mantle composition and processes. In A.D. Saunders & M.J. Norry (eds.): *Magmatism in ocean basins*. Geological Society of London, Special Publication 42, 313–345.
- Whitehouse, M.J., Claesson, S., Sunde, T. & Vestin, J., 1997: Ion-microprobe U–Pb zircon geochronology and correlation of Archaean gneisses from the Lewisian Complex of Gruinard Bay, north-west Scotland. *Geochimica et Cosmochimica Acta* 61, 4 429–4 438.
- Whitehouse, M.J., Kamber, B.S. & Moorbath, S., 1999: Age significance of U–Th–Pb zircon data from Early Archaean rocks of west Greenland: a reassessment based on combined ion-microprobe and imaging studies. *Chemical Geology (Isotope Geoscience Section)* 160, 201–224.
- Wiedenbeck, M., Allé, P., Corfu, F., Griffin, W.L., Meier, M., Oberli, F., Quadt, A.V., Roddick, J.C. & Spiegel, W., 1995: Three natural zircon standards for U-Th-Pb, Lu-Hf, trace element and REE analyses. *Geostandards Newsletter* 19, 1–23.
- Wiedenbeck, M., Hanchar, J.M., Peck, W.H., Sylvester, P., Valley, J., Whitehouse, M., Kronz, A., Morishita, Y., Nasdala, L., Fiebig, J., Franchi, I., Girard, J.P., Greenwood, R.C., Hinton, R., Kita, N., Mason, P.R.D., Norman, M., Ogasawara, M., Piccoli, P.M., Rhede, D., Satoh, H., Schulz-Dobrick, B., Skår, O., Spicuzza, M.J., Terada, K., Tindle, A., Togashi, S., Vennemann, T., Xie, Q. & Zheng, Y.F., 2004: Further Characterisation of the 91500 Zircon Crystal. *Geostandards and Geoanalytical Research* 28, 9–39.

U-Pb ZIRCON AGE OF THE HOST GRANITE OF THE REE AND Mo (U, Th, Nb, Ta) MINERALISATION AT TÅRESÅIVE, MAP SHEET 27J PORJUS SV, NORRBOTTEN COUNTY

Authors: Dick Claesson, Ildikó Antal Lundin, Per-Olof Persson¹ & George Morris

¹Department of Geosciences Swedish Museum of Natural History, Box 50 007, SE-104 05 Stockholm, Sweden

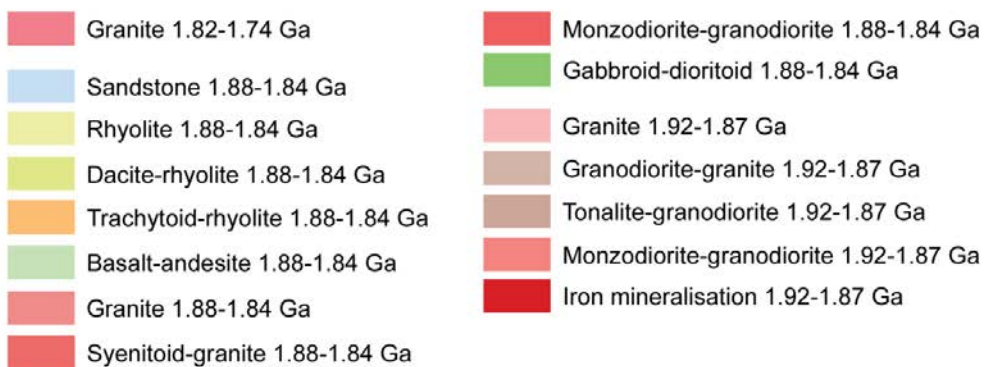
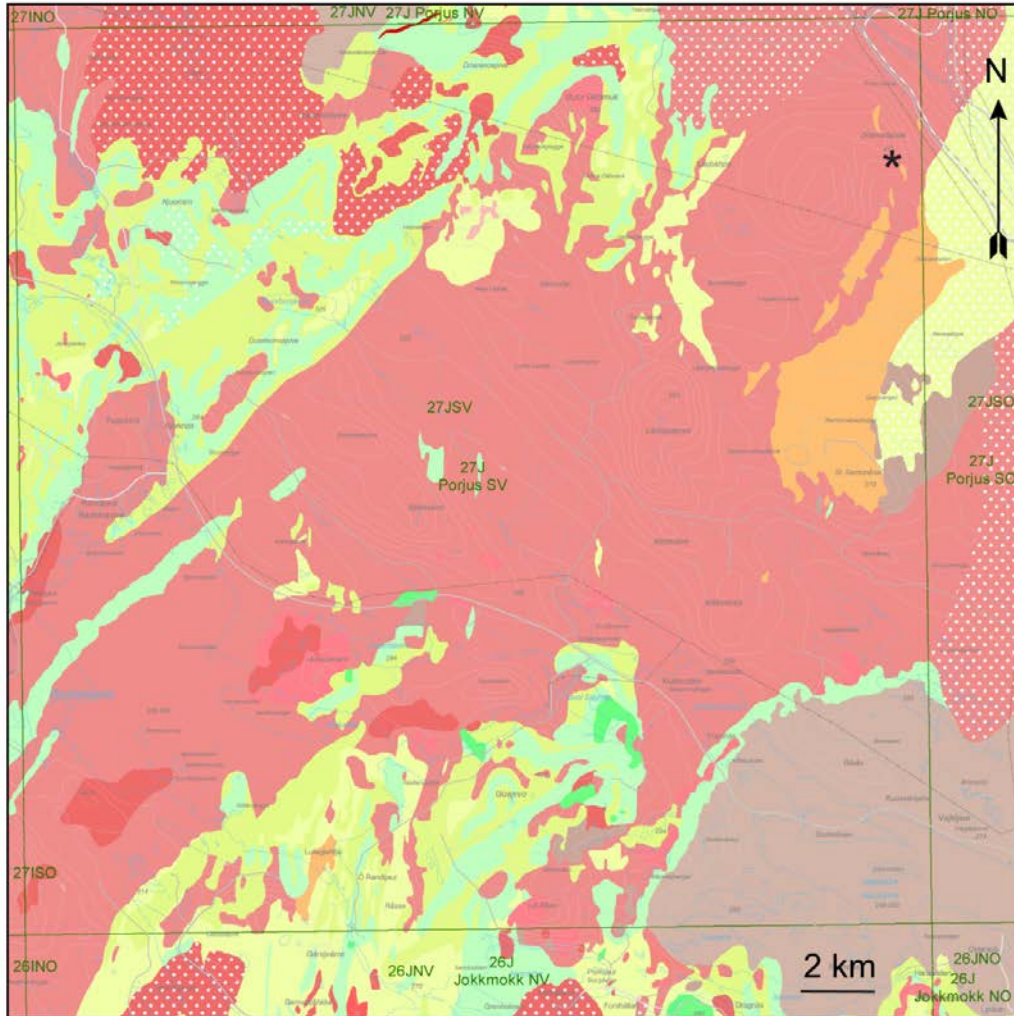


Figure 62. Bedrock map of the area, sampling location marked with black star.

Introduction

Norrbottnen, Sweden is a key area of Europe for future exploration and mining. Molybdenite occurs in hydrothermally altered granite, rhyolite, and pegmatite at Tåresåive within the map area 27J Porjus SV. This granite is part of a larger intrusion and is clearly seen as a low magnetic and gravity anomaly area on both the gravity- and the magnetic anomaly map (Fig. 48, 49, 62). The mineralisation is partly located in fractures or veins but molybdenite also occurs disseminated in the host rocks. This is the only place within the 27J Porjus SV area where this type of mineralisation has been found. Originally it was a mineraljaktfynd (Krister Mattsson 79293) but only molybdenite and high gamma radiation was reported. The newly performed mapping also shows high contents of REE within the sampled mineralisation (Claeson & Antal Lundin *in press a*). The extent or potential of the mineralisation is not known, and it is impossible to estimate from the present investigations.

In order to gain knowledge of when possible economic deposits are formed on a regional scale in the Norrbotten County the host rock at Tåresåive was chosen for age determination. Even the extent of magmatic induced metamorphism is of great importance, by re-heating the crust and producing hydrothermal activity in volcanic rocks, intrusive rocks, or structural zones, or if regional metamorphic events are in any way involved, these ages should be determined.

The aim of this study is to determine the magmatic age of the granite at the Tåresåive REE and Mo mineralisation in map area 27J Porjus SV, and if there are any metamorphic overgrowths, determine these as well, since the latter might indicate ages for the redistribution of elements in the crust.

Sample description

The sample consists of uneven-grained, red granite that is fine-grained to medium-grained (Fig. 63). It is a metamorphic rock displaying foliation, recrystallisation, and hydrothermal alteration. Quartz shows undulose extinction. Potassium feldspar shows cross-hatched twinning. Plagioclase displays optical zonation and very minor sericite alteration (Fig. 64). The sampled monzogranite shows very low content of mafic minerals, mostly opaque minerals and biotite, making it a hololeucocratic rock with less than 1 % mafic minerals. Some muscovite and apatite crystals are present in thin-section. The Zr content of the rock is 304 ppm.

Magnetic susceptibility measured at the outcrop varies between 0 and 313×10^{-5} SI. Petrophysical measurements of a sample show density at 2.597 kg/m^3 , magnetic susceptibility 77×10^{-5} SI, and remanent magnetization intensity of 265 mA/m. The granite was measured at the mineralisation and nearby outcrops where it shows elevated gamma ray radiation values $K = 4.6\text{--}4.8 \%$, $U = 29\text{--}31 \text{ ppm}$, and $Th = 70\text{--}92 \text{ ppm}$. Measurements on the molybdenite mineralisation shows major gamma ray radiation values $K = 1.2\text{--}3.3 \%$, $U = 173\text{--}780 \text{ ppm}$, and $Th = 352\text{--}827 \text{ ppm}$. A measurement of granite c. 100m northwest of the mineralisation also shows elevated gamma ray radiation values $K = 4.5\text{--}4.8 \%$, $U = 19\text{--}25 \text{ ppm}$, and $Th = 68\text{--}81 \text{ ppm}$. Molybdenite occurs disseminated in the granite and as aggregates (Fig. 64). The molybdenite displays bireflectance as well as reflection pleochroism, whitish grey to white (Fig. 64). There are also minor amounts of chalcopyrite in the granite (Fig. 64).

The granite at Tåresåive shows a slightly LREE-enriched and flat HREE pattern, with negative Eu anomaly and Ce anomaly (Fig. 65). The minor LREE enrichment is due to fractional crystallisation, the flat, unfractionated HREE pattern shows that no garnet was left in the residue at the location of magma genesis, and the Eu anomaly is indicative of plagioclase fractionation. The negative Ce anomaly seen in the granite may be due to crystallisation of Ce-allanite in the mineralisation. The negative anomalies shown in the multi-element diagram of Sr is due to

plagioclase fractionation, the P anomaly of apatite fractionation, and the Ti anomaly of Fe-Ti oxide fractionation (Fig. 65). The strong negative Nb anomaly and positive Pb anomaly suggest a subduction related petrogenesis (Fig. 65).



Figure 63. A. Sampled granite from Tåresåive. B. Fractures filled with compact molybdenite within hydrothermally altered granite, rhyolite and pegmatite (7421196/709317). Photos: Ildikó Antal Lundin.

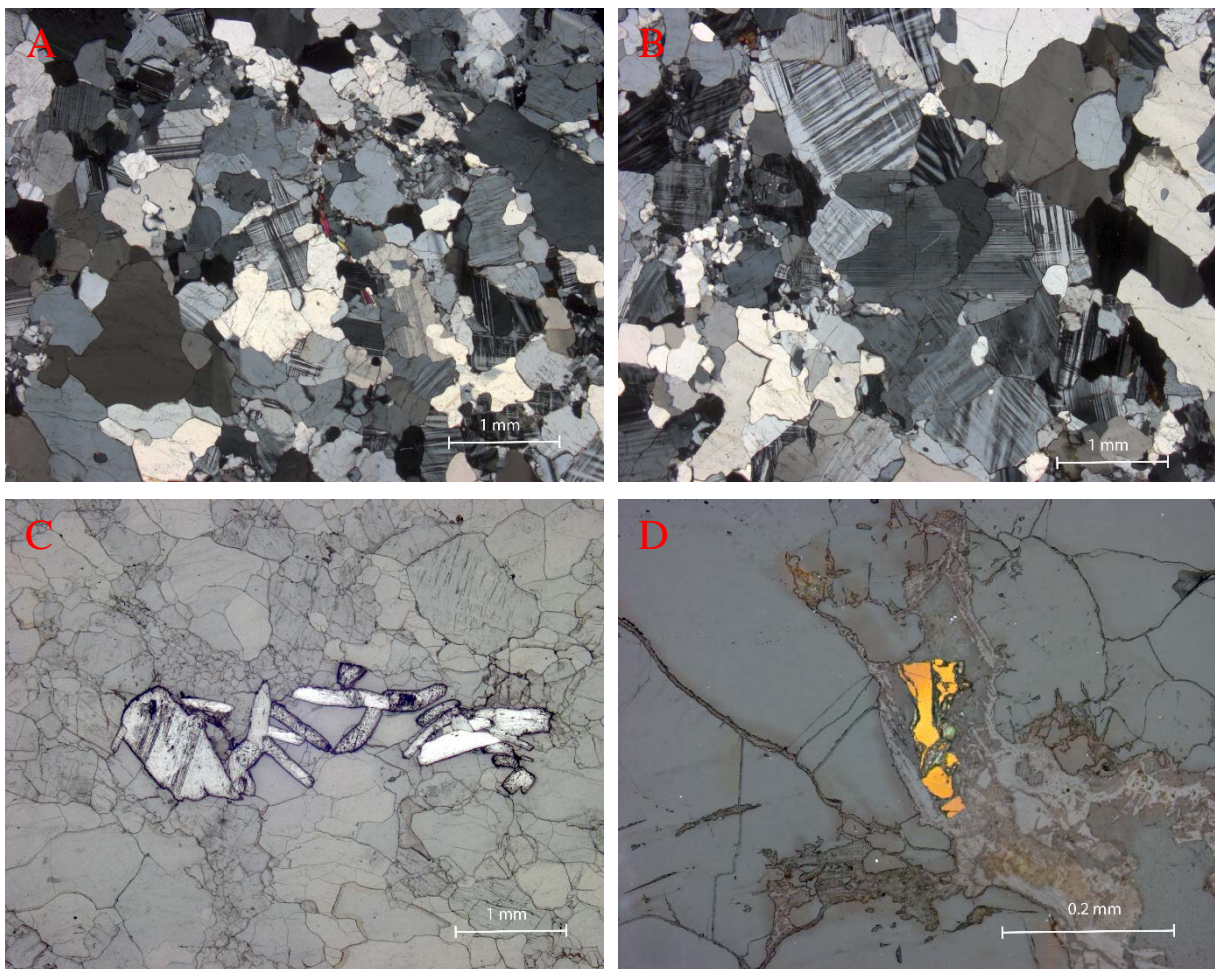


Figure 64. A. Groundmass with small muscovite crystals in granite, crossed nicols. B. Optically-zoned plagioclase in granite, crossed nicols. C. Molybdenite crystals in granite, reflected light. D. Chalcopyrite crystals in granite, reflected light. Micrographs: Dick Claeson.

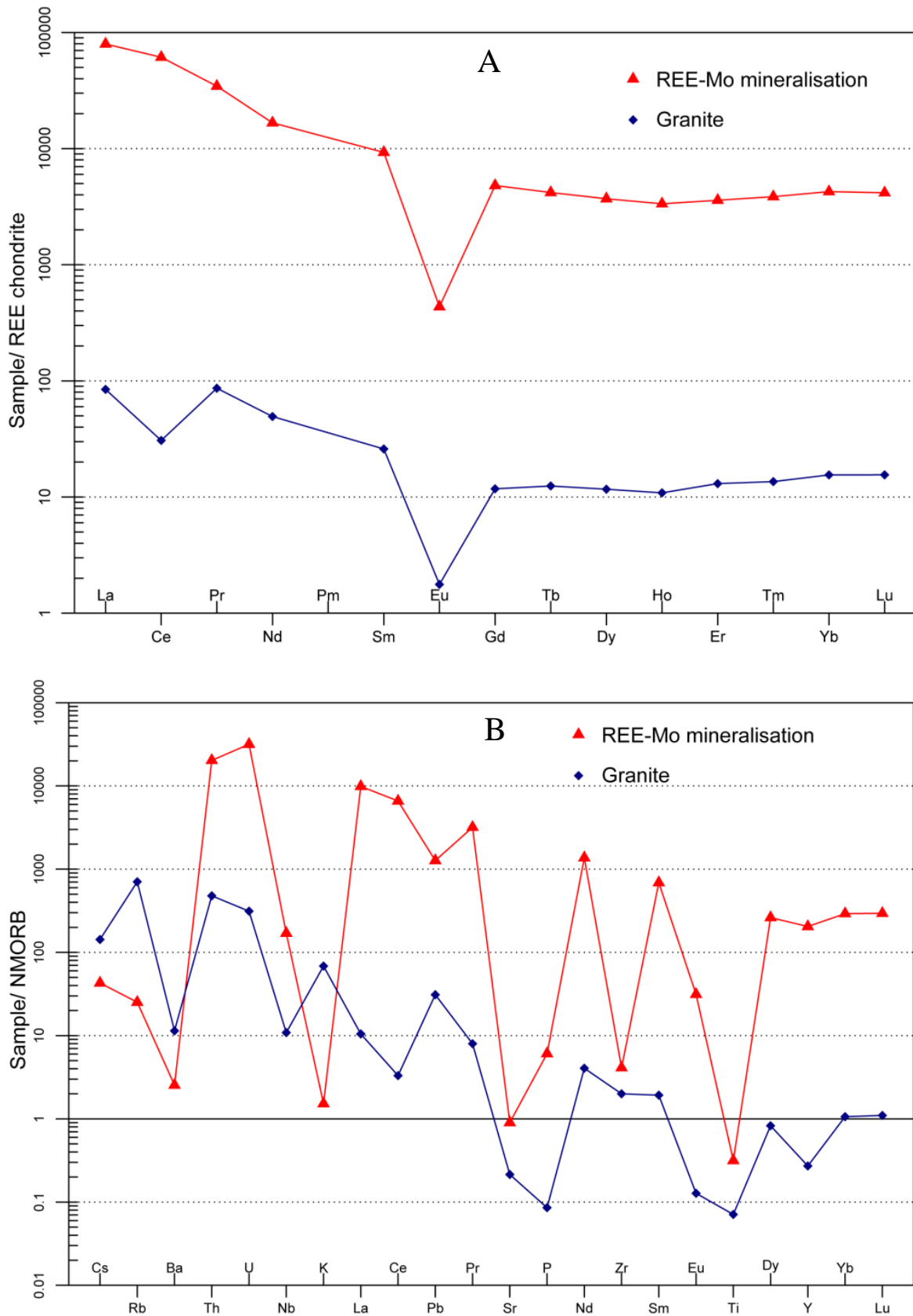


Figure 65. A. REE-diagram with data from lithogeochemical analyses of the host rock granite and the REE-Mo mineralisation at Târesâive. Normalizing values for chondrite from Boynton (1984). **B.** Multi-element diagram, rocks as in A. Normalizing values for N-MORB from Sun & McDonough (1989).

Analytical results and interpretation of geochronological data

Zircon were obtained from a density separate of a crushed rock sample using a Wilfley water table. The magnetic minerals were removed by a hand magnet. Handpicked crystals were mounted in transparent epoxy resin together with chips of reference zircon 91 500. The zircon mounts were polished and after gold coating examined at the Swedish Museum of Natural History in Stockholm. High-spatial resolution secondary ion massspectrometer (SIMS) analysis was done in November 2015 using a Cameca IMS 1 280 at the Nordsim facility at the Swedish Museum of Natural History in Stockholm. Detailed descriptions of the analytical procedures are given in Whitehouse et al. (1997, 1999) and Whitehouse & Kamber (2005).

A c. 6 nA O^{2-} primary ion beam was used, yielding spot sizes of c. 15 μm . Pb/U ratios, elemental concentrations and Th/U ratios were calibrated relative to the Geostandards zircon 91 500 reference, which has an age of c. 1 065 Ma (Wiedenbeck et al. 1995, 2004). Common Pb corrected isotope values were calculated using modern common Pb composition (Stacey & Kramers 1975) and measured ^{204}Pb , in cases of a ^{204}Pb count rate above the detection limit. Decay constants follow the recommendations of Steiger & Jäger (1977). Diagrams and age calculations of isotopic data were made using software Isoplot 4.15 (Ludwig 2012). All age uncertainties are presented at the 95 percent confidence level.

Many of the zircon are brown or reddish brown but colourless grains also occur. Several zircon are turbid and metamict. Most are euhedral, often with somewhat rounded terminations. Rounded crystals also occur and some have a corroded appearance. Cores are common but most of the selected crystals lack visible cores (Fig. 66). The cathodoluminescence appearance differs greatly between the mounted zircon crystals. Some are more or less homogeneous, sometimes with a faint zonation or blotchy. Others have pronounced zonation that can be either oscillatory or irregular (Fig. 66).

Ten crystals were analysed with one spot in each. All ten data points are discordant in the concordia diagram. Three are strongly discordant and seven are reversely discordant. One of the latter (spot 10) is very discordant and plots far from the other six and shows an older $^{207}\text{Pb}/^{206}\text{Pb}$ age. It is not possible to calculate a meaningful discordia age using the Isoplot program. The $^{207}\text{Pb}/^{206}\text{Pb}$ ages of the six reversely discordant points (spot 10 excluded) differ substantially so it is not possible to calculate a meaningful average age (Fig. 67). Analyses 5, 7, and 8 have roughly similar $^{207}\text{Pb}/^{206}\text{Pb}$ ages with an average of $1\,882.5 \pm 3.4$ Ma (2σ).

The zircon display very high U concentration at 1 917–5 369 ppm, except for analysis 3 that shows 314 ppm (Table 21). The high U content is probably the reason for the disturbance of the U-Pb system making the zircon unsuitable for exact geochronology. The measured Th/U ratio varies from 0.07 to 0.36 but for analysis 3 that shows 0.83 (Table 21). The average $^{207}\text{Pb}/^{206}\text{Pb}$ age of analyses 5, 7, and 8 around 1.88 Ga is chosen as the best age estimate interpreted to date igneous crystallisation of the granite at Tåresåive.

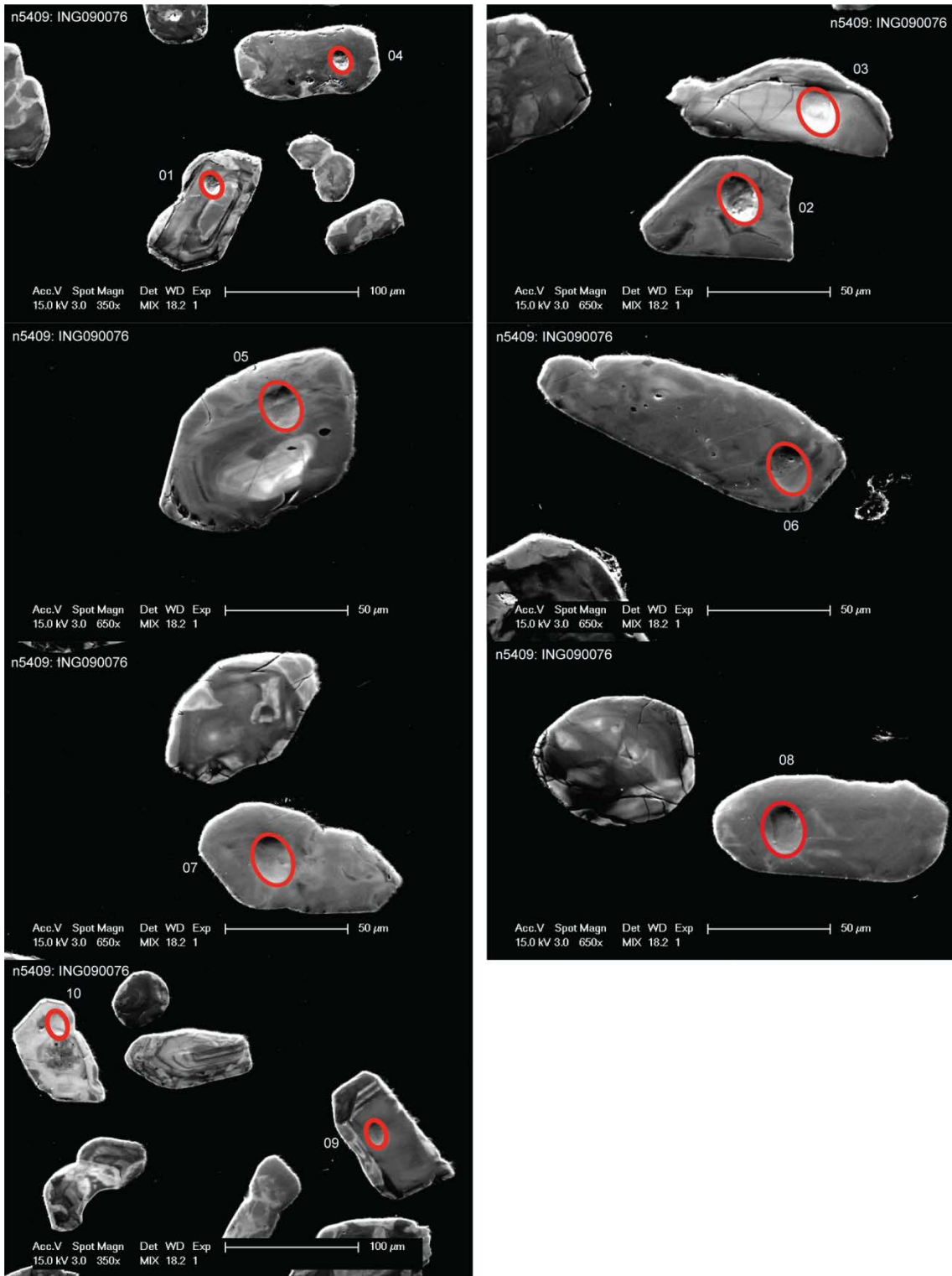


Figure 66. Cathodoluminescence images of the analysed zircon grains. Red ellipses mark the approximate locations of analyses. Numbers refer to analytical spot number in Table 21.

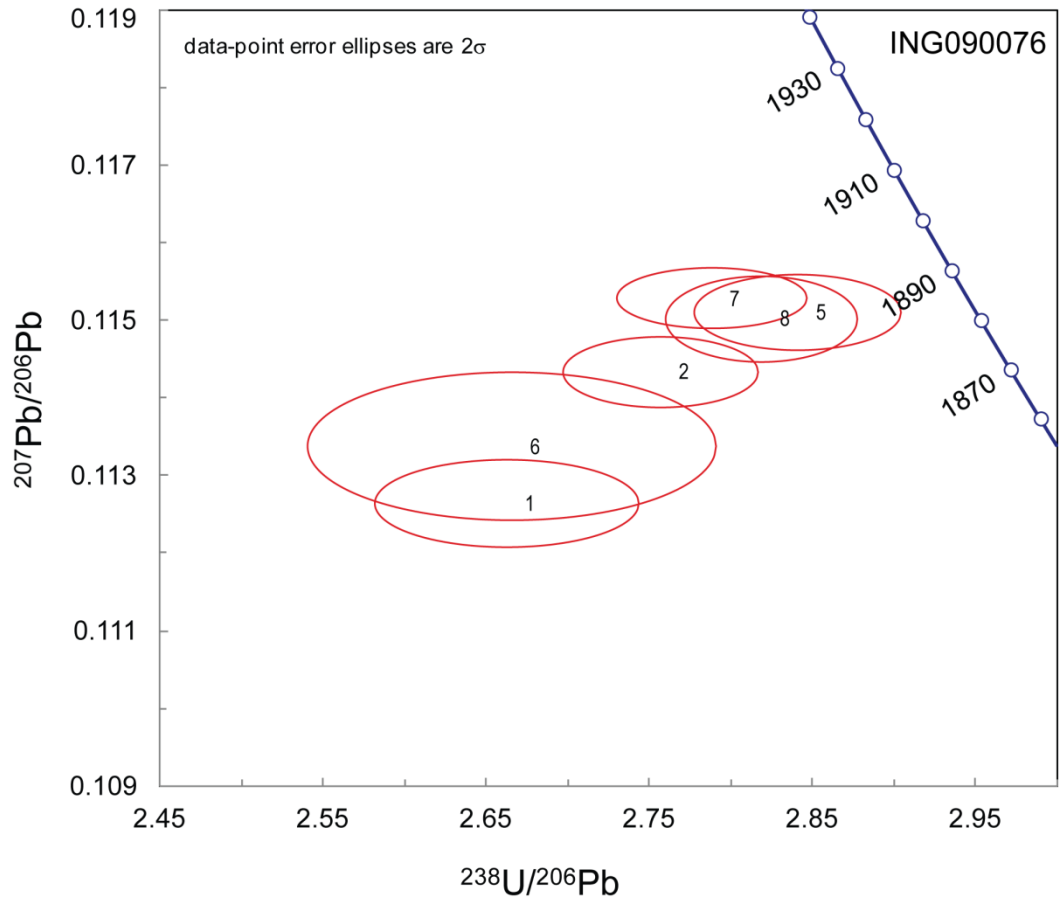


Figure 67. Tera-Wasserburg diagram showing U-Pb SIMS zircon data, all analyses except 3, 4, 9, and 10 are shown.

Table 21. SIMS U-Pb-Th zircon data.

Sample/ spot #	U ppm	Th ppm	Pb ppm	Th/U calc ^{*1}	²⁰⁷ Pb ²³⁵ U	±σ %	²⁰⁸ Pb ²³² Th	±σ %	²³⁸ U ²⁰⁶ Pb	±σ %	²⁰⁷ Pb ²⁰⁶ Pb	±σ %	ρ *2	Disc. % conv. *3	²⁰⁷ Pb ²⁰⁶ Pb	±σ (Ma)	²⁰⁶ Pb ²³⁸ U	±σ (Ma)	²⁰⁶ Pb/ ²⁰⁴ Pb measured	f ₂₀₆ % *4
n5409-01	2172	516	974	0.32	5.833	1.26	0.1278	2.9	2.663	1.24	0.1126	0.21	0.99	13.5	1842	4	2056	22	4846	0.39
n5409-02	2568	490	1092	0.22	5.718	0.90	0.1105	3.6	2.757	0.89	0.1143	0.16	0.98	7.8	1869	3	1995	15	12125	0.15
n5409-03	314	262	89	0.36	3.309	1.08	0.0389	3.7	4.401	0.90	0.1056	0.59	0.84	-26.0	1725	11	1320	11	3043	0.61
n5409-04	5895	1297	802	0.13	1.340	8.43	0.0372	14.4	8.467	8.36	0.0823	1.07	0.99	-44.9	1253	21	720	57	1493	1.25
n5409-05	2632	826	1116	0.32	5.586	0.92	0.1003	2.7	2.841	0.91	0.1151	0.17	0.98	3.8	1881	3	1944	15	54377	0.03
n5409-06	5369	636	2313	0.14	5.864	1.94	0.1105	4.3	2.666	1.91	0.1134	0.34	0.98	12.6	1854	6	2053	34	185650	0.01
n5409-07	2888	264	1182	0.10	5.700	0.87	0.1026	4.0	2.788	0.86	0.1153	0.14	0.99	5.6	1884	2	1976	15	189261	0.01
n5409-08	2097	168	855	0.13	5.626	0.87	0.1531	4.5	2.819	0.85	0.1150	0.20	0.97	4.7	1880	4	1957	14	161054	0.01
n5409-09	1917	688	224	0.19	1.018	1.47	0.0293	2.9	10.129	1.28	0.0748	0.71	0.88	-44.9	1063	14	607	7	3092	0.60
n5409-10	2298	155	1215	0.15	7.471	0.87	0.2263	2.8	2.176	0.86	0.1179	0.13	0.99	32.1	1925	2	2437	17	13951	0.13

Isotope values are common Pb corrected using modern common Pb composition (Stacey & Kramers 1975) and measured ²⁰⁴Pb.

*1 Th/U ratios calculated from ²⁰⁸Pb/²⁰⁶Pb and ²⁰⁷Pb/²⁰⁶Pb ratios, assuming single stage of closed U-Th-Pb evolution.

*2 Error correlation in conventional concordia space. Do not use for Tera-Wasserburg plots.

*3 Age discordance in conventional concordia space. Positive numbers are reverse discordant.

*4 Figures in parentheses are given when no correction has been applied, and indicate a value calculated assuming present-day Stacey-Kramers common Pb.

Discussion and conclusion

Age determination of the granite shows that there is a heterogeneous disturbance of the analysed zircon, which results in a poorly constrained age, but the average $^{207}\text{Pb}/^{206}\text{Pb}$ age of analyses 5, 7, and 8 around 1.88 Ga is the best age estimate for igneous crystallisation of the granite at Tåresåive with the data at hand. The REE and Mo (U, Th, Nb, Ta) mineralisation and processes related to its genesis with elevated U and Th contents in the rocks, suggest an origin of the magmatic zircon population of the granite to be coeval with the mineralisation event. This is apparent from the granite zircon as generally very high U and Th concentrations (Table 21).

Thus, the earlier suggested genetic model where fluids and vapour phases in a late-magmatic hydrothermal system formed in connection with degassing and reduction of internal pressure, in connection with the late-magmatic event fractures arise, where molybdenum- and REE-rich solutions form the basis of the fracture-hosted mineralisation, is a viable interpretation (Claeson & Antal Lundin *in press a*). The results were integrated in the mapping of the 27I Tjåmotis SV, SO area (Claeson & Antal Lundin *in press a*). Summary of sample data is given in Table 22.

Table 22. Summary of sample data.

Rock type	Granite
Lithotectonic unit	Norrbottn lithotectonic unit of the Svecokarelian orogen
Lithological unit	
Sample number	ING090076B
Lab_id	n5409
Coordinates	7421196/709317 (Sweref99TM)
Map sheet	27J Porjus SV (RT90)
Locality	Tåresåive
Project	Sydvästra Norrbotten (80025)

References

- Boynnton, W.V., 1984: Cosmochemistry of the Rare Earth Elements: Meteorite studies. *In* P. Henderson (ed.): *Rare earth element geochemistry*. Elsevier Science B.V. 63–114.
- Claeson, D. & Antal Lundin, I., *in press a*: Beskrivning till berggrundskartan 27J Porjus SV. *Sveriges geologiska undersökning*.
- Ludwig, K.R., 2012: User's manual for Isoplot 3.75. A Geochronological Toolkit for Microsoft Excel. *Berkeley Geochronology Center Special Publication No. 5*, 75 pp.
- Stacey, J.S. & Kramers, J.D., 1975: Approximation of terrestrial lead isotope evolution by a two-stage model. *Earth and Planetary Science Letters* 26, 207–221.
- Steiger, R.H. & Jäger, E., 1977: Convention on the use of decay constants in geo- and cosmochronology. *Earth and Planetary Science Letters* 36, 359–362.
- Sun, S.S. & McDonough, W.F., 1989: Chemical and isotopic systematic of oceanic basalts: implications for mantle composition and processes. *In* A.D. Saunders & M.J. Norry (eds.): *Magmatism in ocean basins*. Geological Society of London, Special Publication 42, 313–345.
- Whitehouse, M.J., Claesson, S., Sunde, T. & Vestin, J., 1997: Ion-microprobe U–Pb zircon geochronology and correlation of Archaean gneisses from the Lewisian Complex of Gruinard Bay, north-west Scotland. *Geochimica et Cosmochimica Acta* 61, 4 429–4 438.
- Whitehouse, M.J., Kamber, B.S. & Moorbath, S., 1999: Age significance of U–Th–Pb zircon data from Early Archaean rocks of west Greenland: a reassessment based on combined ion-microprobe and imaging studies. *Chemical Geology (Isotope Geoscience Section)* 160, 201–224.
- Whitehouse, M., J. & Kamber, B.S., 2005: Assigning Dates to Thin Gneissic Veins in High-Grade Metamorphic Terranes: A Cautionary Tale from Akilia, Southwest Greenland. *Journal of Petrology* 46, 291–318.
- Wiedenbeck, M., Allé, P., Corfu, F., Griffin, W.L., Meier, M., Oberli, F., Quadt, A.V., Roddick, J.C. & Spiegel, W., 1995: Three natural zircon standards for U-Th-Pb, Lu-Hf, trace element and REE analyses. *Geostandards Newsletter* 19, 1–23.
- Wiedenbeck, M., Hanchar, J.M., Peck, W.H., Sylvester, P., Valley, J., Whitehouse, M., Kronz, A., Morishita, Y., Nasdala, L., Fiebig, J., Franchi, I., Girard, J.P., Greenwood, R.C., Hinton, R., Kita, N., Mason, P.R.D., Norman, M., Ogasawara, M., Piccoli, P.M., Rhede, D., Satoh, H., Schulz-Dobrick, B., Skår, O., Spicuzza, M.J., Terada, K., Tindle, A., Togashi, S., Vennemann, T., Xie, Q. & Zheng, Y.F., 2004: Further Characterisation of the 91500 Zircon Crystal. *Geostandards and Geoanalytical Research* 28, 9–39.

U-Pb ZIRCON AGE OF MONZONITE AT NJUORRAMJAURATJ, MAP SHEET 27J PORJUS SV, NORRBOTTEN COUNTY

Authors: Dick Claeson, Ildikó Antal Lundin & Fredrik Hellström

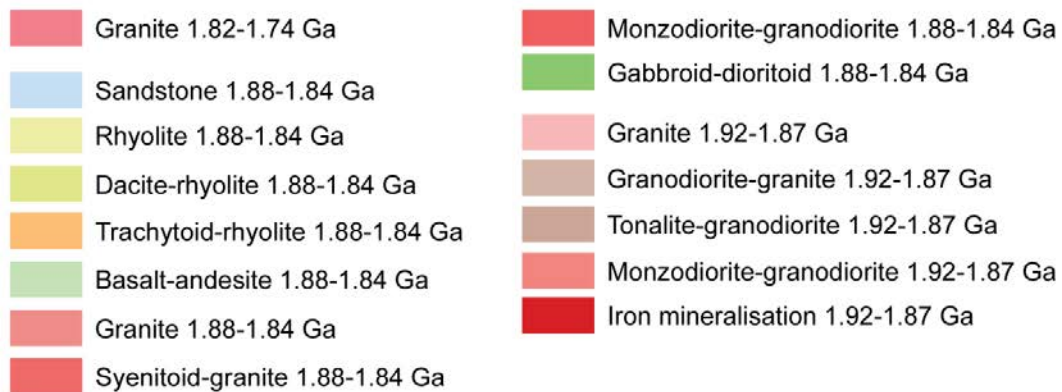
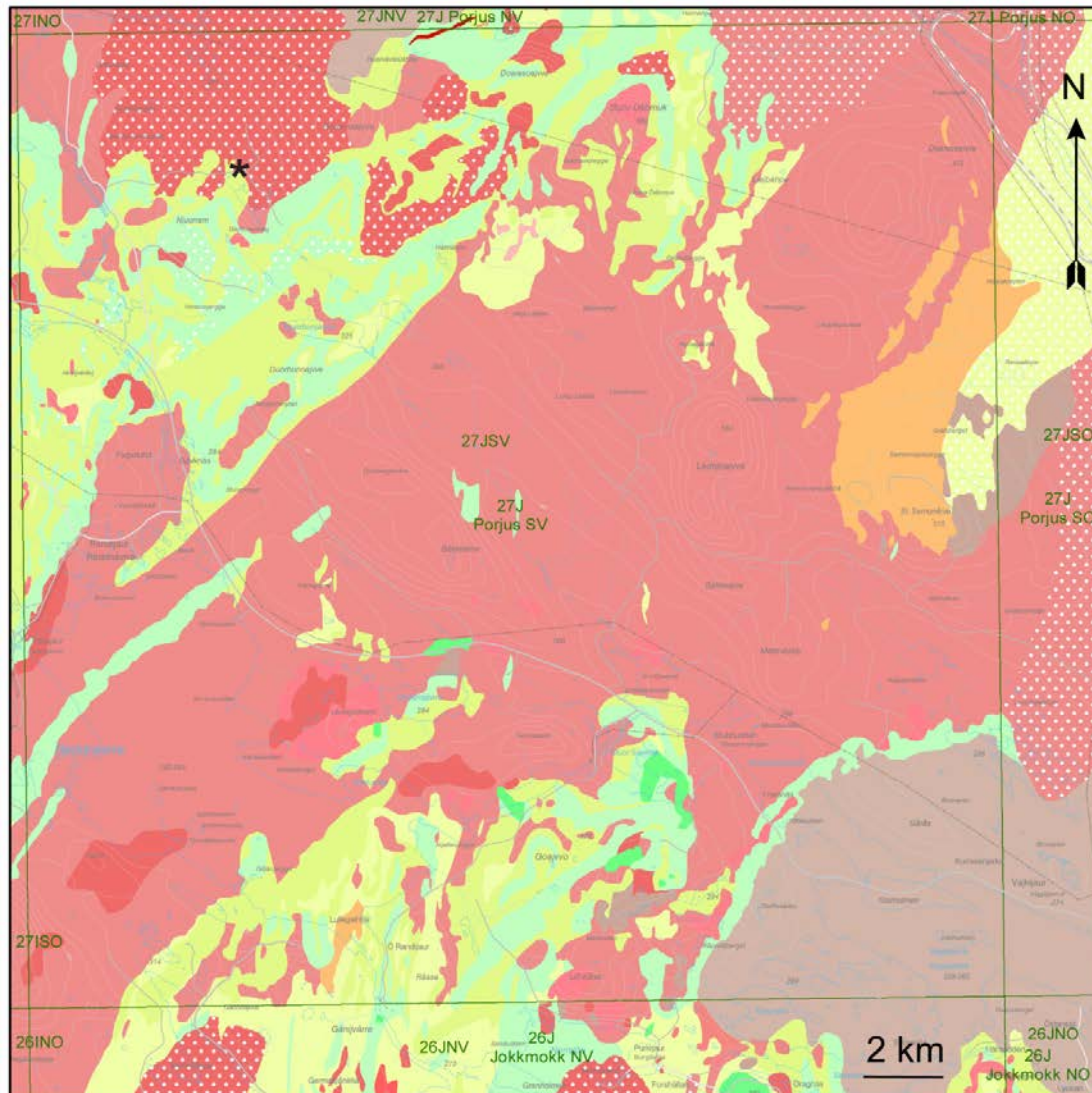


Figure 68. Bedrock map of the area, sampling location marked with black star.

Introduction

Norrbottnen, Sweden is a key area of Europe for future exploration and mining. In order to establish age relations for magmatic activity and metamorphic overprinting in this area, the sampled rock was selected (Fig. 48, 49, 68). The igneous age of the monzonite at Njuorramjauratj is unknown. The aim of this study is to date igneous crystallisation of a monzonite that occurs with coeval granite, quartz monzodiorite to monzodiorite in the 27J Porjus SV map area. These rocks are heterogeneously deformed and metamorphosed. Another issue would be to date the metamorphic recrystallisation of the foliated and at places lineated monzonite, i.e., to date regional metamorphism of the area if possible.

Sample description

The sampled monzonite is associated with granite, quartz monzodiorite and monzodiorite. The rock is red to greyish red or reddish grey, lineated, foliated, porphyric, recrystallised and medium-grained to coarse-grained (Fig. 69). There are 10–25 mm large potassium feldspar phenocrysts (0–20 %). Amphibole and biotite occur in the groundmass, where amphibole clearly dominates (Fig. 70). Accessory minerals are quartz, biotite, opaque minerals, titanite, apatite, and zircon. Titanite is relatively abundant and some display fish-tail twinning. Outcrop measurement of magnetic susceptibility yielded $3\,030\text{--}5\,090 \times 10^{-5}$ SI, geometric mean at $3\,960 \times 10^{-5}$ SI. Ground measurement of radiation shows $K = 3.9\%$, $U = 4.8$ ppm, and $Th = 19.0$ ppm. Petrophysical measurements of two samples show density at $2\,661$ and $2\,766$ kg/m³, magnetic susceptibility $6\,961$ and $15\,314 \times 10^{-5}$ SI, and remanent magnetization intensity of 530 and 660 mA/m.

The monzonite at Njuorramjauratj shows a slightly LREE-enriched and flat HREE pattern, with a pronounced negative Eu anomaly (Fig. 71). The LREE enrichment is due to fractional crystallisation, the flat, unfractionated HREE pattern shows that no garnet was left in the residue at the location of magma genesis, and the Eu anomaly is indicative of extensive plagioclase fractionation. The negative anomalies shown in the multi-element diagram of Sr and Eu are due to plagioclase fractionation, the P anomaly of apatite fractionation, and the Ti anomaly of Fe-Ti oxide fractionation (Fig. 71). The strong negative Nb anomaly may suggest a subduction related petrogenesis (Fig. 71).

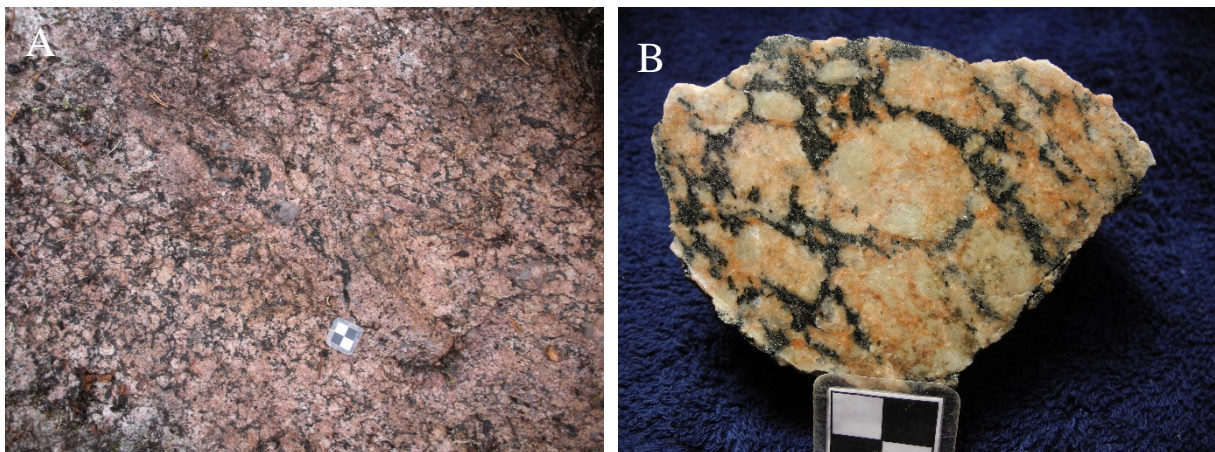


Figure 69. A. Outcrop of the dated monzonite (cm-scale). B. Cut and wetted sample of monzonite. Photos: Dick Claeson.

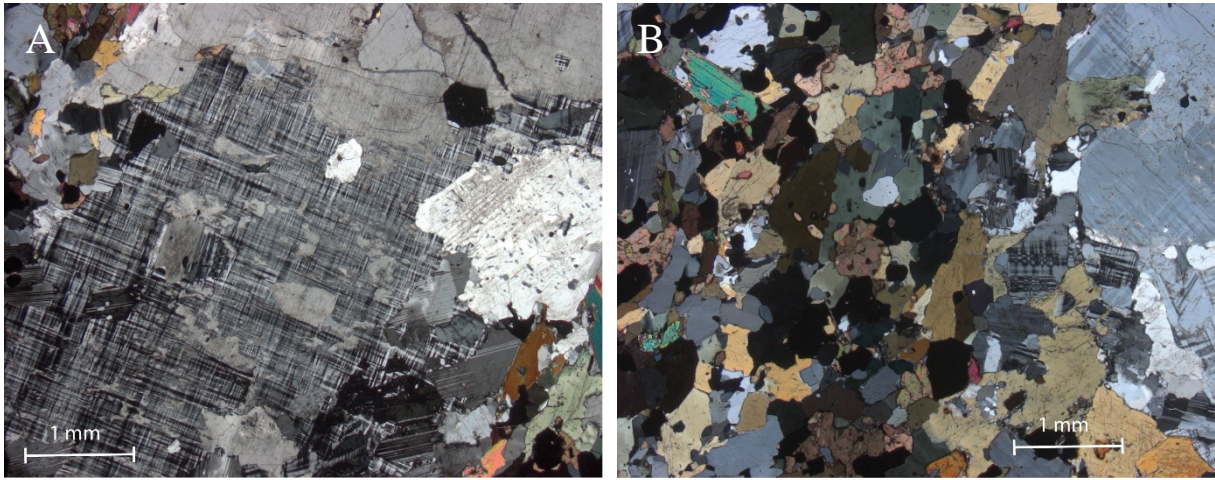


Figure 70. A. Potassium feldspar phenocryst with inclusions of plagioclase in monzonite. **B.** Amphibole, biotite, titanite, and Fe-Ti oxide in monzonite. Micrographs: Dick Claeson.

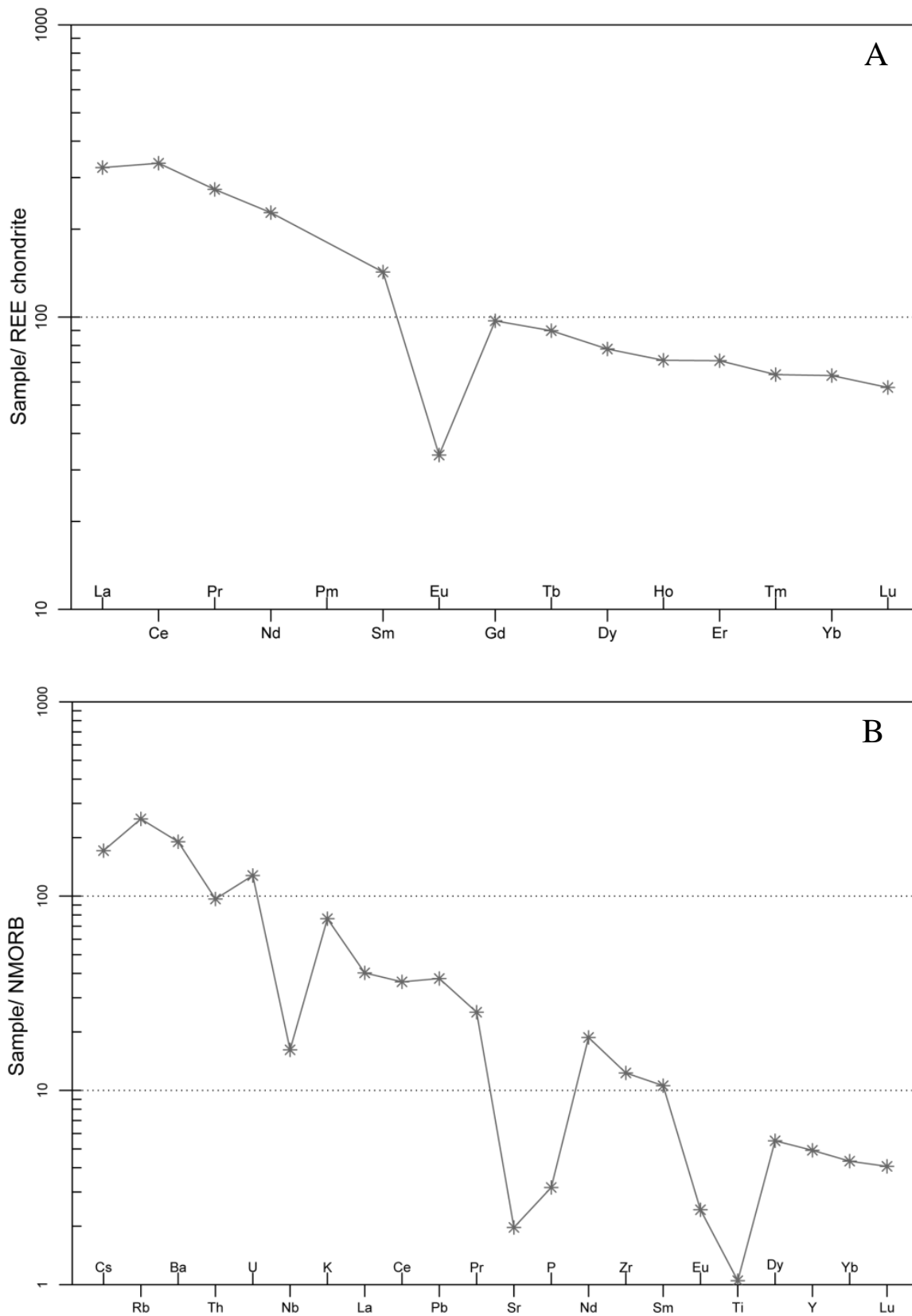


Figure 71. A. REE-diagram of monzonite. Normalizing values for chondrite from Boynton (1984). **B.** Multi-element diagram, rock as in A. Normalizing values for N-MORB from Sun & McDonough (1989).

Analytical results and interpretation of geochronological data

In situ U-Pb-Th SIMS analysis of zircon was performed at the NORDSIM facility at the Museum of Natural History in Mars 2010. Detailed descriptions of the analytical procedures are given in Whitehouse et al. (1997, 1999). Pb/U ratios, elemental concentrations and Th/U ratios were calibrated relative to the Geostandards zircon 91 500 reference, which has an age of c. 1 065 Ma (Wiedenbeck et al. 1995, 2004). Common Pb corrected isotope values were calculated using modern common Pb composition (Stacey & Kramers 1975) and measured ^{204}Pb . Decay constants follow the recommendations of Steiger & Jäger (1977). Diagrams and age calculations of isotopic data were made using software Isoplot 4.15 (Ludwig 2012).

The analytical results are shown in Table 23. The zircon grains in the sample have subhedral to euhedral prismatic shapes. Most grains have inclusions and are usually black turbid. BSE-images show an internal oscillatory growth zonation in the zircon (Fig. 72). The zircon are interpreted as igneous with no secondary recrystallisation.

The U content of the analysed zircon is 57–231 ppm and Th/U ratios are 0.33–0.98 ($n = 10$, Table 23), except one data point (No. 15a) which has 1 061 ppm U and a Th/U ratio of 0.29. This analysis has a high value of common lead and is also strongly discordant (Table 23). A concordia age at $1\,876 \pm 8$ Ma (95 % confidence, MSWD = 0.06, $n = 9$) can be calculated from eight concordant and a less than 0.2 % discordant analysis (No. 1a). The weighted average $^{207}\text{Pb}/^{206}\text{Pb}$ age for the same analyses is $1\,875 \pm 6$ Ma (2σ , MSWD = 0.77; $n = 9$, Fig. 73). The weighted average $^{207}\text{Pb}/^{206}\text{Pb}$ age at $1\,875 \pm 6$ Ma is interpreted to date igneous crystallisation of the monzonite.

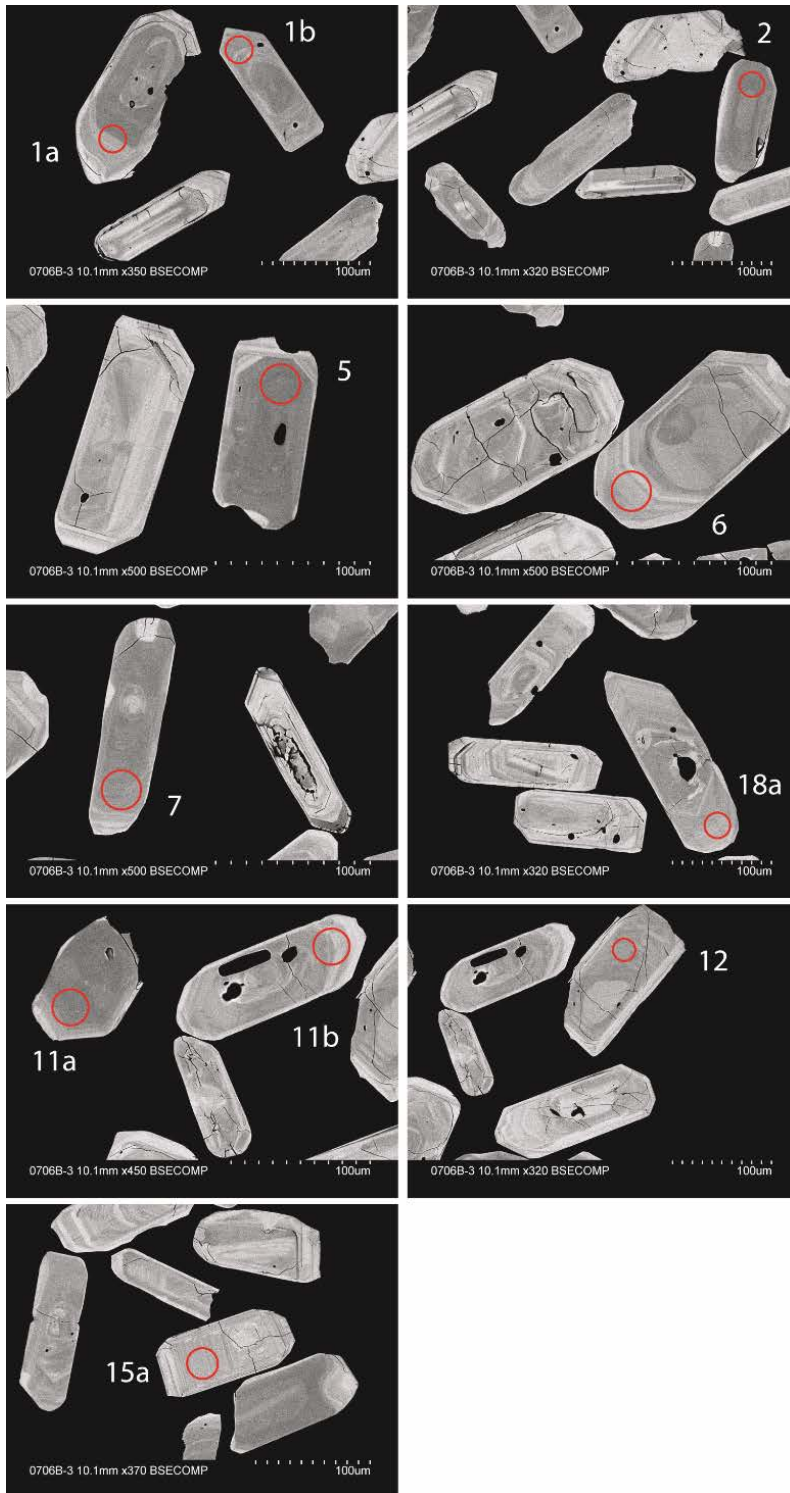


Figure 72. BSE-images of zircon from the monzonite. Red circles mark the approximate location of analyses spots. Numbers refer to analytical spot number in Table 23.

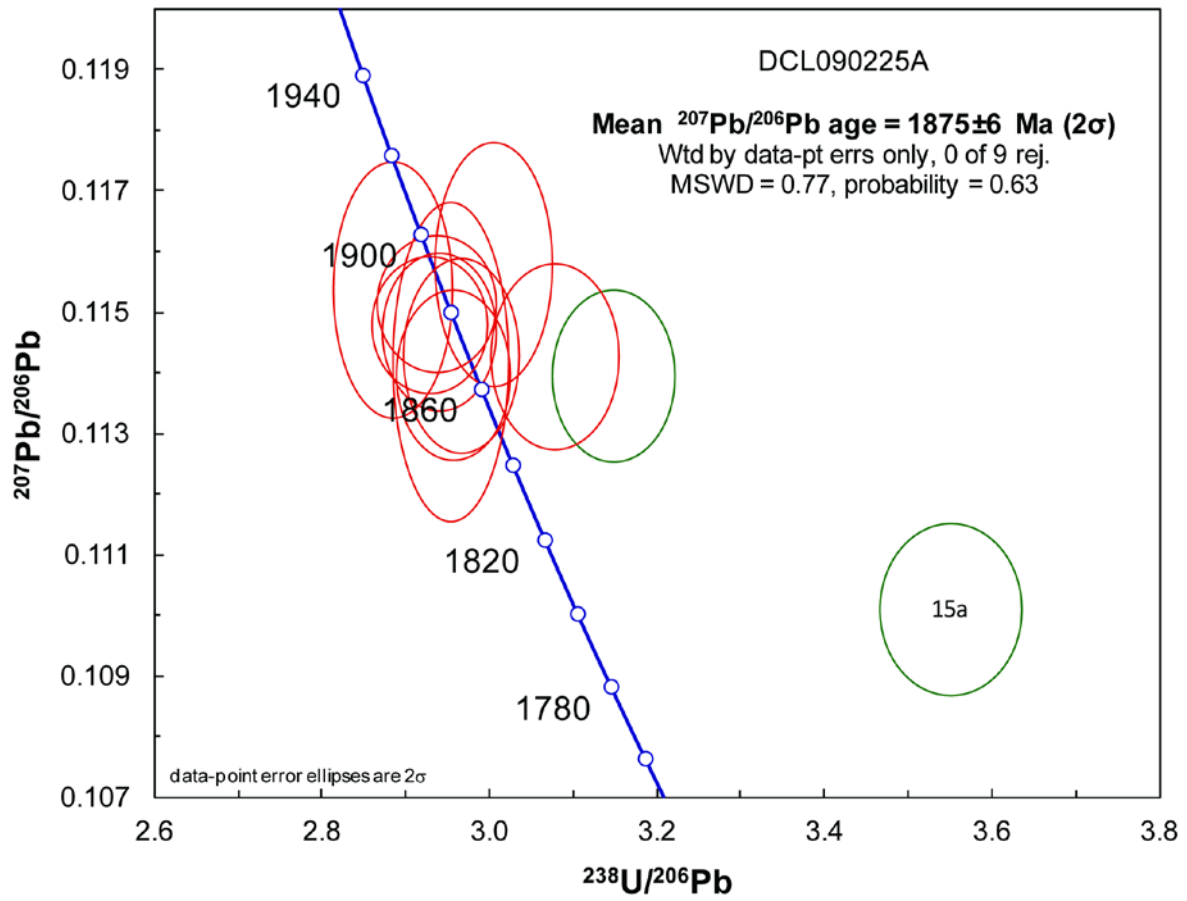


Figure 73. Tera-Wasserburg diagram showing U-Pb SIMS zircon data. Analyses used in age calculation are shown in red.

Table 23. SIMS U-Pb-Th zircon data.

Sample/ spot #	U ppm	Th ppm	Pb ppm	Th/U calc ^{*1}	²⁰⁷ Pb ²³⁵ U	±σ %	²⁰⁸ Pb ²³² Th	±σ %	²³⁸ U ²⁰⁶ Pb	±σ %	²⁰⁷ Pb ²⁰⁶ Pb	±σ %	ρ ^{*2}	Disc. % conv. ^{*3}	²⁰⁷ Pb ²⁰⁶ Pb	±σ (Ma)	²⁰⁶ Pb ²³⁸ U	±σ (Ma)	²⁰⁶ Pb/ ²⁰⁴ Pb measured	f ₂₀₆ % ^{*4}
n3580-01a	188	79	80	0.44	5.405	1.07	0.1018	3.8	2.937	0.99	0.1151	0.40	0.93	0.4	1882	7	1889	16	68540	0.03
n3580-01b	144	62	58	0.42	5.119	1.15	0.0939	3.9	3.078	1.01	0.1143	0.54	0.88	-3.4	1868	10	1814	16	29140	0.06
n3580-5	57	44	26	0.78	5.330	1.35	0.0980	4.0	2.954	0.96	0.1142	0.94	0.72	0.8	1867	17	1880	16	35629	{0.05}
n3580-6	186	68	72	0.33	4.989	1.08	0.0870	4.0	3.149	0.95	0.1139	0.51	0.88	-5.3	1863	9	1778	15	4820	0.39
n3580-7	105	53	45	0.52	5.311	1.12	0.0996	3.9	2.967	0.96	0.1143	0.58	0.86	0.3	1868	10	1873	16	65060	{0.03}
n3580-02a	83	77	39	0.98	5.312	1.19	0.1038	3.9	3.006	0.95	0.1158	0.71	0.80	-2.5	1892	13	1852	15	31239	{0.06}
n3580-11a	61	39	28	0.66	5.515	1.26	0.1013	4.0	2.884	1.01	0.1154	0.75	0.80	2.1	1886	13	1919	17	43216	{0.04}
n3580-11b	157	74	67	0.48	5.378	1.06	0.0997	3.9	2.940	0.95	0.1147	0.47	0.90	0.8	1875	8	1887	16	118244	{0.02}
n3580-12	139	59	58	0.44	5.313	1.07	0.0999	3.9	2.957	0.95	0.1140	0.50	0.88	0.9	1863	9	1878	15	145004	{0.01}
n3580-15a	1069	355	363	0.29	4.274	1.11	0.0816	4.1	3.552	0.98	0.1101	0.53	0.88	-12.7	1801	10	1599	14	405	4.62
n3580-18a	231	111	99	0.48	5.404	1.04	0.0977	3.8	2.929	0.97	0.1148	0.40	0.92	1.1	1876	7	1894	16	56398	0.03

Isotope values are common Pb corrected using modern common Pb composition (Stacey & Kramers 1975) and measured ²⁰⁴Pb.

*1 Th/U ratios calculated from ²⁰⁸Pb/²⁰⁶Pb and ²⁰⁷Pb/²⁰⁶Pb ratios, assuming single stage of closed U-Th-Pb evolution.

*2 Error correlation in conventional concordia space. Do not use for Tera-Wasserburg plots.

*3 Age discordance in conventional concordia space. Positive numbers are reverse discordant.

*4 Figures in parentheses are given when no correction has been applied, and indicate a value calculated assuming present-day Stacey-Kramers common Pb.

Discussion and conclusion

Igneous crystallisation of the monzonite at $1\,875 \pm 6$ Ma shows that the monzonite and associated intrusive rocks in the Porjus area are part of the Perthite monzonite suite of 1.88–1.86 Ga age, and not older, which could be suggested by their sometimes strongly deformed and metamorphic appearance. Metamorphic overprinting of the monzonite did apparently not affect the zircon in the sample enough to develop secondary growth or major recrystallisation. Thus, the degree of deformation and metamorphic overprinting is not to be used straight forward to assign age of the early Svecokarelian intrusive rocks of the area. The results were integrated in the mapping of the 27J Porjus SV area (Claeson & Antal Lundin *in press a*). Summary of sample data is given in Table 24.

Table 24. Summary of sample data.

Rock type	Monzonite
Lithotectonic unit	Norrbottnen lithotectonic unit of the Svecokarelian orogen
Lithological unit	
Sample number	DCL090225A
Lab_id	n3580
Coordinates	7421360/690793 (Sweref99TM)
Map sheet	27J Porjus SV (RT90)
Locality	Njuorramjauratj
Project	Sydvästra Norrbotten (80025)

References

- Boynnton, W.V., 1984: Cosmochemistry of the Rare Earth Elements: Meteorite studies. In P. Henderson (ed.): *Rare earth element geochemistry*. Elsevier Science B.V. 63–114.
- Claeson, D. & Antal Lundin, I., *in press a*: Beskrivning till berggrundskartan 27J Porjus SV. *Sveriges geologiska undersökning*.
- Ludwig, K.R., 2012: User's manual for Isoplot 3.75. A Geochronological Toolkit for Microsoft Excel. *Berkeley Geochronology Center Special Publication No. 5*, 75 pp.
- Stacey, J.S. & Kramers, J.D., 1975: Approximation of terrestrial lead isotope evolution by a two-stage model. *Earth and Planetary Science Letters* 26, 207–221.
- Steiger, R.H. & Jäger, E., 1977: Convention on the use of decay constants in geo- and cosmochronology. *Earth and Planetary Science Letters* 36, 359–362.
- Sun, S.S. & McDonough, W.F., 1989: Chemical and isotopic systematic of oceanic basalts: implications for mantle composition and processes. In A.D. Saunders & M.J. Norry (eds.): *Magmatism in ocean basins*. Geological Society of London, Special Publication 42, 313–345.
- Whitehouse, M.J., Claesson, S., Sunde, T. & Vestin, J., 1997: Ion-microprobe U–Pb zircon geochronology and correlation of Archaean gneisses from the Lewisian Complex of Gruinard Bay, north-west Scotland. *Geochimica et Cosmochimica Acta* 61, 4 429–4 438.
- Whitehouse, M.J., Kamber, B.S. & Moorbath, S., 1999: Age significance of U–Th–Pb zircon data from Early Archaean rocks of west Greenland: a reassessment based on combined ion-microprobe and imaging studies. *Chemical Geology (Isotope Geoscience Section)* 160, 201–224.
- Wiedenbeck, M., Allé, P., Corfu, F., Griffin, W.L., Meier, M., Oberli, F., Quadt, A.V., Roddick, J.C. & Spiegel, W., 1995: Three natural zircon standards for U–Th–Pb, Lu–Hf, trace element and REE analyses. *Geostandards Newsletter* 19, 1–23.
- Wiedenbeck, M., Hanchar, J.M., Peck, W.H., Sylvester, P., Valley, J., Whitehouse, M., Kronz, A., Morishita, Y., Nasdala, L., Fiebig, J., Franchi, I., Girard, J.P., Greenwood, R.C., Hinton, R., Kita, N., Mason, P.R.D., Norman, M., Ogasawara, M., Piccoli, P.M., Rhede, D., Satoh, H., Schulz-Dobrick, B., Skår, O., Spicuzza, M.J., Terada, K., Tindle, A., Togashi, S., Vennemann, T., Xie, Q. & Zheng, Y.F., 2004: Further Characterisation of the 91500 Zircon Crystal. *Geostandards and Geoanalytical Research* 28, 9–39.

MAP SHEET 26J JOKKMOKK NV, NO AREA

Four rocks were sampled for age determination, one volcanic and three intrusive, in order to better constrain the mapping effort and contribute to new data and knowledge of the magmatic events in the area.

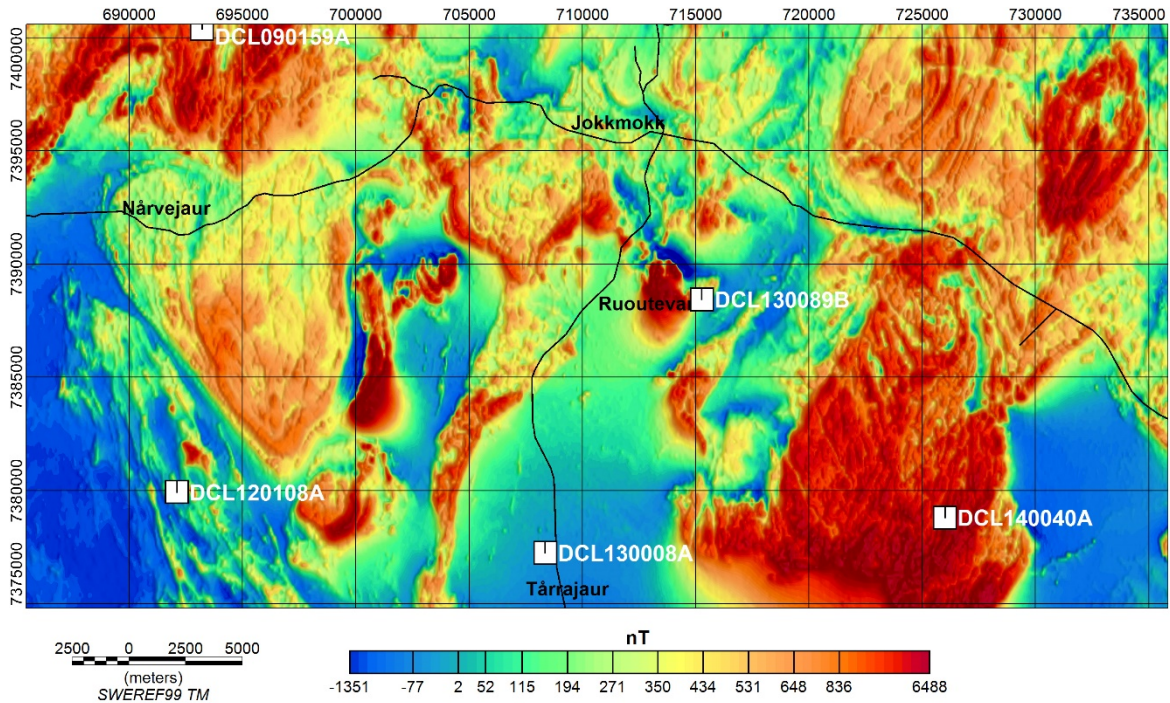


Figure 74. Magnetic total field after subtraction of the geomagnetic reference field (DGRF 1965.0) over the map area 26J Jokkmokk NO and NV. The sample locations are shown with white rectangles.

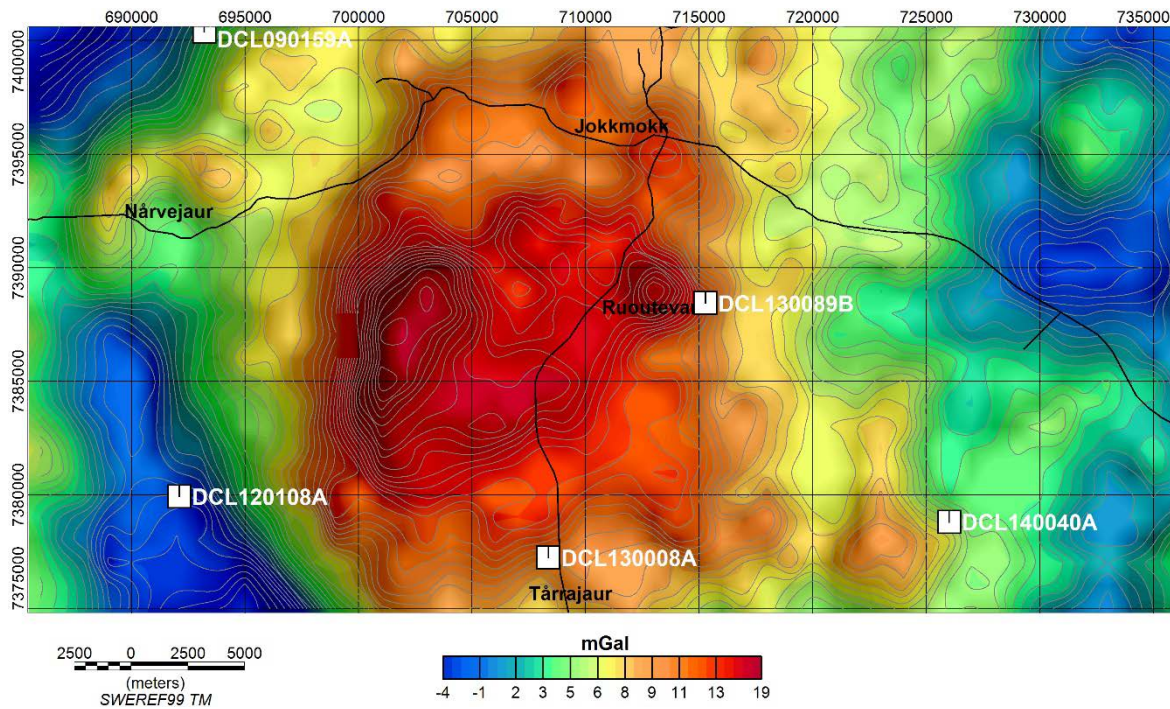


Figure 75. Residual gravity anomaly map over the map sheet 26J Jokkmokk NO and NV. The sample locations are shown with white rectangles.

U-Pb ZIRCON AGE OF RHYOLITE TO TRACHYTE WEST OF LAGMANS- GRAVEN, MAP SHEET 26J JOKKMOKK NV, NORRBOTTEN COUNTY

Authors: Dick Claeson, Ildikó Antal Lundin & Fredrik Hellström

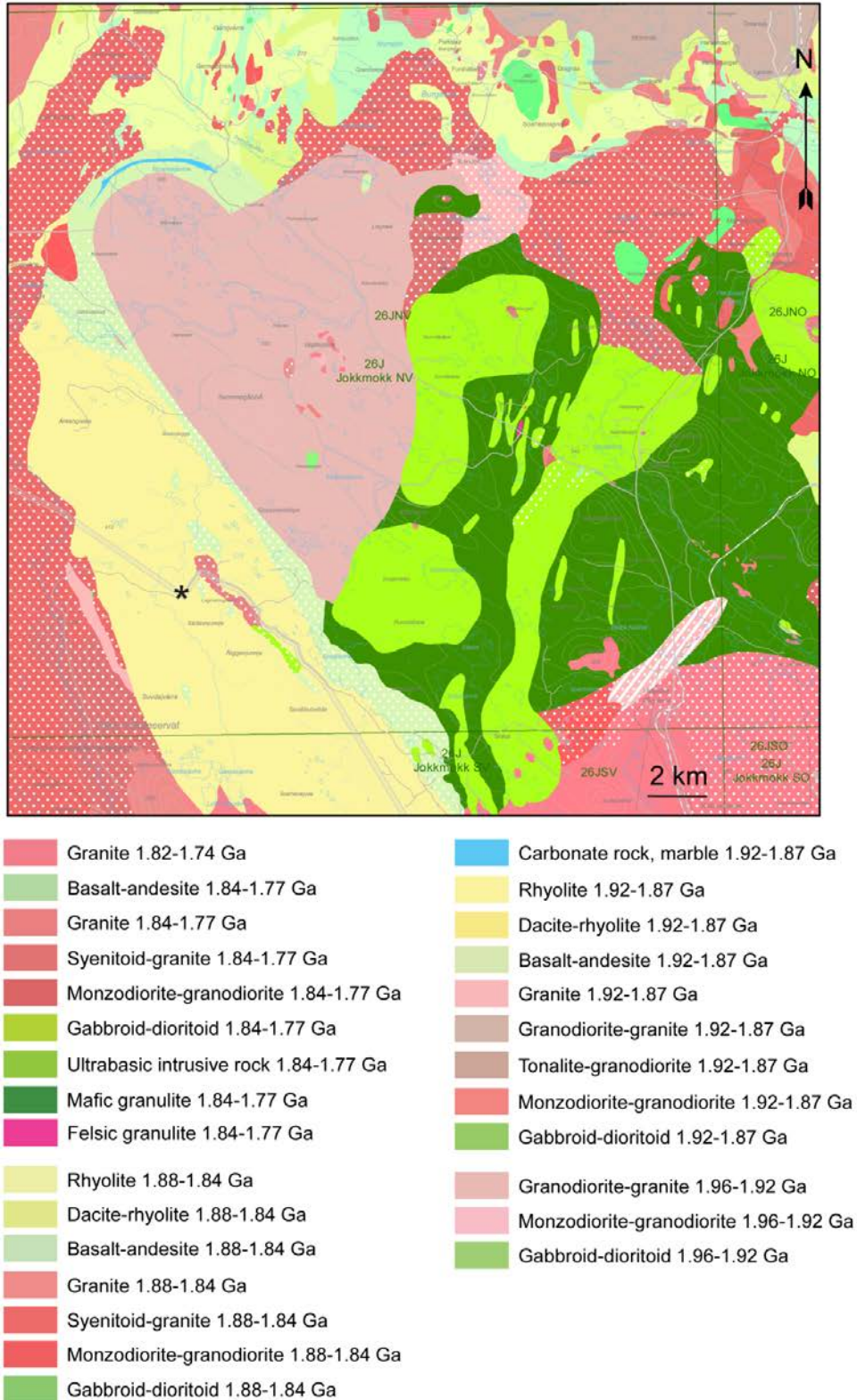


Figure 76. Bedrock map of the area, sampling location marked with black star.

Introduction

Norrbotten, Sweden is a key area of Europe for future exploration and mining. The sampled rock is part of a larger structure that is well-documented by the aeromagnetic data produced by the SGU. Both on the magnetic and gravity anomaly maps the structure is clearly seen as a high magnetic, banded pattern and as a gravity low (Fig. 75–77).

The structure is interpreted as a northwest-southeast trending body of extrusive rocks, which covers parts of the map areas 26J Jokkmokk NV and SV. BHP Billiton and Intrepid Minerals Corp. have made recent exploration efforts regarding base metals of the volcanic rocks of this structure, but the outcome is unknown to date. Since some of the extrusive rocks in the map area are gold and base-metal anomalous, knowing their age is of great interest from an exploration point of view.

If metamorphic rims or other overgrowths are present on the zircon, these should also be studied since this may be of huge significance for the interpretation of the genesis of an ore body/deposit. For example, where multiple episodes of concentration of sulphides are indicated in recent work at Aitik (Wanhainen et al. 2003, 2005) or in iron oxide–copper–gold (IOCG) mineralization in this region (Smith et al. 2009). In order to gain knowledge of when metamorphic events are in any way involved in the genesis of the formation of economic deposits on a regional scale in the Norrbotten county, by re-heating the crust and producing hydrothermal activity in volcanic rocks or structural zones, their age have to be determined. The size of the sampled anomaly on the aeromagnetic map indicates that the extrusive rocks are present for at least 35 km at the surface.

The aim of this study is to determine the magmatic age of the rhyolite to trachyte part of a major structure seen in map areas 26J Jokkmokk NV and SV, and if there are any metamorphic overgrowths, determine these as well, since the latter might show ages for the genesis of ore by redistribution of elements in the crust.

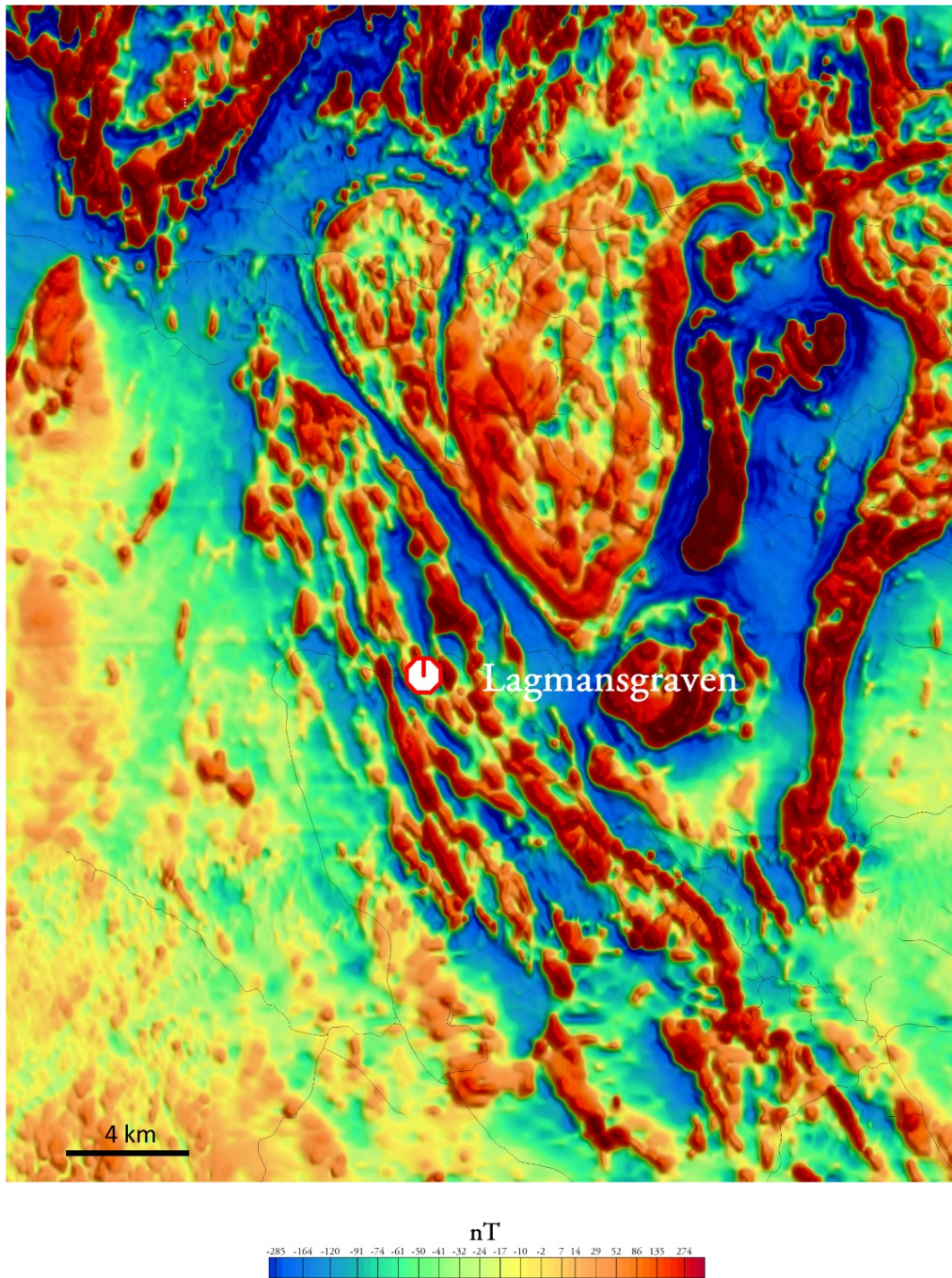


Figure 77. Magnetic anomaly map indicating the distribution of the major structures in the area, part of the map sheet 26J Jokkmokk NV with surroundings. The red and white dot shows the sample location.

Sample description

The sampled outcrop is located approximately 1 km west of the Lagmansgraven, some 25 km SW of Jokkmokk. The sample consists of rhyolite that is deformed, hydrothermally altered, recrystallised, light grey to greyish red (hydrothermally altered rocks are whitish), and varies from very fine-grained to fine-grained (Fig. 78). Fragments of other volcanic rocks are present (Fig. 78). The extrusive rocks are compositionally layered showing a banded appearance with mostly rhyolite and trachyte, minor parts of dacite are also present at the outcrop. The rocks at the outcrop are sometimes porphyritic with feldspar 2–5 mm (0–8 %) and quartz 1–2 mm (0–1 %).

Foliation/layering is oriented 160/86. The Zr content of the rhyolite is 178 ppm and at least 40 to 50 μm large zircon are present in thin-section (Fig. 79). Biotite and muscovite along with opaque minerals define the foliation seen in thin-section (Fig. 80). Magnetic susceptibility at the outcrop varies between 34 and $1\,070 \times 10^{-5}$ SI. Gamma ray measurements at the outcrop shows K = 4.6–4.7 %, U = 2.8–2.9 ppm, and Th = 14.7–15.3 ppm. Petrophysical measurements of a sample show density at $2\,602 \text{ kg/m}^3$, magnetic susceptibility 572×10^{-5} SI, and remanent magnetization intensity of 80 mA/m.

The age determined rhyolite at Lagmansgraven and an interpreted coeval andesite at the northern part of the volcanic successions, shows a LREE-enriched and flat HREE pattern, with a large and a small negative Eu anomaly, respectively (Fig. 81). The LREE enrichment is due to fractional crystallization, the flat, unfractionated HREE pattern shows that no garnet was left in the residue at the location of magma genesis, and the Eu anomaly is indicative of significant plagioclase fractionation for the rhyolite but less so for the andesite. The negative anomaly shown in the multi-element diagram of Sr and Eu suggest plagioclase fractionation (Fig. 81). The P anomaly suggests apatite fractionation and the Ti anomaly extensive Fe-Ti oxide fractionation for the rhyolite and some for the andesite (Fig. 81). The strong negative anomaly of Nb and the strong positive anomaly of Pb both suggest a subduction related petrogenesis for these rocks (Fig. 81).

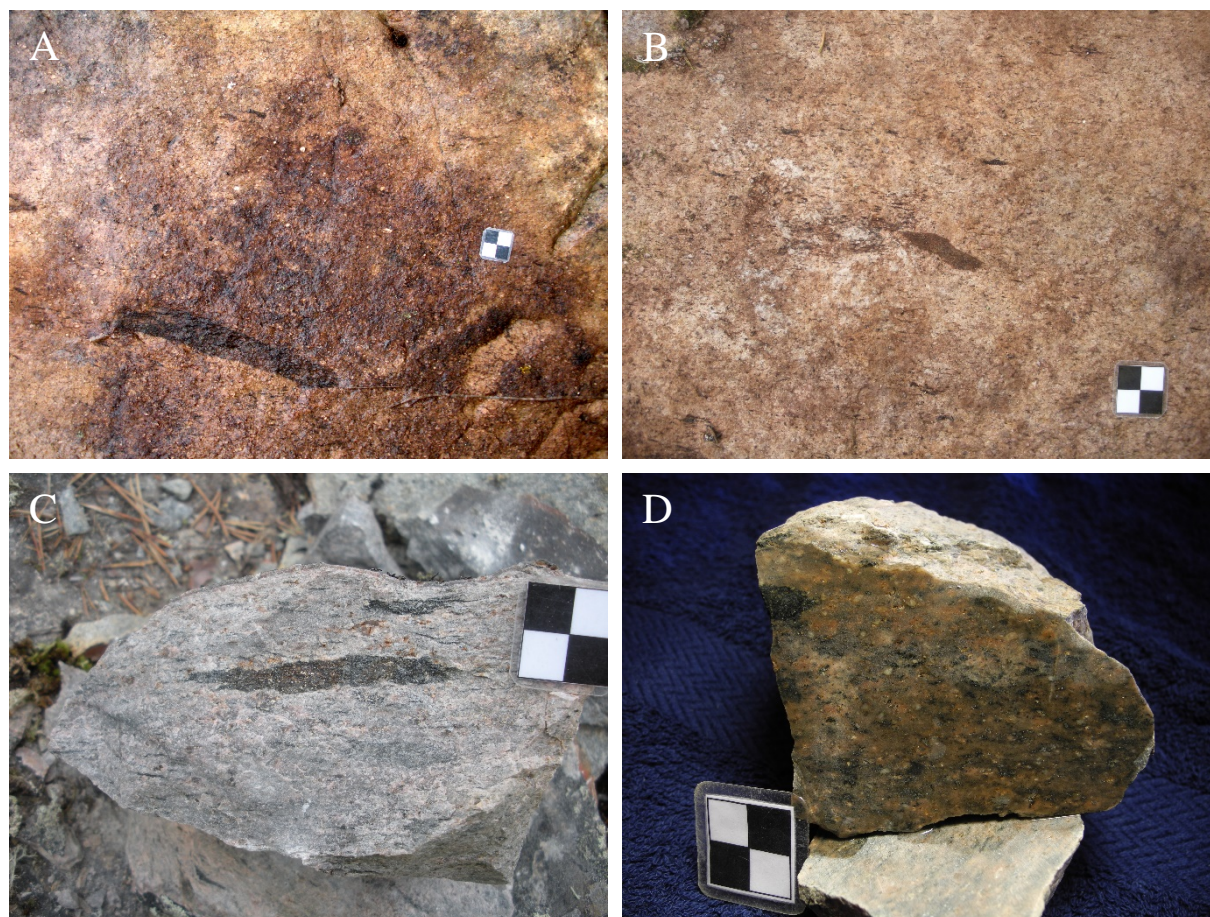


Figure 78. A. wetted and B. dry surface of rhyolite to trachyte, outcrop adjacent to sampling site of DCL120108 with fragments of basic volcanic rocks. C. Fresh rock specimen of rhyolite to trachyte showing light gray colour and with a fragment of a mafic volcanic rock, sampling site. D. Cut and wetted sample of rhyolite DCL120108A (cm-scale). Photos: Dick Claeson.

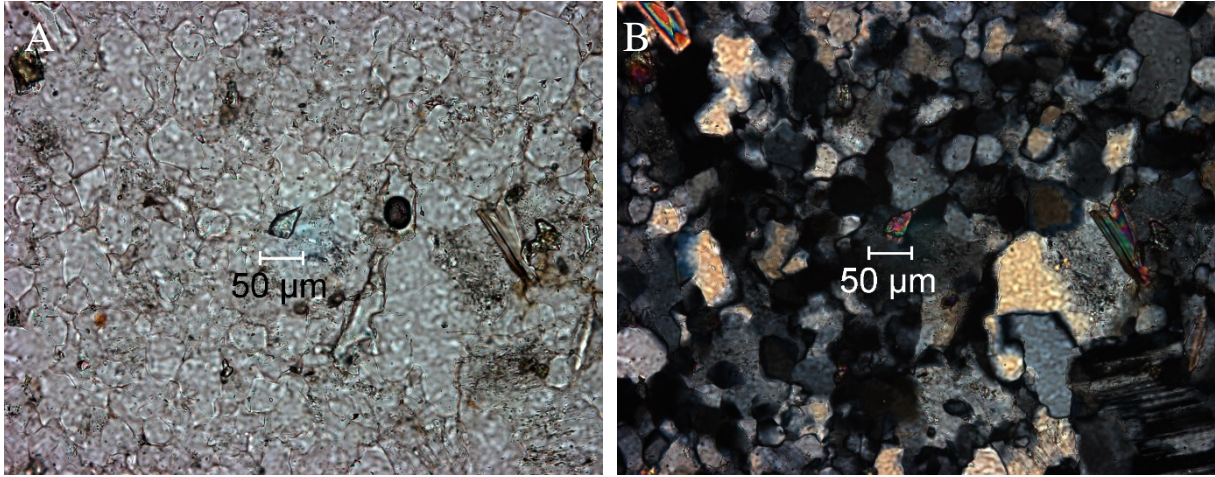


Figure 79. Zircon in thin-section of rhyolite from sampling site DCL120108, **A.** plane-polarized light and **B.** crossed-polarized light.

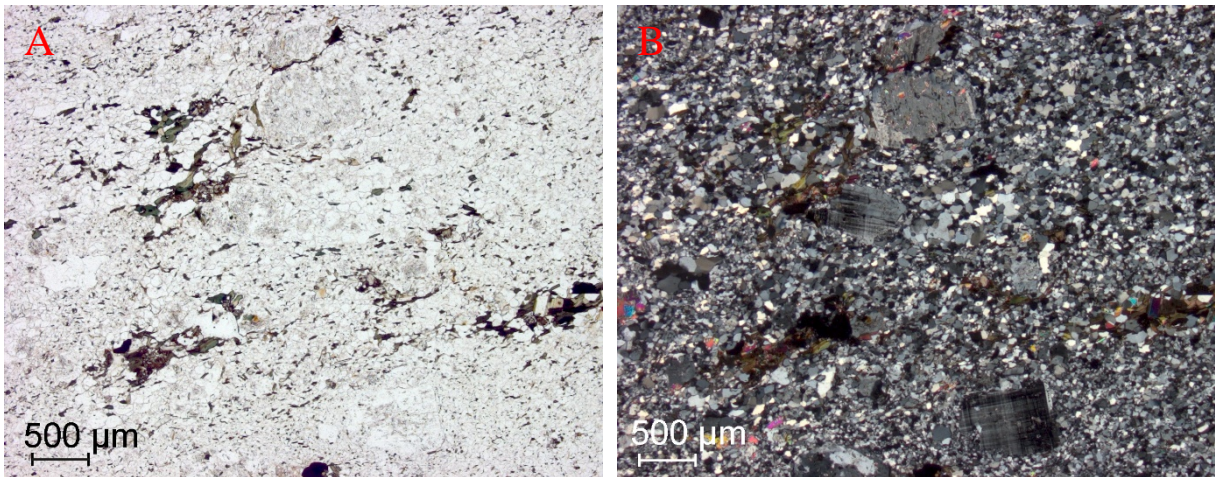


Figure 80. Biotite and muscovite along with opaque minerals define the foliation in thin-section. Phenocrysts of feldspars and quartz are seen, the latter now as aggregates of several distinct grains, **A.** plane-polarized light and **B.** crossed-polarized light.

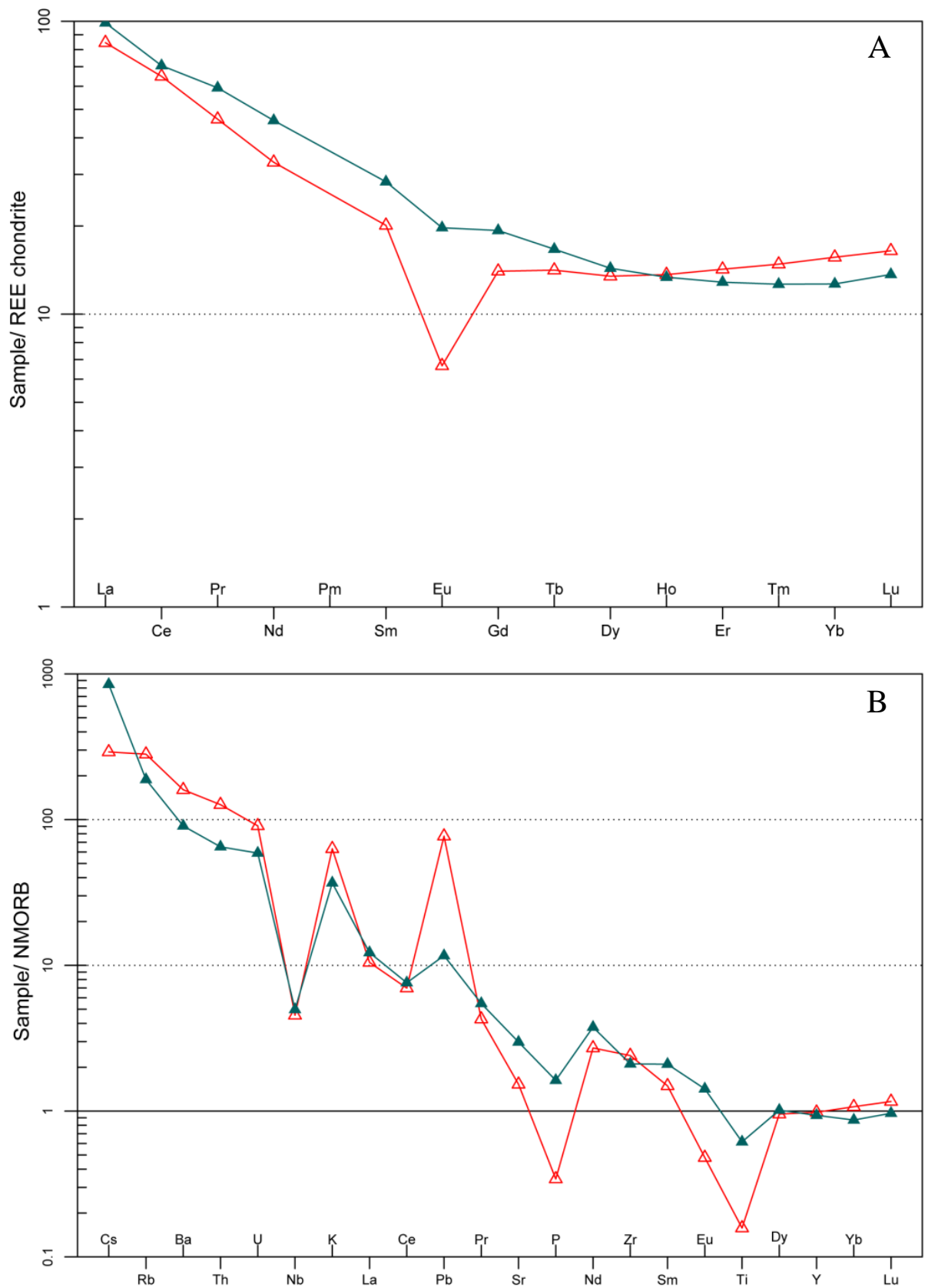


Figure 81. A. REE-diagram of the age determined rhyolite in red and coeval andesite. Normalizing values for chondrite from Boynton (1984). **B.** Multi-element diagram, rock as in A. Normalizing values for N-MORB from Sun & McDonough (1989).

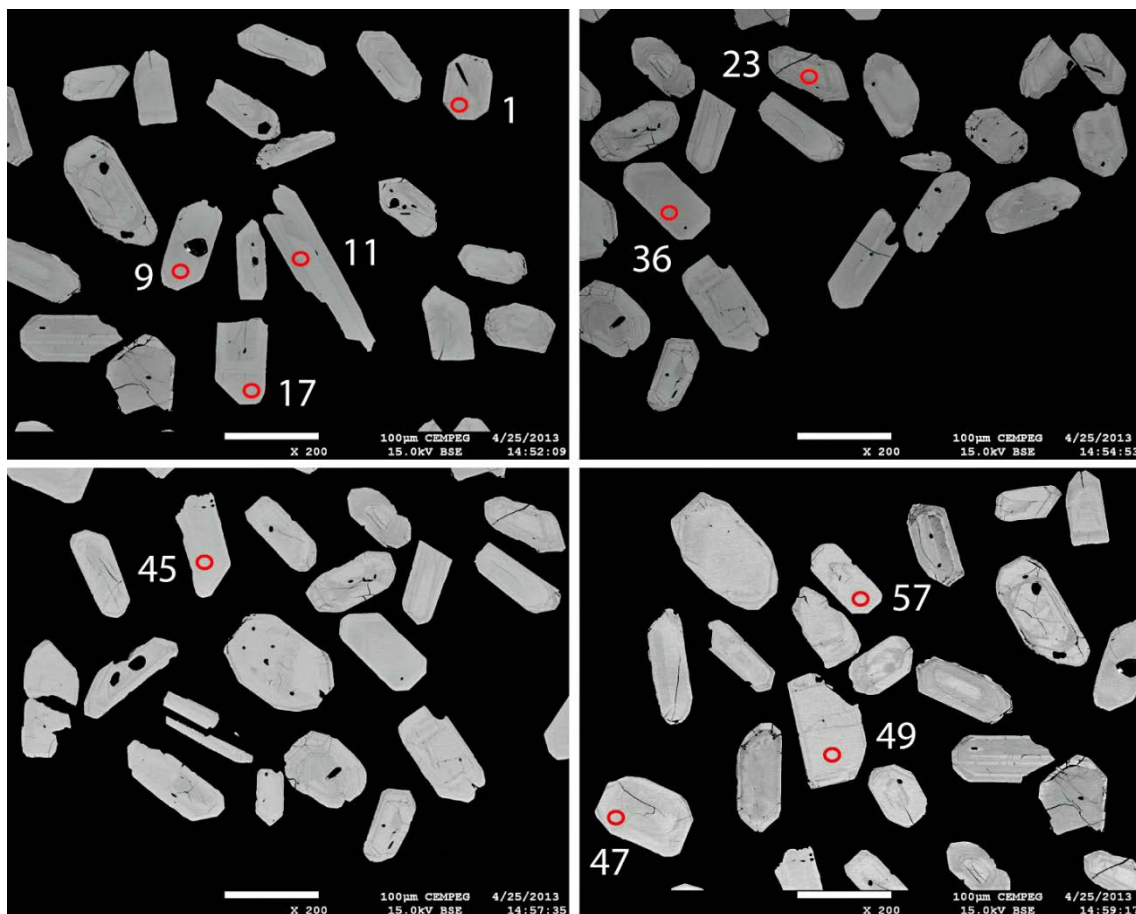


Figure 82. BSE-images of analysed zircon grains. Red ellipses mark the approximate locations of analyses. Numbers refer to analytical spot number in Table 25.

Analytical results and interpretation of geochronological data

Zircon were obtained from a density separate of a crushed rock sample using a Wilfley water table. The magnetic minerals were removed by a hand magnet. Handpicked crystals were mounted in transparent epoxy resin together with chips of reference zircon 91 500. The zircon mounts were polished and after gold coating examined by BSE- and CL-imaging using electron microscopy at the Department of Geology, Uppsala University.

High-spatial resolution secondary ion mass spectrometer (SIMS) analysis was done in May 2013 using a Cameca IMS 1270 at the Nordsim facility at the Swedish Museum of Natural History in Stockholm. Detailed descriptions of the analytical procedures are given in Whitehouse et al. (1997, 1999). Pb/U ratios, elemental concentrations and Th/U ratios were calibrated relative to the Geostandards zircon 91 500 reference, which has an age of c. 1 065 Ma (Wiedenbeck et al. 1995, 2004). Common Pb corrected isotope values were calculated using modern common Pb composition (Stacey & Kramers 1975) and measured ^{204}Pb . Decay constants follow the recommendations of Steiger & Jäger (1977). Diagrams and age calculations of isotopic data were made using software Isoplot 4.15 (Ludwig 2012).

Zircon in the sample have subhedral to euhedral, prismatic shapes (Fig. 82). Microcracks are common. In some grains there are possibly, inherited cores. BSE-images reveal an internal oscillatory zonation in most zircon grains, but the zonation is in part only weakly developed and there are grains that have a homogenous BSE-level. One analysis (No. 1) has high uranium

content at 1 562 ppm, shows a high value of common lead and is 26 % discordant (Table 25). The remaining nine analyses are all concordant at the 2σ limit, with 248–805 ppm U and uniform Th/U ratios, 0.26–0.45. A concordia age can be calculated at $1\ 886 \pm 6$ Ma (95 % confidence, MSWD of concordance = 2.8, probability = 0.092, $n = 9$). Evident from plot, there is some scatter of the data and one analysis shows a relatively large error (Fig. 83). The weighted average $^{207}\text{Pb}/^{206}\text{Pb}$ age is calculated at $1\ 885 \pm 4$ Ma (2σ , MSWD = 1.6, probability = 0.11, $n = 9$), i.e., within error identical to the concordia age (Fig. 83). The weighted average age is chosen as the best age estimate, interpreted to date igneous crystallisation of the rhyolite at $1\ 885 \pm 4$ Ma.

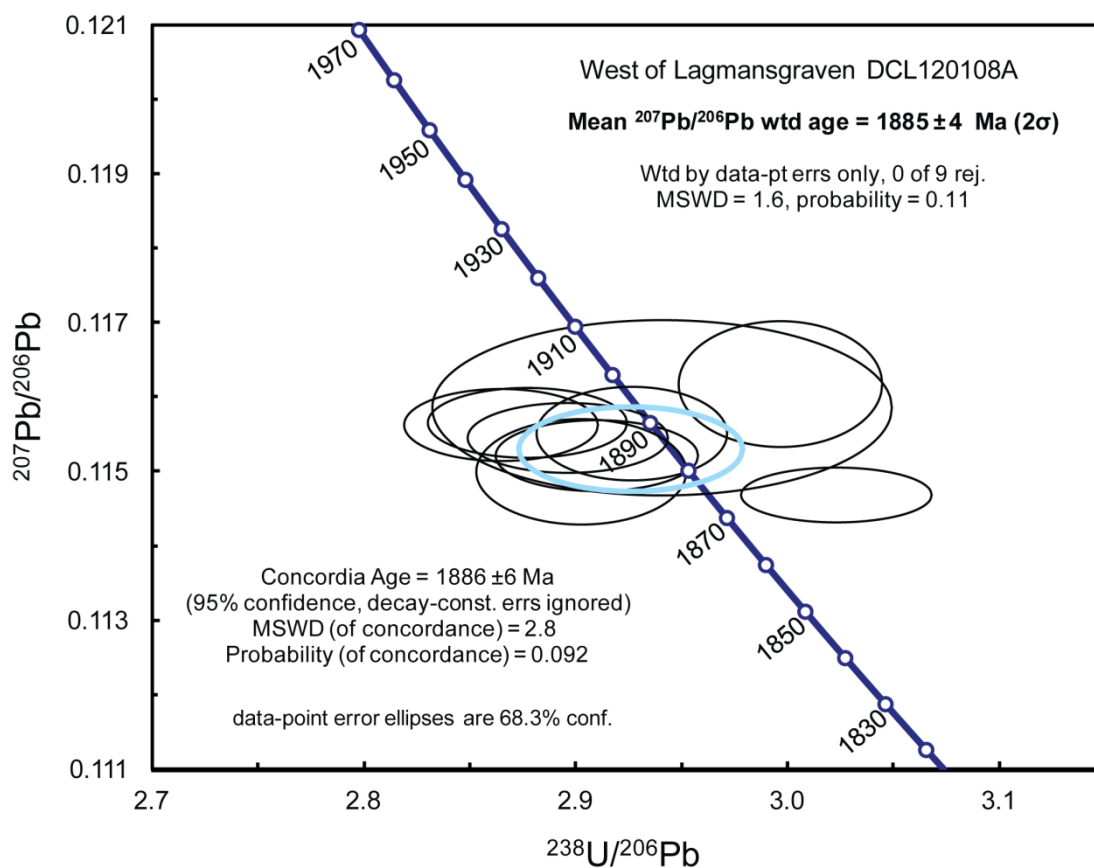


Figure 83. Tera-Wasserburg diagram showing U-Pb SIMS data of zircon analyses. One highly discordant analysis (No. 1) plot outside the extent of the diagram and is excluded from the age calculations, see Table 25 and comments in text.

Table 25. SIMS U-Pb-Th zircon data.

Sample/ spot #	U ppm	Th ppm	Pb ppm	Th/U calc ^{*1}	²⁰⁷ Pb ²³⁵ U	±σ %	²⁰⁸ Pb ²³² Th	±σ %	²³⁸ U ²⁰⁶ Pb	±σ %	²⁰⁷ Pb ²⁰⁶ Pb	±σ %	ρ ^{*2}	Disc. % conv. ^{*3}	²⁰⁷ Pb ²⁰⁶ Pb	±σ (Ma)	²⁰⁶ Pb ²³⁸ U	±σ (Ma)	²⁰⁶ Pb/ ²⁰⁴ Pb measured	f ₂₀₆ % ^{*4}
n4591-1	1562	545	426	0.25	3.292	1.09	0.0641	3.9	4.413	0.99	0.1054	0.48	0.90	-26.0	1721	9	1317	12	3659	0.51
n4591-9	498	251	207	0.45	5.345	1.16	0.0878	5.0	2.997	1.06	0.1162	0.48	0.91	-2.5	1898	9	1856	17	8456	0.22
n4591-11	277	147	115	0.37	5.432	2.53	0.0690	15.2	2.941	2.44	0.1159	0.67	0.96	-0.4	1893	12	1887	40	23978	0.08
n4591-17	455	119	187	0.26	5.496	1.11	0.0980	3.3	2.896	1.08	0.1154	0.27	0.97	1.5	1887	5	1912	18	32698	0.06
n4591-23	805	335	329	0.41	5.230	1.01	0.0959	3.3	3.023	0.99	0.1147	0.21	0.98	-2.0	1875	4	1842	16	29397	0.06
n4591-36	302	116	127	0.38	5.463	1.20	0.0974	3.3	2.903	1.12	0.1150	0.41	0.94	1.8	1880	7	1908	19	67798	0.03
n4591-45	400	160	172	0.42	5.565	1.09	0.1029	3.3	2.865	1.06	0.1156	0.28	0.97	2.5	1890	5	1930	18	503872	{0.00}
n4591-47	248	77	102	0.31	5.442	1.08	0.0990	3.6	2.926	1.02	0.1155	0.36	0.94	0.4	1888	6	1895	17	58492	0.03
n4591-49	416	125	172	0.31	5.459	1.12	0.1018	3.3	2.910	1.09	0.1152	0.28	0.97	1.3	1883	5	1904	18	198587	{0.01}
n4591-57	590	164	246	0.29	5.542	1.11	0.1031	3.3	2.877	1.08	0.1156	0.27	0.97	2.0	1890	5	1923	18	212897	{0.01}

Isotope values are common Pb corrected using modern common Pb composition (Stacey & Kramers 1975) and measured ²⁰⁴Pb.

*1 Th/U ratios calculated from ²⁰⁸Pb/²⁰⁶Pb and ²⁰⁷Pb/²⁰⁶Pb ratios, assuming single stage of closed U-Th-Pb evolution.

*2 Error correlation in conventional concordia space. Do not use for Tera-Wasserburg plots.

*3 Age discordance in conventional concordia space. Positive numbers are reverse discordant.

*4 Figures in parentheses are given when no correction has been applied, and indicate a value calculated assuming present-day Stacey-Kramers common Pb.

Discussion and conclusion

The rhyolite to trachyte age of $1\,885 \pm 4$ Ma is older than some other volcanic rocks in this area (this issue). Even though the typical compositions are rhyolite to trachyte in the more than 35 km long volcanic succession seen in the geophysical data (Fig. 74, 75, 77), there also occur coeval dacite, andesite, and basalt, of which some are porphyritic with potassium feldspar and plagioclase phenocrysts, respectively (Fig. 76). These types of compositions are more or less identical to the younger volcanic rocks allocated to the Arvidsjaur group but too old to be considered as a proper member. The results were integrated in the mapping of the 26J Jokkmokk NV area (Claeson & Antal Lundin *in press b*). Summary of sample data is given in Table 26.

Table 26. Summary of sample data.

Rock type	Rhyolite to trachyte
Lithotectonic unit	Norrbottnen lithotectonic unit of the Svecokarelian orogen
Lithological unit	
Sample number	DCL120108A
Lab_id	n4591
Coordinates	7379927/692113 (Sweref99TM)
Map sheet	26J Jokkmokk NV (RT90)
Locality	West of Lagmansgraven
Project	Sydvästra Norrbotten (80025)

Acknowledgments

Martin Whitehouse, Lev Ilyinsky and Kerstin Lindén at the NordSIM analytical facility are greatly acknowledged for their support with SIMS-analyses. Jarek Majka and Abigail Barker at the Department of Geology, Uppsala University are much thanked for their assistance during BSE/CL-imaging of zircon.

References

- Boynnton, W.V., 1984: Cosmochemistry of the Rare Earth Elements: Meteorite studies. *In* P. Henderson (ed.): *Rare earth element geochemistry*. Elsevier Science B.V. 63–114.
- Claeson, D. & Antal Lundin, I., *in press b*: Beskrivning till berggrundskartorna 26J Jokkmokk NV, NO. *Sveriges geologiska undersökning*.
- Ludwig, K.R., 2012: User's manual for Isoplot 3.75. A Geochronological Toolkit for Microsoft Excel. *Berkeley Geochronology Center Special Publication No. 5*, 75 pp.
- Smith, M.P., Storey, C.D., Jeffries, T.E., & Ryan, C., 2009: *In Situ* U–Pb and Trace Element Analysis of Accessory Minerals in the Kiruna District, Norrbotten, Sweden: New Constraints on the Timing and Origin of Mineralization. *Journal of Petrology* 50, 2 063–2 094.
- Stacey, J.S. & Kramers, J.D., 1975: Approximation of terrestrial lead isotope evolution by a two-stage model. *Earth and Planetary Science Letters* 26, 207–221.
- Steiger, R.H. & Jäger, E., 1977: Convention on the use of decay constants in geo- and cosmochronology. *Earth and Planetary Science Letters* 36, 359–362.
- Sun, S.S. & McDonough, W.F., 1989: Chemical and isotopic systematic of oceanic basalts: implications for mantle composition and processes. *In* A.D. Saunders & M.J. Norry (eds.): *Magmatism in ocean basins*. Geological Society of London, Special Publication 42, 313–345.
- Wanhainen, C., Broman, C. and Martinsson, O., 2003. The Aitik Cu–Au–Ag deposit in northern Sweden: a product of high salinity fluids. *Mineralium Deposita* 38, 715–726.
- Wanhainen, C., Billström, K., Martinsson, O., Stein, H. and Nordin, R., 2005. 160 Ma of magmatic/hydrothermal and metamorphic activity in the Gällivare area: Re–Os dating of molybdenite and U–Pb dating of titanite from the Aitik Cu–Au–Ag deposit, northern Sweden. *Mineralium Deposita* 40, 435–447.
- Whitehouse, M.J., Claesson, S., Sunde, T. & Vestin, J., 1997: Ion-microprobe U–Pb zircon geochronology and correlation of Archaean gneisses from the Lewisian Complex of Gruinard Bay, north-west Scotland. *Geochimica et Cosmochimica Acta* 61, 4 429–4 438.
- Whitehouse, M.J., Kamber, B.S. & Moorbath, S., 1999: Age significance of U–Th–Pb zircon data from Early Archaean rocks of west Greenland: a reassessment based on combined ion-microprobe and imaging studies. *Chemical Geology (Isotope Geoscience Section)* 160, 201–224.
- Wiedenbeck, M., Allé, P., Corfu, F., Griffin, W.L., Meier, M., Oberli, F., Quadt, A.V., Roddick, J.C. & Spiegel, W., 1995: Three natural zircon standards for U–Th–Pb, Lu–Hf, trace element and REE analyses. *Geostandards Newsletter* 19, 1–23.
- Wiedenbeck, M., Hanchar, J.M., Peck, W.H., Sylvester, P., Valley, J., Whitehouse, M., Kronz, A., Morishita, Y., Nasdala, L., Fiebig, J., Franchi, I., Girard, J.P., Greenwood, R.C., Hinton, R., Kita, N., Mason, P.R.D., Norman, M., Ogasawara, M., Piccoli, P.M., Rhede, D., Satoh, H., Schulz-Dobrick, B., Skår, O., Spicuzza, M.J., Terada, K., Tindle, A., Togashi, S., Vennemann, T., Xie, Q. & Zheng, Y.F., 2004: Further Characterisation of the 91500 Zircon Crystal. *Geostandards and Geoanalytical Research* 28, 9–39.

U-Pb ZIRCON AGE OF GRANITE TO QUARTZ MONZONITE NORTH OF TÅRRAJAUR, MAP SHEET 26J JOKKMOKK NV, NORRBOTTEN COUNTY

Authors: Dick Claeson, Ildikó Antal Lundin & Fredrik Hellström

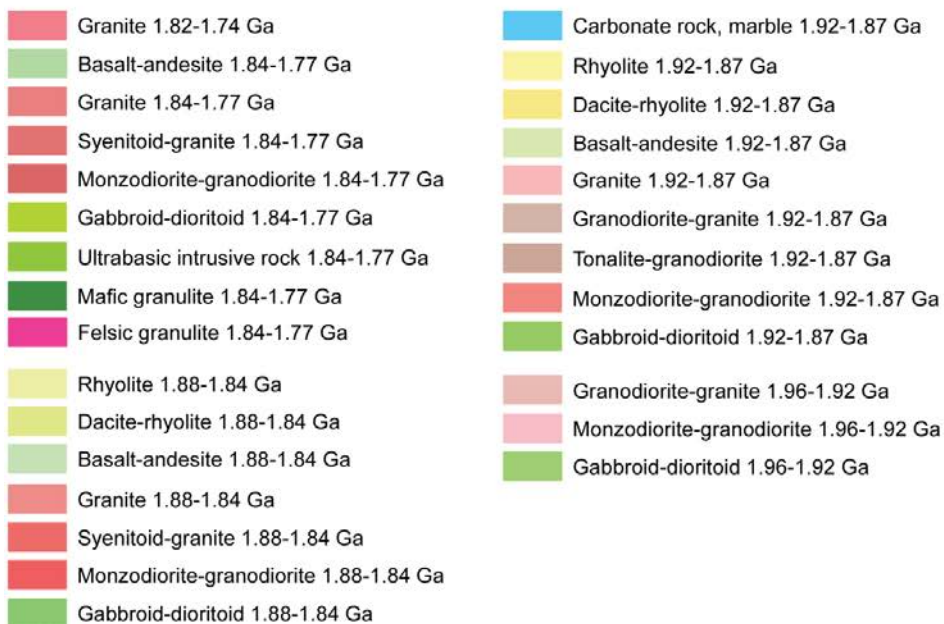
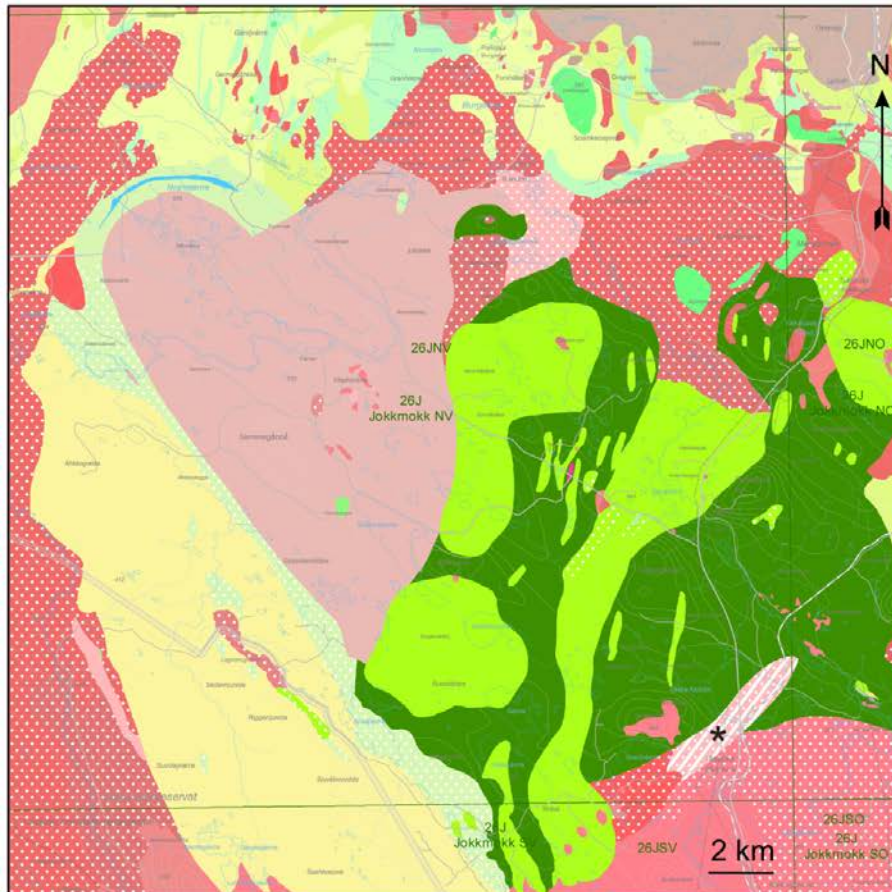


Figure 84. Bedrock map of the area, sampling location marked with black star.

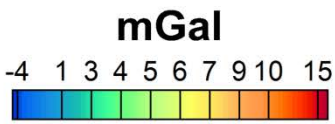
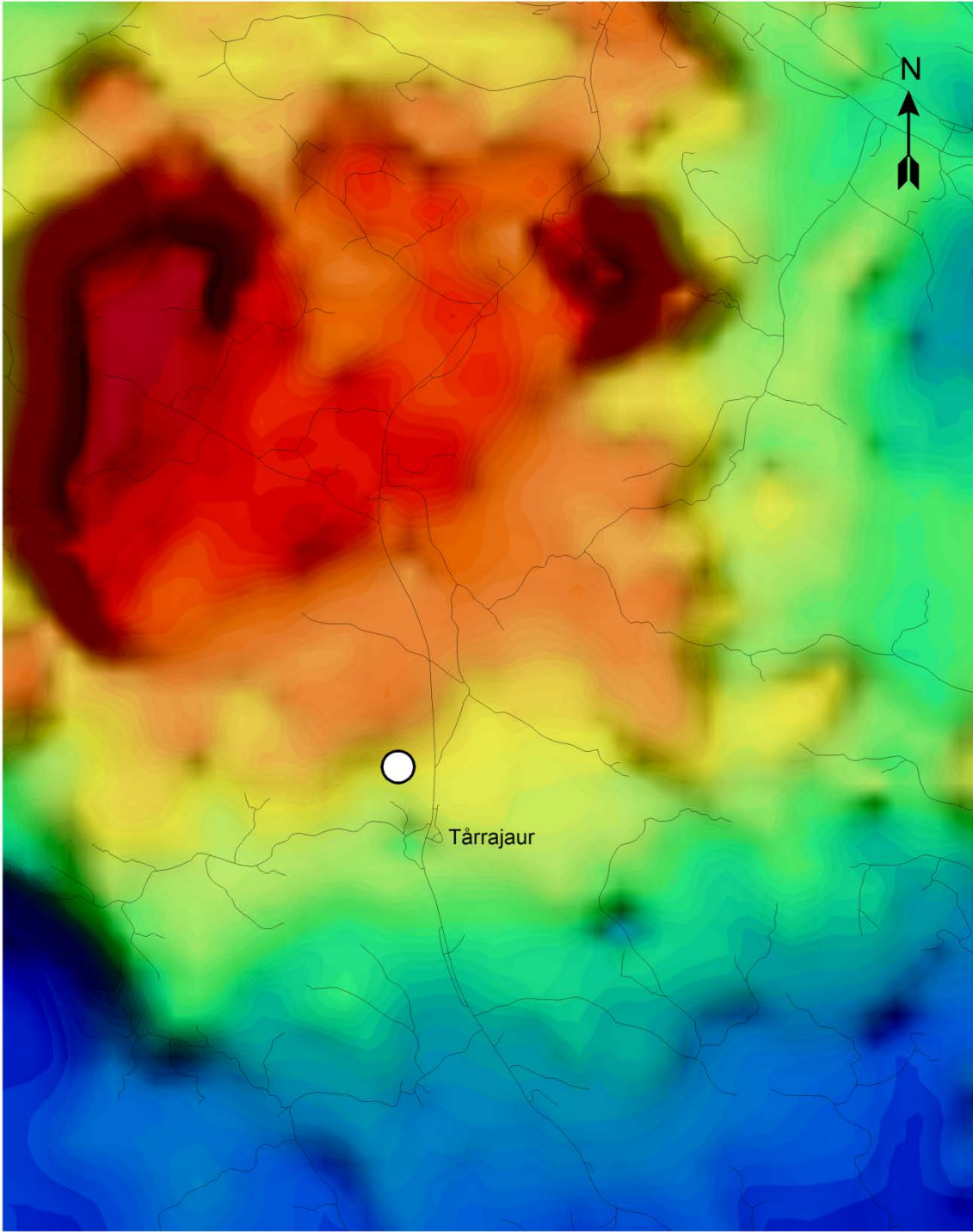
Introduction

Norrbotten, Sweden is a key area of Europe for future exploration and mining. The sampled rock is part of a distinctive low magnetic area seen on the aeromagnetic data produced by the SGU (Fig. 84, 85).

If metamorphic rims or other overgrowths are present on the zircon of the sample, these should also be studied since this may be of significance for the interpretation of the genesis of this low magnetic area, because several other rock types are also present and have the same magnetic signature. In order to gain knowledge of when metamorphic events are in any way involved in the genesis of the formation of economic deposits on a regional scale in the Norrbotten County, by reheating the crust and producing hydrothermal activity in volcanic rocks, intrusive rocks or structural zones, their age have to be determined.

The aim of this study is to determine the magmatic age of the granite to quartz monzonite part of this area seen on map sheets 26J Jokkmokk NV and NO, and if there are any metamorphic overgrowths, determine these as well, since the latter might show ages for the genesis of this low magnetic area by redistribution of elements in the crust.

To our knowledge, this particular type of rock has not been discovered in the project area of SV Norrbotten (Jokkmokk NV, NO, Luvos NV, NO, SV, Porjus SV and Tjåmotis SV, SO) and there is also the possibility that this rock is much older, possibly even Archean.



4 km

Figure 85. A. Gravity map in colour, part of the map sheet 26J Jokkmokk NV and NO with surroundings. The white dot shows the sample location.

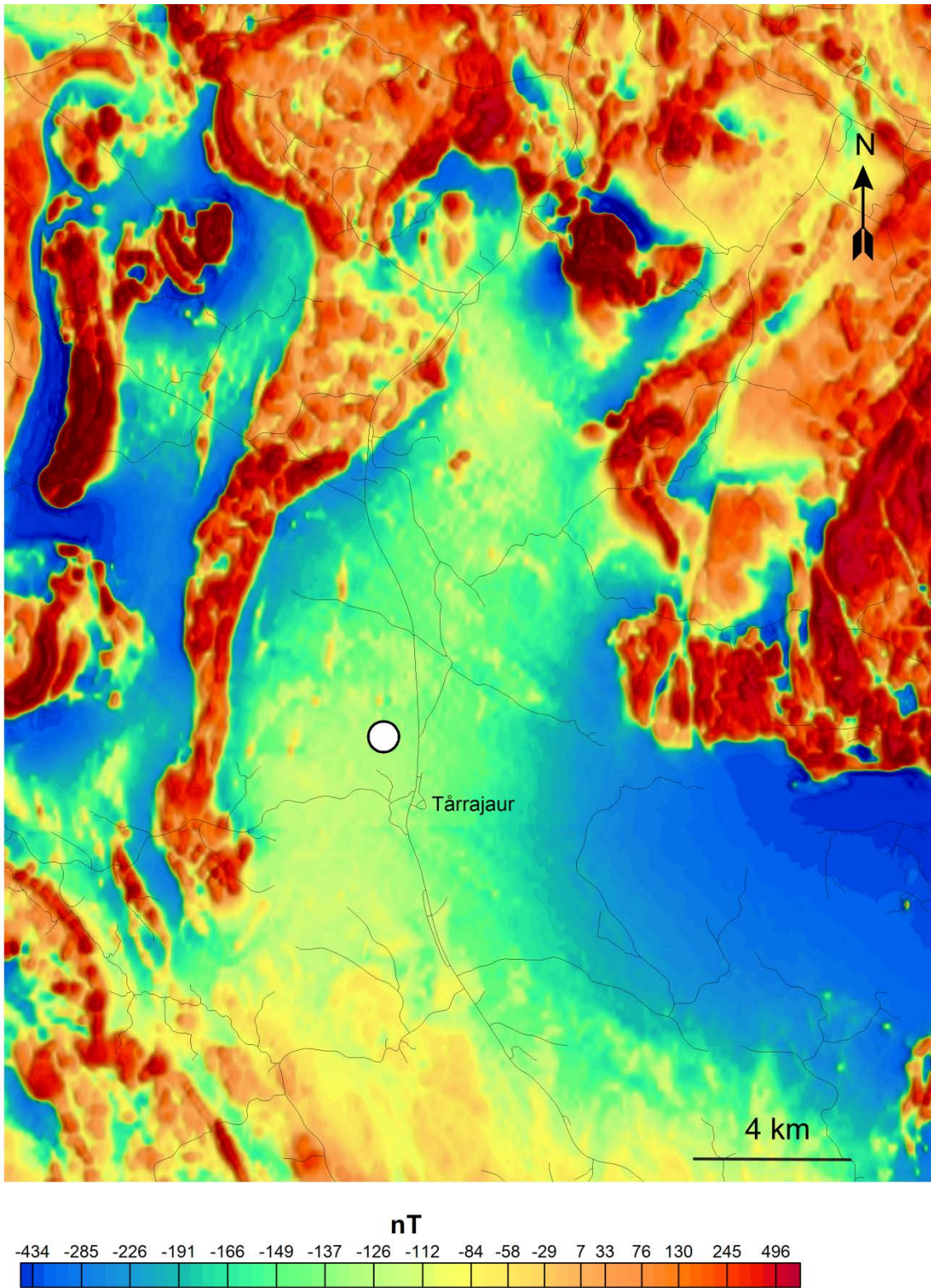


Figure 85. B. Magnetic anomaly map indicating the distribution of the major structures in the area, part of the map sheet 26J Jokkmokk NV and NO with surroundings. The white dot shows the sample location.

Sample description

The sampled outcrop is located approximately 1 km north of the Tårrajaur, some 25 km S of Jokkmokk. The sample consists of granite to quartz monzonite that is deformed, possibly hydrothermally altered, recrystallised, light grey to grey, and varies from fine-grained to medium-grained (Fig. 86). The rocks at the outcrop are augen-bearing with roundish K-feldspar megacrysts and phenocrysts 5–20 mm (2–7 %) and contain biotite + amphibole (~ 10 %). The K-feldspar megacrysts varies in colour between red, pink, grey, and white at the different outcrops. It is not always obvious if they are phenocrysts or augen or both (Fig. 86). The potassium feldspar shows Carlsbad and cross-hatched twinning, perthite and microperthite intergrowths (Fig. 87). The phenocrysts have inclusions of plagioclase, amphibole, biotite, and quartz (Fig. 87).

Plagioclase shows minor sericite alteration and minor blobs of myrmekite are present. Amphibole and biotite are present in the groundmass at 6 and 3 %, respectively. Magmatic amphibole is pleochroic, dark to light green and pleochroic biotite brownish red to pale yellow. Quartz shows undulose extinction. Accessory minerals are opaque minerals, mostly magnetite, apatite, titanite, and small zircon. Especially at outcrops showing severe deformation are the K-feldspar megacrysts rounded to lensoid in shape. Foliation is oriented 210/86. The hydrothermal alteration is at places intense and results in light-coloured rocks. Massive pegmatite, probably of Granite-Pegmatite association affinity, occurs as dykes cutting the foliation. The Zr content of the rock is 199 ppm. Magnetic susceptibility at the outcrop varies between 12 and 17×10^{-5} SI. Gamma-ray measurements resulted in K = 2.6 %, U = 1.2 ppm, Th = 9.1 ppm, mean values for three measurements at the locality.

Five outcrops thought to be of the same lithological unit are present within an area of roughly 4 km² and at none of these five are other rocks present than the presumed late Svecokarelian pegmatite. Rocks that occur in the surrounding area are metamorphosed basaltoid to andesitoid and minor dacitoid, monzodiorite, and well-preserved late Svecokarelian granite to pegmatite (Claeson & Antal Lundin *in press b*).

The sampled granite north of Tårrajaur shows a LREE-enriched and flat HREE pattern, with a negative Eu anomaly (Fig. 88). The LREE enrichment is due to fractional crystallisation, the flat, unfractionated HREE pattern shows that no garnet was left in the residue at the location of magma genesis, and the Eu anomaly is indicative of plagioclase fractionation. The negative anomalies shown in the multi-element diagram of P and Ti are indicative of apatite fractionation and Fe-Ti oxide fractionation, respectively (Fig. 88). The strong negative Nb anomaly and positive Pb anomaly suggest a subduction related petrogenesis (Fig. 88).

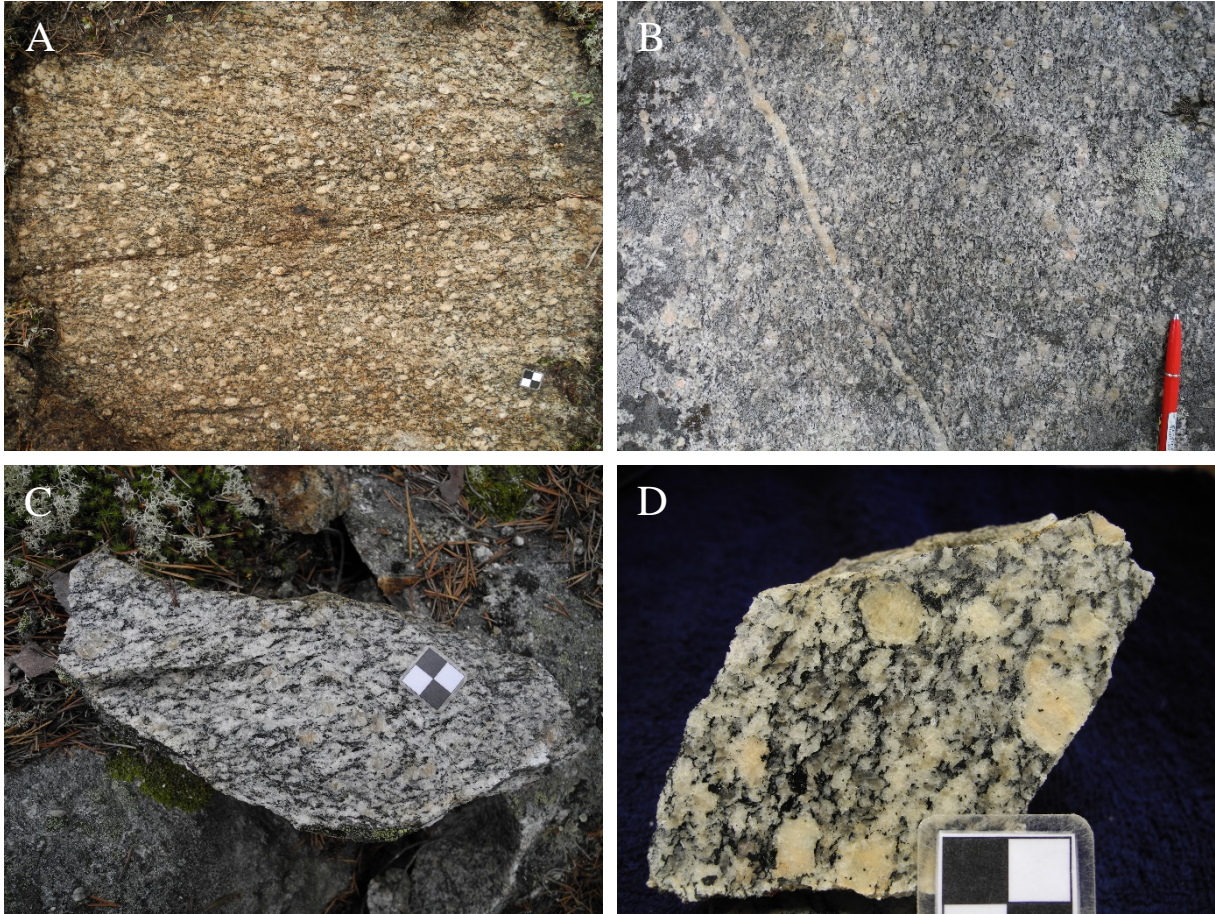


Figure 86. A. Granite to quartz monzonite, outcrop adjacent to sampling site. B. Close-up of granite to quartz monzonite, outcrop adjacent to sampling site. C. Close-up of age determined sample of granite. D. Cut and wetted granite of DCL130008 (cm-scale). Photos: Dick Claeson.

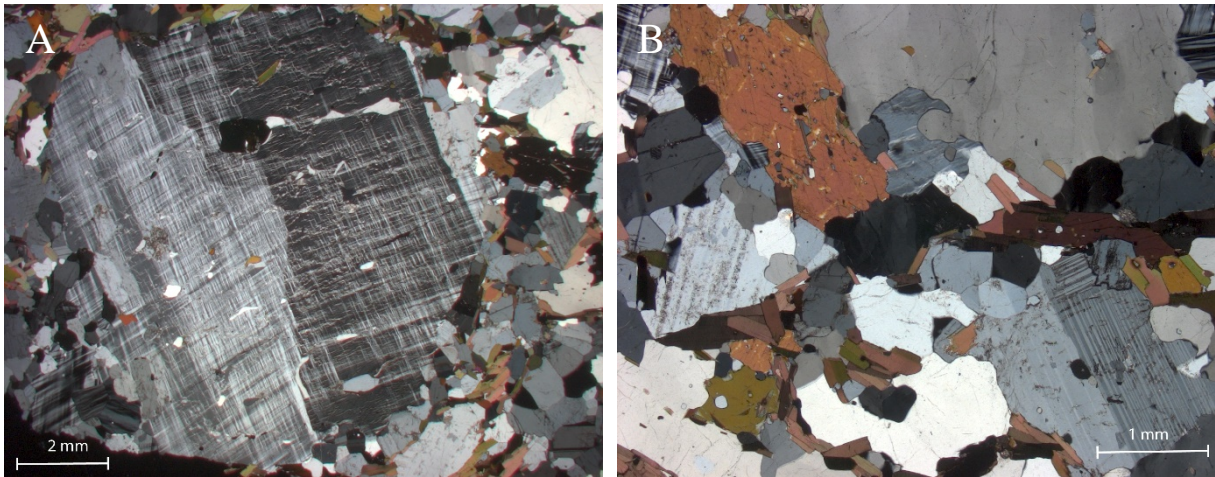


Figure 87. A. Phenocryst of potassium feldspar in granite DCL130008, crossed nicols. B. Matrix of granite DCL130008 with plagioclase, K-feldspar, quartz, biotite, and amphibole, crossed nicols. Micrographs: Dick Claeson.

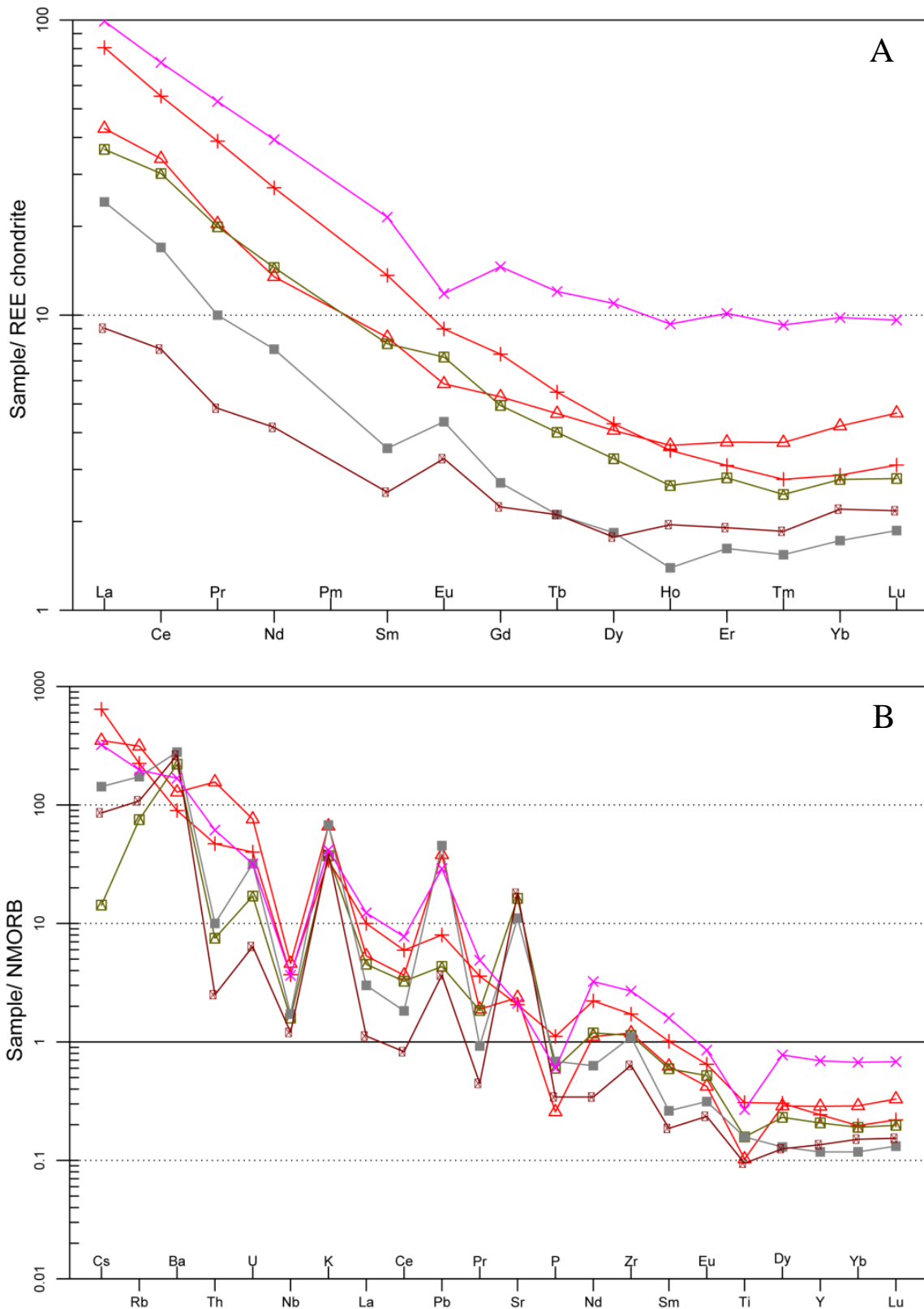


Figure 88. A. REE-diagram of granite from Tårrajaur in pink, granodiorite and granite samples from the 1.93 Ga Närkejaur intrusion in bright red, and three granitoid samples of the 1.88 Ga Jokkmokk granitoid in green to brown. Normalizing values for chondrite from Boynton (1984). B. Multi-element diagram, rocks as in A. Normalizing values for N-MORB from Sun & McDonough (1989).

Analytical results and interpretation of geochronological data

Zircon were obtained from a density separate of a crushed rock sample using a Wilfley water table. The magnetic minerals were removed by a hand magnet. Handpicked crystals were mounted in transparent epoxy resin together with chips of reference zircon 91 500. The zircon mounts were polished and after gold coating examined by back-scattered electron (BSE) and cathodoluminescence (CL) imaging using electron microscopy at EBC, Uppsala University and at the Swedish Museum of Natural History in Stockholm. High-spatial resolution secondary ion mass spectrometer (SIMS) analysis was done in November and December 2014 using a Cameca IMS 1 280 at the Nordsim facility at the Swedish Museum of Natural History in Stockholm. Detailed descriptions of the analytical procedures are given in Whitehouse et al. (1997, 1999) and Whitehouse & Kamber (2005).

A c. 6 nA O^{2-} primary ion beam was used, yielding spot sizes of c. 15 μm . Pb/U ratios, elemental concentrations and Th/U ratios were calibrated relative to the Geostandards zircon 91 500 reference, which has an age of c. 1 065 Ma (Wiedenbeck et al. 1995, 2004). Common Pb corrected isotope values were calculated using modern common Pb composition (Stacey & Kramers 1975) and measured ^{204}Pb , in cases of a ^{204}Pb count rate above the detection limit. Decay constants follow the recommendations of Steiger & Jäger (1977). Diagrams and age calculations of isotopic data were made using software Isoplot 4.15 (Ludwig 2012). All age uncertainties are presented at the 95 % confidence level. BSE- and CL imaging of the dated zircon was performed using electron microscopy at the Department of Geology, Uppsala University.

The heavy mineral concentrate contains, euhedral, usually medium to long, prismatic, weakly pinkish zircon. Nearly all zircon are turbid and of poor analytical quality. BSE-images show a weakly developed oscillatory zonation and areas of homogenous BSE-level zircon (Fig. 89). All ten analyses are concordant within the 2σ limit and with low values of common lead (Table 27). The uranium content is rather uniform at 346–737 ppm. Also, the Th/U ratios show trivial variation, 0.26–0.33. A concordia age is calculated at $1\,887 \pm 3$ Ma (2σ , $n = 10$), but the MSWD and probability of concordance is low resulting from analyses being slightly reversely discordant (Fig. 90). A weighted average $^{207}\text{Pb}/^{206}\text{Pb}$ age is calculated at $1\,885 \pm 3$ Ma (MSWD = 0.49, Probability = 0.88, $n = 10$), i.e., within error the same as the concordia age (Fig. 90). The weighted average $^{207}\text{Pb}/^{206}\text{Pb}$ age at $1\,885 \pm 3$ Ma is chosen as the best age estimate, interpreted to date igneous crystallisation of the granite to quartz monzonite rock north of Tårarjaur.

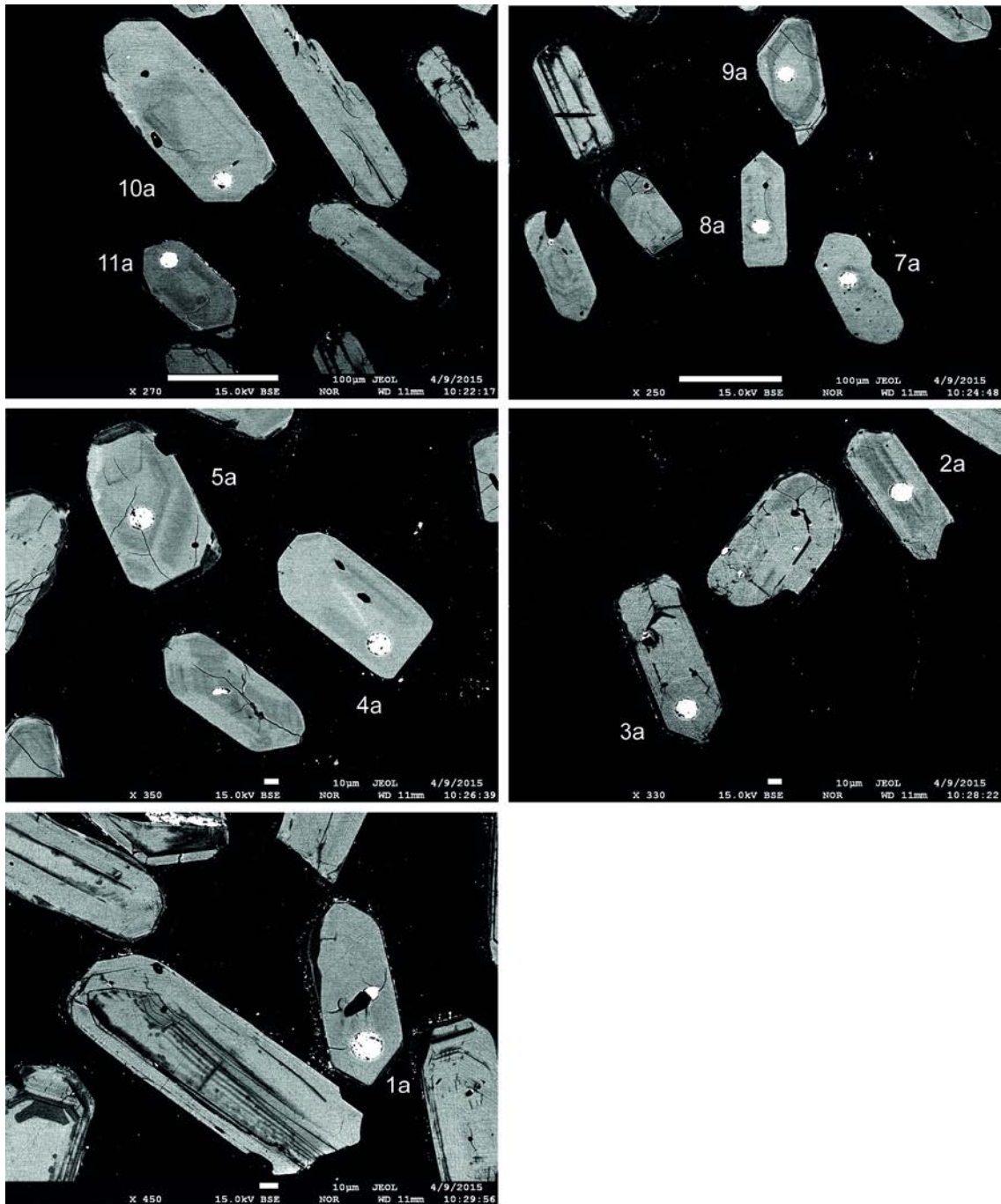


Figure 89. Back-scattered electron images of analysed zircon grains. Numbers refer to analytical spot number in Table 27.

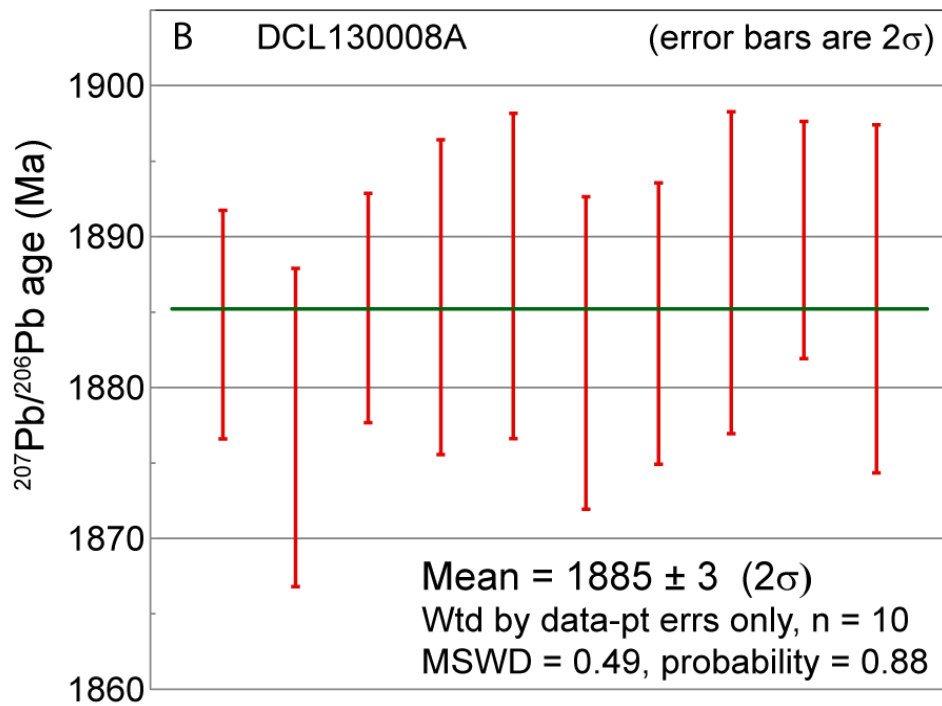
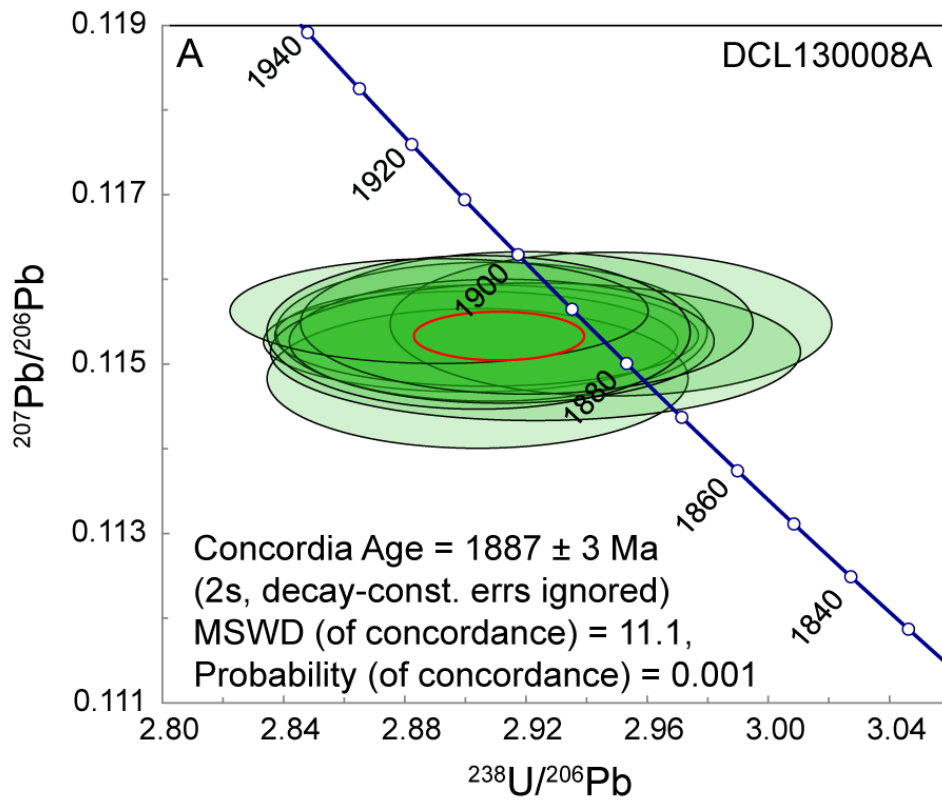


Figure 90. A. Tera-Wasserburg diagram showing U-Pb SIMS data of zircon analyses. Error ellipse of calculated weighted mean age is shown in red. B. $^{207}\text{Pb}/^{206}\text{Pb}$ age diagram.

Table 27. SIMS U-Pb-Th zircon data.

Sample/ spot #	U ppm	Th ppm	Pb ppm	Th/U calc ^{*1}	²⁰⁷ Pb ²³⁵ U	±σ %	²⁰⁸ Pb ²³² Th	±σ %	²³⁸ U ²⁰⁶ Pb	±σ %	²⁰⁷ Pb ²⁰⁶ Pb	±σ %	ρ *2	Disc. % conv. *3	²⁰⁷ Pb ²⁰⁶ Pb	±σ (Ma)	²⁰⁶ Pb ²³⁸ U	±σ (Ma)	²⁰⁶ Pb/ ²⁰⁴ Pb measured	f ₂₀₆ % *4
n5168_01a	737	227	307	0.32	5.477	0.99	0.1020	2.0	2.902	0.96	0.1153	0.21	0.98	1.5	1884	4	1909	16	276285	{0.01}
n5168_02a	373	104	154	0.29	5.452	1.02	0.1025	2.1	2.904	0.98	0.1148	0.29	0.96	1.9	1877	5	1907	16	726497	{0.00}
n5168_03a	718	204	296	0.29	5.470	1.01	0.1009	2.1	2.907	0.98	0.1153	0.21	0.98	1.3	1885	4	1906	16	169558	{0.01}
n5168_04a	488	123	200	0.26	5.469	1.04	0.1008	2.1	2.909	1.00	0.1154	0.29	0.96	1.2	1886	5	1905	17	>1e6	{0.00}
n5168_05a	411	84	164	0.21	5.401	1.05	0.1001	2.6	2.948	1.01	0.1155	0.30	0.96	-0.3	1887	5	1883	17	>1e6	{0.00}
n5168_07a	682	178	278	0.27	5.431	1.26	0.1002	2.6	2.923	1.22	0.1152	0.29	0.97	0.9	1882	5	1897	20	25772	0.07
n5168_08a	461	111	188	0.25	5.458	1.02	0.1017	2.1	2.912	0.98	0.1153	0.26	0.97	1.1	1884	5	1903	16	449952	{0.00}
n5168_09a	346	112	144	0.33	5.453	1.09	0.1005	2.2	2.920	1.05	0.1155	0.30	0.96	0.7	1888	5	1898	17	124730	{0.01}
n5168_10a	647	136	264	0.22	5.514	1.00	0.1028	2.1	2.892	0.98	0.1156	0.22	0.98	1.5	1890	4	1915	16	647548	{0.00}
n5168_11a	391	59	156	0.16	5.477	1.03	0.1030	2.1	2.905	0.98	0.1154	0.32	0.95	1.3	1886	6	1907	16	958708	{0.00}

Isotope values are common Pb corrected using modern common Pb composition (Stacey & Kramers 1975) and measured ²⁰⁴Pb.

*1 Th/U ratios calculated from ²⁰⁸Pb/²⁰⁶Pb and ²⁰⁷Pb/²⁰⁶Pb ratios, assuming single stage of closed U-Th-Pb evolution.

*2 Error correlation in conventional concordia space. Do not use for Tera-Wasserburg plots.

*3 Age discordance in conventional concordia space. Positive numbers are reverse discordant.

*4 Figures in parentheses are given when no correction has been applied, and indicate a value calculated assuming present-day Stacey-Kramers common Pb.

Discussion and conclusion

The age of $1\,885 \pm 3$ Ma shows that the granite to quartz monzonite north of Tårrajaur is part of the early Svecokarelian intrusions of the area. The rocks north of Tårrajaur is departing in its visual appearance and metamorphic overprinting from most similar rocks of the south-western Norrbotten project area, which lead to it being singled out as a possible Archaean rock and candidate for age determination (Claeson & Antal Lundin 2013). The granite to quartz monzonite at Tårrajaur compared with the grey granodiorite and light grey granite from the Närkejaur intrusion (1.93 Ga, Hellström 2015, map area 26J Jokkmokk NV), show similar lithogeochemical signatures for both generations and are most probably generated from the same type of source and under analogous conditions, even though 45 Ma separate the events (Fig. 88). The principal difference seen by the eye is the potassium phenocrysts, hydrothermal alteration, and the extensive deformation with possible development of augen in the Tårrajaur granite to quartz monzonite.

In the northern parts of map areas 26J Jokkmokk NV, NO and the southern parts of 27J Porjus SV, SO, a grey to light grey granitoid intrusion called “Jokkmokk granitoid” was age determined using multi-fraction zircon to $1\,883 \pm 15$ Ma (U-Pb TIMS, Lundmark et al. 2005). A lithogeochemical comparison with the 1.88 Ga Jokkmokk granitoid shows distinct differences in the multi-element diagram, where the ratio Th/U, the trend from Cs to Ba, and the positive Sr and Eu anomalies are the most prominent differences (Fig. 88). Their petrogenesis is obviously completely different even if they are more or less coeval and the Jokkmokk granitoid is designated to be an albite granite intrusion (Claeson & Antal Lundin *in press a*). The results were integrated in the mapping of the 26J Jokkmokk NV, NO area (Claeson & Antal Lundin *in press b*). Summary of sample data is given in Table 28.

Table 28. Summary of sample data.

Rock type	Potassium porphyric granite
Lithotectonic unit	Norrbotten lithotectonic unit of the Svecokarelian orogen
Lithological unit	
Sample number	DCL130008A
Lab_id	n5168
Coordinates	7377242/708368 (Sweref99TM)
Map sheet	26J Jokkmokk NV (RT90)
Locality	North of Tårrajaur
Project	Sydvästra Norrbotten (80025)

Acknowledgements

U-Pb isotopic zircon data were obtained from beneficial co-operation with the Laboratory for Isotope Geology of the Swedish Museum of Natural History in Stockholm. The Nordsim facility is operated under an agreement between the research funding agencies of Denmark, Norway and Sweden, the Geological Survey of Finland and the Swedish Museum of Natural History. Martin Whitehouse, Lev Ilyinsky and Kerstin Lindén at the Nordsim analytical facility are gratefully acknowledged for their first-class analytical support with SIMS-analyses. Martin Whitehouse reduced the zircon analytical data, Lev Ilyinsky assisted during ion probe analyses and Kerstin Lindén prepared the zircon mounts. Milos Bartol at EBC, as well as Jarek Majka at the Department of Geology, Uppsala University, are much thanked for their support during BSE-imaging of zircon.

References

- Boynton, W.V., 1984: Cosmochemistry of the Rare Earth Elements: Meteorite studies. In P. Henderson (ed.): *Rare earth element geochemistry*. Elsevier Science B.V. 63–114.
- Claeson, D. & Antal Lundin, I., 2013: Berggrundsgeologisk undersökning, sydvästra Norrbotten. Sammanfattning av pågående verksamhet 2013. *Sveriges geologiska undersökning SGU-rapport 2013:18*, 27 pp.
- Claeson, D. & Antal Lundin, I., *in press a*: Beskrivning till berggrundskartan 27J Porjus SV. *Sveriges geologiska undersökning*.
- Claeson, D. & Antal Lundin, I., *in press b*: Beskrivning till berggrundskartorna 26J Jokkmokk NV, NO. *Sveriges geologiska undersökning*.
- Hellström, F., 2015: SIMS geochronology of a 1.93 Ga basement metagranitoid at Norvijaur west of Jokkmokk, northern Sweden. *Sveriges geologiska undersökning SGU-rapport 2015:01*, 18 pp.
- Ludwig, K.R., 2012: User's manual for Isoplot 3.75. A Geochronological Toolkit for Microsoft Excel. *Berkeley Geochronology Center Special Publication No. 5*, 75 pp.
- Lundmark, C., Billström, K. & Weihed, P., 2005: The Jokkmokk granitoid, an example of 1.88 Ga juvenile magmatism at the Archaean-Proterozoic border in northern Sweden. *GFF* 127, 83–98.
- Stacey, J.S. & Kramers, J.D., 1975: Approximation of terrestrial lead isotope evolution by a two-stage model. *Earth and Planetary Science Letters* 26, 207–221.
- Steiger, R.H. & Jäger, E., 1977: Convention on the use of decay constants in geo- and cosmochronology. *Earth and Planetary Science Letters* 36, 359–362.
- Sun, S.S. & McDonough, W.F., 1989: Chemical and isotopic systematic of oceanic basalts: implications for mantle composition and processes. In A.D. Saunders & M.J. Norry (eds.): *Magmatism in ocean basins*. Geological Society of London, Special Publication 42, 313–345.
- Whitehouse, M.J., Claesson, S., Sunde, T. & Vestin, J., 1997: Ion-microprobe U–Pb zircon geochronology and correlation of Archaean gneisses from the Lewisian Complex of Gruinard Bay, north-west Scotland. *Geochimica et Cosmochimica Acta* 61, 4 429–4 438.
- Whitehouse, M.J., Kamber, B.S. & Moorbath, S., 1999: Age significance of U–Th–Pb zircon data from Early Archaean rocks of west Greenland: a reassessment based on combined ion-microprobe and imaging studies. *Chemical Geology (Isotope Geoscience Section)* 160, 201–224.
- Whitehouse, M., J. & Kamber, B.S., 2005: Assigning Dates to Thin Gneissic Veins in High-Grade Metamorphic Terranes: A Cautionary Tale from Akilia, Southwest Greenland. *Journal of Petrology* 46, 291–318.
- Wiedenbeck, M., Allé, P., Corfu, F., Griffin, W.L., Meier, M., Oberli, F., Quadt, A.V., Roddick, J.C. & Spiegel, W., 1995: Three natural zircon standards for U-Th-Pb, Lu-Hf, trace element and REE analyses. *Geostandards Newsletter* 19, 1–23.
- Wiedenbeck, M., Hanchar, J.M., Peck, W.H., Sylvester, P., Valley, J., Whitehouse, M., Kronz, A., Morishita, Y., Nasdala, L., Fiebig, J., Franchi, I., Girard, J.P., Greenwood, R.C., Hinton, R., Kita, N., Mason, P.R.D., Norman, M., Ogasawara, M., Piccoli, P.M., Rhede, D., Satoh, H., Schulz-Dobrick, B., Skår, O., Spicuzza, M.J., Terada, K., Tindle, A., Togashi, S., Vennemann, T., Xie, Q. & Zheng, Y.F., 2004: Further Characterisation of the 91500 Zircon Crystal. *Geostandards and Geoanalytical Research* 28, 9–39.

U-Pb ZIRCON AGE OF GABBRO PEGMATITE AT THE RUOUTEVARE INTRUSION, MAP SHEET 26J JOKKMOKK NO, NORRBOTTEN COUNTY

Authors: Dick Claeson, Ildikó Antal Lundin & Fredrik Hellström

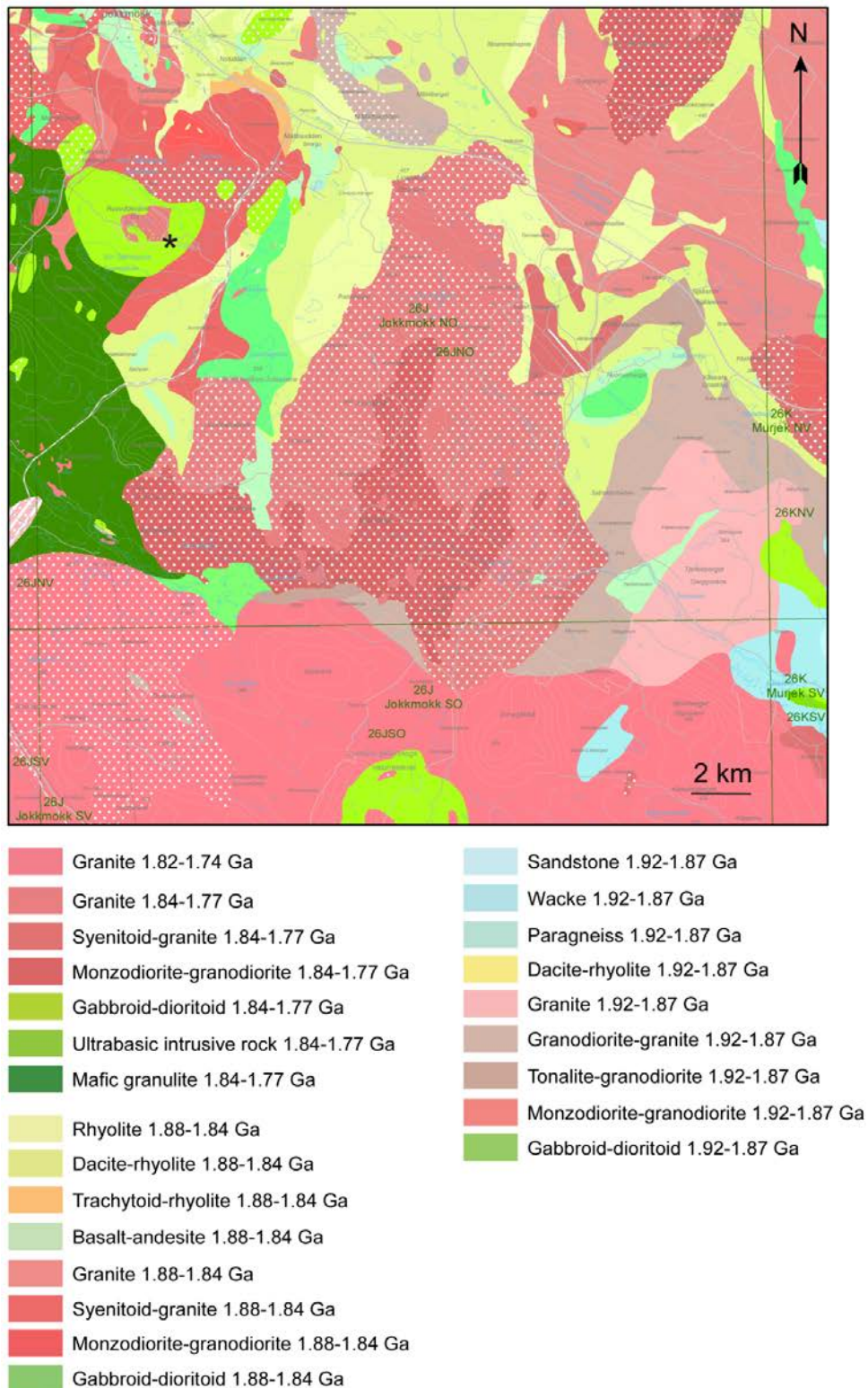


Figure 91. Bedrock map of the area, sampling location marked with black star.

Introduction

Norrbottnen, Sweden is a key area of Europe for future exploration and mining. The sampled gabbro pegmatite is part of the mountain Ruotevare positioned 6 km south of Jokkmokk (Fig. 91). The aeromagnetic data produced by the SGU shows a distinctive high magnetic anomaly at the sample location (Fig. 92). The high magnetic anomaly area consists mostly of outcrops of gabbroic rocks that are parts of a layered intrusion and occurrences of granite pegmatite (Fig. 91, 92). Modelling of the area using geophysical data has been presented earlier (Claeson & Antal Lundin 2013, Antal Lundin et al. 2017, Claeson & Antal Lundin *in press b*).

The contacts between gabbroic rocks and granite pegmatite are interpreted as showing that they formed at the same time, since hardly any contacts observed are chilled and several show a soft wavy contact (Claeson & Antal Lundin 2013). The layered intrusion is at some places mineralised and new data show that there is at least a horizon with anomalous PGE-Au content (Claeson & Antal Lundin 2013). Gabbroic compositions dominate but vary and at several places evidence of multiple pulses of mafic magma can be seen (Claeson & Antal Lundin 2013). Ultramafic rocks are seen both as cumulate layers as well as a few cm-wide dykes (Claeson & Antal Lundin 2013). Synmagmatic brecciation and enclaves are also seen (Claeson & Antal Lundin 2013).

In the area close to the intrusion, south to southeast, there are rocks earlier interpreted as clastic sediments whereas our current interpretation of these rocks is andesitoid to basaltoid for the most part, which are sometimes severely metamorphosed, to granulite facies. Just north of the intrusion coeval potassium feldspar porphyritic monzonite and monzodiorite are present. The rest of the bordering rocks are mostly monzonitoid and granitoid rocks, interpreted to be 1.87–1.89 Ga old (Fig. 91).

The aim of this study is to determine the magmatic age of the gabbro pegmatite. Since there are extremely few age determinations of gabbroic rocks in the area, an effort should be done by the SGU to at least try to determine some of these, in order to examine what age the gabbros in the Norrbotten County might span, Ruotevare being a PGE-Au anomalous intrusion makes the case even stronger. The sampled intrusion is seen as a possibly young intrusion, related to the magmatic events around 1.80 Ga.

The age determination of the gabbroic intrusion will most probably also tell at what point the andesitoid to basaltoid rocks were metamorphosed to granulite conditions. The magmatic age determination will also contribute to the knowledge of the extent of bimodal magmatism or if there are no corresponding felsic rocks intruding at the time of its formation in the Norrbotten County. Furthermore, the age will also be of use for inferring the age of the coexisting granite pegmatite, which has been quarried at Ruotevare (Sundius 1952, Senften 2008).

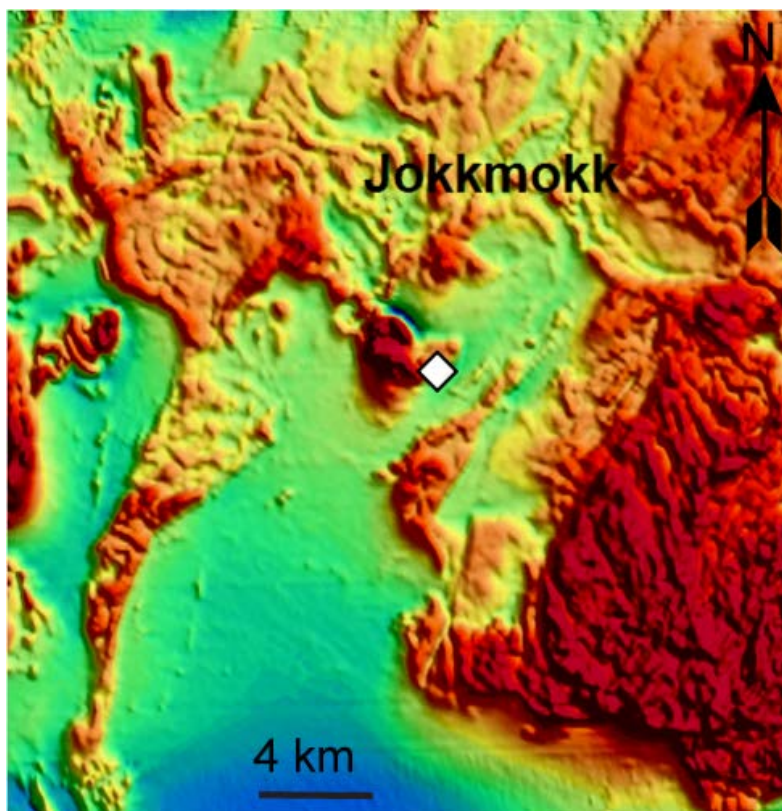


Figure 92. Magnetic anomaly map indicating the distribution of the major structures in the area, part of the map sheets 26J Jokkmokk NV, NO with surroundings. The white diamond shows the sample location.

Sample description

The sampled outcrop is located at the mountain Ruotevare approximately 6 km south of Jokkmokk. The sampled gabbro pegmatite consists mostly of plagioclase, clinopyroxene, amphibole, with minor biotite. The gabbro pegmatite lacks deformation and metamorphic overprinting. The outcrop shows a tremendous variation among rock compositions and there is ordinary gabbro, ultramafic, and ultrabasic rocks along with the gabbro pegmatite with evidence of several pulses of gabbroic magma that has interacted (Claeson & Antal Lundin *in press b*). The gabbro pegmatite is located next to an ultramafic gabbroic layer and the contact is interfingering (Fig. 93). A few meters from the gabbro pegmatite an ultramafic and ultrabasic cumulate occurs that shows anomalous PGE-Au content (Claeson & Antal Lundin 2013, *in press b*). Petrophysical measurements of a sample from the ultramafic and ultrabasic cumulate show density at $3\,186\text{ kg/m}^3$, magnetic susceptibility $14\,939 \times 10^{-5}\text{ SI}$, and remanent magnetization intensity of $8\,319\text{ mA/m}$. Gabbro at the outcrop displays low gamma ray radiation, $K = 0.3\%$, $U = 0.2\text{--}0.5\text{ ppm}$, and $\text{Th} = 1\text{--}1.3\text{ ppm}$.

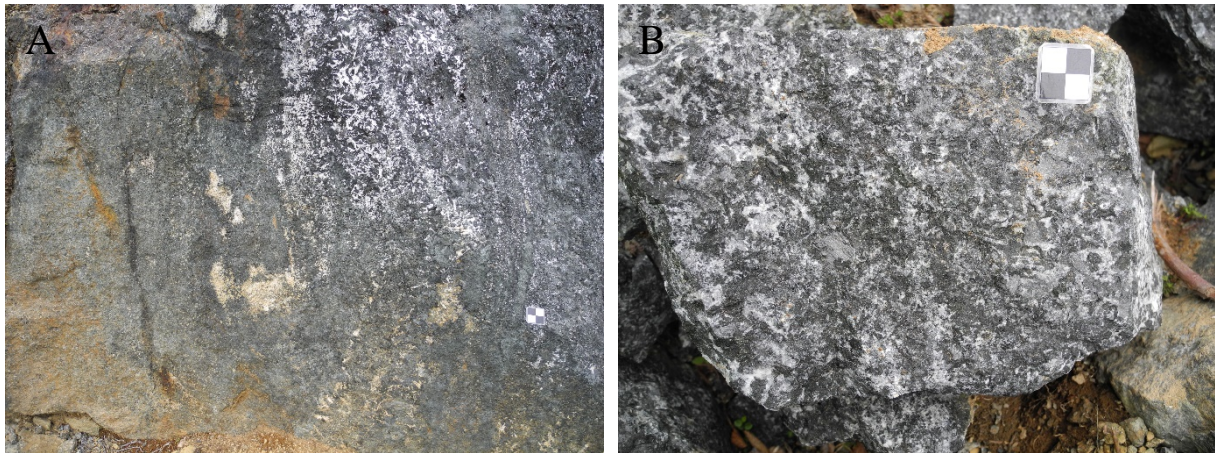


Figure 93. A. Gabbro pegmatite outcrop with surrounding ultramafic gabbroic layer. B. Close-up of sampled gabbro pegmatite.

Analytical results and interpretation of geochronological data

Zircon were obtained from a density separate of a crushed rock sample using a Wilfley water table. The magnetic minerals were removed by a hand magnet. Handpicked crystals were mounted in transparent epoxy resin together with chips of reference zircon 91 500. The zircon mounts were polished and after gold coating examined by Back scattered electron (BSE) and Cathodoluminescence (CL) imaging using electron microscopy at EBC, Uppsala University and at the Swedish Museum of Natural History in Stockholm. High-spatial resolution secondary ion mass spectrometer (SIMS) analysis was done in November and December 2014 using a Cameca IMS 1 280 at the Nordsim facility at the Swedish Museum of Natural History in Stockholm. Detailed descriptions of the analytical procedures are given in Whitehouse et al. (1997, 1999), and Whitehouse & Kamber (2005).

A c. 6 nA O^{2-} primary ion beam was used, yielding spot sizes of c. 15 μm . Pb/U ratios, elemental concentrations and Th/U ratios were calibrated relative to the Geostandards zircon 91 500 reference, which has an age of c. 1 065 Ma (Wiedenbeck et al. 1995, 2004). Common Pb corrected isotope values were calculated using modern common Pb composition (Stacey & Kramers 1975) and measured ^{204}Pb , in cases of a ^{204}Pb count rate above the detection limit. Decay constants follow the recommendations of Steiger & Jäger (1977). Diagrams and age calculations of isotopic data were made using software Isoplot 4.15 (Ludwig 2012). All age uncertainties are presented at the 2σ confidence level. BSE- and CL imaging of the age determined zircon was performed using electron microscopy at the Department of Geology, Uppsala University.

Most of the mounted grains from the heavy mineral separate turned out to be titanite, but there are also a small number of weakly pinkish crystal fragments of zircon. Back-scattered electron (BSE) and cathodoluminescence (CL) images show a weakly developed, diffuse and broad zoning or a homogenous BSE/CL-level (Fig. 94). Grain No. 7 displays CL-bright domains.

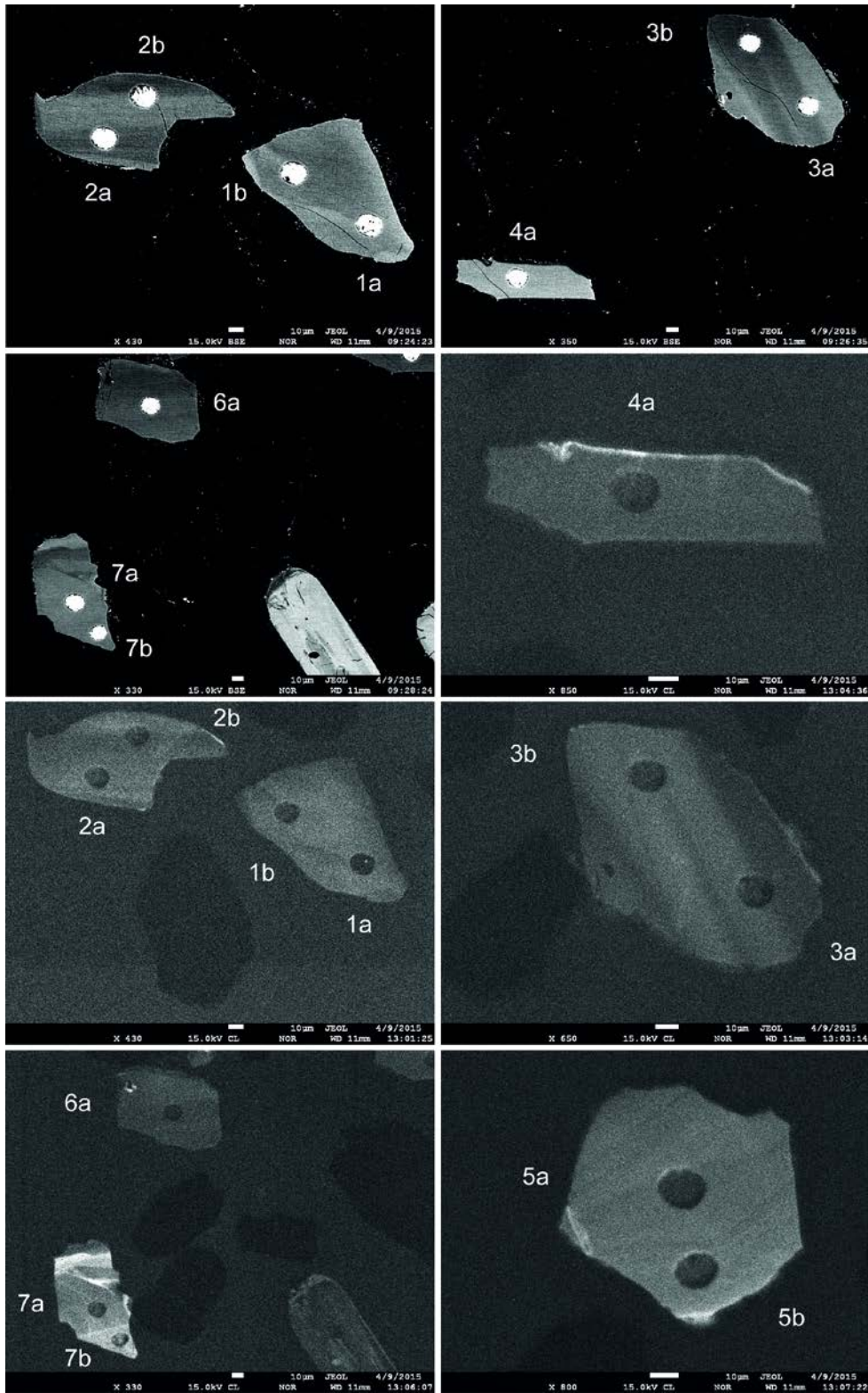


Figure 94. BSE-images, three in the upper left corner with dark background and CL-images of analysed zircon grains. Numbers refer to analytical spot number in Table 29. Spot size is c. 15–20µm.

The 12 zircon analyses performed are concordant with low amounts of common lead and are divided into two age groups. One old group with eight analyses that record generally higher Th/U ratios (0.21–0.77), compared to a group of four analyses showing a younger age done in two zircon grains, No. 5 and 7 (Fig. 95, Th/U = 0.01–0.22). The old group records a concordia age of 1883 ± 5 Ma (Fig. 95), identical with the mean $^{207}\text{Pb}/^{206}\text{Pb}$ weighted age of 1884 ± 5 Ma (2σ , $n = 8$, MSWD = 1.17, probability = 0.32). The young group demonstrates a mean $^{207}\text{Pb}/^{206}\text{Pb}$ weighted age of 1785 ± 13 Ma (2σ , $n = 4$, MSWD = 1.7, probability = 0.19), but one of the analyses (7b) is somewhat younger, preventing calculation of a concordia age since data are not equivalent. Analysis 7b is low in uranium and record a large age error (Table 29), excluding this analysis, a concordia age can be calculated at 1785 ± 10 Ma (Fig. 95). The young zircon grains No. 5 and 7 have apparently not a different morphology or internal texture compared to the zircon of the old group, as revealed by the BSE- and CL-images (Fig. 94). Grain 7 differs however slightly in having CL bright domains. The analyses of the two young zircon grains differ in being low in Th, resulting in low Th/U ratios.

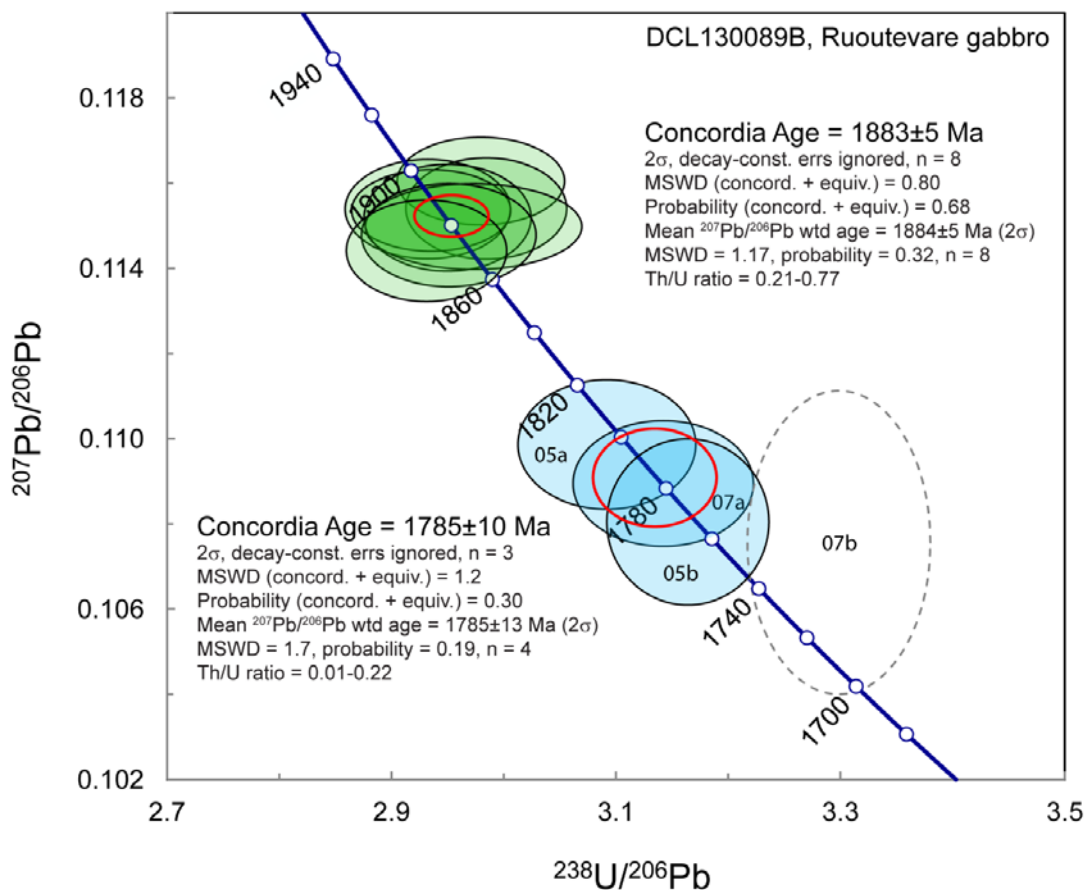


Figure 95. Tera-Wasserburg diagram showing U-Pb SIMS data of zircon analyses. Analysis 7b, shown with broken line, was excluded from calculation of the lower concordia age (see text). Error ellipse of calculated weighted mean age is shown in red.

Table 29. SIMS U-Pb-Th zircon data.

Sample/ spot #	U ppm	Th ppm	Pb ppm	Th/U calc ^{*1}	²⁰⁷ Pb	$\pm\sigma$	²⁰⁸ Pb	$\pm\sigma$	²³⁸ U	$\pm\sigma$	²⁰⁷ Pb	$\pm\sigma$	ρ *2	Disc. % conv. *3	²⁰⁷ Pb	$\pm\sigma$	²⁰⁶ Pb	$\pm\sigma$	²⁰⁶ Pb/ ²⁰⁴ Pb	f ₂₀₆ % *4
					²³⁵ U %	²³² Th %	²⁰⁶ Pb %	²⁰⁶ Pb %	²⁰⁶ Pb (Ma)	²³⁸ U (Ma)	measured									
n5165_01a	192	133	86	0.71	5.364	1.16	0.1001	2.2	2.951	1.08	0.1148	0.43	0.93	0.3	1877	8	1881	18	153378	{0.01}
n5165_01b	194	126	87	0.67	5.383	1.08	0.1005	2.1	2.931	1.00	0.1144	0.43	0.92	1.3	1871	8	1892	16	302905	{0.01}
n5165_02a	201	41	81	0.21	5.427	1.11	0.1026	2.3	2.932	1.03	0.1154	0.41	0.93	0.3	1886	7	1892	17	95100	{0.02}
n5165_02b	319	115	131	0.37	5.332	1.07	0.1008	2.3	2.984	0.98	0.1154	0.42	0.92	-1.4	1886	8	1863	16	127168	{0.01}
n5165_03a	266	206	120	0.77	5.371	1.09	0.0981	2.1	2.979	1.02	0.1161	0.36	0.94	-1.9	1896	6	1866	17	58778	{0.03}
n5165_03b	168	104	74	0.63	5.385	1.12	0.0995	2.1	2.950	1.03	0.1152	0.44	0.92	-0.1	1883	8	1882	17	183536	{0.01}
n5165_04a	288	77	117	0.28	5.420	1.04	0.1028	2.1	2.935	0.99	0.1154	0.34	0.95	0.3	1886	6	1890	16	>1e6	{0.00}
n5165_05a	113	1	41	0.01	4.900	1.19	0.1001	5.6	3.092	1.05	0.1099	0.56	0.88	0.6	1797	10	1807	17	>1e6	{0.00}
n5165_05b	108	3	38	0.03	4.709	1.19	0.0981	5.1	3.164	0.93	0.1081	0.74	0.78	0.2	1767	13	1770	14	36500	{0.05}
n5165_06a	288	159	124	0.56	5.333	1.37	0.0984	2.4	2.973	1.33	0.1150	0.36	0.97	-0.7	1880	6	1869	22	579757	{0.00}
n5165_07a	123	26	46	0.22	4.782	1.18	0.0958	2.4	3.142	1.04	0.1090	0.55	0.88	-0.1	1782	10	1781	16	142517	{0.01}
n5165_07b	77	11	27	0.14	4.496	1.69	0.0906	3.7	3.299	1.01	0.1076	1.35	0.60	-3.3	1759	25	1707	15	19844	{0.09}

Isotope values are common Pb corrected using modern common Pb composition (Stacey & Kramers 1975) and measured ²⁰⁴Pb.

*1 Th/U ratios calculated from ²⁰⁸Pb/²⁰⁶Pb and ²⁰⁷Pb/²⁰⁶Pb ratios, assuming single stage of closed U-Th-Pb evolution.

*2 Error correlation in conventional concordia space. Do not use for Tera-Wasserburg plots.

*3 Age discordance in conventional concordia space. Positive numbers are reverse discordant.

*4 Figures in parentheses are given when no correction has been applied, and indicate a value calculated assuming present-day Stacey-Kramers common Pb.

Discussion and conclusion

The interpretation of the age determination is not straight forward; one option is that the old analyses at $1\,883 \pm 5$ Ma date igneous crystallisation of the gabbro and that the analyses of grains No. 5 and 7 at $1\,785 \pm 10$ Ma represent a secondary, metamorphic age. Another option is that the zircon in the sample are mostly inherited from a felsic rock that is totally dissolved and possibly the reason for the increased amount of fluid in order to produce the pegmatite gabbro body. If that is correct, the inheritance of zircon occurs at $1\,785 \pm 10$ Ma of the $1\,883 \pm 5$ Ma old zircon, which is interpreted as the igneous age of the dissolved felsic rock.

The newly formed zircon or domains at $1\,785 \pm 10$ Ma represents the timing of the gabbro intrusion and dissolution of that rock. This scenario would also result in low Th/U ratio among the newly formed zircon domains, since it is the process of growth of secondary zircon that normally is attributed to explain low Th/U ratios, even if basic rocks may have primary zircon with low Th/U ratios (Hanchar & Hoskin 2003). In addition, the morphology of the zircon fragments of the gabbro pegmatite (Fig. 94) does resemble the shape of magmatically resorbed zircon (cf. Corfu et al. 2003).

The total lack of high-grade metamorphic alteration and the well-preserved appearance, at outcrops and in thin-sections of the gabbroic rocks, are supporting evidence for the option of inheritance of zircon (Claeson & Antal Lundin *in press b*). Since there is no evidence for a major metamorphic event, because that is needed in order to grow secondary zircon within a large gabbroic intrusion and of the same size as the other zircon of the igneous event, the option invoking a metamorphic event is discarded. Furthermore, the coexisting granitic pegmatite at Ruotevare is interpreted as coeval because of their contact relations and both lack major metamorphic overprinting (Claeson & Antal Lundin *in press b*). Earlier results indicate an age of c. $1\,795$ Ma for the granite pegmatite using allanite and fergusonite (Welin & Blomqvist 1964, Welin 1979).

The most prominent positive gravity anomaly in southern Norrbotten appears in the Jokkmokk area and the Ruotevare gabbro is part of this anomaly (Antal Lundin et al. 2017). A 3D inversion of gravity field data of the regional anomaly indicates a substantial volume of 297 km^3 of a high-density body, interpreted as gabbroids, which is considered sufficient for the heat input required for the observed granulite facies metamorphism and partial melting of e.g. andesitoid rocks (Antal Lundin et al. 2017). This would then have occurred at around $1\,785 \pm 10$ Ma ago.

In the nearby area, several large sized magmatic intrusions do occur around 1.78–1.81 Ga e.g. Tvärträsket Jokkmokk NO, Hárrevárddo intrusion Tjåmotis SV, Urtjuvare and Ahmavaara Nattavaara and some of these do show bimodal magmatism with a basic magmatic component (this issue). All of these rocks do not have the same petrogenesis as the in Norrbotten County wide-spread S-type Granite-Pegmatite association that also appears around 1.80 Ga.

The results were integrated in the mapping of the 26J Jokkmokk NV, NO area (Claeson & Antal Lundin *in press b*). Summary of sample data is given in Table 30.

Table 30. Summary of sample data.

Rock type	Gabbro pegmatite
Lithotectonic unit	Norrbottnen lithotectonic unit of the Svecokarelian orogen
Lithological unit	
Sample number	DCL130089B
Lab_id	n5165
Coordinates	7388439/715280 (Sweref99TM)
Map sheet	26J Jokkmokk NO (RT90)
Locality	Ruotevare
Project	Sydvästra Norrbotten (80025)

Acknowledgements

U-Pb isotopic zircon data were obtained from beneficial co-operation with the Laboratory for Isotope Geology of the Swedish Museum of Natural History in Stockholm. The Nordsim facility is operated under an agreement between the research funding agencies of Denmark, Norway and Sweden, the Geological Survey of Finland and the Swedish Museum of Natural History. Martin Whitehouse, Lev Ilyinsky and Kerstin Lindén at the Nordsim analytical facility are gratefully acknowledged for their first-class analytical support with SIMS-analyses. Martin Whitehouse reduced the zircon analytical data, Lev Ilyinsky assisted during ion probe analyses and Kerstin Lindén prepared the zircon mounts. Milos Bartol at EBC, and Jaroslaw Majka at the Department of Geology, Uppsala University, as well as Kerstin Lindén at NRM are all much thanked for their support during BSE/CL-imaging of zircon.

References

- Antal Lundin, I., Claeson, D. & Persson, L., 2017: Gravity inversion and its implication for basic magmatism and associated high-grade metamorphism, Northern Sweden. Abstract SAGA's 15th Biennial Conference & Exhibition.
- Claeson, D. & Antal Lundin, I., 2013: Berggrundsgeologisk undersökning, sydvästra Norrbotten. Sammanfattning av pågående verksamhet 2013. *Sveriges geologiska undersökning SGU-rapport 2013:18*, 27 pp.
- Claeson, D. & Antal Lundin, I., *in press b*: Beskrivning till berggrundskartorna 26J Jokkmokk NV, NO. *Sveriges geologiska undersökning*.
- Corfu, F., Hanchar, J.M., Hoskin, P.W.O. & Kinny, P., 2003: Atlas of zircon textures. In J.M. Hanchar & P.W.O. Hoskin (eds.): *Zircon. Reviews in Mineralogy and Geochemistry* 53, Mineralogical Society of America. 469–500.
- Hanchar J.M. & Hoskin P.W.O. (eds.), 2003: *Zircon. Reviews in Mineralogy and Geochemistry, vol. 53, Mineralogical Society of America/Geochemical Society*. 500 pp.
- Ludwig, K.R., 2012: User's manual for Isoplot 3.75. A Geochronological Toolkit for Microsoft Excel. *Berkeley Geochronology Center Special Publication No. 5*, 75 pp.
- Senften, T., 2008: Dokumentation av gruvlämningar i Ruotevare, Jokkmokks kommun. *Länsstyrelsen i Norrbottens län, rapportserie 1/2008*, 46 pp.

- Skiöld, T., Öhlander, B., Markkula, H., Widenfalk, L. & Claesson, L.-Å. 1993: Chronology of Proterozoic processes at the Archaean continental margin in northern Sweden. *Precambrian Research* 64, 225–238.
- Sundius, N., 1952: Kvarts, fältspat och glimmer samt förekomster därav i Sverige. *Sveriges geologiska undersökning C 520*, 231 pp.
- Stacey, J.S. & Kramers, J.D., 1975: Approximation of terrestrial lead isotope evolution by a two-stage model. *Earth and Planetary Science Letters* 26, 207–221.
- Steiger, R.H. & Jäger, E., 1977: Convention on the use of decay constants in geo- and cosmochronology. *Earth and Planetary Science Letters* 36, 359–362.
- Welin, E., 1979: Tabulation of recalculated radiometric ages published 1960–1979 for rocks and minerals in Sweden. *GFF* 101, 309–320.
- Welin, E. & Blomqvist, G., 1964: Age measurements on radioactive minerals from Sweden. *GFF* 86, 33–50.
- Whitehouse, M.J., Claesson, S., Sunde, T. & Vestin, J., 1997: Ion-microprobe U–Pb zircon geochronology and correlation of Archaean gneisses from the Lewisian Complex of Gruinard Bay, north-west Scotland. *Geochimica et Cosmochimica Acta* 61, 4 429–4 438.
- Whitehouse, M.J., Kamber, B.S. & Moorbath, S., 1999: Age significance of U–Th–Pb zircon data from Early Archaean rocks of west Greenland: a reassessment based on combined ion-microprobe and imaging studies. *Chemical Geology (Isotope Geoscience Section)* 160, 201–224.
- Whitehouse, M., J. & Kamber, B.S., 2005: Assigning Dates to Thin Gneissic Veins in High-Grade Metamorphic Terranes: A Cautionary Tale from Akilia, Southwest Greenland. *Journal of Petrology* 46, 291–318.
- Wiedenbeck, M., Allé, P., Corfu, F., Griffin, W.L., Meier, M., Oberli, F., Quadt, A.V., Roddick, J.C. & Spiegel, W., 1995: Three natural zircon standards for U-Th-Pb, Lu-Hf, trace element and REE analyses. *Geostandards Newsletter* 19, 1–23.

U-Pb ZIRCON AGE OF PORPHYRIC QUARTZ MONZONITE TO MONZONITE SOUTH OF TVÄRTRÄSKET, MAP SHEET 26J JOKKMOKK NO, NORRBOTTEN COUNTY

Authors: Dick Claeson, Ildikó Antal Lundin & Fredrik Hellström

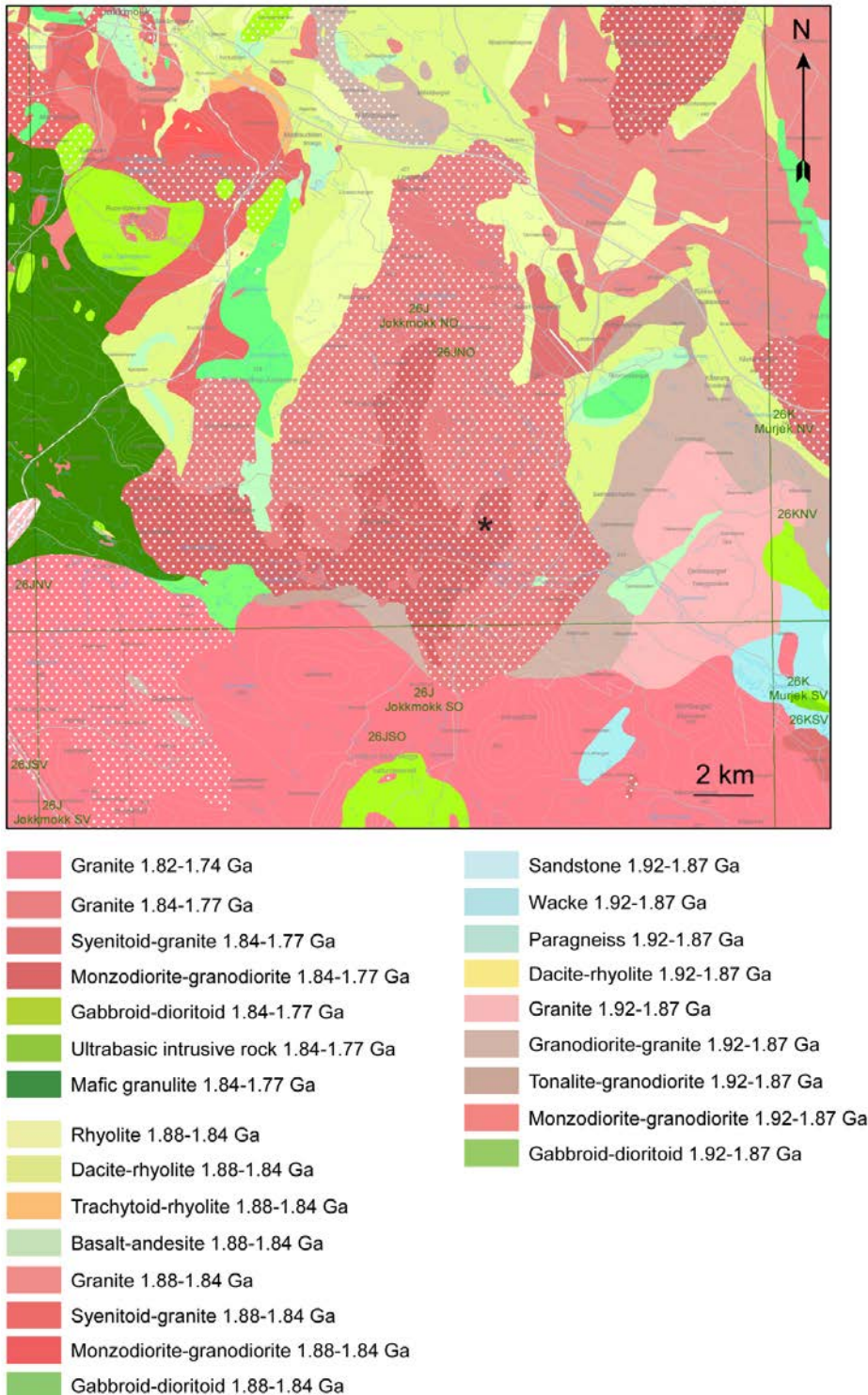


Figure 96. Bedrock map of the area, sampling location marked with black star.

Introduction

Norrbottnen, Sweden is a key area of Europe for future exploration and mining. The sampled rock is part of a distinctive high magnetic area seen on the magnetic anomaly maps (Fig. 96, 97). The high magnetic area covers a major part of the map area 26J Jokkmokk NO of the project mapping area and a similar but smaller anomaly is seen to the northeast on the map sheet that is interpreted to consist of a similar type of rock and to be coeval (Fig. 96, 97).

A tentative age estimate from the appearance of the rock would suggest an age around 1.80 Ga. However, if metamorphic rims or other overgrowths are present on the zircon of the sample, these should also be studied since this may be of significance for the interpretation of the genesis of the causative rock of this high magnetic area. Furthermore, several other rock types are also present and have the same magnetic signature. In order to gain knowledge of when metamorphic events are in any way involved in the genesis of the formation of economic deposits on a regional scale in the Norrbotten County, by re-heating the crust and producing hydrothermal activity in volcanic rocks, intrusive rocks or structural zones, their age have to be determined. Even the extent of magmatic induced metamorphism is of great importance.

A few larger intrusions of mostly quartz monzonite, granite to monzonite, and subordinate quartz monzodiorite to monzodiorite occur within the area of map sheet 26J Jokkmokk NO. The two younger, largest, acid to intermediate intrusions within the area 26J Jokkmokk NO consist of rocks with a strong variation in compositions (Claeson & Antal Lundin *in press b*). Three main rock types occur: 1) red to greyish red, even- to uneven-grained quartz monzonite to granite, 2) reddish grey to greyish red, coarsely K-feldspar porphyric quartz monzonite to granite, and 3) grey to greyish red, coarsely K-feldspar porphyric quartz monzodiorite, monzonite, quartz monzonite to monzodiorite, in both intrusions. The northern intrusion shows a higher proportion of intermediate compositions, quartz monzodiorite to monzonite, compared with the southern intrusion. A more extensive description of the geology of the area is found in Claeson & Antal Lundin (*in press b*). A 3D model of the intrusion using magnetic susceptibility is presented in Claeson & Antal Lundin (2015).

The aim of this study is to determine the magmatic age of the quartz monzonite to monzonite part of the southern intrusion seen in map area 26J Jokkmokk NO, and if there are any metamorphic overgrowths, determine these as well, since the latter might show ages for the redistribution of elements in the crust.

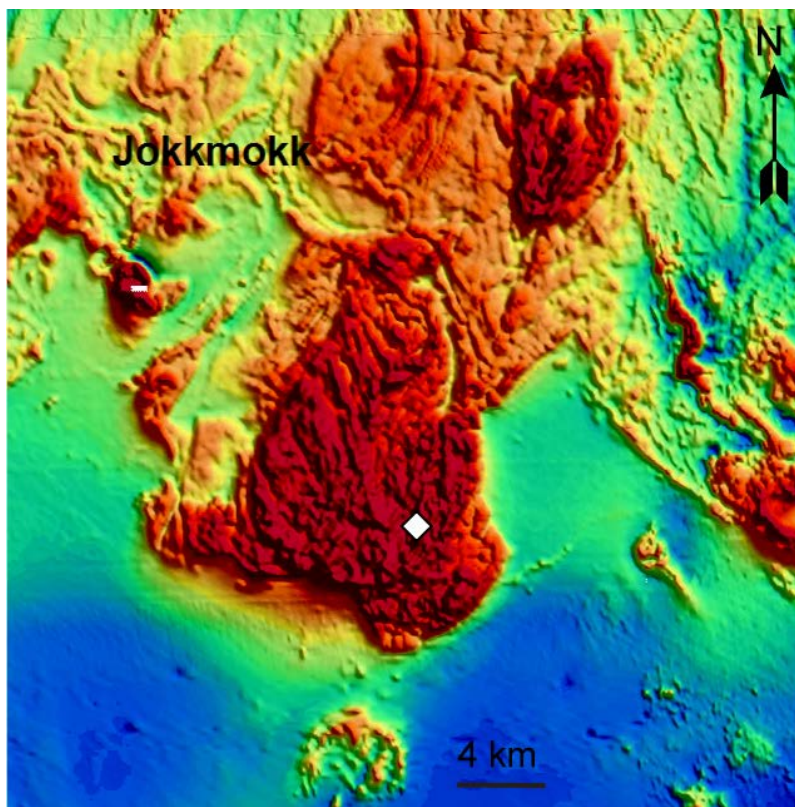


Figure 97. Magnetic anomaly map indicating the distribution of the major structures in the area, part of the map sheet 26J Jokkmokk NO with surroundings. The white diamond shows the sample location.

Sample description

The sampled outcrop is located just south of Tvärträsket, some 20 km southeast of Jokkmokk. The sample consists of monzonite to quartz monzonite, with minor amounts of granite appearing at the outcrop. The rock is greyish red to reddish grey, medium- to coarse grained. The rock is porphyric with potassium feldspar phenocrysts 10–40 mm (10–30 %) and some show rapakivi texture (Fig. 98). The potassium feldspar shows Carlsbad and cross-hatched twinning, perthite and microperthite intergrowths (Fig. 99). The phenocrysts have inclusions of plagioclase and quartz (Fig. 99). Plagioclase shows minor sericite alteration and blobs of myrmekite are present (Fig. 99). Biotite and amphibole are present in the groundmass at 12 and 2 %, respectively. Magmatic amphibole is pleochroic, dark to light green and pleochroic biotite brownish red to pale yellow and green. Quartz shows undulose extinction and bulging recrystallisation with subgrains (Fig. 99).

Accessory minerals are opaque minerals, mostly magnetite, apatite, titanite, and small zircon. Magmatic foliation and flow related parallel orientation of the phenocrysts is oriented 260/74–84 and massive parts are also present (Fig. 98). Some xenoliths of andesitoid are present at the outcrop. Pyrite crystals are seen in the groundmass and fracture-filling epidote. The Zr content of the rock is 408 ppm. Magnetic susceptibility at the outcrop varies between $2\,610$ and $5\,090 \times 10^{-5}$ SI with a geometric mean of $3\,630 \times 10^{-5}$ SI. Determination of the radiation properties of the rock, using gamma-ray spectrometry, resulted in $K = 4.6 \%$, $U = 1.2$ ppm, $Th = 7.3$ ppm. Petrophysical measurements show density at $2\,693$ kg/m³, magnetic susceptibility $6\,356 \times 10^{-5}$ SI, and Q-value at 0.0. The sample is from an outcrop that has seen an attempt at quarrying dimension stone, where at least a c. 8×4 metre large part has been removed and some of it is still present at the location (Fig. 98).

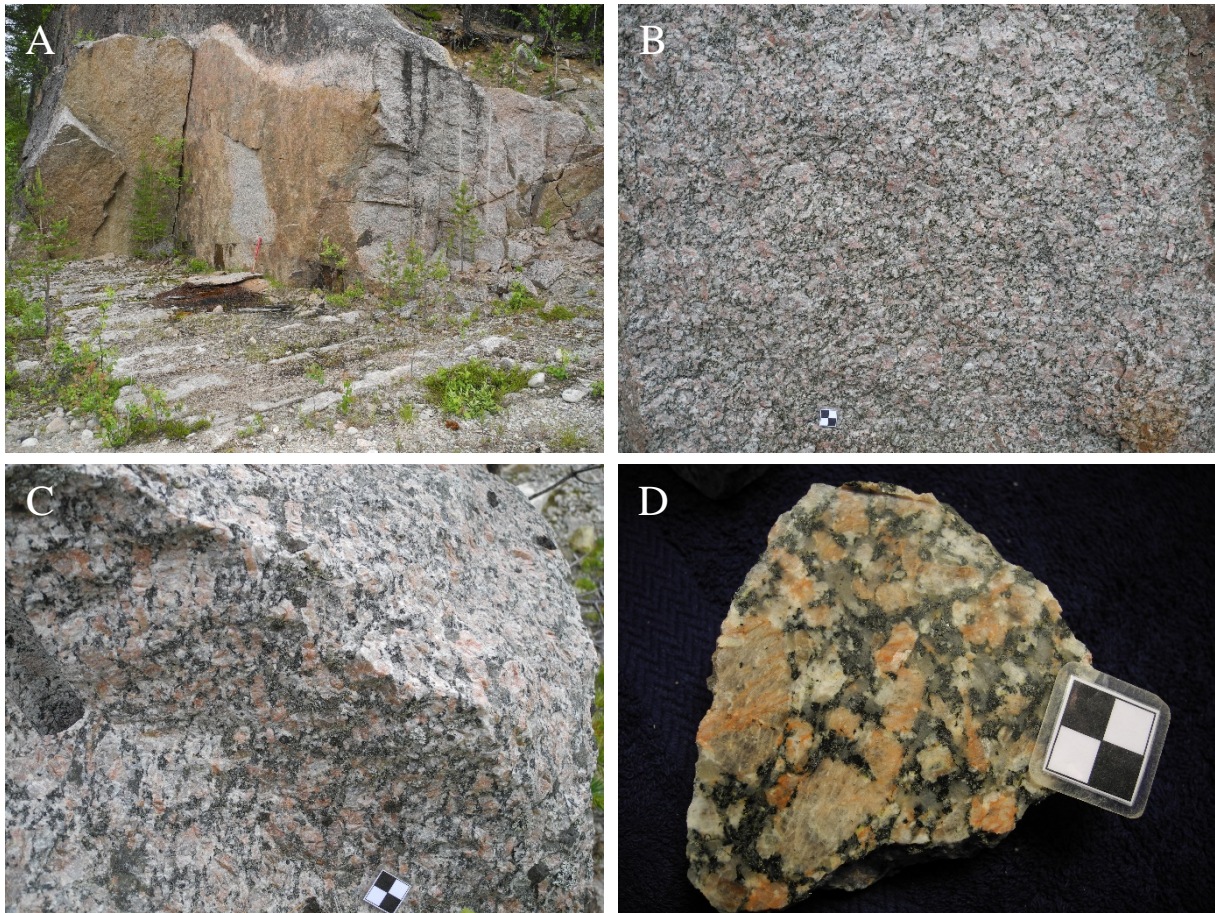


Figure 98. A. Potassium feldspar porphyritic monzonite to quartz monzonite outcrop showing attempt at quarrying dimension stone. B. Close-up of porphyritic monzonite to quartz monzonite. C. Porphyritic monzonite to quartz monzonite showing magmatic foliation and flow related parallel orientation of K-feldspar phenocrysts. D. Cut and wetted quartz monzonite of DCL140040 (cm-scale). Photos: Dick Claeson.

The quartz monzonite south of Tvärträsket shows a LREE-enriched and flat HREE pattern, with a minor negative Eu anomaly (Fig. 100). The LREE enrichment is due to fractional crystallisation, the flat, unfractionated HREE pattern shows that no garnet was left in the residue at the location of magma genesis, and the minor Eu anomaly is indicative of plagioclase fractionation. The negative anomalies shown in the multi-element diagram of Sr is due to plagioclase fractionation, the P anomaly of apatite fractionation, and the Ti anomaly of Fe-Ti oxide fractionation (Fig. 100). The strong negative Nb anomaly and positive Pb anomaly suggest a subduction related petrogenesis (Fig. 100).

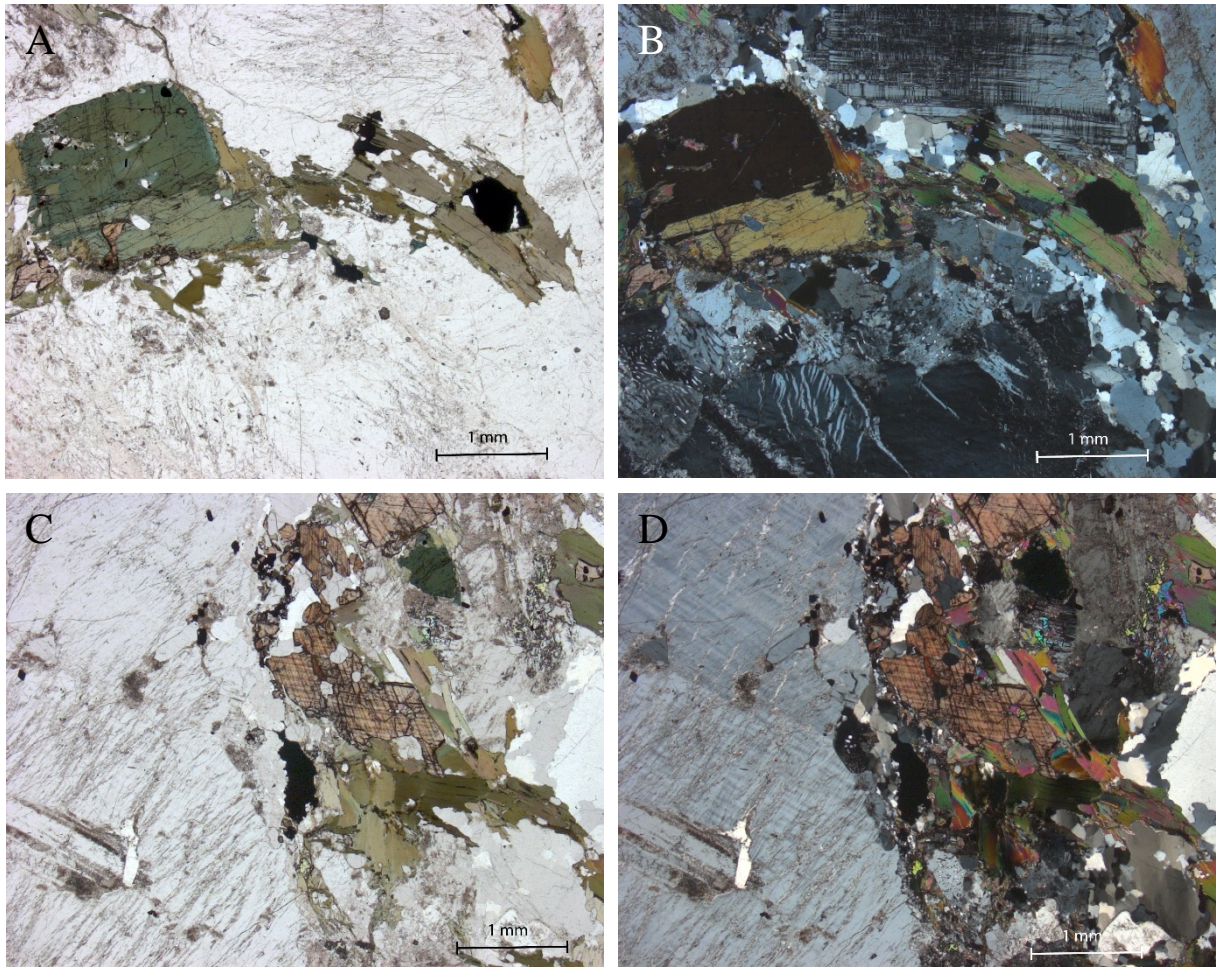


Figure 99. Potassium feldspar, plagioclase, amphibole, biotite, and quartz in quartz monzonite DCL140040, **A.** plane-polarized light, **B.** crossed nicols. Phenocryst of potassium feldspar to the left with plagioclase and quartz inclusions, in centre biotite, titanite, and zircon in quartz monzonite DCL140040, **C.** plane-polarized light, **D.** crossed nicols. Micrographs: Dick Claeson.

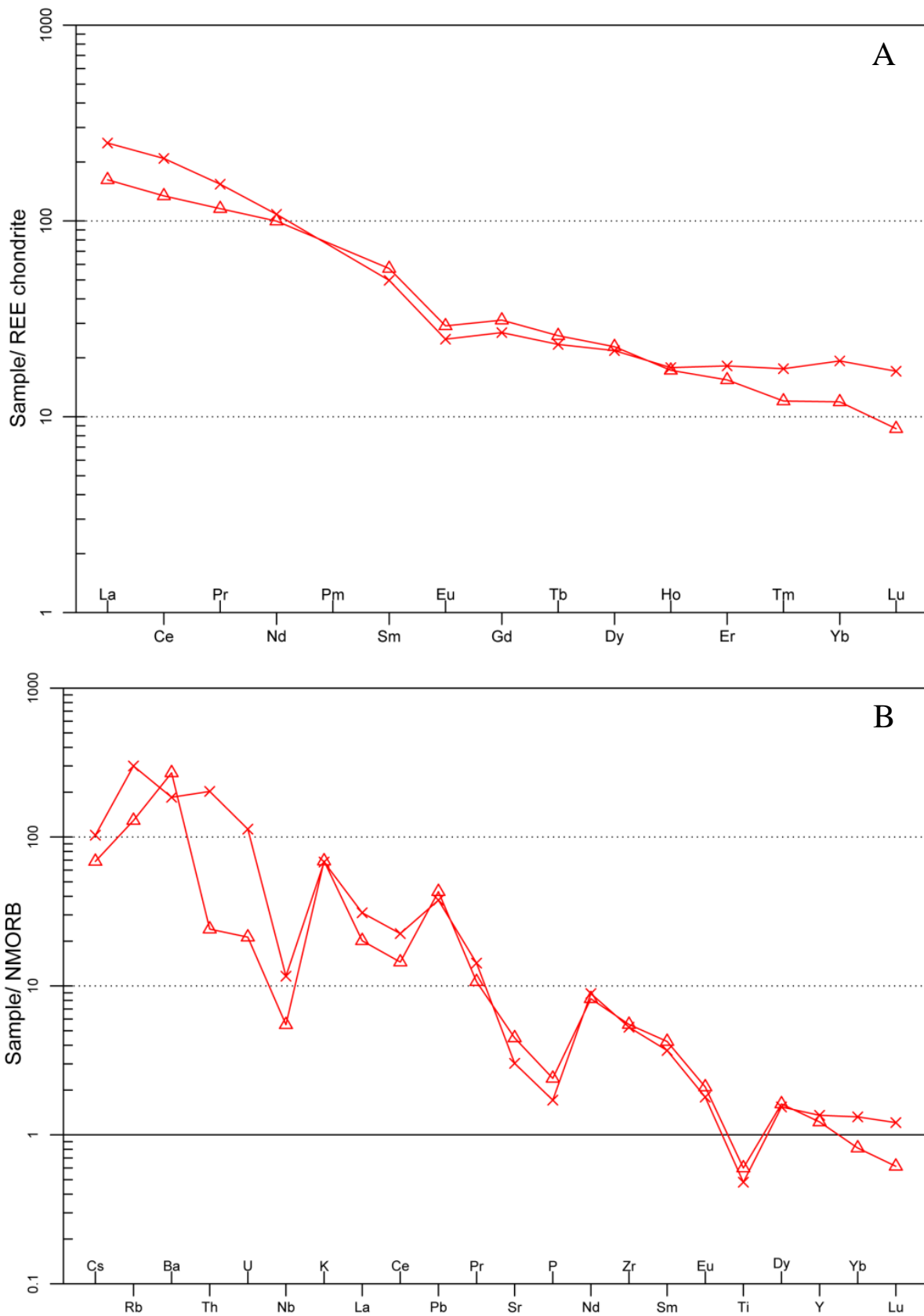


Figure 100. A. REE-diagram of quartz monzonite from Tvärträsket (rectangle) and Ammaberget (cross). Normalizing values for chondrite from Boynton (1984). B. Multi-element diagram, rocks as in A. Normalizing values for N-MORB from Sun & McDonough (1989).

Analytical results and interpretation of geochronological data

Zircon were obtained from a density separate of a crushed rock sample using a Wilfley water table. The magnetic minerals were removed by a hand magnet. Handpicked crystals were mounted in transparent epoxy resin together with chips of reference zircon 91 500. The zircon mounts were polished and after gold coating examined by back-scattered electron (BSE) and cathodoluminescence (CL) imaging using electron microscopy at EBC, Uppsala University and at the Swedish Museum of Natural History in Stockholm. High-spatial resolution secondary ion mass spectrometer (SIMS) analysis was done in November and December 2014 using a Cameca IMS 1 280 at the Nordsim facility at the Swedish Museum of Natural History in Stockholm. Detailed descriptions of the analytical procedures are given in Whitehouse et al. (1997, 1999) and Whitehouse & Kamber (2005).

A c. 6 nA O^{2-} primary ion beam was used, yielding spot sizes of c. 15 μm . Pb/U ratios, elemental concentrations and Th/U ratios were calibrated relative to the Geostandards zircon 91 500 reference, which has an age of c. 1 065 Ma (Wiedenbeck et al. 1995, 2004). Common Pb corrected isotope values were calculated using modern common Pb composition (Stacey & Kramers 1975) and measured ^{204}Pb , in cases of a ^{204}Pb count rate above the detection limit. Decay constants follow the recommendations of Steiger & Jäger (1977). Diagrams and age calculations of isotopic data were made using software Isoplot 4.15 (Ludwig 2012). All age uncertainties are presented at the 2σ confidence level. BSE-imaging of the dated zircon was performed using electron microscopy at the Department of Geology, Uppsala University.

The heavy mineral concentrate contains plenty of zircon and titanite. The zircon are colourless and transparent with subhedral, prismatic crystal shapes. Inclusions and microcracks are common. BSE-images show a concentric, oscillatory internal zonation in the zircon (Fig. 101). All eleven analyses are concordant at the 2σ error limit and record low values of common lead, except analysis No. 1a (Table 31). The uranium content of the zircon is low, 63–163 ppm, and Th/U ratios vary between 0.34 and 1.0. A concordia age is calculated at $1\,794 \pm 5$ Ma (Fig. 102, $n = 11$, MSWD of conc. & equiv. = 1.08, probability of conc. & equiv. = 0.36), which is within error the same as the weighted average $^{207}\text{Pb}/^{206}\text{Pb}$ age at $1\,798 \pm 6$ Ma (MSWD = 0.73, probability = 0.70). The concordia age at $1\,794 \pm 5$ Ma is chosen as the best age estimate interpreted to date igneous crystallisation of the porphyric monzonite to quartz monzonite.

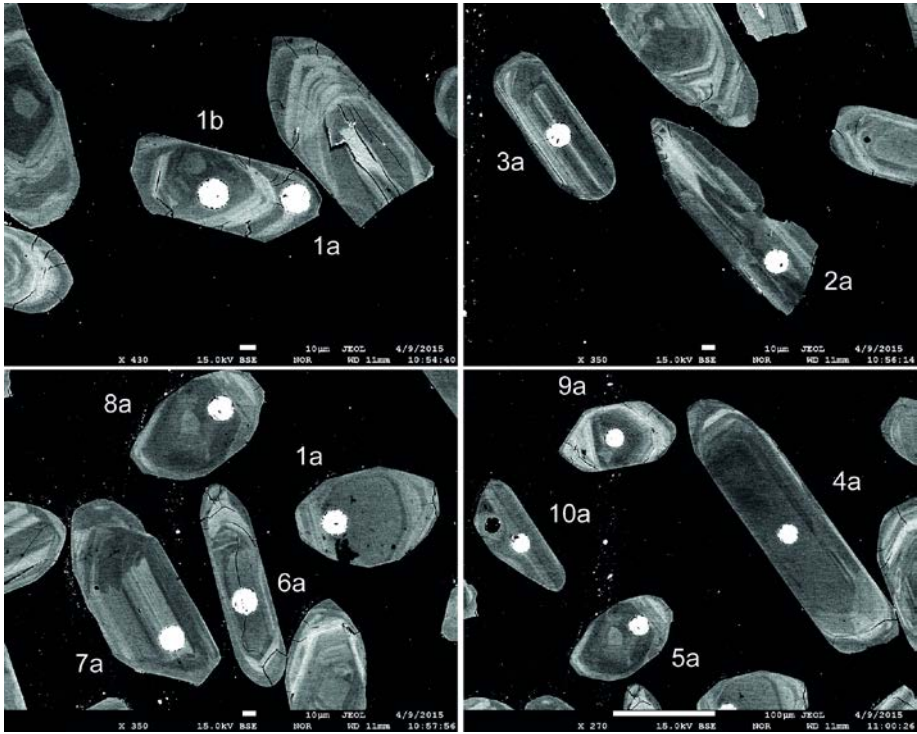


Figure 101. Back-scattered electron images of the analysed zircon grains. White ellipses mark the approximate locations of analyses. Numbers refer to analytical spot number in Table 31.

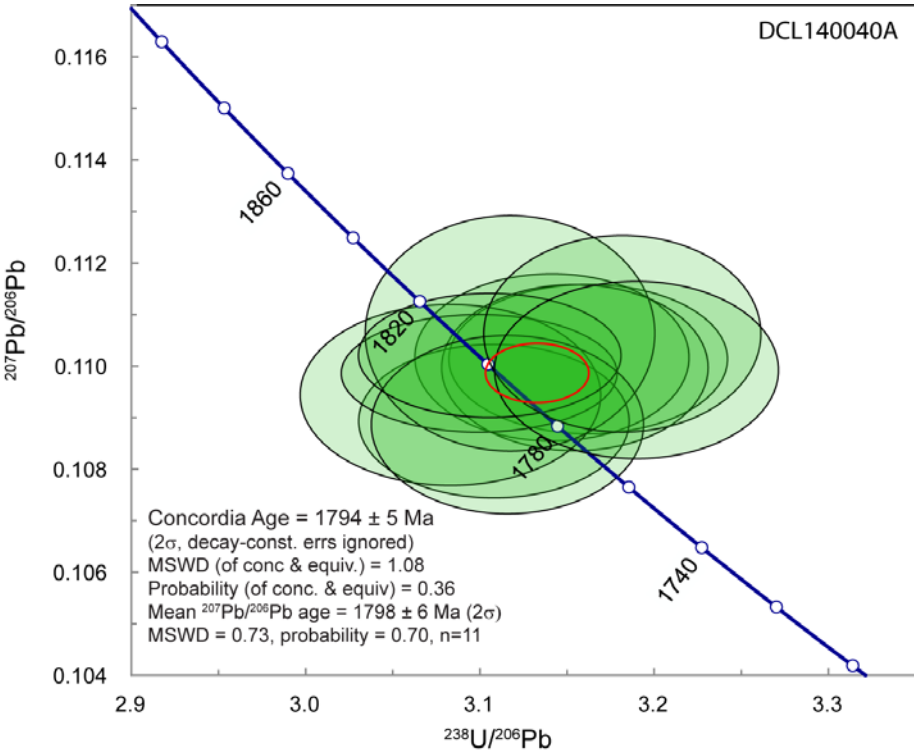


Figure 102. Tera-Wasserburg diagram showing U-Pb SIMS zircon data. Error ellipse of calculated weighted mean age is shown in red.

Table 31. SIMS U-Pb-Th zircon data.

Sample/ spot #	U ppm	Th ppm	Pb ppm	Th/U calc *1	²⁰⁷ Pb ²³⁵ U	±s %	²⁰⁸ Pb ²³² Th	±s %	²³⁸ U ²⁰⁶ Pb	±s %	²⁰⁷ Pb ²⁰⁶ Pb	±s %	ρ *2	Disc. % conv. *3	²⁰⁷ Pb ²⁰⁶ Pb (Ma)	±s (Ma)	²⁰⁶ Pb ²³⁸ U (Ma)	±s (Ma)	²⁰⁶ Pb/ ²⁰⁴ Pb measured	f ₂₀₆ % *4
n5175_01a	163	55	62	0.34	4.803	1.16	0.0935	2.4	3.162	1.03	0.1101	0.54	0.89	-1.9	1802	10	1771	16	1957	0.96
n5175_01b	86	50	35	0.59	4.836	1.19	0.0944	2.2	3.141	1.02	0.1102	0.60	0.86	-1.3	1802	11	1782	16	>1e6	{0.00}
n5175_02a	100	45	39	0.46	4.807	1.16	0.0937	2.4	3.154	0.99	0.1100	0.60	0.86	-1.5	1799	11	1775	15	64792	{0.03}
n5175_03a	123	84	52	0.70	4.833	1.16	0.0947	2.2	3.108	1.02	0.1089	0.56	0.88	1.1	1782	10	1798	16	>1e6	{0.00}
n5175_04a	63	46	27	0.74	4.895	1.32	0.0939	3.9	3.083	1.14	0.1095	0.65	0.87	1.3	1790	12	1811	18	42417	{0.04}
n5175_05a	110	84	46	0.76	4.795	1.24	0.0933	2.1	3.182	1.02	0.1106	0.70	0.82	-3.0	1810	13	1762	16	>1e6	{0.00}
n5175_06a	70	50	29	0.71	4.752	1.22	0.0925	2.5	3.190	1.04	0.1099	0.64	0.85	-2.6	1798	12	1758	16	52888	{0.04}
n5175_07a	148	145	67	1.00	4.888	1.13	0.0953	2.1	3.100	1.04	0.1099	0.42	0.93	0.3	1797	8	1803	16	181681	{0.01}
n5175_08a	77	47	32	0.61	4.894	1.38	0.0935	2.2	3.117	1.09	0.1106	0.84	0.79	-1.0	1810	15	1794	17	95365	{0.02}
n5175_09a	75	49	31	0.67	4.818	1.21	0.0940	2.2	3.116	1.02	0.1089	0.65	0.84	0.9	1781	12	1794	16	159538	{0.01}
n5175_10a	129	107	56	0.85	4.893	1.09	0.0954	2.1	3.106	0.99	0.1102	0.45	0.91	-0.2	1803	8	1799	16	195447	{0.01}

Isotope values are common Pb corrected using modern common Pb composition (Stacey & Kramers 1975) and measured ²⁰⁴Pb.

*1 Th/U ratios calculated from ²⁰⁸Pb/²⁰⁶Pb and ²⁰⁷Pb/²⁰⁶Pb ratios, assuming a single stage of closed U-Th-Pb evolution

*2 Error correlation in conventional concordia space. Do not use for Tera-Wasserburg plots.

*3 Age discordance in conventional concordia space. Positive numbers are reverse discordant.

*4 Figures in parentheses are given when no correction has been applied, and indicate a value calculated assuming present-day Stacey-Kramers common Pb.

Discussion and conclusion

There are two intrusions close to each other in the map area 26J Jokkmokk NO that show similar lithological characteristics (Fig. 96). The lithochemical data from the larger, southern intrusion at Tvärträsket is for the most part more or less identical to that of the sample from northern intrusion at Ammaberget (Fig. 100). The only real difference shown in the plots between the two rocks is the content of Th and U (Fig. 100). So even though the northern intrusion is not age determined, field appearance, lithochemical and rock compositions indicate that they are coeval and comagmatic (Claeson & Antal Lundin *in press b*). The concordia age at $1\,794 \pm 5$ Ma is the best age estimate interpreted to date igneous crystallisation of these intrusions. The results were integrated in the mapping of the 26J Jokkmokk NV, NO area (Claeson & Antal Lundin *in press b*). Summary of sample data is given in Table 32.

Table 32. Summary of sample data.

Rock type	Potassium porphyric monzonite to quartz monzonite
Lithotectonic unit	Norrbottnen lithotectonic unit of the Svecokarelian orogen
Lithological unit	
Sample number	DCL140040A
Lab_id	n5175
Coordinates	7378805/726008 (Sweref99TM)
Map sheet	26J Jokkmokk NO (RT90)
Locality	Tvärträsket
Project	Sydvästra Norrbotten (80025)

Acknowledgements

U-Pb isotopic zircon data were obtained from beneficial co-operation with the Laboratory for Isotope Geology of the Swedish Museum of Natural History in Stockholm. The Nordsim facility is operated under an agreement between the research funding agencies of Denmark, Norway and Sweden, the Geological Survey of Finland and the Swedish Museum of Natural History. Martin Whitehouse, Lev Ilyinsky and Kerstin Lindén at the Nordsim analytical facility are gratefully acknowledged for their first-class analytical support with SIMS-analyses. Martin Whitehouse reduced the zircon analytical data, Lev Ilyinsky assisted during ion probe analyses and Kerstin Lindén prepared the zircon mounts. Milos Bartol at EBC, and Jaroslaw Majka at the Department of Geology, Uppsala University, as well as Kerstin Lindén at NRM are all much thanked for their support during BSE/CL-imaging of zircon.

References

- Boynton, W.V., 1984: Cosmochemistry of the Rare Earth Elements: Meteorite studies. In P. Henderson (ed.): *Rare earth element geochemistry*. Elsevier Science B.V. 63–114.
- Claeson, D. & Antal Lundin, I., 2015: Berggrundsgeologisk undersökning, sydvästra Norrbotten. Sammanfattning av pågående verksamhet 2014. *Sveriges geologiska undersökning SGU-rapport 2015:03*, 32 pp.
- Claeson, D. & Antal Lundin, I., *in press b*: Beskrivning till berggrundskartorna 26J Jokkmokk NV, NO. *Sveriges geologiska undersökning*.
- Ludwig, K.R., 2012: User's manual for Isoplot 3.75. A Geochronological Toolkit for Microsoft Excel. *Berkeley Geochronology Center Special Publication No. 5*, 75 pp.
- Stacey, J.S. & Kramers, J.D., 1975: Approximation of terrestrial lead isotope evolution by a two-stage model. *Earth and Planetary Science Letters* 26, 207–221.
- Steiger, R.H. & Jäger, E., 1977: Convention on the use of decay constants in geo- and cosmochronology. *Earth and Planetary Science Letters* 36, 359–362.
- Sun, S.S. & McDonough, W.F., 1989: Chemical and isotopic systematic of oceanic basalts: implications for mantle composition and processes. In A.D. Saunders & M.J. Norry (eds.): *Magmatism in ocean basins*. Geological Society of London, Special Publication 42, 313–345.
- Whitehouse, M.J., Claesson, S., Sunde, T. & Vestin, J., 1997: Ion-microprobe U–Pb zircon geochronology and correlation of Archaean gneisses from the Lewisian Complex of Gruinard Bay, north-west Scotland. *Geochimica et Cosmochimica Acta* 61, 4 429–4 438.
- Whitehouse, M.J., Kamber, B.S. & Moorbath, S., 1999: Age significance of U–Th–Pb zircon data from Early Archaean rocks of west Greenland: a reassessment based on combined ion-microprobe and imaging studies. *Chemical Geology (Isotope Geoscience Section)* 160, 201–224.
- Whitehouse, M., J. & Kamber, B.S., 2005: Assigning Dates to Thin Gneissic Veins in High-Grade Metamorphic Terranes: A Cautionary Tale from Akilia, Southwest Greenland. *Journal of Petrology* 46, 291–318.
- Wiedenbeck, M., Allé, P., Corfu, F., Griffin, W.L., Meier, M., Oberli, F., Quadt, A.V., Roddick, J.C. & Spiegel, W., 1995: Three natural zircon standards for U-Th-Pb, Lu-Hf, trace element and REE analyses. *Geostandards Newsletter* 19, 1–23.
- Wiedenbeck, M., Hanchar, J.M., Peck, W.H., Sylvester, P., Valley, J., Whitehouse, M., Kronz, A., Morishita, Y., Nasdala, L., Fiebig, J., Franchi, I., Girard, J.P., Greenwood, R.C., Hinton, R., Kita, N., Mason, P.R.D., Norman, M., Ogasawara, M., Piccoli, P.M., Rhede, D., Satoh, H., Schulz-Dobrick, B., Skår, O., Spicuzza, M.J., Terada, K., Tindle, A., Togashi, S., Vennemann, T., Xie, Q. & Zheng, Y.F., 2004: Further Characterisation of the 91500 Zircon Crystal. *Geostandards and Geoanalytical Research* 28, 9–39.

MAP SHEET 271 TJÅMOTIS SV, SO AREA

Four rocks were sampled for age determination, two volcanic and two intrusive, in order to better constrain the mapping effort and contribute to new data and knowledge of the magmatic events in the area.

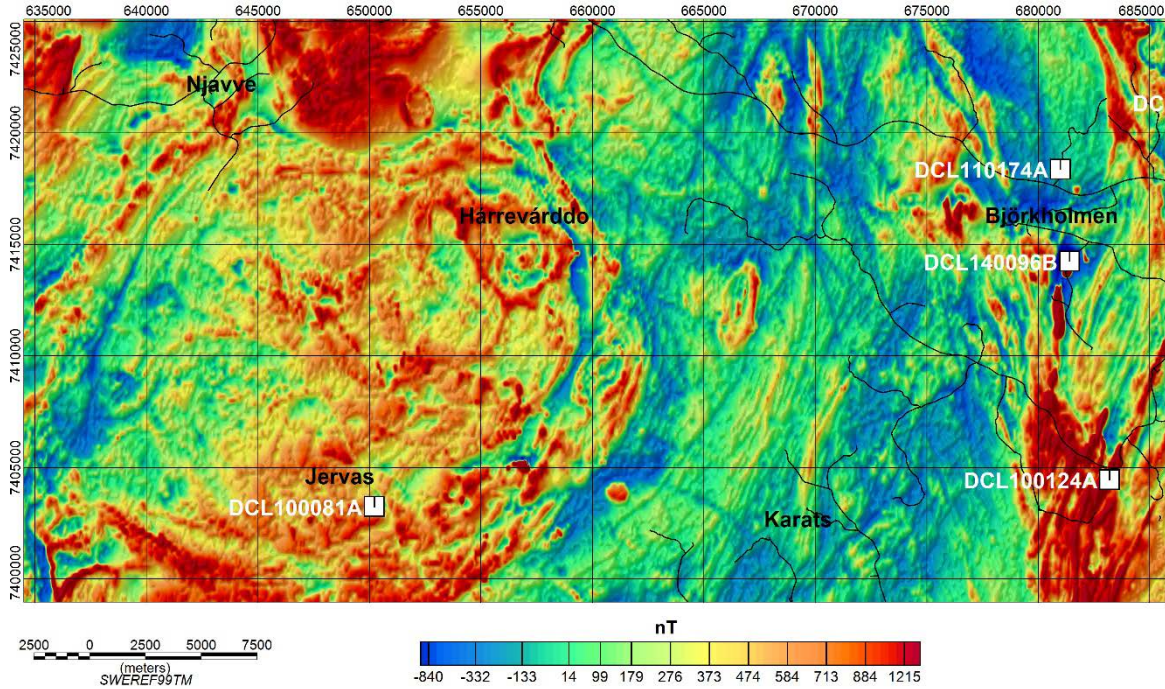


Figure 103. Magnetic total field after subtraction of the geomagnetic reference field (DGRF 1965.0) over the map area 271 Tjåmotis SO and SV. The sample locations are shown with white rectangles.

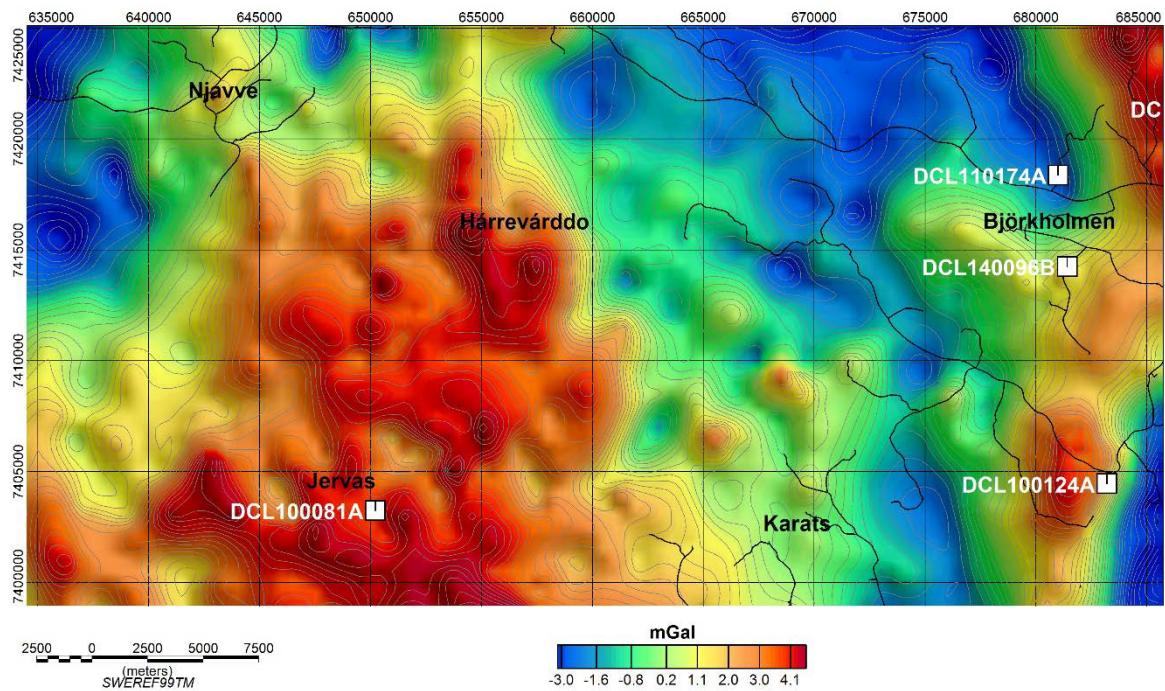


Figure 104. Residual gravity anomaly map over the map sheet 271 Tjåmotis SO and SV. The sample locations are shown with white rectangles.

Introduction

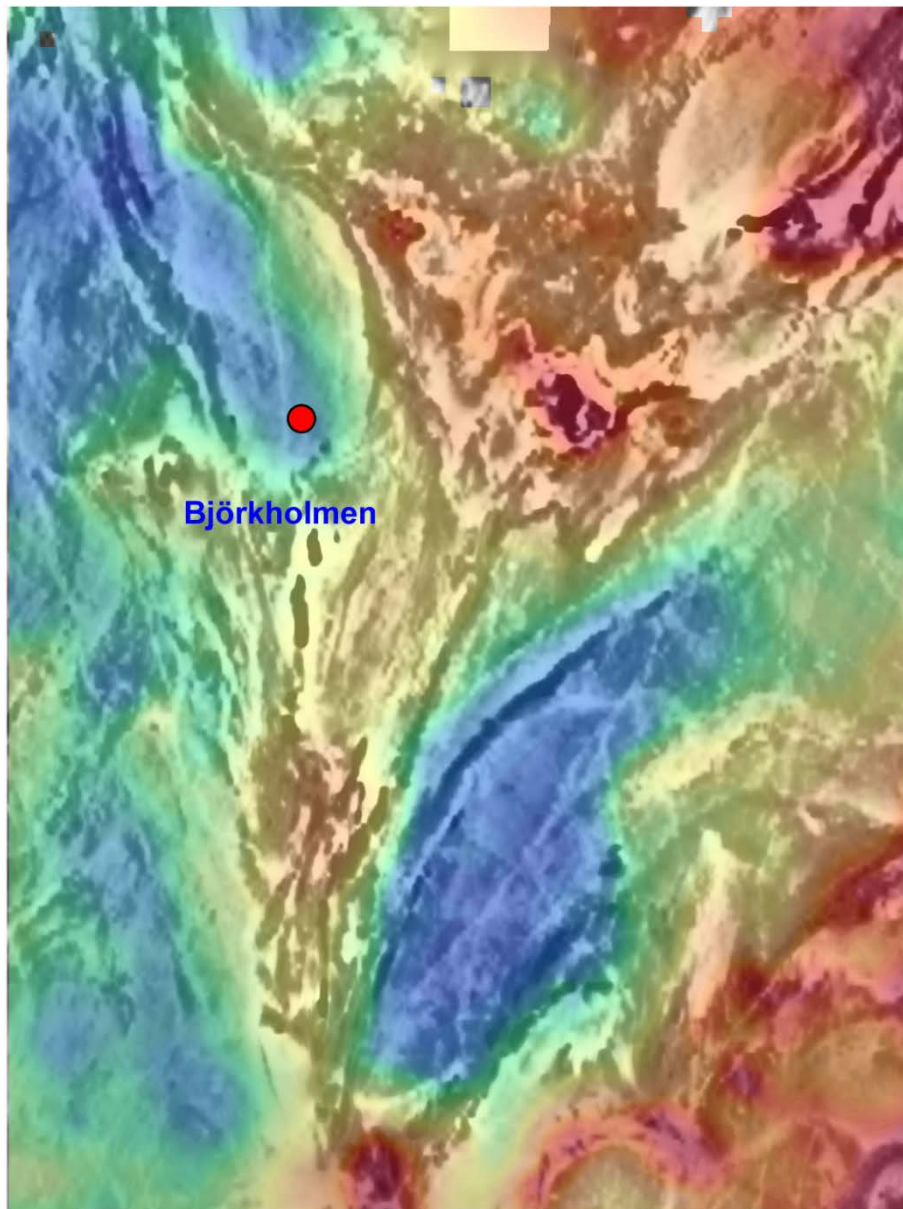
Norrbottnen, Sweden is a key area of Europe for future exploration and mining. The sampled rock is part of a large structure that is well-documented by the aeromagnetic data produced by the SGU (Fig. 103–106). Both on magnetic maps and Bouguer anomaly maps the structure is clearly seen as a well-defined gravity low and a low magnetic, elliptic anomaly pattern (Fig. 106) caused by low density and relatively low susceptibility rocks. The gravity low indicates that the structure consists mostly of felsic rocks. The structure is interpreted as a body of intrusive rocks and is 5×10 km in diameter, which covers parts of the map area 27I Tjåmotis SO.

Interpretation of the magnetic anomaly pattern suggests that this intrusion's relation to the surrounding extrusive rocks is different compared to other intrusive rocks found on map sheet 27I Tjåmotis SO. The elliptic body cuts the high-magnetic pattern, mainly consisting of volcanic rocks, to the south. Other intrusions in map area 27I Tjåmotis SO, with similar metamorphic overprinting as the rocks of the elliptic body, show more irregular patterns and the surrounding extrusive rocks are forming parallel patterns.

If there are zircon with metamorphic rims or other overgrowths, these should also be studied since this may be of huge significance for the interpretation of the genesis of an ore body/deposit, in this case the Kallak iron ore c. 4 km south of the sampled granite. For example, where multiple episodes of concentration of sulphides are indicated in recent work at Aitik (Wanhainen et al. 2003, 2005) or in iron oxide–copper–gold (IOCG) mineralisation in this region (Smith et al. 2009). In order to gain knowledge of when metamorphic events are in any way involved in the genesis of the formation of economic deposits on a regional scale in the Norrbotten county, by re-heating the crust and producing hydrothermal activity in volcanic rocks or structural zones, their age have to be determined.

If intrusions are in any way involved in the genesis of the formation of economic deposits on a regional scale in the Norrbotten county, by re-heating the crust and producing hydrothermal activity in volcanic rocks or structural zones, their age should be determined in order to get a fundamental understanding of the intrusions spatial distribution. But we believe this is a field for future research. Knowledge about the magmatic age of the intrusion and metamorphic overprinting is consequently important.

The aim of this study is to determine the magmatic age of the granite to quartz monzonite as part of a major structure on the map sheet 27I Tjåmotis SO and if there are any metamorphic overgrowths, determine these as well, since the latter might show ages for the genesis of ore by redistribution of elements in the crust.



5 km

Figure 106. Residual gravity map in colour, superimposed on the magnetic anomaly map in grey, map sheet 271 Tjåmotis SV with surroundings. The red dot shows the sample location.

Sample description

The sampled outcrop is located at the southeast part of Ritavare, some 10 km northwest of Randijaur. The sample consists of granite that is deformed, recrystallised, red to greyish red, and medium-grained (Fig. 107, 108). The rock is equigranular to porphyric with feldspar megacrysts 5–10 mm (0–3 %). Biotite content is around 8 %. Foliation is oriented 200/45 and mineral lineation 20/30. Magnetic susceptibility at the outcrop varies between 930 and $1\,830 \times 10^{-5}$ SI. Petrophysical measurements of a sample show density at $2\,632 \text{ kg/m}^3$, magnetic susceptibility $1\,544 \times 10^{-5}$ SI, and remanent magnetization intensity of 160 mA/m. Gamma ray spectrometry on the outcrop shows K = 5 %, U = 5 ppm, and Th = 31 ppm. The Zr content of the rock is 206 ppm.

The granite to quartz monzonite at Ritavare shows a LREE-enriched and flat HREE pattern, with a pronounced negative Eu anomaly (Fig. 109). The LREE enrichment is due to fractional crystallisation, the flat, unfractionated HREE pattern shows that no garnet was left in the residue at the location of magma genesis, and the Eu anomaly is indicative of extensive plagioclase fractionation. The negative anomalies shown in the multi-element diagram of Sr and Eu are due to plagioclase fractionation, the P anomaly of apatite fractionation, and the Ti anomaly of Fe-Ti oxide fractionation (Fig. 109). The strong negative Nb anomaly and positive Pb anomaly suggest a subduction related petrogenesis (Fig. 109).

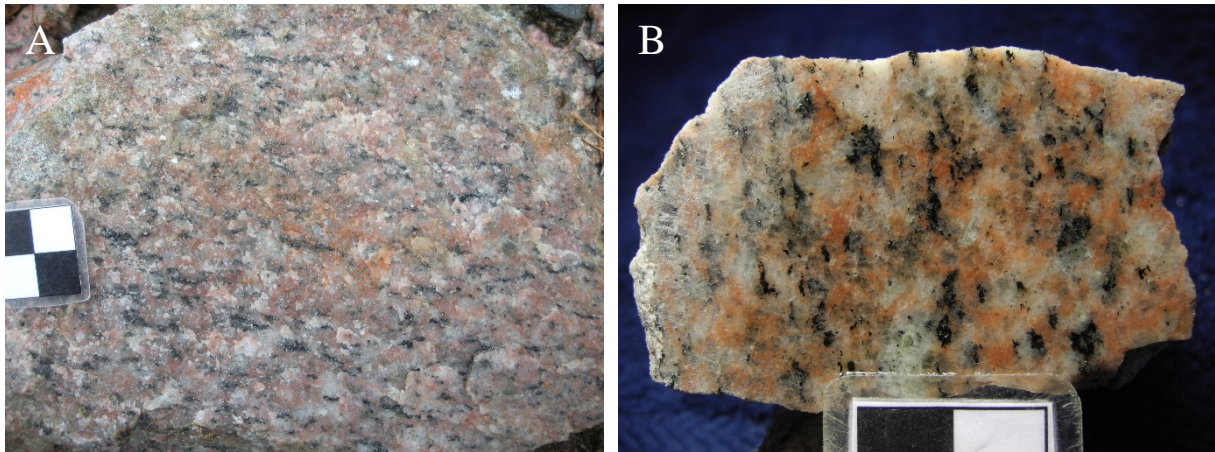


Figure 107. A. Granite to quartz monzonite, outcrop adjacent to sampling site of DCL110174A. B. Cut and wetted sample of granite (cm-scale). Photos: Dick Claeson.

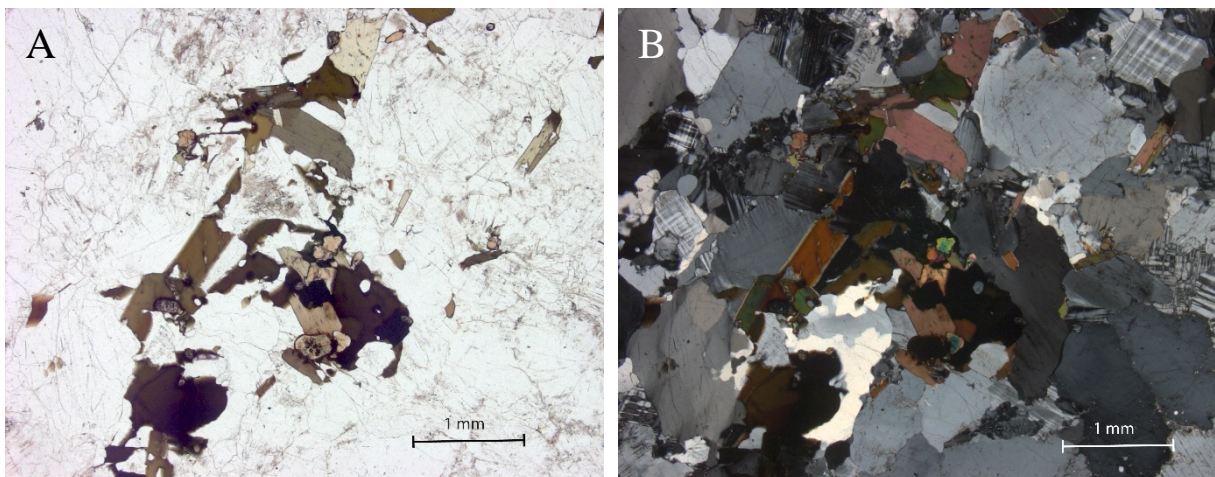


Figure 108. A. Potassium feldspar, plagioclase, quartz, biotite, and Fe-Ti oxide, plane-polarized light. B. Crossed nicols of same view. Micrographs: Dick Claeson.

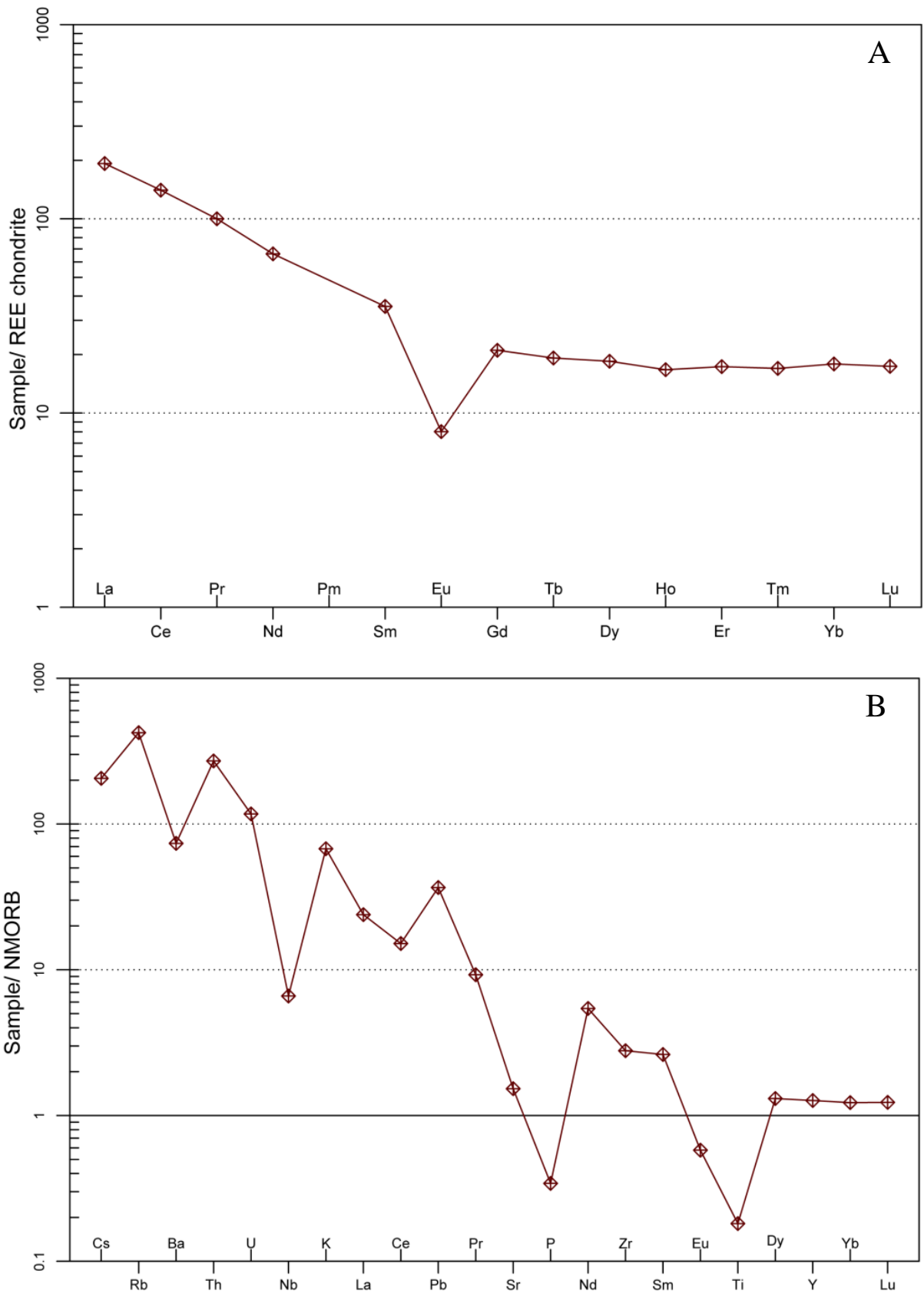


Figure 109. A. REE-diagram of granite to quartz monzonite. Normalizing values for chondrite from Boynton (1984). **B.** Multi-element diagram, rock as in A. Normalizing values for N-MORB from Sun & McDonough (1989).

Analytical results and interpretation of geochronological data

Zircon were obtained from a density separate of a crushed rock sample using a Wilfley water table. The magnetic minerals were removed by a hand magnet. Handpicked crystals were mounted in transparent epoxy resin together with chips of reference zircon 91 500. The zircon mounts were polished and after gold coating examined by Back-Scattered Electron (BSE) imaging, using standard electron microscopy at the Evolutionary Biology Centre (EBC), Uppsala University. High-spatial resolution secondary ion mass spectrometer (SIMS) analysis was done in December 2012 using a Cameca IMS 1 270 at the Nordsim facility at the Swedish Museum of Natural History in Stockholm. Detailed descriptions of the analytical procedures are given in Whitehouse et al. (1997, 1999).

Pb/U ratios, elemental concentrations and Th/U ratios were calibrated relative to the Geostandards zircon 91 500 reference, which has an age of c. 1 065 Ma (Wiedenbeck et al. 1995, 2004). Common Pb corrected isotope values were calculated using modern common Pb composition (Stacey & Kramers 1975) and measured ^{204}Pb . Decay constants follow the recommendations of Steiger & Jäger (1977). Diagrams and age calculations of isotopic data were made using software Isoplot 4.15 (Ludwig 2012). BSE/CL-imaging was also done after SIMS-analyses at the Department of Geology, Uppsala University.

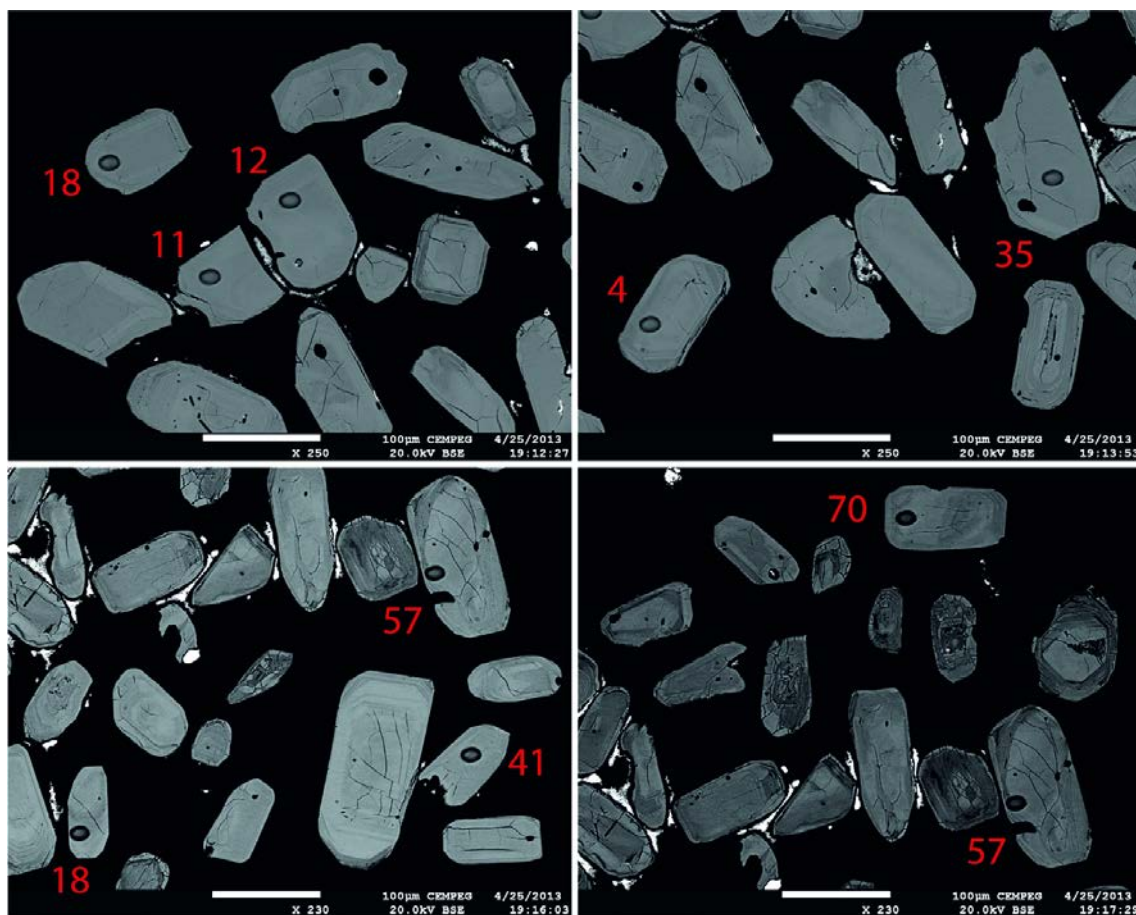


Figure 110. BSE-images of analysed zircon grains. Numbers refer to analytical spot number in Table 33.

The heavy mineral separate contains, subhedral zircon, mostly greyish turbid grains of poor analytical quality. BSE-images of the zircon show an internal oscillatory zonation, typical of magmatic zircon (Fig. 110). Microcracks are common in most grains and BSE-dark domains probably represent metamict zircon. The ten analyses are variable in uranium, 210–1 371 ppm, and show Th/U ratios at 0.19 to 0.32. Most analyses exhibit high values of common lead and are highly discordant (Table 33).

A discordia line through all analyses results in intercept ages at $1\,868 \pm 55$ Ma and 417 ± 180 Ma, with a poor fit indicated by a high MSWD of 15. Only one analysis is concordant at the 2σ limit, with a concordia age at $1\,881 \pm 15$ Ma (2σ , MSWD of concordance = 2.0, probability of concordance = 0.16). Including two 2.9 % and 3.6 % discordant analyses (35, 70), a weighted average $^{207}\text{Pb}/^{206}\text{Pb}$ age is calculated at $1\,881 \pm 30$ Ma (Fig. 111; 95 % confidence, MSWD = 3.4, probability = 0.033, $n = 3$). One of these analyses, No. 35, is slightly older than the others, possibly containing an inherited component and excluding that analysis the weighted average $^{207}\text{Pb}/^{206}\text{Pb}$ age is calculated at $1\,875 \pm 9$ Ma (2σ , MSWD = 0.013, probability = 0.91, $n = 2$). Although poorly constrained and based on only a few analyses it is suggested that the igneous crystallisation age of the granite is dated at c. 1.88 Ga.

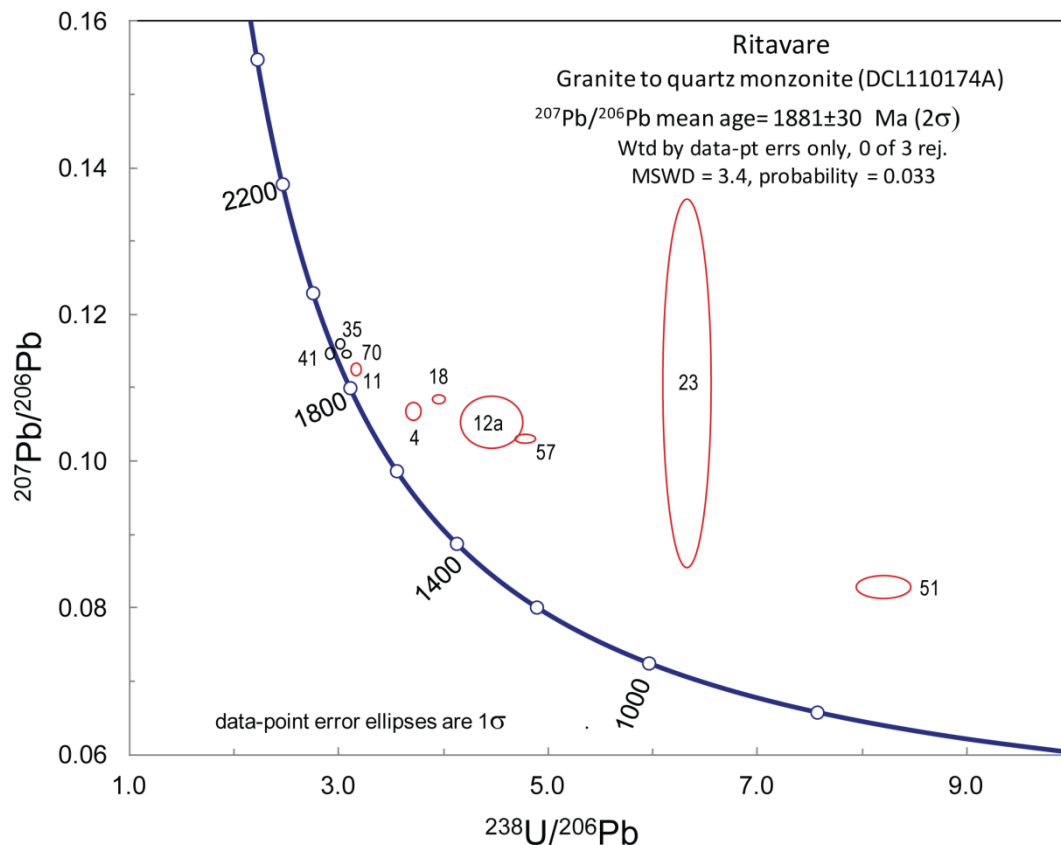


Figure 111. Tera-Wasserburg diagram showing U-Pb SIMS data of zircon analyses. Analyses used in age calculation are marked in black, excluded analyses in red.

Table 33. SIMS U-Pb-Th zircon data.

Sample/ spot #	U ppm	Th ppm	Pb ppm	Th/U calc ^{*1}	²⁰⁷ Pb		²⁰⁸ Pb		²³⁸ U		²⁰⁷ Pb		ρ	Disc. % conv. ^{*3}	²⁰⁷ Pb		²⁰⁶ Pb		²⁰⁶ Pb/ ²⁰⁴ Pb measured	f ₂₀₆ % ^{*4}
					²³⁵ U %	±σ	²³² Th %	±σ	²⁰⁶ Pb %	±σ	²⁰⁶ Pb %	±σ			²³⁸ U (Ma)	±σ	²³⁸ U (Ma)	±σ		
n4397-04	520	243	175	0.42	3.964	1.51	0.0815	3.4	3.714	1.30	0.1068	0.77	0.86	-13.4	1745	14	1537	18	4167	0.45
n4397-11	403	86	150	0.20	4.903	1.12	0.0902	4.5	3.163	0.99	0.1125	0.53	0.88	-4.3	1840	10	1771	15	13533	0.14
n4397-12	880	390	246	0.35	3.252	4.92	0.0709	8.8	4.464	4.41	0.1053	2.19	0.90	-26.7	1719	40	1303	52	893	2.09
n4397-18	791	329	247	0.35	3.781	1.03	0.0770	3.0	3.956	0.96	0.1085	0.35	0.94	-20.2	1774	6	1453	13	2385	0.78
n4397-23	1226	771	253	0.33	2.410	15.2	0.0494	24.3	6.326	2.38	0.1106	15.0	0.16	-51.2	1809	250	946	21	181	10.34
n4397-35	243	138	104	0.56	5.316	1.04	0.0972	4.1	3.010	0.97	0.1161	0.39	0.93	-2.9	1896	7	1849	16	155714	{0.01}
n4397-41	210	68	87	0.34	5.427	1.11	0.1011	3.0	2.914	1.01	0.1147	0.47	0.91	1.6	1875	8	1902	17	24898	0.08
n4397-51	1370	520	198	0.20	1.392	2.43	0.0333	6.2	8.205	2.07	0.0828	1.27	0.85	-43.8	1265	25	741	15	290	6.44
n4397-57	655	177	162	0.19	2.972	1.35	0.0623	3.2	4.781	1.29	0.1031	0.40	0.96	-29.7	1680	7	1224	14	3965	0.47
n4397-70	552	130	212	0.22	5.140	1.00	0.0917	3.7	3.075	0.96	0.1146	0.30	0.95	-3.6	1874	5	1815	15	6750	0.28

Isotope values are common Pb corrected using modern common Pb composition (Stacey & Kramers 1975) and measured ²⁰⁴Pb.

*1 Th/U ratios calculated from ²⁰⁸Pb/²⁰⁶Pb and ²⁰⁷Pb/²⁰⁶Pb ratios, assuming single stage of closed U-Th-Pb evolution.

*2 Error correlation in conventional concordia space. Do not use for Tera-Wasserburg plots.

*3 Age discordance in conventional concordia space. Positive numbers are reverse discordant.

*4 Figures in parentheses are given when no correction has been applied, and indicate a value calculated assuming present-day Stacey-Kramers common Pb.

Discussion and conclusion

The granite to quartz monzonite at Ritavare is more or less coeval with the folded, surrounding extrusive rocks at c. 1.88 Ga. The amphibolite facies metamorphic event that these rocks have been subjected to did not result in any secondary growth of zircon at this location (Fig. 110). The results were integrated in the mapping of the Tjåmotis SO area (Claeson & Antal Lundin *in press c*). Summary of sample data is given in Table 34.

Table 34. Summary of sample data.

Rock type	Granite to quartz monzonite
Lithotectonic unit	Norrbottnen lithotectonic unit of the Svecokarelian orogen
Lithological unit	
Sample number	DCL110174A
Lab_id	n4397
Coordinates	7418372/680995 (Sweref99TM)
Map sheet	27I Tjåmotis SO (RT90)
Locality	Ritavare
Project	Sydvästra Norrbotten (80025)

References

- Boynton, W.V., 1984: Cosmochemistry of the Rare Earth Elements: Meteorite studies. *In* P. Henderson (ed.): *Rare earth element geochemistry*. Elsevier Science B.V. 63–114.
- Claeson, D. & Antal Lundin, I., *in press*: Beskrivning till berggrundskartorna 27I Tjåmotis SV, SO. *Sveriges geologiska undersökning*.
- Ludwig, K.R., 2012: User's manual for Isoplot 3.75. A Geochronological Toolkit for Microsoft Excel. *Berkeley Geochronology Center Special Publication No. 5*, 75 pp.
- Smith, M.P., Storey, C.D., Jeffries, T.E., and Ryan, C., 2009. *In Situ* U–Pb and Trace Element Analysis of Accessory Minerals in the Kiruna District, Norrbotten, Sweden: New Constraints on the Timing and Origin of Mineralization. *Journal of Petrology* 50, 2 063–2 094.
- Stacey, J.S. & Kramers, J.D., 1975: Approximation of terrestrial lead isotope evolution by a two-stage model. *Earth and Planetary Science Letters* 26, 207–221.
- Steiger, R.H. & Jäger, E., 1977: Convention on the use of decay constants in geo- and cosmochronology. *Earth and Planetary Science Letters* 36, 359–362.
- Sun, S.S. & McDonough, W.F., 1989: Chemical and isotopic systematic of oceanic basalts: implications for mantle composition and processes. *In* A.D. Saunders & M.J. Norry (eds.): *Magmatism in ocean basins*. Geological Society of London, Special Publication 42, 313–345.
- Wanhainen, C., Billström, K., Martinsson, O., Stein, H. and Nordin, R., 2005: 160 Ma of magmatic/hydrothermal and metamorphic activity in the Gällivare area: Re–Os dating of molybdenite and U–Pb dating of titanite from the Aitik Cu–Au–Ag deposit, northern Sweden. *Mineralium Deposita*, 40, 435–447.
- Wanhainen, C., Broman, C. and Martinsson, O., 2003: The Aitik Cu–Au–Ag deposit in northern Sweden: a product of high salinity fluids. *Mineralium Deposita* 38, 715–726.
- Whitehouse, M.J., Claesson, S., Sunde, T. & Vestin, J., 1997: Ion-microprobe U–Pb zircon geochronology and correlation of Archaean gneisses from the Lewisian Complex of Gruinard Bay, north-west Scotland. *Geochimica et Cosmochimica Acta* 61, 4 429–4 438.
- Whitehouse, M.J., Kamber, B.S. & Moorbath, S., 1999: Age significance of U–Th–Pb zircon data from Early Archaean rocks of west Greenland: a reassessment based on combined ion-microprobe and imaging studies. *Chemical Geology (Isotope Geoscience Section)* 160, 201–224.
- Wiedenbeck, M., Allé, P., Corfu, F., Griffin, W.L., Meier, M., Oberli, F., Quadt, A.V., Roddick, J.C. & Spiegel, W., 1995: Three natural zircon standards for U–Th–Pb, Lu–Hf, trace element and REE analyses. *Geostandards Newsletter* 19, 1–23.
- Wiedenbeck, M., Hanchar, J.M., Peck, W.H., Sylvester, P., Valley, J., Whitehouse, M., Kronz, A., Morishita, Y., Nasdala, L., Fiebig, J., Franchi, I., Girard, J.P., Greenwood, R.C., Hinton, R., Kita, N., Mason, P.R.D., Norman, M., Ogasawara, M., Piccoli, P.M., Rhede, D., Satoh, H., Schulz-Dobrick, B., Skår, O., Spicuzza, M.J., Terada, K., Tindle, A., Togashi, S., Vennemann, T., Xie, Q. & Zheng, Y.F., 2004: Further Characterisation of the 91500 Zircon Crystal. *Geostandards and Geoanalytical Research* 28, 9–39.

U-Pb ZIRCON AGE DETERMINATION OF THE HÁRREVÁRDDO INTRUSION USING QUARTZ MONZONITE AT JERVAS, MAP SHEET 271 TJÅMOTIS SV, NORRBOTTEN COUNTY

Authors: Dick Claeson, Ildikó Antal Lundin & Fredrik Hellström

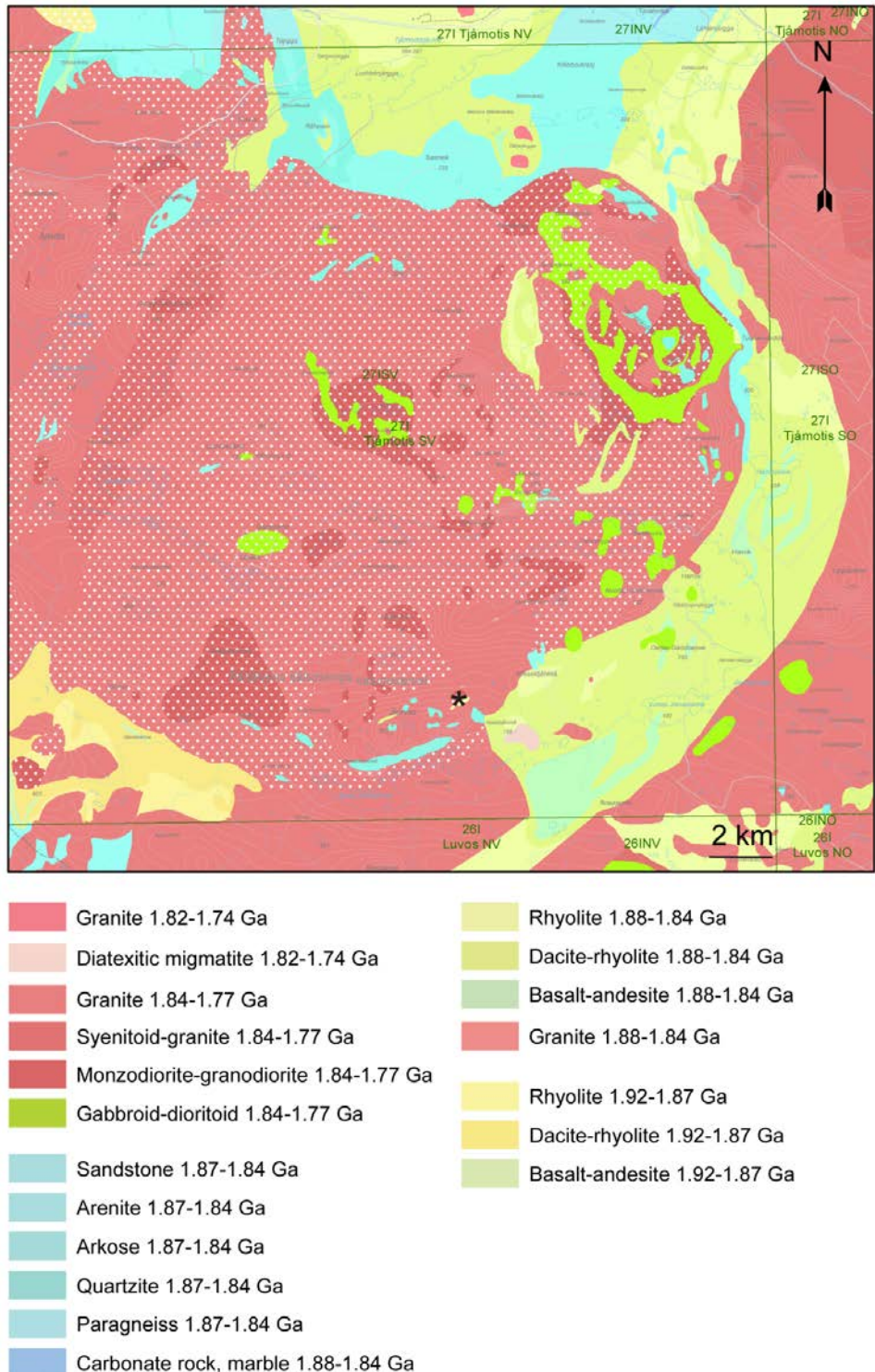


Figure 112. Bedrock map of the area, sampling location marked with black star.

Introduction

Norrbottn County, Sweden is a key area of Europe for future exploration and mining. The sampled rock is part of a large structure that is well-documented by the aeromagnetic data produced by the SGU. Both on magnetic- and gravity anomaly maps the structure is clearly seen as a more or less circular pattern. The large, circular magnetic anomaly that roughly occurs on the map area 27I Tjåmotis SV consists of multiple, coeval intrusions of bimodal magmatism, i.e., both basic rocks, gabbro to diorite and intermediate to acidic rocks from quartz monzodiorite, quartz monzonite, to granite (Fig. 112). These are intimately related with each other and there is no doubt based on field observations that all of these rock types are coeval (Antal Lundin et al. 2010, 2011, 2012a, 2012b, Claeson & Antal Lundin 2013, 2015). On the magnetic anomaly map (Fig. 113) the structure appears with varying levels of magnetization and the structure partly coincides with a moderate gravity surplus with small, internal variations (Antal Lundin et al. 2012a).

The geophysical signature suggests a circular but also complex built multiple intrusion, where the supracrustal rocks found in the area making the patterns even more complex. Within the large, nearly circular anomaly pattern, a smaller ring shaped positive magnetic anomaly having a diameter of about 4.5 km appears at Hárrevárddo. This, together with the variety of rocks with a large element of basic rocks within the smaller circular anomaly, shows that the more than 500 km² large, round structure consists of several intrusions and pulses of magmatism, but all of which are more or less of the same age. With the rocks outside the circular anomaly that are interpreted to be of the same age, the more or less coeval magmatism occupies more than 800 km². The best area to see most of the varieties of rocks within the large, circular anomaly and the multiple intrusive character is at Hárrevárddo and therefore it was named the Hárrevárddo intrusion (Claeson & Antal Lundin *in press c*). The outcrop at Jervas is located in a remote part of the Norrbotten County that lacks roads and we were transported to the area of interest by helicopter for regular bedrock mapping.

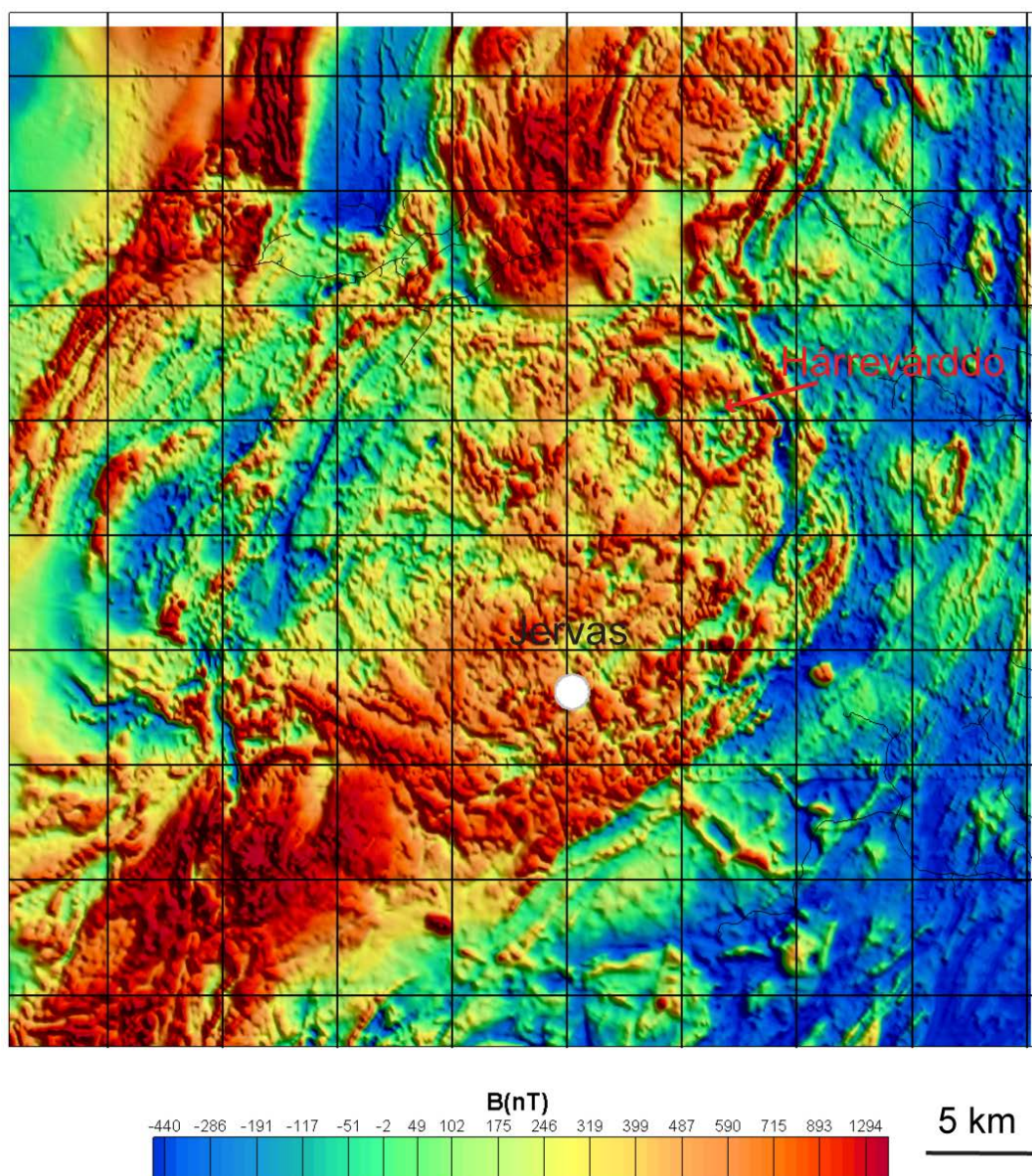


Figure 113. Magnetic anomaly map, reduced to the pole with apparent circular structure, map sheet 27I Tjåmotis SV with surroundings. The white dot shows the sample location.

New age results from the Ahmavaara during work in the map area 27K Nattavaara (Claeson & Antal Lundin 2012), west of the Boliden mine Aitik, show that a large 1.80 Ga intrusion, earlier thought to belong to the 1.88–86 Ga Perthite monzonite suite (Witschard 1996), is situated next to the mine and there was no knowledge of this prior to the SGU dating effort (Claeson et al. this issue). This may be of huge significance for the interpretation of the genesis of an ore body/deposit, where multiple episodes of concentration of sulphides are indicated in recent work at e.g. Aitik (Wanhainen et al. 2003, 2005) or in iron oxide–copper–gold (IOCG) mineralisation in this region (Smith et al. 2009). If these 1.80 Ga intrusions (or younger) are in any way involved in the genesis of the formation of economic deposits on a regional scale in the Norrbotten county, by re-heating the crust and producing hydrothermal activity in volcanic rocks or structural zones, their age should be determined in order to get a fundamental understanding of the younger intrusions spatial distribution. But we believe this is a field for future research. The size of the

sampled anomaly on the aeromagnetic map indicate that if this intrusion has played any role in producing economically interesting deposits, it may be on the scale of the entire map sheet 27I Tjåmotis SV, knowledge about the age is consequently paramount.

Further, a more speculative hypothesis that could be tested by the dating of this sample; is it possible that the pattern seen further to the south in the Transscandinavian Igneous Belt (TIB, e.g. Gorbatshev & Bogdanova 1993) where in general magmatic ages are younger to the west, starting with minor exposed areas of rocks intruded at around 1.85 Ga in the east and several 1.80 Ga intrusions in the middle and mostly 1.70–1.65 Ga in the western parts of southern Sweden, most of the latter parts now referred to as the Eastern Segment (e.g. Berthelsen 1980) of the Sveconorwegian orogen. No rocks in this part of Sweden (southwestern Norrbotten), to the knowledge of the authors, are as young as the 1.70 Ga TIB rocks further south. The location of this sample is close to as far west as you get before the Scandinavian Caledonides appear. Work has been done in northwestern Norway, where TIB-rocks are suggested to emerge through windows in the Caledonian nappes, which resulted in ages around 1.80–1.77 and 1.72–1.70 Ga (Romer et al. 1992).

The aim of this study is to determine the magmatic age of the quartz monzonite and thus the age of the major structure in the map area 27I Tjåmotis SV. Are these rocks 1.80 Ga or are they 1.88–1.86 Ga rocks or may they even be part of a more westerly, younger suite of rocks, possibly 1.72–1.7 Ga?

Sample description

The sampled outcrop is located at Jervas, some 23.5 km SSW of Tjåmotis. The sample consists of quartz monzonite associated with granite, monzonite, quartz monzodiorite, and monzodiorite that is undeformed. The rock is well-preserved, massive, grey, and varies from medium-grained to coarse-grained (Fig. 114, 115). The quartz monzonite is uneven-grained to porphyritic with potassium feldspar 10–20 mm (0–3 %). The potassium feldspar shows Carlsbad twinning and phenocrysts have inclusions of plagioclase (Fig. 115). Plagioclase shows minor sericite alteration and minor blobs of myrmekite are present (Fig. 115). Amphibole and biotite are present in the groundmass at 6 and 3 %, respectively. Magmatic amphibole is pleochroic, dark to light green and biotite brownish coloured. Quartz shows weakly developed undulose extinction. Accessory minerals are opaque minerals, mostly magnetite and not many sulphide mineral grains, apatite, and small zircon. Magnetic susceptibility at the outcrop varies between 2 210 and 6 300 $\times 10^{-5}$ SI. Petrophysical measurements show density at 2 742 kg/m³, magnetic susceptibility 5 951 $\times 10^{-5}$ SI, and remanent magnetization intensity of 590 mA/m. Gamma ray measured at the outcrop shows K = 4.8–5.2 %, U = 5.4–6.6 ppm, and Th = 2–2.6 ppm. The Zr content of the rock is 1 030 ppm and large zircon are easily found in thin-section.

The quartz monzonite at Jervas shows a LREE-enriched and flat HREE pattern, with a pronounced negative Eu anomaly (Fig. 116). The LREE enrichment is due to fractional crystallisation, the flat, unfractionated HREE pattern shows that no garnet was left in the residue at the location of magma genesis, and the Eu anomaly is indicative of extensive plagioclase fractionation. The negative anomalies shown in the multi-element diagram of Sr and Eu are due to plagioclase fractionation, the P anomaly of apatite fractionation, and the Ti anomaly of Fe-Ti oxide fractionation (Fig. 116). The strong negative Nb anomaly may suggest a subduction related petrogenesis but the negative Pb anomaly indicates that possibly less subducted sediment was involved in their petrogenesis compared with typical lithochemical signatures of arc magmas (Fig. 116).

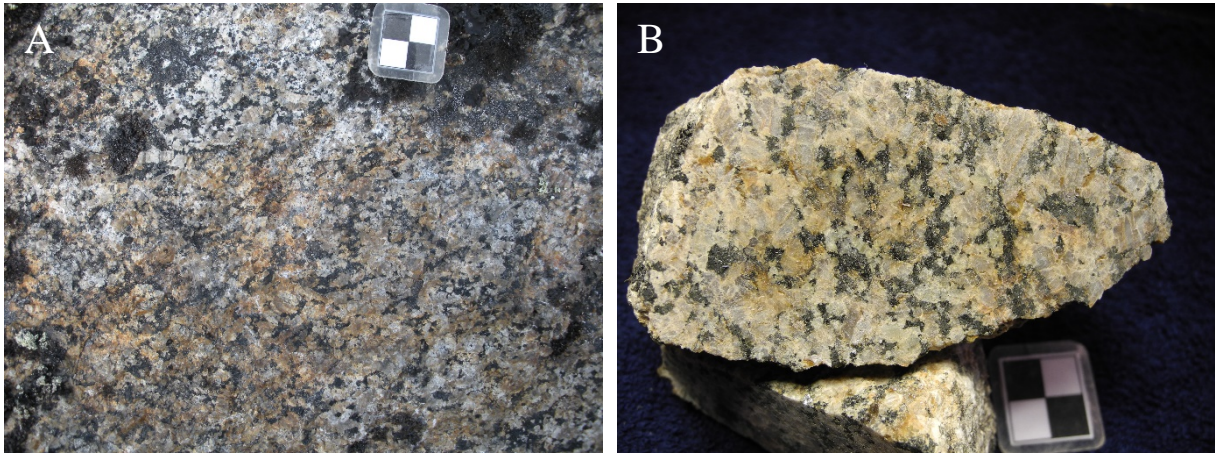


Figure 114. A. Quartz monzonite, outcrop adjacent to sampling site (cm-scale). **B.** Cut sample of quartz monzonite. Photos: Dick Claeson.

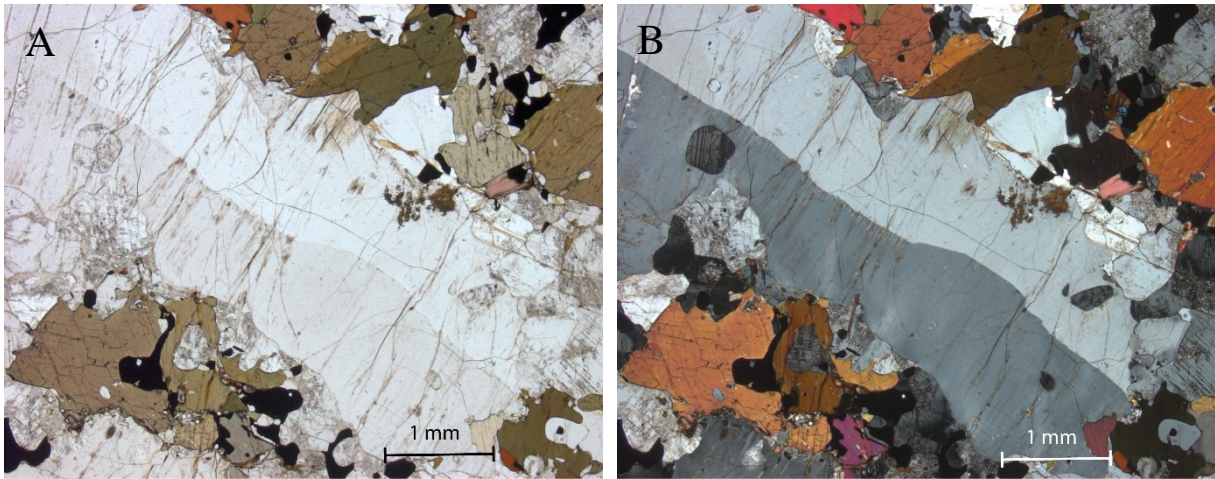


Figure 115. A. Potassium feldspar phenocryst with inclusions of plagioclase in quartz monzonite, with matrix amphibole, biotite, and Fe-Ti oxide, plane-polarized light. **B.** Crossed nicols of same view. Micrographs: Dick Claeson.

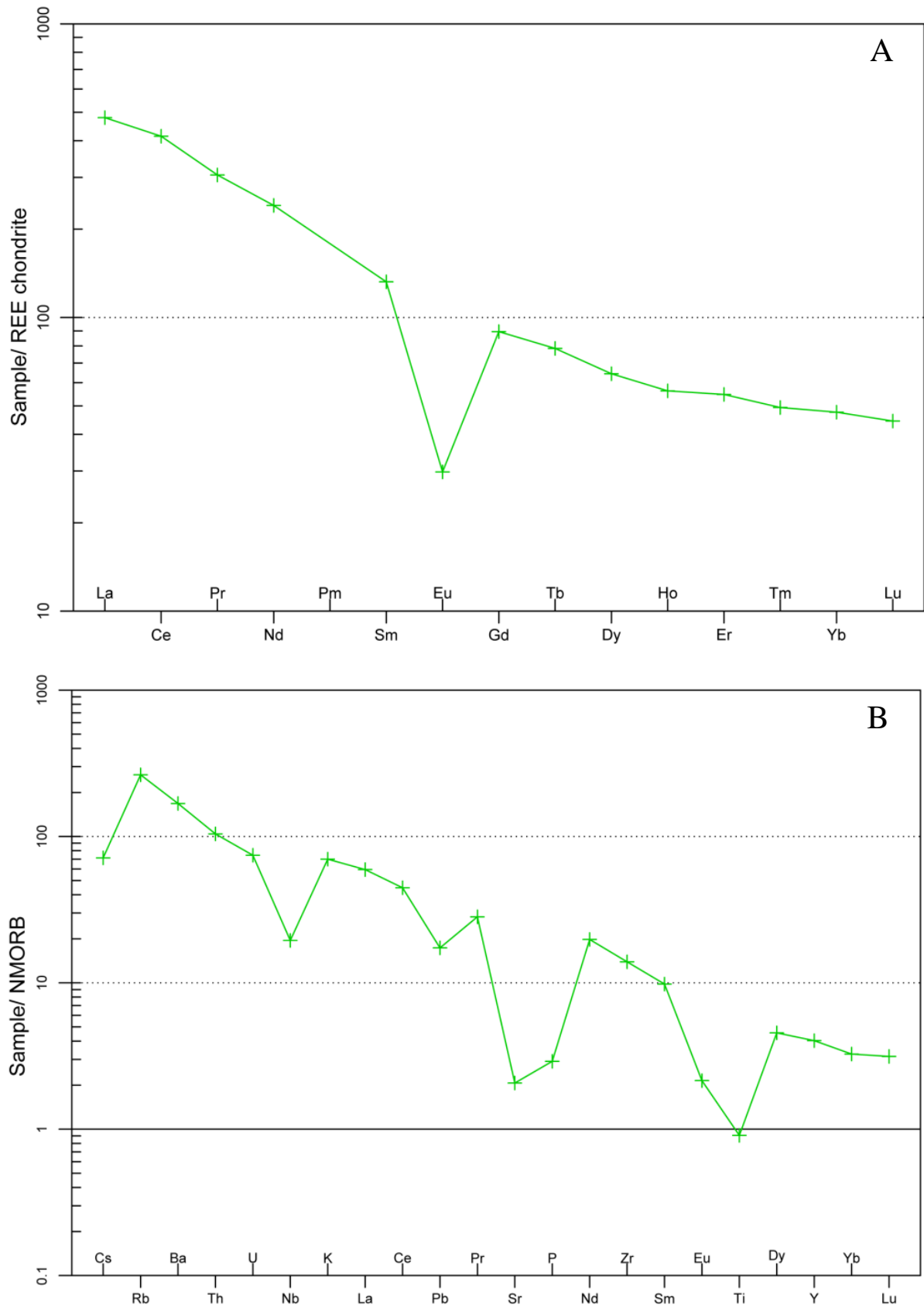


Figure 116. A. REE-diagram of quartz monzonite. Normalizing values for chondrite from Boynton (1984). **B.** Multi-element diagram, rock as in A. Normalizing values for N-MORB from Sun & McDonough (1989).

Analytical results and interpretation of geochronological data

U-Pb-Th SIMS analysis of zircon was performed using a Cameca IMS 1 270 at the Nordsim facility at the Museum of Natural History in November 2011. Detailed descriptions of the analytical procedures are given in Whitehouse et al. (1997, 1999). Pb/U ratios, elemental concentrations and Th/U ratios were calibrated relative to the Geostandards zircon 91 500 reference, which has an age of c. 1 065 Ma (Wiedenbeck et al. 1995, 2004). Common Pb corrected isotope values were calculated using modern common Pb composition (Stacey & Kramers 1975) and measured ^{204}Pb . Decay constants follow the recommendations of Steiger & Jäger (1977). Diagrams and age calculations of isotopic data were made using software Isoplot 4.15 (Ludwig 2012).

The analytical results are shown in Table 35. The heavy mineral concentrate from 475 g of processed sample contains abundant clear, colourless subhedral to euhedral zircon, but there are also turbid grains, especially in the coarser fractions. BSE-images show an internal oscillatory zonation in the zircon, interpreted as a magmatic growth zonation (Fig. 117). Most grains are BSE-dark in the centre with lighter coloured outer domains.

The zircon U content varies between 45 and 510 ppm. Core and rim analyses of grain No. 4 show distinctly higher Th/U ratios from 0.96 to 1.10, compared to the rest of the analyses that record Th/U ratios between 0.23 and 0.59 (Table 35). The concordant analyses from this grain (4, 4b) show a much older age, with apparent $^{207}\text{Pb}/^{206}\text{Pb}$ ages at about 1.98 Ga. Four of the analyses (10, 15, 21r, 22r) are discordant at the 2σ level, the other 17 analyses are near concordant, with a concordia age of $1\,784 \pm 5$ (MSWD of concordance = 14; probability of concordance = 0.000) and a $^{207}\text{Pb}/^{206}\text{Pb}$ weighted mean age of $1\,781 \pm 4$ Ma (MSWD = 0.79, probability = 0.70).

Analyses that are less than 3.0 % discordant give a concordia age of $1\,784 \pm 4$ Ma (Fig. 118; MSWD = 4.7 probability of concordance = 0.031) and a $^{207}\text{Pb}/^{206}\text{Pb}$ weighted mean age of $1\,782 \pm 5$ Ma (MSWD = 0.64, probability = 0.82). The concordia age of $1\,784 \pm 4$ Ma is chosen as the best age estimate of igneous crystallisation of the quartz monzonite at Jervas. The older age of the zircon grain No. 4, suggest that this grain probably is inherited from the source rock.

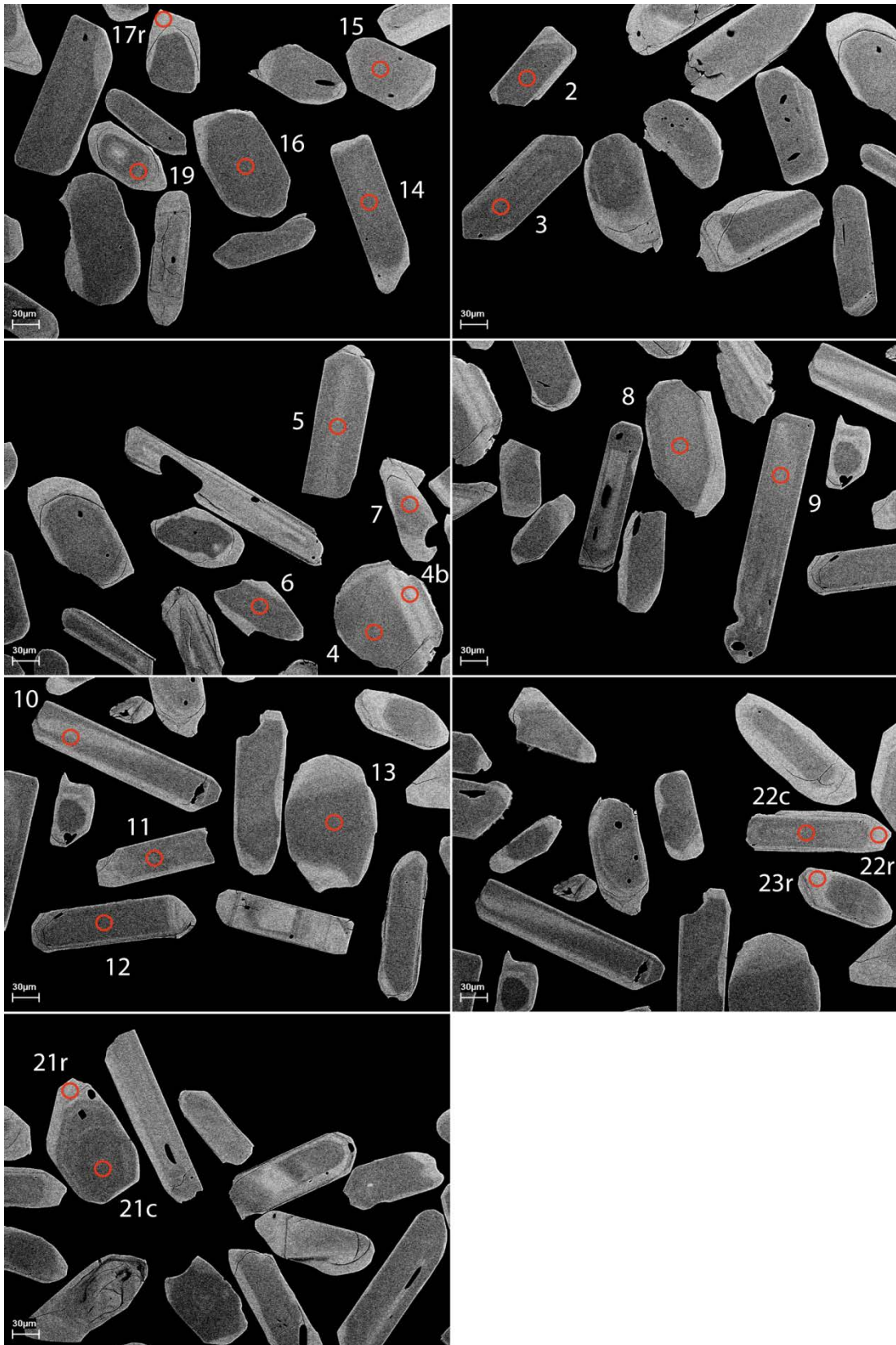


Figure 117. BSE-images of zircon grains with the approximate location of spot analyses marked. Numbers refer to analytical spot number in Table 35.

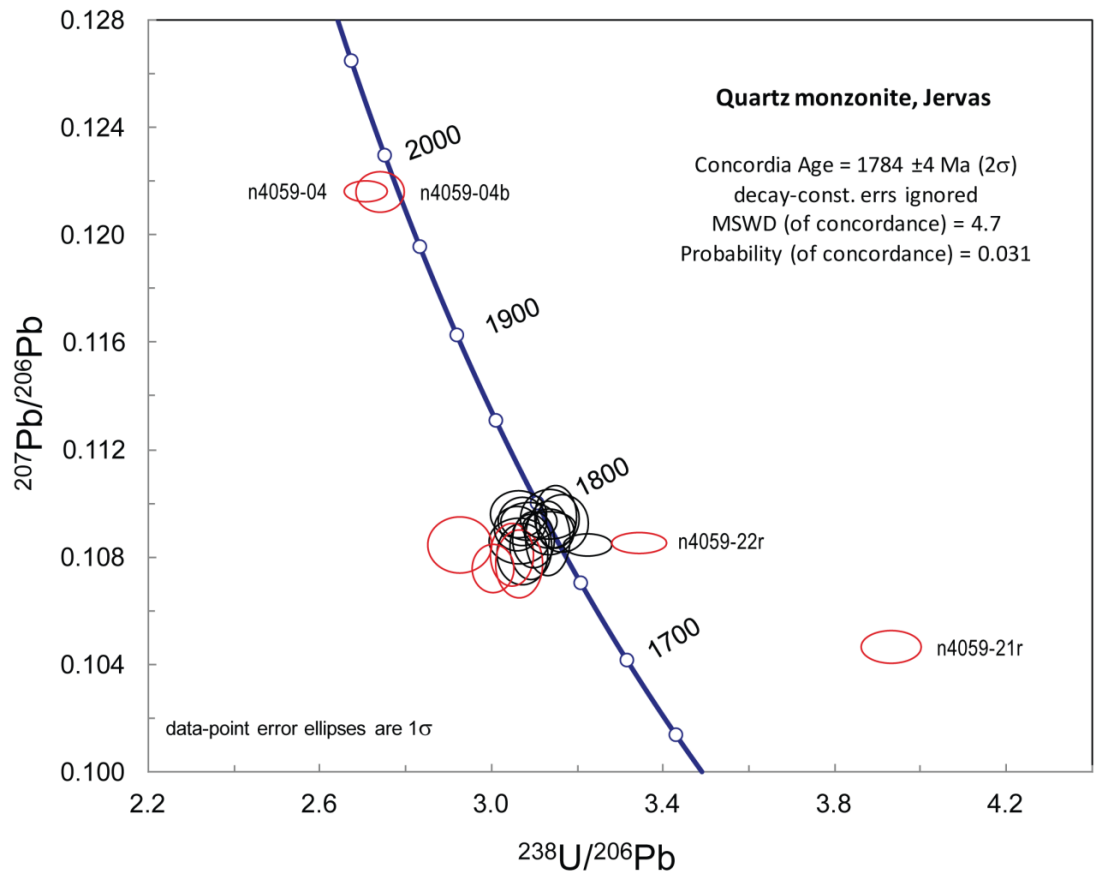


Figure 118. Tera-Wasserburg diagram showing U-Pb SIMS zircon data from quartz monzonite at Jervas. Analyses used for age calculation are shown in black.

Table 35. SIMS U-Pb-Th zircon data.

Sample/ spot #	U ppm	Th ppm	Pb ppm	Th/U calc ^{*1}	²⁰⁷ Pb ²³⁵ U	±σ %	²⁰⁸ Pb ²³² Th	±σ %	²³⁸ U ²⁰⁶ Pb	±σ %	²⁰⁷ Pb ²⁰⁶ Pb	±σ %	ρ *2	Disc. % conv. *3	²⁰⁷ Pb ²⁰⁶ Pb	±σ (Ma)	²⁰⁶ Pb ²³⁸ U	±σ (Ma)	²⁰⁶ Pb/ ²⁰⁴ Pb measured	f ₂₀₆ % *4
n4059-02	91	49	38	0.56	4.885	1.62	0.0958	3.8	3.065	1.53	0.1086	0.53	0.95	2.9	1776	10	1820	24	86017	{0.02}
n4059-03	59	27	24	0.49	4.833	1.27	0.0982	7.3	3.092	1.03	0.1084	0.75	0.81	2.2	1772	14	1807	16	46095	{0.04}
n4059-04	478	438	245	0.96	6.196	1.23	0.1079	3.6	2.707	1.21	0.1216	0.21	0.99	2.7	1980	4	2027	21	169398	0.01
n4059-04b	131	137	68	1.10	6.120	1.42	0.1083	3.6	2.739	1.36	0.1216	0.4	0.96	1.5	1980	7	2006	23	>1e6	{0.00}
n4059-05	107	57	43	0.55	4.759	1.42	0.0959	4.1	3.164	1.26	0.1092	0.65	0.89	-1.0	1787	12	1770	20	101088	{0.02}
n4059-06	58	25	23	0.43	4.810	1.58	0.0943	4.1	3.137	1.43	0.1094	0.67	0.91	-0.4	1790	12	1784	22	60006	{0.03}
n4059-07	95	35	38	0.39	4.934	1.52	0.0979	3.7	3.063	1.42	0.1096	0.52	0.94	1.8	1793	9	1821	23	61568	{0.03}
n4059-08	77	32	30	0.44	4.785	1.40	0.0967	5.0	3.131	1.12	0.1087	0.84	0.8	0.6	1777	15	1787	17	75943	{0.02}
n4059-09	145	67	59	0.48	4.883	1.48	0.0967	3.7	3.088	1.41	0.1093	0.43	0.96	1.3	1788	8	1809	22	69554	{0.03}
n4059-10	83	43	36	0.54	5.111	1.79	0.0953	3.8	2.926	1.68	0.1084	0.63	0.94	7.9	1774	11	1895	28	492613	{0.00}
n4059-11	121	50	48	0.42	4.907	1.32	0.0960	3.6	3.072	1.20	0.1093	0.55	0.91	1.8	1788	10	1817	19	46541	0.04
n4059-12	88	43	35	0.51	4.793	1.24	0.0968	3.7	3.150	1.03	0.1095	0.69	0.83	-0.9	1791	13	1777	16	46746	0.04
n4059-13	57	32	24	0.59	4.852	1.46	0.0960	3.7	3.072	1.29	0.1081	0.68	0.88	3.2	1768	12	1817	20	86311	{0.02}
n4059-14	94	47	39	0.54	4.892	1.29	0.0992	3.8	3.047	1.08	0.1081	0.71	0.84	4.0	1768	13	1830	17	31730	0.06
n4059-15	83	44	35	0.58	4.938	1.18	0.1006	3.6	3.003	1.04	0.1076	0.56	0.88	6.2	1759	10	1853	17	89058	{0.02}
n4059-16	46	21	19	0.50	4.849	1.42	0.0978	3.8	3.063	1.18	0.1077	0.78	0.83	3.9	1762	14	1821	19	17953	0.10
n4059-17r	442	121	167	0.25	4.803	1.30	0.0852	3.7	3.134	1.26	0.1092	0.3	0.97	0.0	1786	5	1785	20	4893	0.38
n4059-19	121	39	48	0.35	4.915	1.25	0.0990	3.6	3.059	1.15	0.1091	0.49	0.92	2.5	1784	9	1823	18	64017	{0.03}
n4059-21c	61	34	25	0.58	4.836	1.23	0.0966	3.6	3.098	1.06	0.1087	0.63	0.86	1.7	1777	12	1803	17	161314	{0.01}
n4059-21r	510	173	156	0.29	3.669	1.24	0.0749	3.6	3.933	1.17	0.1046	0.39	0.95	-16.2	1708	7	1460	15	7278	0.26
n4059-22c	102	42	40	0.43	4.791	1.34	0.0964	5.3	3.135	1.24	0.1089	0.51	0.93	0.2	1782	9	1785	19	51874	{0.04}
n4059-22r	497	122	175	0.23	4.474	1.26	0.0854	3.6	3.345	1.24	0.1085	0.23	0.98	-5.7	1775	4	1686	18	46982	0.04
n4059-23r	493	130	181	0.27	4.638	1.16	0.0925	3.5	3.224	1.13	0.1085	0.25	0.98	-2.1	1774	5	1742	17	83635	0.02

Isotope values are common Pb corrected using modern common Pb composition (Stacey & Kramers 1975) and measured ²⁰⁴Pb.

*1 Th/U ratios calculated from ²⁰⁸Pb/²⁰⁶Pb and ²⁰⁷Pb/²⁰⁶Pb ratios, assuming single stage of closed U-Th-Pb evolution.

*2 Error correlation in conventional concordia space. Do not use for Tera-Wasserburg plots.

*3 Age discordance in conventional concordia space. Positive numbers are reverse discordant.

*4 Figures in parentheses are given when no correction has been applied, and indicate a value calculated assuming present-day Stacey-Kramers common Pb.

Discussion and conclusion

The igneous crystallisation age of $1\,784 \pm 4$ Ma of the quartz monzonite at Jervas also determines the age of the Hárrevárddo intrusion. The Hárrevárddo intrusion comprise a Paleoproterozoic late-Orosirian to early-Statherian magmatism that will in future research be used as a case study, that allows us to study magmatic processes and pluton growth without major subsequent tectonic activity from that era.

The results show that even though the Hárrevárddo intrusion is among the youngest Svecokarelian intrusions in the area, it belongs to the older 1.80–1.77 Ga and not a 1.72–1.70 Ga younger generation (cf. Romer et al. 1992).

The older age of the zircon grain No. 4, suggest that this grain probably is inherited, either from the source rock or assimilation early on en route to higher levels within the crust or from some completely dissolved host rock at the level of emplacement.

The results were integrated in the mapping of the 27I Tjåmotis SV, SO area (Claeson & Antal Lundin *in press c*). Summary of sample data is given in Table 36.

Table 36. Summary of sample data.

Rock type	Quartz monzonite
Lithotectonic unit	Norrbottnen lithotectonic unit of the Svecokarelian orogen
Lithological unit	
Sample number	DCL100081A
Lab_id	n4059
Coordinates	7403249/650222 (Sweref99TM)
Map sheet	27I Tjåmotis SV (RT90)
Locality	Jervas/Hárrevárddo intrusion
Project	Sydvästra Norrbotten (80025)

References

- Antal Lundin, I., Claeson, D. & Hellström, F., 2011: Sydvästra Norrbotten, berg. *In* S. Lundqvist (ed.): *Sammanfattning av pågående verksamhet 2010. Berggrundsgeologisk undersökning. Sveriges geologiska undersökning SGU-rapport 2011:6*, 86–105.
- Antal Lundin, I., Claeson, D., Hellström, F. & Berggren, L., 2012a: Berggrundsgeologisk undersökning, sydvästra Norrbotten. Sammanfattning av pågående verksamhet 2011. *Sveriges geologiska undersökning SGU-rapport 2012:3*, 34 pp.
- Antal Lundin, I., Claeson, D., Hellström, F. & Berggren, L., 2012b: Berggrundsgeologisk undersökning, sydvästra Norrbotten. Sammanfattning av pågående verksamhet 2012. *Sveriges geologiska undersökning SGU-rapport 2012:21*, 44 pp.
- Antal Lundin, I., Claeson, D., Hellström, F. & Kero, L., 2010: Sydvästra Norrbotten. *In* H. Delin (ed.): *Berggrundsgeologisk undersökning. Sammanfattning av pågående verksamhet 2009. Sveriges geologiska undersökning SGU-rapport 2010:2*, 43–69.
- Berthelsen, A., 1980: Towards a palinspastic tectonic analysis of the Baltic shield. *International Geological Congress Colloque C6*, 5–21.
- Boynton, W.V., 1984: Cosmochemistry of the Rare Earth Elements: Meteorite studies. *In* P. Henderson (ed.): *Rare earth element geochemistry*. Elsevier Science B.V. 63–114.
- Claeson, D. & Antal Lundin, I., 2012: Beskrivning till berggrundskartorna 27K Nattavaara NV, NO, SV & SO. *Sveriges geologiska undersökning K 383–386*, 22 pp.
- Claeson, D. & Antal Lundin, I., 2013: Berggrundsgeologisk undersökning, sydvästra Norrbotten. Sammanfattning av pågående verksamhet 2013. *Sveriges geologiska undersökning SGU-rapport 2013:18*, 27 pp.
- Claeson, D. & Antal Lundin, I., 2015: Berggrundsgeologisk undersökning, sydvästra Norrbotten. Sammanfattning av pågående verksamhet 2014. *Sveriges geologiska undersökning SGU-rapport 2015:03*, 32 pp.
- Claeson, D. & Antal Lundin, I., *in press c*: Beskrivning till berggrundskartorna 27I Tjåmotis SV, SO. *Sveriges geologiska undersökning*.
- Gorbatshev, R. & Bogdanova, S., 1993: Frontiers in the Baltic Shield. *Precambrian Research* 64, 3–21.
- Ludwig, K.R., 2012: User's manual for Isoplot 3.75. A Geochronological Toolkit for Microsoft Excel. *Berkeley Geochronology Center Special Publication No. 5*, 75 pp.
- Romer, R.L., Kjösnæs, B., Korneliussen, A., Lindahl, I., Skyseth, T., Stendal, M. & Sundvoll, B., 1992: The Archean-Proterozoic boundary beneath the Calidonides of northern Norway and Sweden: U-Pb, Rb-Sr and ϵ Nd isotope data from the Rombak-Tysfjord area: *NGU Rapport 91.225*, 68 pp.
- Smith, M.P., Storey, C.D., Jeffries, T.E., & Ryan, C., 2009: *In Situ* U–Pb and Trace Element Analysis of Accessory Minerals in the Kiruna District, Norrbotten, Sweden: New Constraints on the Timing and Origin of Mineralization. *Journal of Petrology* 50, 2 063–2 094.
- Stacey, J.S. & Kramers, J.D., 1975: Approximation of terrestrial lead isotope evolution by a two-stage model. *Earth and Planetary Science Letters* 26, 207–221.

- Steiger, R.H. & Jäger, E., 1977: Convention on the use of decay constants in geo- and cosmochronology. *Earth and Planetary Science Letters* 36, 359–362.
- Sun, S.S. & McDonough, W.F., 1989: Chemical and isotopic systematic of oceanic basalts: implications for mantle composition and processes. In A.D. Saunders & M.J. Norry (eds.): *Magmatism in ocean basins*. Geological Society of London, Special Publication 42, 313–345.
- Wanhainen, C., Broman, C. & Martinsson, O., 2003: The Aitik Cu–Au–Ag deposit in northern Sweden: a product of high salinity fluids. *Mineralium Deposita* 38, 715–726.
- Wanhainen, C., Billström, K., Martinsson, O., Stein, H. & Nordin, R., 2005: 160 Ma of magmatic/hydrothermal and metamorphic activity in the Gällivare area: Re–Os dating of molybdenite and U–Pb dating of titanite from the Aitik Cu–Au–Ag deposit, northern Sweden. *Mineralium Deposita* 40, 435–447.
- Whitehouse, M.J., Claesson, S., Sunde, T. & Vestin, J., 1997: Ion-microprobe U–Pb zircon geochronology and correlation of Archaean gneisses from the Lewisian Complex of Gruinard Bay, north-west Scotland. *Geochimica et Cosmochimica Acta* 61, 4 429–4 438.
- Whitehouse, M.J., Kamber, B.S. & Moorbath, S., 1999: Age significance of U–Th–Pb zircon data from Early Archaean rocks of west Greenland: a reassessment based on combined ion-microprobe and imaging studies. *Chemical Geology (Isotope Geoscience Section)* 160, 201–224.
- Wiedenbeck, M., Allé, P., Corfu, F., Griffin, W.L., Meier, M., Oberli, F., Quadt, A.V., Roddick, J.C. & Spiegel, W., 1995: Three natural zircon standards for U–Th–Pb, Lu–Hf, trace element and REE analyses. *Geostandards Newsletter* 19, 1–23.
- Wiedenbeck, M., Hanchar, J.M., Peck, W.H., Sylvester, P., Valley, J., Whitehouse, M., Kronz, A., Morishita, Y., Nasdala, L., Fiebig, J., Franchi, I., Girard, J.P., Greenwood, R.C., Hinton, R., Kita, N., Mason, P.R.D., Norman, M., Ogasawara, M., Piccoli, P.M., Rhede, D., Satoh, H., Schulz-Dobrick, B., Skår, O., Spicuzza, M.J., Terada, K., Tindle, A., Togashi, S., Vennemann, T., Xie, Q. & Zheng, Y.F., 2004: Further Characterisation of the 91500 Zircon Crystal. *Geostandards and Geoanalytical Research* 28, 9–39.
- Witschard, F., 1996: Berggrundskartan 28K Gällivare SV. *Sveriges geologiska undersökning Ai* 100.

U-Pb ZIRCON AGE OF HOST QUARTZ TRACHYTE AT THE KALLAK IRON ORE DEPOSIT EAST OF BJÖRKHOLMEN, MAP SHEET 27I TJÅMOTIS SO, NORRBOTTEN COUNTY

Authors: Dick Claeson, Ildikó Antal Lundin, Per-Olof Persson¹ & George Morris

¹Department of Geosciences Swedish Museum of Natural History, Box 50 007, SE-104 05 Stockholm, Sweden

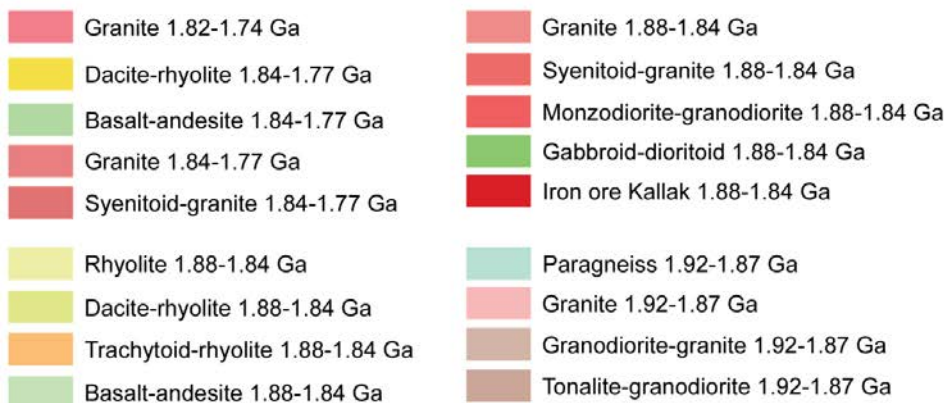
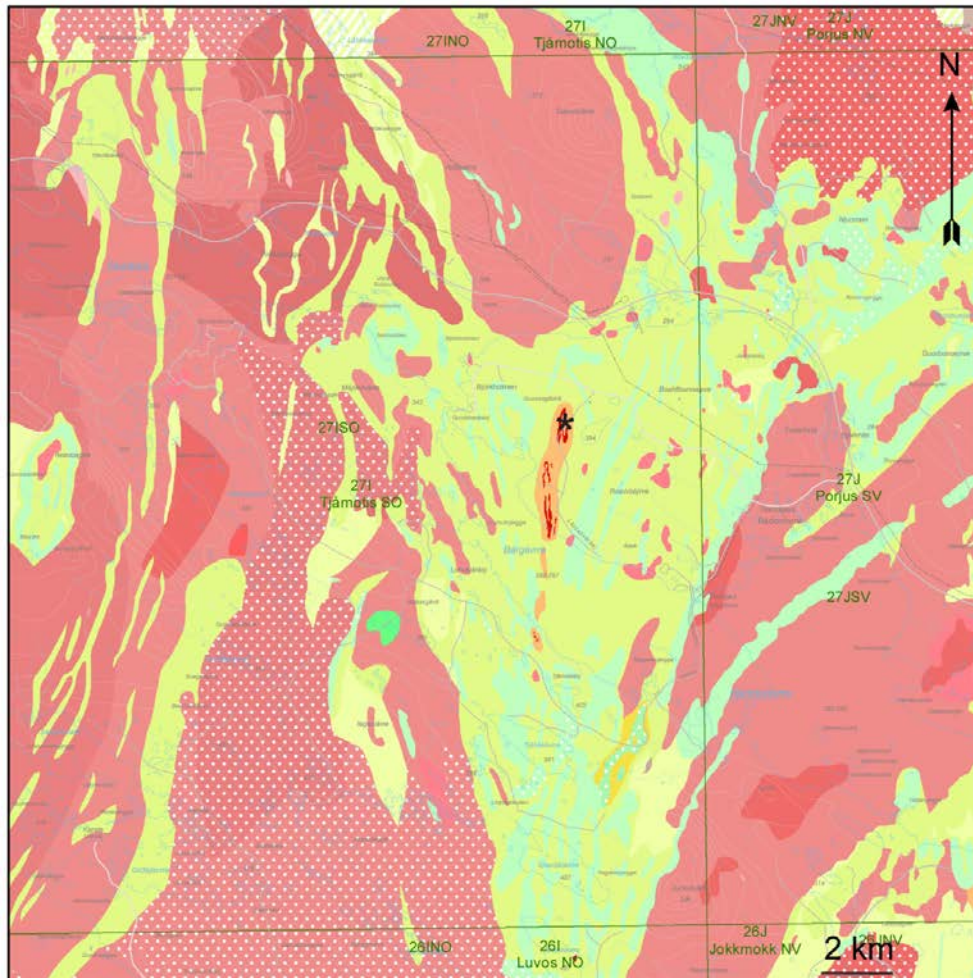


Figure 119. Bedrock map of the area, sampling location marked with black star.

Introduction

The Norrbotten County, Sweden is a key area of Europe for future exploration and mining. A north–south to north-northeast–south-southwest trending zone of iron mineralisations, hosted by supracrustal rocks is found within the map areas 27J Porjus NV, SV, 27I Tjåmotis SO, and 26I Luvos NO. The deposits at Kallak, Parkijaure, Akkihaure, and Åkosjegge are relatively well investigated and thus considered to be ore deposits whereas Pakko, Maivesvare, and Tjårovaratj are regarded as possible ore targets (Johansson 1980). Both Kallak and Åkosjegge are interpreted to occur associated with volcanic host rocks, the latter deposit in gneissic skarn rocks however, suggesting metasedimentary rock components as well. The sampled rock is part of the host rock of the iron ore deposit at Kallak, the latter seen as a distinctive high magnetic area in the magnetic data and on the gravity anomaly map (Fig. 103, 104).

In order to gain knowledge of when economic deposits are formed on a regional scale in the Norrbotten County the host rock at Kallak was chosen for age determination. Even the extent of magmatic induced metamorphism is of great importance, by re-heating the crust and producing hydrothermal activity in volcanic rocks, intrusive rocks or structural zones, or if regional metamorphic events are in any way involved, these ages should be determined.

The aim of this study is to determine the magmatic age of the quartz trachyte at the Kallak ore deposit in map area 27I Tjåmotis SO, and if there are any metamorphic overgrowths, determine these as well, since the latter might show ages for the redistribution of elements in the crust. Furthermore, age determinations of volcanic rocks in the region are scarce.

Sample description

The very magnetite-rich bedrock, ore at Kallak shows foliation and lineation, contain fragments of both felsic and mafic volcanic rocks and banding with the surrounding acid volcanic rock is obvious (Fig. 120). Structures were not measured because the very high magnetite content in the bedrock, which gives varying magnetic deviation, but a consistent lineation, dips southward. In connection with SGU fieldwork 2014, the trenches and blasted test pits done by Jokkmokk Iron Mines AB in the iron ore deposit at Kallak were visited (Fig. 120).

The acid volcanic rock found in the pits and trenches is a garnet-bearing quartz trachyte with empty or rusty amygdules. Smaller amounts of skarn consisting of amphibole, garnet, epidote, pink to orange calcite, and greenish apatite was found in both the quartz trachyte and the iron mineralisation. The volcanic quartz trachyte that was sampled at the trench for lithogeochemical analysis shows a high content of barium 2 350 ppm, possibly indicating that volcanic-hydrothermal processes have been active. There was also andesitoid volcanic rocks present at the trenches.

The sampled outcrop is one of the trenches mentioned above at Kallak. The sample consists of reddish grey to grey quartz trachyte that is very fine-grained to fine-grained. Sparse potassium feldspar phenocrysts occur, up to 2 mm in size, displaying amphibole and plagioclase inclusions and are not severely altered (Fig. 121). Potassium feldspar shows cross-hatched twinning. Plagioclase shows minor sericite alteration. Amphibole and biotite are present in the groundmass at 11 and 4 %, respectively. Amphibole is pleochroic, green to light green and pleochroic biotite is brownish red to pale yellow and green. Quartz shows undulose extinction. Accessory minerals are magnetite, garnet, apatite, and small zircon. Small garnets are present in the quartz trachyte and easily observed in thin-section (Fig. 121). The Zr content of the rock is 222 ppm. Foliation is pronounced even in thin-section. Magnetic susceptibility varies between 151 and $3\ 100 \times 10^{-5}$ SI. Petrophysical measurements of a sample show density at $2\ 742\ \text{kg/m}^3$, magnetic susceptibility 184×10^{-5} SI, and remanent magnetization intensity of 181 mA/m.

The quartz trachyte at Kallak shows a LREE-enriched and flat HREE pattern, with a negative Eu anomaly (Fig. 122). The LREE enrichment is due to fractional crystallisation, the flat, unfractionated HREE pattern shows that no garnet was left in the residue at the location of magma genesis, and the Eu anomaly is indicative of plagioclase fractionation. The negative anomalies shown in the multi-element diagram of Sr is due to plagioclase fractionation, the P anomaly of apatite fractionation, and the Ti anomaly of Fe-Ti oxide fractionation (Fig. 122). The strong negative Nb anomaly and positive Pb anomaly suggest a subduction related petrogenesis (Fig. 122).

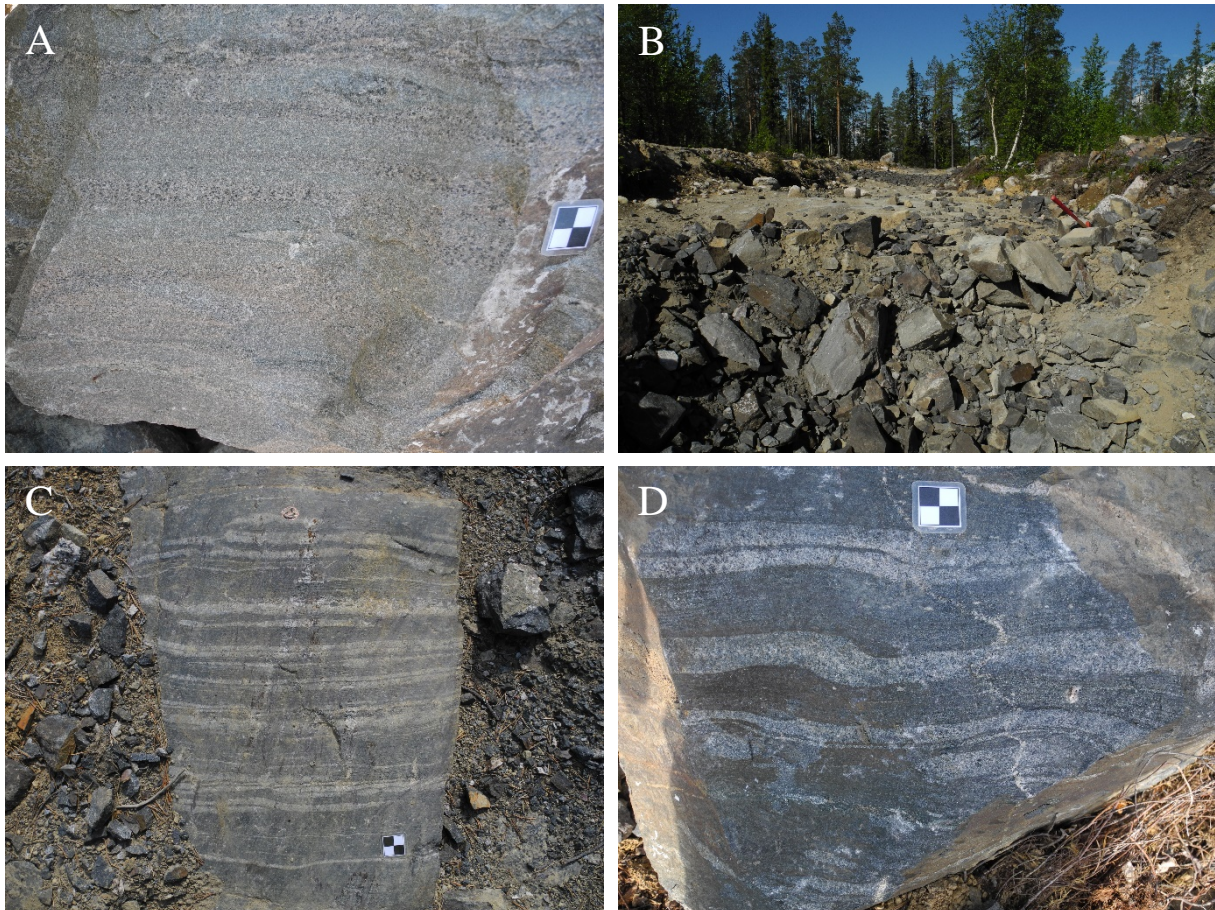


Figure 120. A. Close-up of the sampled quartz trachyte volcanic rock from the excavation trench at Kallak (7414247/681408). B. Excavation trench and test pits at Kallak. C. Outcrop of iron mineralisation at Kallak with bands of quartz trachyte in magnetite ore. D. Close-up of banding in millimetre- and centimetre scale, which is made up of magnetite-rich and quartz trachyte bands, respectively (cm-scale). Photos: Dick Claeson.

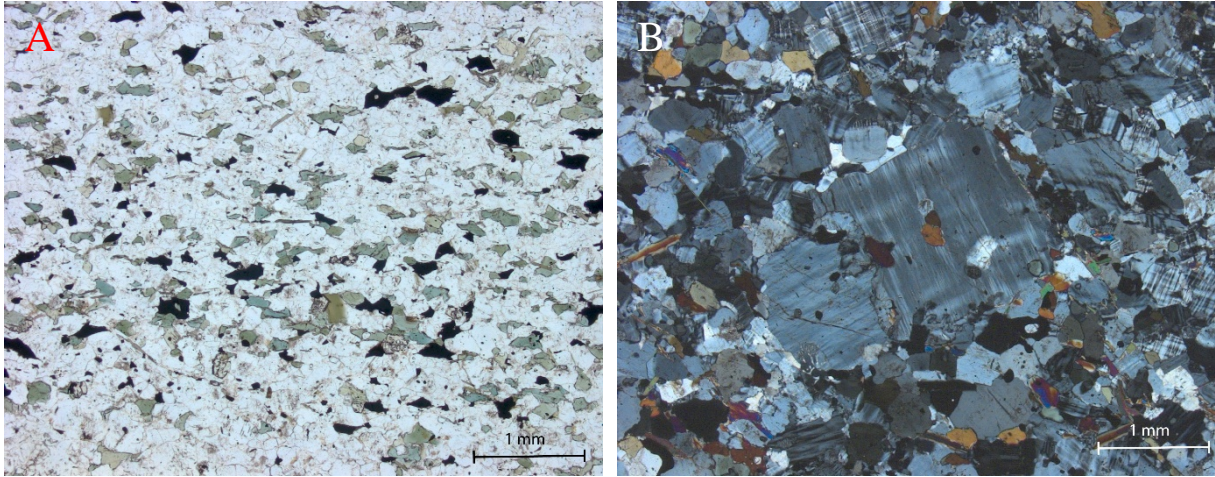


Figure 121. **A.** Up to 200 μm large garnet crystals in quartz trachyte, plane polarised light. **B.** Phenocrysts of potassium feldspar in quartz trachyte with inclusions of amphibole and plagioclase, crossed nicols. Micrographs: Dick Claeson.

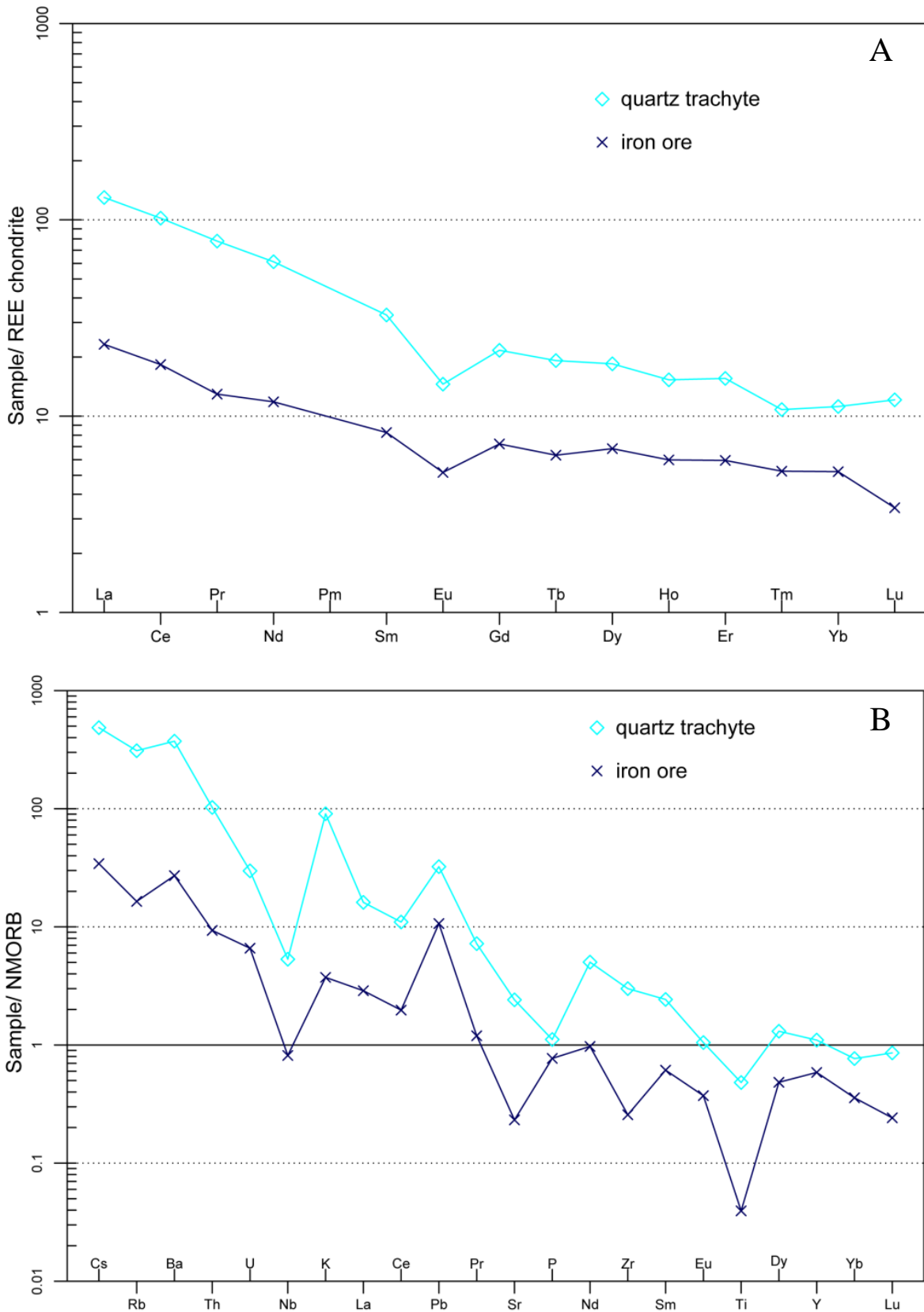


Figure 122. A. REE-diagram with data from lithochemical analyses of the host rock quartz trachyte and the iron ore at Kallak. Normalizing values for chondrite from Boynton (1984). **B.** Multi-element diagram, rocks as in A. Normalizing values for N-MORB from Sun & McDonough (1989).

Analytical results and interpretation of geochronological data

Zircon were obtained from a density separate of a crushed rock sample using a Wilfley water table. The magnetic minerals were removed by a hand magnet. Handpicked crystals were mounted in transparent epoxy resin together with chips of reference zircon 91 500. The zircon mounts were polished and after gold coating examined at the Swedish Museum of Natural History in Stockholm. High-spatial resolution secondary ion massspectrometer (SIMS) analysis was done in November 2015 using a Cameca IMS 1 280 at the Nordsim facility at the Swedish Museum of Natural History in Stockholm. Detailed descriptions of the analytical procedures are given in Whitehouse et al. (1997, 1999) and Whitehouse & Kamber (2005).

A c. 6 nA O^{2-} primary ion beam was used, yielding spot sizes of c. 15 μm . Pb/U ratios, elemental concentrations and Th/U ratios were calibrated relative to the Geostandards zircon 91 500 reference, which has an age of c. 1 065 Ma (Wiedenbeck et al. 1995, 2004). Common Pb corrected isotope values were calculated using modern common Pb composition (Stacey & Kramers 1975) and measured ^{204}Pb , in cases of a ^{204}Pb count rate above the detection limit. Decay constants follow the recommendations of Steiger & Jäger (1977). Diagrams and age calculations of isotopic data were made using software Isoplot 4.15 (Ludwig 2012). All age uncertainties are presented at the 95 % confidence level.

Most of the zircon are substantially rounded. Both short and elongated crystals are common. Many of the selected crystals are clear. The cathodoluminescence images show magmatic zonation in the majority of the studied grains (Fig. 123). Sometimes the zoning is diffuse or irregular and show resorption textures. Possible overgrowths are seen in some grains as well as inherited cores. The zircon population shows a large variation in luminosity between dark and light crystals. Ten crystals were analysed, three of them with two spots so the total number of analyses is 13. Six analyses were rejected due to too strong discordance.

The obtained ages have a large spread suggesting a strongly heterogeneous zircon population. The analyses 7a, 7b and 8 are concordant within error limits and yield a concordia age of $1\,873 \pm 11$ Ma (2σ , Fig. 124). Analysis 5b is concordant with a $^{207}\text{Pb}/^{206}\text{Pb}$ -age of $1\,929 \pm 14.5$ Ma (1σ). Analysis 3 is concordant with a $^{207}\text{Pb}/^{206}\text{Pb}$ age of $2\,001 \pm 12$ Ma (1σ). Analysis 2 is slightly discordant and has roughly similar $^{207}\text{Pb}/^{206}\text{Pb}$ age of $1\,998 \pm 11$ Ma (1σ). The zircon crystal of analysis 6a is substantially older with a concordant $^{207}\text{Pb}/^{206}\text{Pb}$ -age of $2\,701 \pm 12$ Ma (1σ). Analysis 6b is of similar age but strongly discordant. Also, analysis 9 has a $^{207}\text{Pb}/^{206}\text{Pb}$ age above 2.6 Ga but is strongly discordant. The U concentrations show 131–523 ppm for the concordant and nearly concordant analyses. The 2.7 Ga crystal (6a) has 131 ppm and the others 220–523 ppm. The rejected analyses show U concentrations between 431 and 1 669 ppm. The measured Th/U ratio is 1.02 for point 6a and 0.22–0.58 for the concordant or nearly concordant analyses. Two of the rejected analyses (4 and 5a) have lower ratios (0.06 and 0.10, respectively). The concordia age of $1\,873 \pm 11$ Ma ($n = 3$, 2σ , $\text{MSWD} = 2.1$, probability = 0.15) is chosen as the best age estimate interpreted to date igneous crystallisation of the quartz trachyte at Kallak.

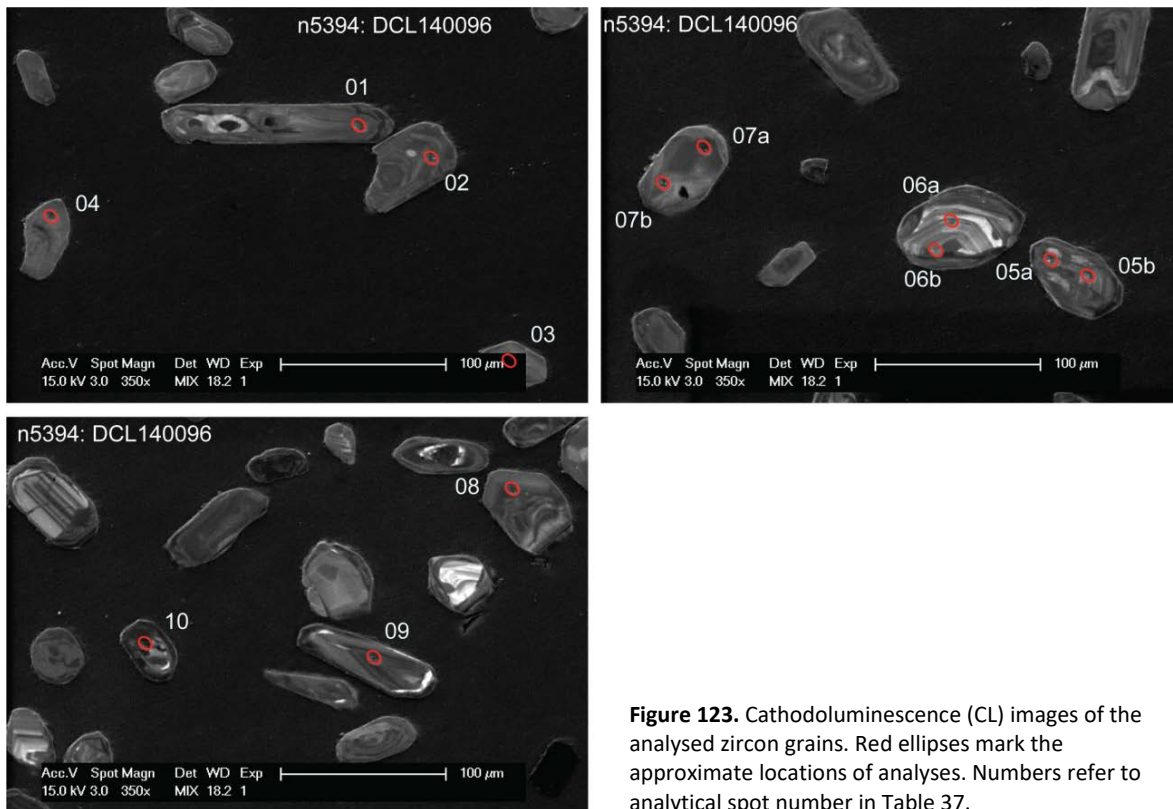


Figure 123. Cathodoluminescence (CL) images of the analysed zircon grains. Red ellipses mark the approximate locations of analyses. Numbers refer to analytical spot number in Table 37.

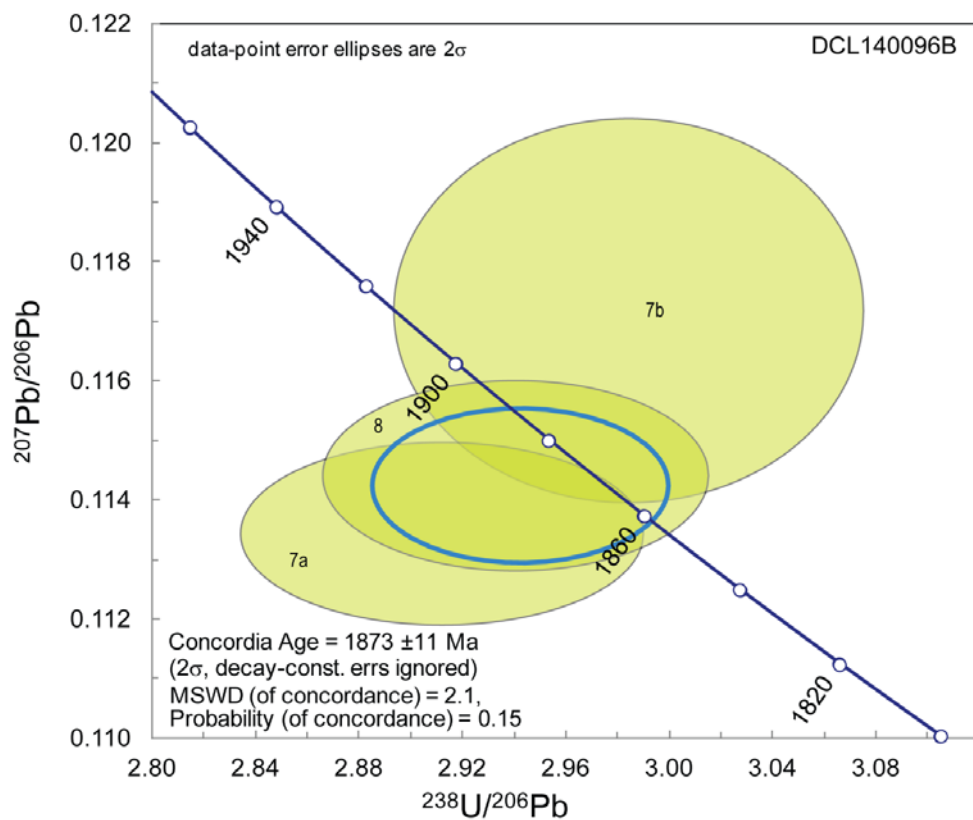


Figure 124. Tera-Wasserburg diagram showing U-Pb SIMS zircon data. Error ellipse of calculated weighted mean age is shown in blue.

Table 37. SIMS U-Pb-Th zircon data of the quartz trachyte.

Sample/ spot #	U ppm	Th ppm	Pb ppm	Th/U calc ^{*1}	²⁰⁷ Pb ²³⁵ U	±σ %	²⁰⁸ Pb ²³² Th	±σ %	²³⁸ U ²⁰⁶ Pb	±σ %	²⁰⁷ Pb ²⁰⁶ Pb	±σ %	ρ ^{*2}	Disc. % conv. ^{*3}	²⁰⁷ Pb ²⁰⁶ Pb	±σ (Ma)	²⁰⁶ Pb ²³⁸ U	±σ (Ma)	²⁰⁶ Pb/ ²⁰⁴ Pb measured	f ₂₀₆ % ^{*4}
n5394-01	463	76	165	0.21	4.777	4.84	0.1244	25.7	3.329	1.16	0.1154	4.70	0.24	-11.6	1885	82	1693	17	115	16.33
n5394-02	413	91	169	0.19	5.873	1.20	0.0914	4.4	2.884	1.03	0.1229	0.61	0.86	-4.6	1998	11	1919	17	6209	0.30
n5394-03	280	163	132	0.57	6.207	1.29	0.1020	4.0	2.734	1.10	0.1231	0.67	0.85	0.5	2001	12	2009	19	9053	0.21
n5394-04	1669	92	427	0.06	3.239	1.43	0.0948	8.1	4.399	1.27	0.1034	0.66	0.89	-23.9	1685	12	1320	15	737	2.54
n5394-05a	639	62	188	0.07	3.757	2.79	0.0657	17.0	3.842	2.58	0.1047	1.05	0.93	-14.3	1709	19	1491	34	1787	1.05
n5394-05b	227	92	97	0.38	5.699	1.35	0.0936	4.4	2.860	1.08	0.1182	0.81	0.80	0.2	1929	15	1933	18	5142	0.36
n5394-06a	131	133	100	1.03	13.245	1.35	0.1442	4.1	1.929	1.15	0.1853	0.70	0.85	-0.4	2701	12	2693	25	13632	0.14
n5394-06b	431	186	115	0.39	4.420	1.52	0.1259	5.2	5.573	1.41	0.1787	0.58	0.93	-64.6	2641	10	1064	14	299	{6.26}
n5394-07a	523	251	224	0.48	5.371	1.22	0.0956	4.0	2.912	1.09	0.1134	0.55	0.89	3.0	1855	10	1903	18	9321	0.20
n5394-07b	220	74	90	0.35	5.414	1.67	0.1035	5.4	2.984	1.24	0.1172	1.12	0.74	-3.1	1914	20	1863	20	2187	0.86
n5394-08	405	108	164	0.26	5.364	1.18	0.0941	4.1	2.941	1.04	0.1144	0.57	0.87	1.0	1871	10	1887	17	10524	0.18
n5394-09	734	236	323	0.16	8.756	1.71	0.0704	11.0	2.827	1.05	0.1795	1.34	0.62	-30.4	2649	22	1952	18	270	6.93
n5394-10	1244	567	262	0.30	2.340	2.69	0.0569	6.5	5.972	1.07	0.1014	2.47	0.40	-42.6	1649	45	998	10	152	12.34

Isotope values are common Pb corrected using modern common Pb composition (Stacey & Kramers 1975) and measured ²⁰⁴Pb.

*1 Th/U ratios calculated from ²⁰⁸Pb/²⁰⁶Pb and ²⁰⁷Pb/²⁰⁶Pb ratios, assuming single stage of closed U-Th-Pb evolution.

*2 Error correlation in conventional concordia space. Do not use for Tera-Wasserburg plots.

*3 Age discordance in conventional concordia space. Positive numbers are reverse discordant.

*4 Figures in parentheses are given when no correction has been applied, and indicate a value calculated assuming present-day Stacey-Kramers common Pb.

Discussion and conclusion

Age determination of the quartz trachyte shows that there is a heterogeneous set of zircon, with the oldest being Archaean, c. 2 700 Ma old, and that the likely formation of the volcanic rocks took place at about $1\,873 \pm 11$ Ma ago. The age of the host quartz trachyte of the Kallak iron ore, overlaps with that of the ore body at Kiirunavaara (c. 1 874 Ma, Westhues et al. 2016). The iron ore at Kallak and the quartz trachyte have similar REE patterns, but the mineralisation shows significantly lower levels of REE (Fig. 122). The same applies to the multi-element diagram, which shows similar trends for the two samples, but the iron ore has significantly lower levels compared with the quartz trachyte (Fig. 122).

The interpretation of the results from the above investigations is that the quartz trachyte and the Kallak iron ore deposit were deposited in a volcanogenic environment during the early Svecokarelian (Claeson & Antal Lundin *in press c*). The results were integrated in the mapping of the 27I Tjåmotis SV, SO area (Claeson & Antal Lundin *in press c*). Summary of sample data is given in Table 38.

Table 38. Summary of sample data.

Rock type	Quartz trachyte
Lithotectonic unit	Norrbottnen lithotectonic unit of the Svecokarelian orogen
Lithological unit	
Sample number	DCL140096B
Lab_id	n5394
Coordinates	7414247/681408 (Sweref99TM)
Map sheet	27I Tjåmotis SO (RT90)
Locality	Kallak
Project	Sydvästra Norrbotten (80025)

Acknowledgements

U-Pb isotopic zircon data were obtained from the Laboratory for Isotope Geology of the Swedish Museum of Natural History in Stockholm. The Nordsim facility is operated under an agreement between the research funding agencies of Denmark, Norway and Sweden, the Geological Survey of Finland and the Swedish Museum of Natural History.

References

- Boynton, W.V., 1984: Cosmochemistry of the Rare Earth Elements: Meteorite studies. *In* P. Henderson (ed.): *Rare earth element geochemistry*. Elsevier Science B.V. 63–114.
- Claeson, D. & Antal Lundin, I., *in press c*: Beskrivning till berggrundskartorna 27I Tjåmotis SV, SO. *Sveriges geologiska undersökning*.
- Johansson, R., 1980: Jokkmokksområdets järnmalmer – Geofysisk tolkning med malmberäkning. *Sveriges geologiska undersökning FM 8012*, 36 pp.
- Ludwig, K.R., 2012: User's manual for Isoplot 3.75. A Geochronological Toolkit for Microsoft Excel. *Berkeley Geochronology Center Special Publication No. 5*, 75 pp.
- Stacey, J.S. & Kramers, J.D., 1975: Approximation of terrestrial lead isotope evolution by a two-stage model. *Earth and Planetary Science Letters* 26, 207–221.
- Steiger, R.H. & Jäger, E., 1977: Convention on the use of decay constants in geo- and cosmochronology. *Earth and Planetary Science Letters* 36, 359–362.
- Sun, S.S. & McDonough, W.F., 1989: Chemical and isotopic systematic of oceanic basalts: implications for mantle composition and processes. *In* A.D. Saunders & M.J. Norry (eds.): *Magmatism in ocean basins*. Geological Society of London, Special Publication 42, 313–345.
- Westhues, A., Hanchar, J.M., Whitehouse, M.J. & Martinsson, O., 2016: New constraints on the timing of host-rock emplacement, hydrothermal alteration, and iron oxide-apatite mineralization in the Kiruna district, Norrbotten, Sweden. *Economic Geology* 111, 1 595–1 618.
- Whitehouse, M.J., Claesson, S., Sunde, T. & Vestin, J., 1997: Ion-microprobe U–Pb zircon geochronology and correlation of Archaean gneisses from the Lewisian Complex of Gruinard Bay, north-west Scotland. *Geochimica et Cosmochimica Acta* 61, 4 429–4 438.
- Whitehouse, M.J., Kamber, B.S. & Moorbath, S., 1999: Age significance of U–Th–Pb zircon data from Early Archaean rocks of west Greenland: a reassessment based on combined ion-microprobe and imaging studies. *Chemical Geology (Isotope Geoscience Section)* 160, 201–224.
- Whitehouse, M., J. & Kamber, B.S., 2005: Assigning Dates to Thin Gneissic Veins in High-Grade Metamorphic Terranes: A Cautionary Tale from Akilia, Southwest Greenland. *Journal of Petrology* 46, 291–318.
- Wiedenbeck, M., Allé, P., Corfu, F., Griffin, W.L., Meier, M., Oberli, F., Quadt, A.V., Roddick, J.C. & Spiegel, W., 1995: Three natural zircon standards for U-Th-Pb, Lu-Hf, trace element and REE analyses. *Geostandards Newsletter* 19, 1–23.
- Wiedenbeck, M., Hanchar, J.M., Peck, W.H., Sylvester, P., Valley, J., Whitehouse, M., Kronz, A., Morishita, Y., Nasdala, L., Fiebig, J., Franchi, I., Girard, J.P., Greenwood, R.C., Hinton, R., Kita, N., Mason, P.R.D., Norman, M., Ogasawara, M., Piccoli, P.M., Rhede, D., Satoh, H., Schulz-Dobrick, B., Skår, O., Spicuzza, M.J., Terada, K., Tindle, A., Togashi, S., Vennemann, T., Xie, Q. & Zheng, Y.F., 2004: Further Characterisation of the 91500 Zircon Crystal. *Geostandards and Geoanalytical Research* 28, 9–39.

NEW VOLCANIC SUCCESSION AT 1.77 Ga DETERMINED BY U-Pb ZIRCON AGE OF ANDESITOID AT TJÄKKAURE, MAP SHEET 271 TJÅMOTIS SO, NORRBOTTEN COUNTY

Authors: Dick Claeson, Ildikó Antal Lundin & Fredrik Hellström

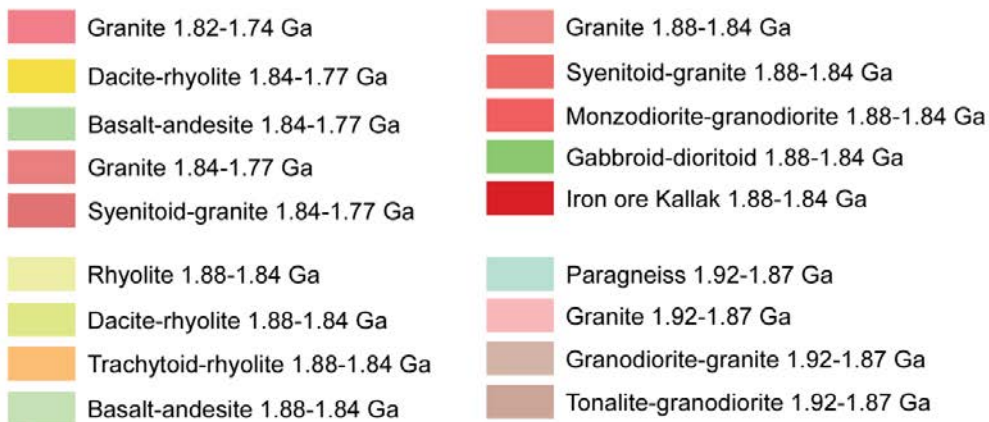
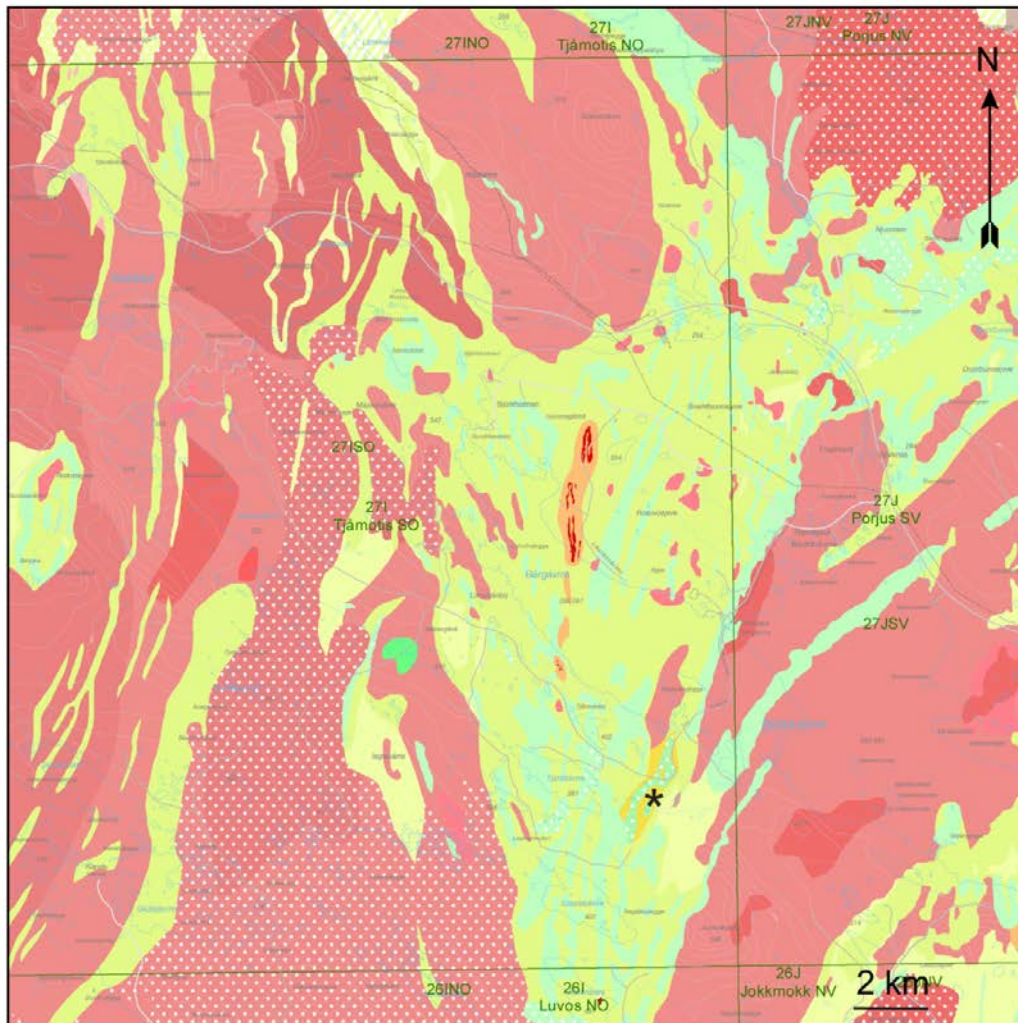


Figure 125. Bedrock map of the area, sampling location marked with black star.

Introduction

Norrbottnen, Sweden is a key area of Europe for future exploration and mining. Both on the magnetic and Bouguer anomaly maps the volcanic rocks are clearly seen as a high magnetic, banded pattern and as a gravity high (Fig. 103, 104). The structure is interpreted as a body of extrusive rocks, which covers parts of the map sheet 27I Tjåmotis SO (Fig. 125). Recent attempts at SGU to determine the age of these has failed due to the poor condition of the zircon (DCL090069). Since some of these extrusive rocks are Au anomalous (failed age determination DCL090069) and the present sample might have a connection to the genesis of the iron-deposit at Kallak, so from an exploration point of view knowing their age is of great interest.

If there are zircon with metamorphic rims or other overgrowths, these should also be studied since this may be of huge significance for the interpretation of the genesis of an ore body/deposit, in this case the Kallak iron ore c. 10 km north of the sampled volcanic rock. For example, where multiple episodes of concentration of sulphides are indicated in recent work at Aitik (Wanhainen et al. 2003, 2005) or in iron oxide–copper–gold (IOCG) mineralisation in this region (Smith et al. 2009). In order to gain knowledge of when metamorphic events are in any way involved in the genesis of the formation of economic deposits on a regional scale in the Norrbotten county, by re-heating the crust and producing hydrothermal activity in volcanic rocks or structural zones, their age have to be determined. But we believe this is a field for future research! The size of the sampled anomaly on the aeromagnetic map indicates that the extrusive rocks are stretching from Björkholmen to Kiruna and far beyond, knowledge about the age is consequently important.

The aim of this study is to determine the magmatic age of an andesitoid part of a major structure on the map area 27I Tjåmotis SO and if there are any metamorphic overgrowths, determine these as well, since the latter might show ages for the genesis of ore by redistribution of elements in the crust. However, the well-preserved nature of the sampled rock compared with the amphibolite facies volcanic rocks for the most part of the extrusive rocks stretching from Björkholmen to Kiruna, suggest that the volcanic successions at Tjåkkaure may belong to a younger generation than the rest. Furthermore, age determinations of volcanic rocks in the region are scarce.

Sample description

A common rock in the volcanic successions at Tjåkkaure is a grey to dark grey basaltic andesite to andesite (Fig. 126). These are very fine-grained to fine-grained, foliated and banded 200/82–88 during primary emplacement. There is at places a noticeable primary lineation present 20/60, where most often mafic fragments best define the lineation (Fig. 126). The genesis of the structures is related to the deposition of hot, extrusive products that moved in a semi-plastic condition and is not related to any regional plastic deformation taking place after 1.77 Ga. These intermediate volcanic rocks are for the most part well-preserved and compared with the surrounding older volcanic rocks extremely so, which at places show evidence of partial melting as veins during amphibolite facies metamorphism (Claeson & Antal Lundin *in press c*).

Only lesser growth of subgrains in quartz and undulose extinction is to be seen in microscope, and aggregates of amphibole glomerocrysts, all indicative of low metamorphic dynamic recrystallisation (Fig. 127). Magnetite occurs as glomerocrysts, often along with amphibole. Parts are hydrothermally altered displaying epidote. At places the andesite is rich in volcanic rock fragments and exhibits a great variation in content of plagioclase phenocrysts 5–10 mm (0–10 %). Dacitoid and basalt occur as well in the successions, where the latter sometimes is plagioclase porphyric. Obviously, these are volcanoclastic deposits, where the fragments show that coeval magmatism and eruption of andesitoid, dacitoid, and basaltoid compositions occurred.

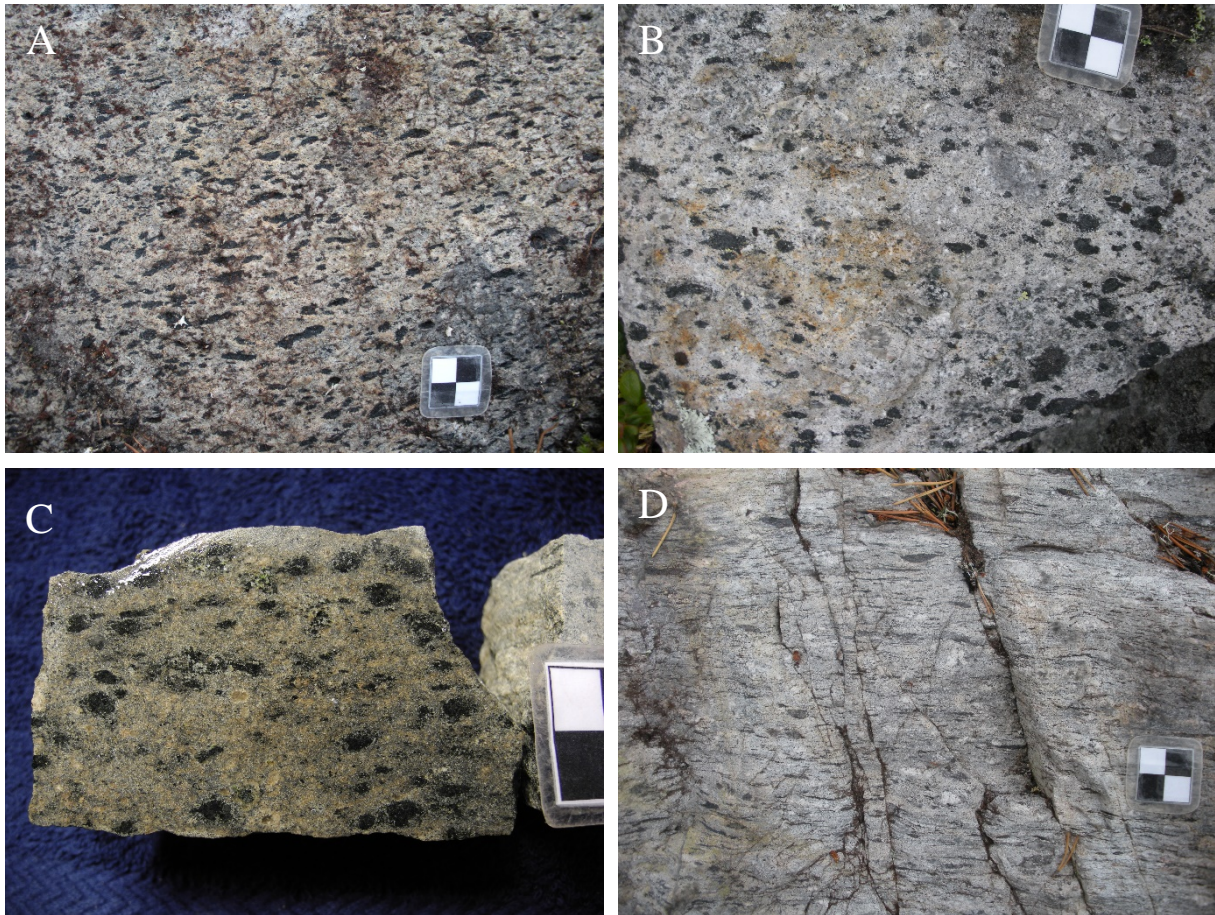


Figure 126. A. and B. Andesitoid, outcrop adjacent to sampling site of DCL100124A (7404458/683199). C. Cut and wetted sample of andesitoid DCL100124A (cm-scale). D. Andesitoid displaying primary foliation and lots of fragments (7405033/683559). Photos: Dick Claeson.

The sampled outcrop is located east of the lake Tjäkkaure, some 10 km SW of Randijaur. The sample consists of trachybasaltic andesite with shoshonite affinity that is deformed during deposition, hydrothermally altered, light grey to dark grey (hydrothermally altered rocks are more pale), and varies from very fine- to fine-grained (Fig. 126, 127). Fragments of other volcanic rocks are present. The extrusive rocks are compositionally layered showing a banded appearance. The more mafic and basic rocks at the outcrop is sometimes porphyric with plagioclase feldspar 2–10 mm (0–10 %). Magnetite and amphibole are present as aggregates and in microscope seen as glomerocrysts, indicating a volcanic origin (Fig. 126, 127). Primary foliation and banding is oriented 200/88 and mineral lineation 20/60. Magnetic susceptibility varies between 11 700 and 23 600 $\times 10^{-5}$ SI. Petrophysical measurements of a sample show density at 2 916 kg/m³, magnetic susceptibility 33 415 $\times 10^{-5}$ SI, and remanent magnetization intensity of 1 230 mA/m. Gamma ray measurements on the outcrop shows K = 1.6 %, U = 3 ppm, and Th = 7.4 ppm. The Zr content of the rock is 309 ppm.

The low degree of deformation and metamorphic overprinting is in stark contrast to the early Svecokarelian volcanic rocks of the surrounding that display amphibolite facies with incipient partial melting (e.g. Claeson & Antal Lundin *in press c*).

The trachybasaltic andesite and trachybasalt at Tjäkkaure shows a LREE-enriched and flat HREE pattern, with a small negative Eu anomaly (Fig. 128). The LREE enrichment is due to fractional crystallisation, the flat, unfractionated HREE pattern shows that no garnet was left in the residue at the location of magma genesis, and the Eu anomaly is indicative of insignificant plagioclase fractionation. The negative anomaly shown in the multi-element diagram of Sr but none in Eu suggest something else than plain plagioclase fractionation for the Sr (Fig. 128). The minor P anomaly indicates apatite fractionation, and the Ti anomaly minor Fe-Ti oxide fractionation (Fig. 128). The strong negative anomaly of Nb may suggest a subduction related petrogenesis but the strong negative anomaly of Pb indicate that this might not be the case or that the transfer of Pb into new magmas that is normally seen in subduction settings did not occur e.g. less subducted sediment was involved in their petrogenesis (Fig. 128).

The lithochemical analysis of the dated rock shows a basaltic andesite to basaltic trachyandesite with a shoshonitic composition ($\text{Na}_2\text{O} - 2.0 < \text{K}_2\text{O}$). Compared with older generations of basalt and andesite in the map area of 27I Tjåmotis SO, the Tjäkkaure samples are generally richer in REE and have lower Cs and Rb content at comparable SiO_2 (Claeson & Antal Lundin *in press c*).

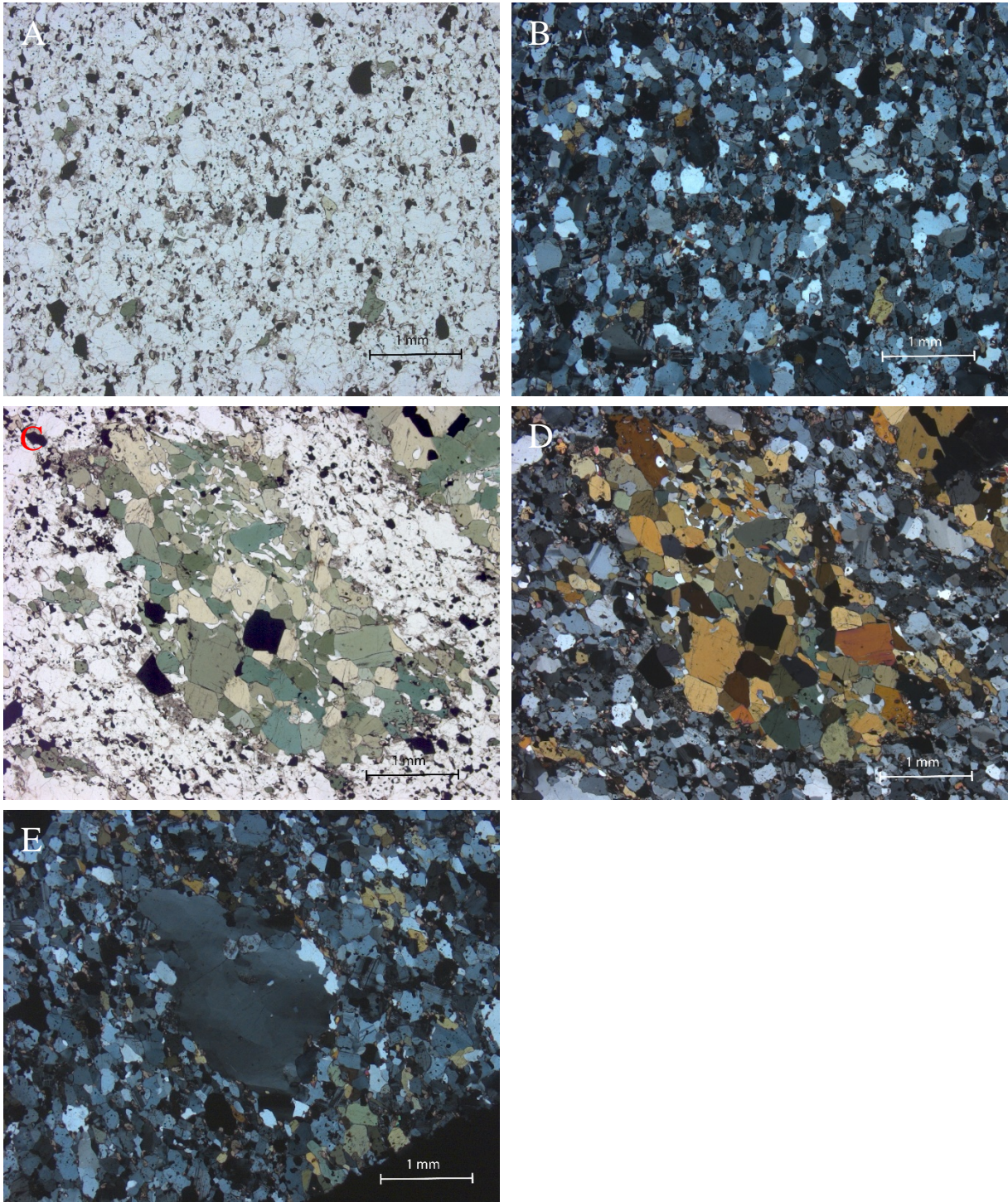


Figure 127. A. Matrix of basaltic trachyandesite, plane-polarized light. B. Crossed nicols of same view. C. Glomerocryst as aggregate of amphibole and Fe-Ti oxide, plane-polarized light. D. Crossed nicols of same view. E. Quartz megacryst showing slight undulose extinction and minor subgrain growth. Micrographs: Dick Claeson.

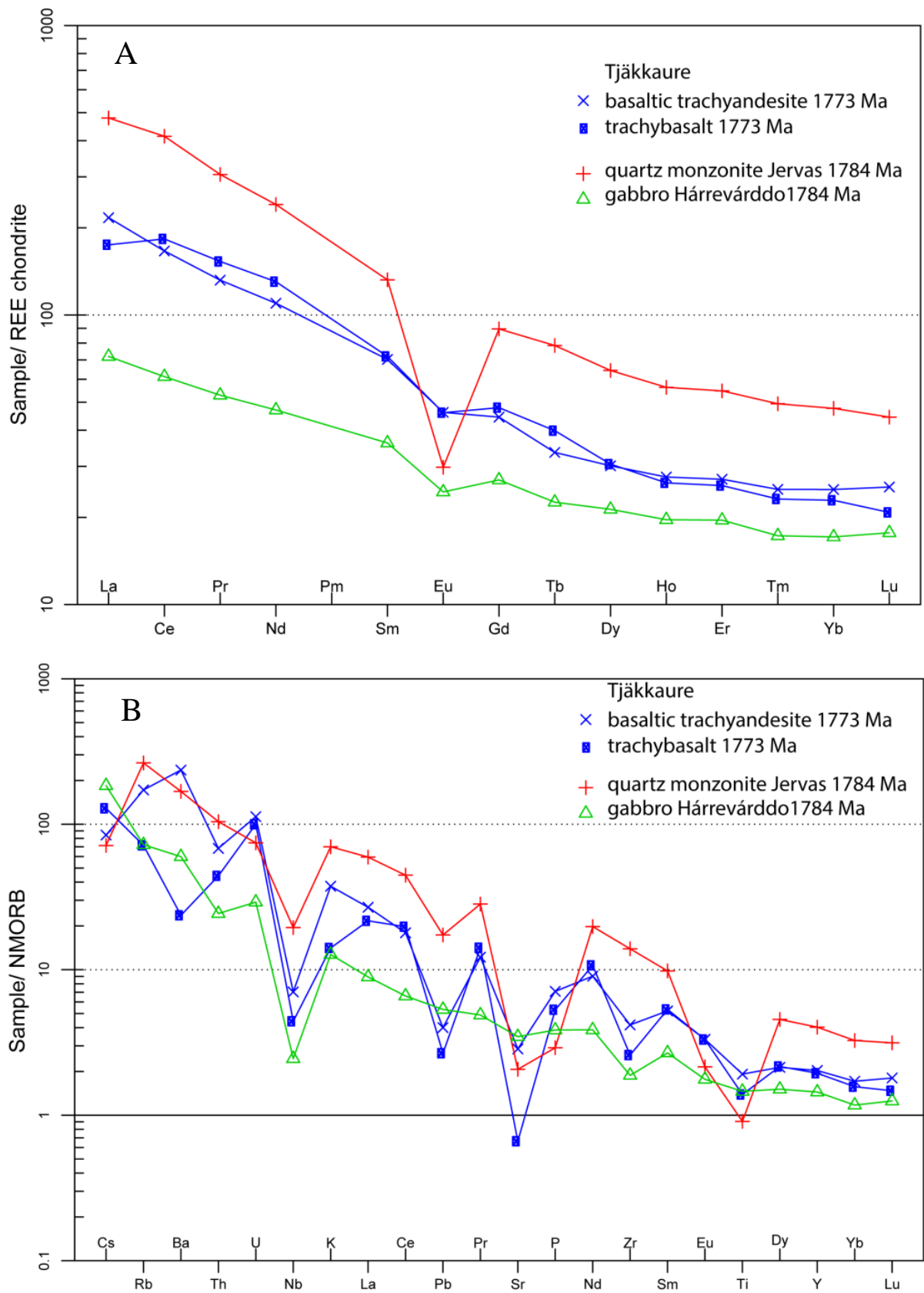


Figure 128. A. REE-diagram of basaltic trachyandesite and trachybasalt of Tjäkkaure compared with quartz monzonite and gabbro from the Hárrevárddo intrusion. Normalizing values for chondrite from Boynton (1984). **B.** Multi-element diagram, rock as in A. Normalizing values for N-MORB from Sun & McDonough (1989).

Analytical results and interpretation of geochronological data

Zircon were obtained from a density separate of a crushed rock sample using a Wilfley water table. The magnetic minerals were removed by a hand magnet. Handpicked crystals were mounted in transparent epoxy resin together with chips of reference zircon 91 500. The zircon mounts were polished and after gold coating examined by Back-Scattered Electron (BSE) imaging, using standard electron microscopy at the Evolutionary Biology Centre (EBC), Uppsala University. High-spatial resolution secondary ion massspectrometer (SIMS) analysis was done in December 2012 using a Cameca IMS 1 270 at the Nordsim facility at the Swedish Museum of Natural History in Stockholm. Detailed descriptions of the analytical procedures are given in Whitehouse et al. (1997, 1999).

Pb/U ratios, elemental concentrations and Th/U ratios were calibrated relative to the Geostandards zircon 91 500 reference, which has an age of c. 1 065 Ma (Wiedenbeck et al. 1995, 2004). Common Pb corrected isotope values were calculated using modern common Pb composition (Stacey & Kramers 1975) and measured ^{204}Pb . Decay constants follow the recommendations of Steiger & Jäger (1977). Diagrams and age calculations of isotopic data were made using software Isoplot 4.15 (Ludwig 2012). BSE/CL-imaging was done at the Department of Geology, Uppsala University after the SIMS-analyses work.

The heavy mineral separate contains elongated, subhedral zircon, mostly transparent and colourless. BSE-images of the zircon show a homogenous colour level and CL-imaging a mottled appearance of the zircon (Fig. 129). The 13 analyses are all low in uranium, 73–131 ppm, and show rather low Th/U ratios, 0.08–0.20. Four analyses (5, 16, 22, 23) record high values of common lead ($f_{206}=0.38\text{--}1.22\%$) and are 6.9–11.8 % discordant (Table 39). Excluding two 3.7 % and 3.9 % reversely discordant analyses (43, 21), the remaining eight analyses give a concordia age at $1\,777 \pm 10$ Ma (95 % confidence, MSWD of concordance = 1.3, Probability of concordance = 0.26, $n=8$). Including the two weakly reversely discordant analyses, a weighted average $^{207}\text{Pb}/^{206}\text{Pb}$ age is calculated at $1\,773 \pm 7$ Ma (Fig. 130; 2σ , MSWD = 0.70, probability = 0.71, $n=10$), which is chosen as the best age estimate of igneous crystallisation of the trachybasaltic andesite.

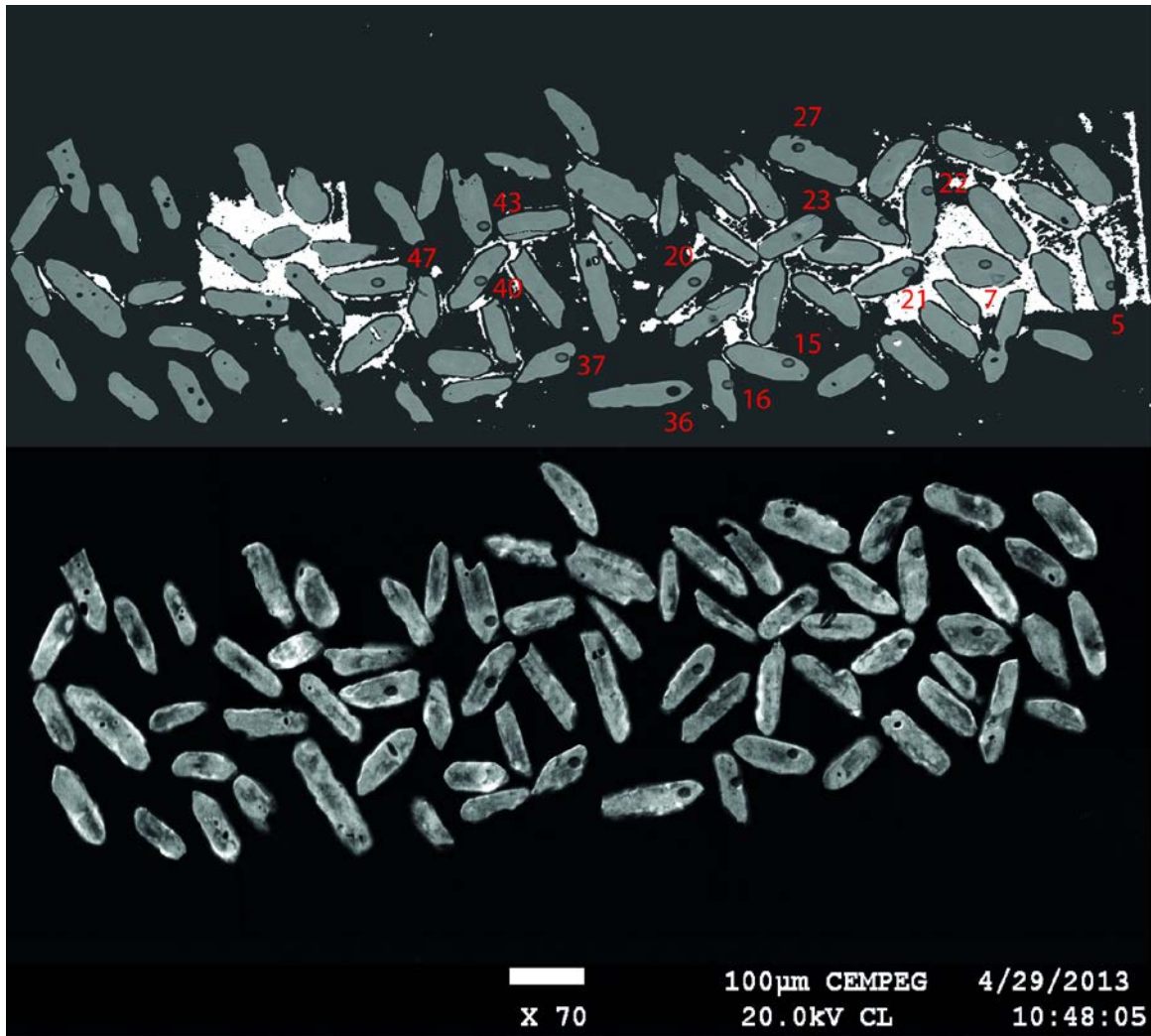


Figure 129. BSE-image (top) and CL-image (below) of analysed zircon grains. Numbers refer to analytical spot number in Table 39

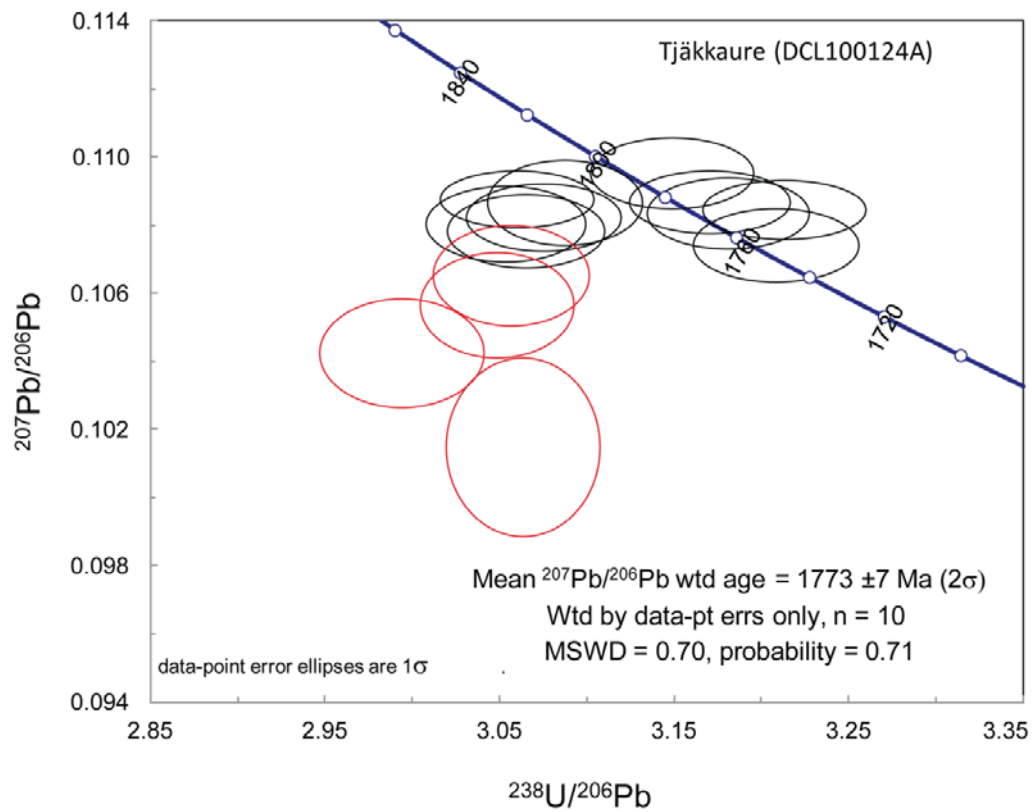


Figure 130. Tera-Wasserburg diagram showing U-Pb SIMS data of zircon analyses. Analyses used in age calculation are marked in black, excluded analyses in red.

Table 39. SIMS U-Pb-Th zircon data

Sample/ spot #	U ppm	Th ppm	Pb ppm	Th/U calc ^{*1}	²⁰⁷ Pb ²³⁵ U	±σ %	²⁰⁸ Pb ²³² Th	±σ %	²³⁸ U ²⁰⁶ Pb	±σ %	²⁰⁷ Pb ²⁰⁶ Pb	±σ %	ρ ^{*2}	Disc. % conv. ^{*3}	²⁰⁷ Pb ²⁰⁶ Pb (Ma)	±σ (Ma)	²⁰⁶ Pb ²³⁸ U (Ma)	±σ (Ma)	²⁰⁶ Pb/ ²⁰⁴ Pb measured	f ₂₀₆ % ^{*4}
n4392-05	95	13	35	0.11	4.805	1.33	0.0697	7.0	3.057	0.97	0.1065	0.91	0.73	5.5	1741	17	1825	15	3092	0.60
n4392-07	118	19	43	0.16	4.726	1.11	0.0932	4.0	3.170	0.96	0.1087	0.55	0.87	-0.6	1777	10	1767	15	87083	{0.02}
n4392-15	101	17	38	0.18	4.852	1.22	0.0954	3.7	3.088	0.95	0.1086	0.76	0.78	2.0	1777	14	1809	15	42790	{0.04}
n4392-16	90	14	33	0.08	4.567	1.95	0.0442	20.8	3.064	0.95	0.1015	1.70	0.49	11.8	1651	31	1821	15	1536	1.22
n4392-20	85	12	31	0.14	4.796	1.17	0.0908	3.4	3.149	0.98	0.1095	0.64	0.84	-0.9	1791	12	1778	15	50528	{0.04}
n4392-21	90	11	34	0.13	4.878	1.20	0.0949	3.7	3.054	0.99	0.1080	0.68	0.82	3.9	1766	12	1826	16	19304	0.10
n4392-22	106	19	40	0.17	4.778	1.36	0.0836	4.0	3.049	0.96	0.1056	0.97	0.70	6.9	1725	18	1829	15	4876	0.38
n4392-23	79	10	30	0.10	4.801	1.44	0.0671	8.2	2.994	1.03	0.1042	1.01	0.72	10.6	1701	18	1858	17	2642	0.71
n4392-27	90	15	33	0.19	4.695	1.15	0.1012	3.8	3.181	0.96	0.1083	0.64	0.83	-0.6	1772	12	1762	15	110039	{0.02}
n4392-36a	73	8	26	0.12	4.616	1.18	0.0927	3.7	3.209	0.98	0.1074	0.66	0.83	-0.5	1756	12	1749	15	66812	{0.03}
n4392-37a	92	14	35	0.16	4.852	1.13	0.0918	3.9	3.075	0.95	0.1082	0.60	0.84	2.9	1770	11	1815	15	44330	0.04
n4392-40a	131	24	50	0.20	4.900	1.08	0.0977	3.1	3.060	0.95	0.1087	0.51	0.88	2.8	1779	9	1823	15	62818	0.03
n4392-43a	80	9	30	0.11	4.850	1.17	0.0924	3.9	3.065	0.97	0.1078	0.66	0.83	3.7	1763	12	1820	15	30091	0.06
n4392-47a	110	19	40	0.17	4.654	1.10	0.0934	3.1	3.213	0.96	0.1085	0.53	0.87	-1.7	1774	10	1747	15	>1e6	{0.00}

Isotope values are common Pb corrected using modern common Pb composition (Stacey & Kramers 1975) and measured ²⁰⁴Pb.

*1 Th/U ratios calculated from ²⁰⁸Pb/²⁰⁶Pb and ²⁰⁷Pb/²⁰⁶Pb ratios, assuming single stage of closed U-Th-Pb evolution.

*2 Error correlation in conventional concordia space. Do not use for Tera-Wasserburg plots.

*3 Age discordance in conventional concordia space. Positive numbers are reverse discordant.

*4 Figures in parentheses are given when no correction has been applied, and indicate a value calculated assuming present-day Stacey-Kramers common Pb.

Discussion and conclusion

The Tjäkkaure volcanic successions at $1\,773 \pm 7$ Ma are the youngest known in the region and until now, not even recognized in an area of relatively major geological and prospecting interest with earlier mapping efforts. Other young volcanic rocks do occur in the region e.g. a rhyolite of the Dobblon Group is $1\,803 \pm 15$ Ma old (Skiöld 1988). However, the Tjäkkaure successions are most probably not related to the Dobblon Group because of the much more acid compositions of the latter. Instead the most likely scenario for the petrogenesis of the Tjäkkaure volcanic rocks is that they are related to the magmatic activity occurring at c. 1 784 Ma, when the multiple Hárrevárddo intrusion forms within the map area 27I Tjåmotis SV (Claeson & Antal Lundin *in press c*, this issue).

The trachybasaltic andesite and trachybasalt at Tjäkkaure are shown along with a gabbro and quartz monzonite from the Hárrevárddo intrusion in Figure 128 and illustrate that they may have the same petrogenetic origin. These types of compositions of magmas have earlier generated similar volcanic rocks during 1.89–1.86 Ga in the region (Claeson & Antal Lundin *in press c*). There is also extensive magmatism in the map areas 26J Jokkmokk NV and NO at around 1 795 Ma (Claeson & Antal Lundin *in press b*, this issue). These were gabbroic intrusions as well as coarse K-feldspar porphyric acid to intermediate intrusions, mostly quartz monzodiorite, monzonite, quartz monzonite, and granite (Claeson & Antal Lundin *in press b*, this issue).

There are several other outcrops of similar volcanic rocks as those found at Tjäkkaure that might belong to these youngest extrusive rocks in the map area 27I Tjåmotis SO and the most adjacent map sheets, but since no efforts to date these have been performed they are all conservatively classified as belonging to the older successions (Claeson & Antal Lundin *in press c*). The results were integrated in the mapping of the 27I Tjåmotis SO area (Claeson & Antal Lundin *in press c*). Summary of sample data is given in Table 40.

Table 40. Summary of sample data.

Rock type	Andesitoid
Lithotectonic unit	Norrbottnen lithotectonic unit of the Svecokarelian orogen
Lithological unit	
Sample number	DCL100124A
Lab_id	n4392
Coordinates	7404458/683199 (Sweref99TM)
Map sheet	27I Tjåmotis SO (RT90)
Locality	Tjäkkaure
Project	Sydvästra Norrbotten (80025)

Acknowledgments

Martin Whitehouse, Lev Ilyinsky and Kerstin Lindén at the Nordsim analytical facility are acknowledged for their great support with the SIMS-analytical work. Gary Wife at EBC, as well as Jarek Majka and Abigail Barker at the Department of Geology, Uppsala University are much thanked for their assistance during BSE/CL-imaging of zircon.

References

- Boynton, W.V., 1984: Cosmochemistry of the Rare Earth Elements: Meteorite studies. *In* P. Henderson (ed.): *Rare earth element geochemistry*. Elsevier Science B.V. 63–114.
- Claeson, D. & Antal Lundin, I., *in press b*: Beskrivning till berggrundskartorna 26J Jokkmokk NV, NO. *Sveriges geologiska undersökning*.
- Claeson, D. & Antal Lundin, I., *in press c*: Beskrivning till berggrundskartorna 27I Tjåmotis SV, SO. *Sveriges geologiska undersökning*.
- Ludwig, K.R., 2012: User's manual for Isoplot 3.75. A Geochronological Toolkit for Microsoft Excel. *Berkeley Geochronology Center Special Publication No. 5*, 75 pp.
- Skiöld, T., 1988: Implications of new U-Pb zircon chronology to early Proterozoic crustal accretion in northern Sweden. *Precambrian Research* 38, 147–164.
- Smith, M.P., Storey, C.D., Jeffries, T.E. & Ryan, C., 2009: *In Situ* U–Pb and Trace Element Analysis of Accessory Minerals in the Kiruna District, Norrbotten, Sweden: New Constraints on the Timing and Origin of Mineralization. *Journal of Petrology*, 50, 2 063–2 094.
- Stacey, J.S. & Kramers, J.D., 1975: Approximation of terrestrial lead isotope evolution by a two-stage model. *Earth and Planetary Science Letters* 26, 207–221.
- Steiger, R.H. & Jäger, E., 1977: Convention on the use of decay constants in geo- and cosmochronology. *Earth and Planetary Science Letters* 36, 359–362.
- Sun, S.S. & McDonough, W.F., 1989: Chemical and isotopic systematic of oceanic basalts: implications for mantle composition and processes. *In* A.D. Saunders & M.J. Norry (eds.): *Magmatism in ocean basins*. Geological Society of London, Special Publication 42, 313–345.
- Wanhainen, C., Broman, C. & Martinsson, O., 2003: The Aitik Cu–Au–Ag deposit in northern Sweden: a product of high salinity fluids. *Mineralium Deposita* 38, 715–726.
- Wanhainen, C., Billström, K., Martinsson, O., Stein, H. & Nordin, R., 2005: 160 Ma of magmatic/hydrothermal and metamorphic activity in the Gällivare area: Re–Os dating of molybdenite and U–Pb dating of titanite from the Aitik Cu–Au–Ag deposit, northern Sweden. *Mineralium Deposita* 40, 435–447.
- Whitehouse, M.J., Claesson, S., Sunde, T. & Vestin, J., 1997: Ion-microprobe U–Pb zircon geochronology and correlation of Archaean gneisses from the Lewisian Complex of Gruinard Bay, north-west Scotland. *Geochimica et Cosmochimica Acta* 61, 4 429–4 438.
- Whitehouse, M.J., Kamber, B.S. & Moorbath, S., 1999: Age significance of U–Th–Pb zircon data from Early Archaean rocks of west Greenland: a reassessment based on combined ion-microprobe and imaging studies. *Chemical Geology (Isotope Geoscience Section)* 160, 201–224.
- Wiedenbeck, M., Allé, P., Corfu, F., Griffin, W.L., Meier, M., Oberli, F., Quadt, A.V., Roddick, J.C. & Spiegel, W., 1995: Three natural zircon standards for U–Th–Pb, Lu–Hf, trace element and REE analyses. *Geostandards Newsletter* 19, 1–23.
- Wiedenbeck, M., Hanchar, J.M., Peck, W.H., Sylvester, P., Valley, J., Whitehouse, M., Kronz, A., Morishita, Y., Nasdala, L., Fiebig, J., Franchi, I., Girard, J.P., Greenwood, R.C., Hinton, R., Kita, N., Mason, P.R.D., Norman, M., Ogasawara, M., Piccoli, P.M., Rhede, D., Satoh, H., Schulz-Dobrick, B., Skår, O., Spicuzza, M.J., Terada, K., Tindle, A., Togashi, S., Vennemann, T., Xie, Q. & Zheng, Y.F., 2004: Further Characterisation of the 91500 Zircon Crystal. *Geostandards and Geoanalytical Research* 28, 9–39.

CONCLUDING REMARKS AND FUTURE ISSUES

Even if the presented age determinations in this report add to our knowledge of geological events and solves some questions we had during mapping of the map sheet areas 27K Nattavaara, 27J Porjus SV, 26J Jokkmokk NV and SV, and 27I Tjåmotis SV and SO, there are a plethora of unresolved and interesting issues left for the future! We list below some related to age determination and isotopic work that we had no financial possibility to perform during ordinary mapping at the SGU.

- Age determination of ore and host at several locations and different types of deposits.
- Age determination of alteration, focused on ore deposits.
- Age determination of metamorphic events, both regional and those related to intrusion of large amounts of magma.
- Isotopic studies of both ore deposits and rocks to document their signatures, petrogenesis, and ore genesis.